LOW TEMPERATURE ANHARMONICITY

IN THE SUPERCONDUCTING SPINELS

A thesis submitted for the degree of;

PHILOSOPHIAE DOCTOR

at The University of Aston in Birmingham, by

PAUL PEARSON DAWES, B.Sc.(Hons), M.Sc.

September, 1975.

SUMMARY

Strong comparisons between the properties of the high transition temperature superconductors in the β- tungsten and NbN groups and the superconducting spinels are described within the framework of present theories of high T_c superconductivity. In particular, emphasis is laid upon the known presence of lattice instabilities in both groups of compounds.

X-Ray diffractometric measurements of the crystallographic parameters of the superconducting spinels have been made and the superconducting transition temperatures determined using the Meissner Effect.

Mössbauer spectrometry experiments have been performed which establish the presence of low temperature anharmonicity within the superconducting spinels by measurement of the recoil-free fraction. Coincident total shift measurements have enabled the present theory of the band structure to be tested.

By making use of recent theories employing Mössbauer effect measurements, the validity of McMillans theory applied to the superconducting spinels has been investigated and shown to be reasonable, within the approximations of the theory.

CONTENTS

CHAPTER 1 SUPERCONDUCTIVITY AND THE SPINELS

"As far as high transition temperatures and any theory are concerned ... (save Hopfields) ... there is a complete and total anti-correlation".

B. T. Matthias. (1968)

1.1 The Phenomena of Superconductivity

It has been known for many years that the specific electrical resistance of metals decreases with temperature. This is because the scattering of electrons which arises from the thermal motion of the atoms decreases at low temperatures, corresponding to the decrease in the amplitude of atomic vibrations. It is found experimentally that the decrease in resistance is approximately linear from room temperature down to about one third of the Debye Characteristic Temperature, (Θ_D). Well below this temperature the resistivity varies as T^5.

In 1911 after succeeding in his attempt to liquify helium, Kamerlingh - Onnes proceeded to investigate the electrical resistance of metals down to 1^oK. He found that for mercury the resistance disappeared apparently completely and quite dramatically just below 4.2^oK (Fig 1.1). This phenomena of zero resistance at finite temperature is now called superconductivity. Kamerlingh - Onnes was not able to obtain the same result with all metals. Even after much repurification some retained a residual low resistance down to the lowest attainable temperature.

The origin of the latter was made clear by the work of Bloch (1928) who showed that an electron can move freely through a perfect crystal structure without resistance and that a finite mean free path can only be due to imperfections in the structure. In general the imperfections correspond predominantly with the thermal vibrations of the atoms, but impurities and crystal structure defects, such as vacancies, and grain boundaries also scatter electrons. The free path length in this case is determined by the number and scattering power of the defects and is

FIG. 1.1 THE ELECTRICAL RESISTANCE OF MERCURY AT LOW TEMPERATURE.

AFTER KAMERLINGH-ONNES, 1911

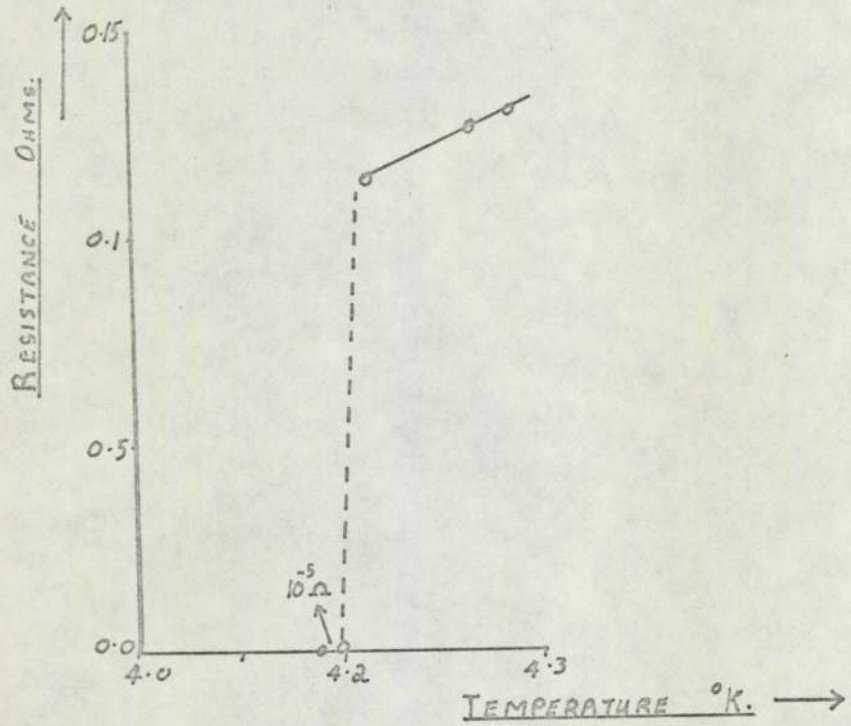

substantially independant of temperature. For related reasons, the temperature at which a superconductor loses its resistance, the superconducting transition temperature T_c, is not always as sharply defined as in Fig. 1.1. The impurities and imperfections cause the transition to broaden (Fig. 1.2). In connection with this it should be noted that Lynton (1969) defines the transition point, T_M as the temperature at which half the original resistance remains. It is however, well established experimental practice to refer to the transition temperature, T_c as the temperature at which the transition commences (See, for example; Matthias, Geballe, Geller and Corenzwit, 1954).

Among the unique aspects of physical behaviour which arise with superconductivity, two properties are particularly important. These are the magnetic behaviour and the thermal capacity. The unusual character of the former was finally established in 1933 by Meissner and Oschenfeld who found that as the temperature of a superconductor is lowered through the transition all magnetic field lines are expelled from the body of the material, i.e. that the flux density within a superconductor is identically zero. This phenomenon is of great importance as one of the principle methods of detecting superconductivity (see section 3.3). The strength of any applied magnetic field is significant, for if the magnetic field is excessively powerful, or if a sufficiently large current is passed through a superconductor the material reverts to its normal state. A superconducting material is therefore often characterised by its critical magnetic field, B_c and critical current density, J_c as well as by its transition temperature.

The heat capacity of a superconductor is equally remarkable. Here, as the material passes through its transition temperature, the heat capacity is observed to increase sharply (Fig 1.3). On the other hand by maintaining the same sample in its normal state by the application of a magnetic field the heat capacity which would exist in the absence of the contribution from the superconducting electrons can be measured. This contribution has been

FIG. 1.2. TRANSITION CURVES OF TIN

AFTER JACKSON, 1955

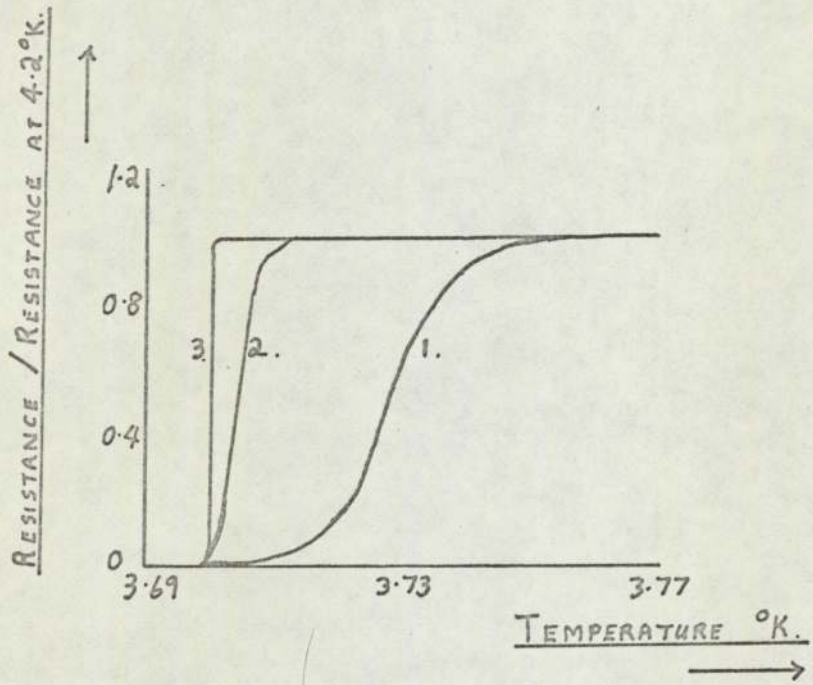

1. POLYCRYSTALLINE
2. WIRE CONTAINING FEW CRYSTALS
3. SINGLE CRYSTAL.

FIG. 1.3 THE HEAT CAPACITY OF TIN IN THE NORMAL AND SUPERCONDUCTING STATES.

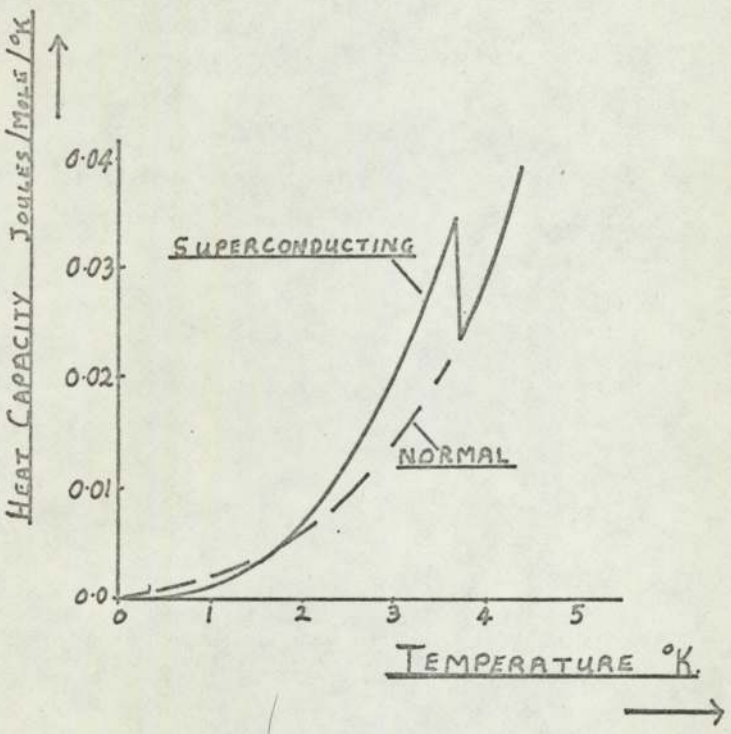

found to vary exponentially with temperature and in analogy with the semi-conductors, some form of energy gap must exist between the normal and superconducting states. (See Lynton (1969) for details).

The results of the investigations of the heat capacity and magnetic behaviour of superconductors stimulated the development of macroscopic phenomenological theories such as those of Gorter and Casimir (1934) on the thermodynamics and F. and H. London (1935a, 1935b) on the magnetic behaviour. All attempts at a microscopic theory however, had proved entirely futile, despite the obvious success of the "free-electron" theory of metals as developed by Sommerfeld and Bloch.

In 1947 Heisenberg introduced the Coulomb interaction between electrons into the free-electron model of conductivity and concluded that at low temperatures it might be possible for a certain fraction of the conduction electrons to 'condense' in momentum space to form a state of higher order. A major problem was however the source of attraction between electrons to overcome their Coulomb repulsion. Significantly, in the light of more recent developments it was apparently believed that the ion cores forming a crystal, because of their large mass, compared with the electrons, could play no part in the establishment of the superconducting state. (See Fröhlich, 1961). The entirely contrary proposal of Fröhlich, (1950) that the phonons might provide the missing attractive mechanism was therefore something of a revolution in the thinking of that time.

1.2 Microscopic Theory

Fröhlich pointed out that as an electron moved through the lattice its electrostatic interaction with the ion cores produces oscillatory distortions which may be pictured as the emission and absorption of phonons by the electrons (Fig 1.4). Such phonons are termed virtual since their short lifetime and the Uncertainty Principle renders the Conservation of Energy unnecessary. This "electron-phonon" interaction lowers the free energy proportionally as the square of the average phonon energy i.e. inversely

FIG. 1.4 REPRESENTATION OF THE ELECTRON PAIRING MECHANISM VIA THE DISTORTION OF THE LATTICE.

AFTER LITTLE, 1965

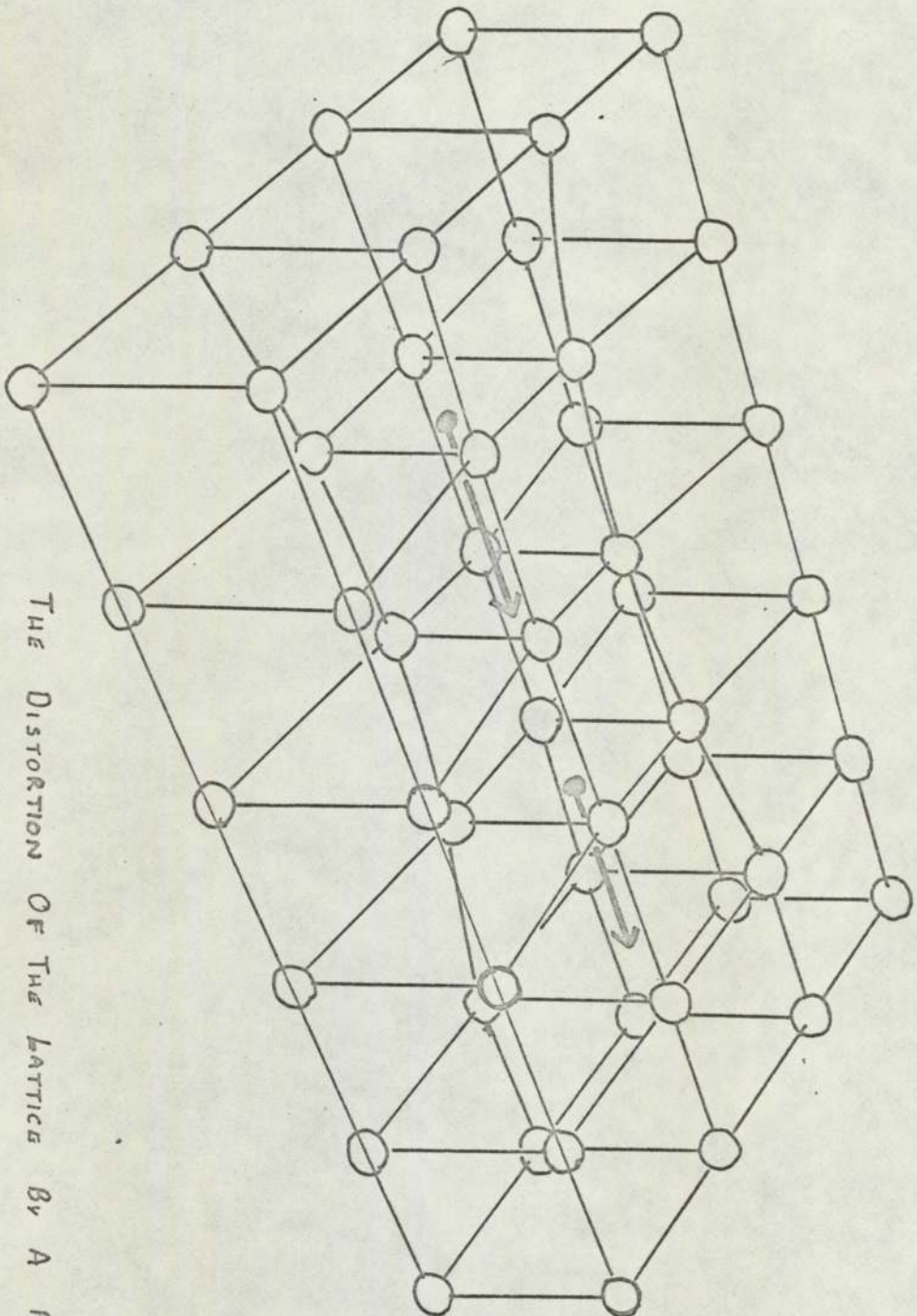

THE DISTORTION OF THE LATTICE BY A PASSING ELECTRON PRODUCING A REGION WHICH IS ATTRACTIVE TO A SECOND ELECTRON.

proportionally as the isotopic mass. The reduction in free energy is also proportional to $\frac{B_c^2}{8\pi}$ and thus the theory leads to the prediction that B_c and T_c should vary inversely as the square root of the isotopic mass. This is the Isotope Effect which was independantly discovered by Maxwell (1950) and by Reynolds, Serin and Nesbitt (1950), during their investigation of the T_c's of isotopically pure samples of mercury. Fröhlich's theory however did not give the correct order of magnitude for the energy difference between the normal and superconducting states.

The next step was made by Cooper (1956) who showed that if there is a net attraction between two electrons, just above the Fermi Energy, then these electrons will form a bound state the binding energy of which is a sensitive function of the vector sum of the individual electron momenta. The resultant lowering of the total energy comes to a sharp maximum when the two electrons of the "Cooper Pair" have equal and opposite momenta and spin. The required net attraction was shown by Bardeen, Cooper and Schrieffer (B.C.S. 1957) to be due to the interchange of virtual phonons. This can best be illustrated with the aid of a Feynmann Diagram (Fig 1.5) Here the emission of a virtual phonon $\underset{\sim}{q}$, by an electron with wave vector $\underset{\sim}{k}$, is followed by the absorption of the phonons by a second electron $\underset{\sim}{k}'$. The first electron is scattered into $\underset{\sim}{k} - \underset{\sim}{q}$ and the second into $\underset{\sim}{k}' + \underset{\sim}{q}$. Since the process is virtual it does not require the Conservation of Energy; and the electron - electron interaction depends upon the relative magnitudes of the electronic energy change involved and the virtual phonons energy. If the latter is greater than the former, the interaction is positive and the electrons are attracted. The fundamental postulate of the B.C.S. Theory therefore is that superconductivity occurs when such attractive mechanisms between Cooper Pairs dominate their Coulomb repulsion.

In order to obtain the correct order of magnitude for the energy reduction on passage into the superconducting state, Bardeen et al assumed that all interactions except the electron - phonon pairing mechanism are the

FIG. 1.5 FEYNMAN DIAGRAM OF ELECTRON-PHONON COUPLING

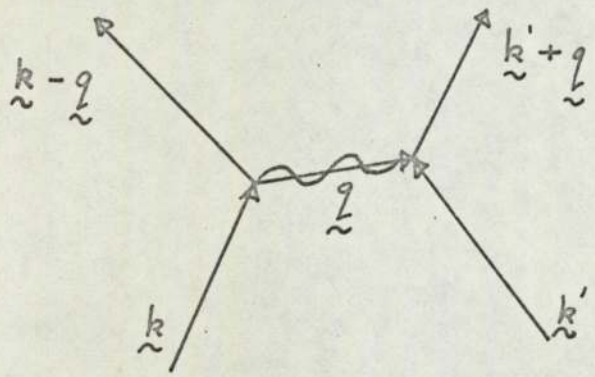

same for the superconducting and normal states, at $0^{o}K$. Thus they calculated the superconducting ground state energy due solely to the Cooper-Pair and Coulomb interactions, as;

$$W(o) = \frac{-2N(o)(\hbar\omega_c)^2}{\exp\left[2/N(o)V - 1\right]} \qquad 1.1$$

Here N(o) is the electronic density of states and ω_c is the phonon cut - off frequency corresponding to θ_D. V is a parameter describing the Cooper - Pair and Coulomb interactions between two electrons. In order to simplify the mathematical problems Bardeen et al made the assumption that V was isotropic, instantaneous and constant for all electrons in a narrow shell of energy less than $\hbar\omega_c$ around the Fermi Energy and was zero elsewhere. This assumption was based upon the experimental fact that the similarities between the superconducting characteristics of widely different metals seemed to imply that the responsible interaction can not crucially depend upon the detailed electronic structure of individual substances.

An important feature of the theory is that the number of electrons involved in pairing was large as a consequence of the large coherence length of the electron wave function involved. This follows since the intervals of importance in momentum space $\frac{\Delta k}{k} \simeq \frac{kT_c}{E_f}$ and therefore $\Delta k \sim 10^{+4}$ cms^{-1}. Using the Uncertainty Principle this yields $\Delta x \sim 10^{-4}$ cms. Now the number of electrons with energies within $k T_c$ of the Fermi Surface is approximately $\frac{kT_c}{E} \simeq 10^{-4}$, and these are the electrons which can interact. Assuming an electron density of 10^{22} electrons per cm^3 the number of electrons capable of interacting with a given electron is $\sim 10^{6}$.

Among the predictions of the Bardeen, Cooper, Schrieffer theory is that the temperature dependant energy gap, Δ, separating the normal and superconducting states, decreases to zero as the temperature rises from $0^{o}K$ to T_c according to the relation;

$$\Delta = (\hbar\omega_c) \exp - \left(\frac{1}{N(o)V}\right) \qquad 1.2$$

Their derviation of an expression for the superconducting transition temperature, viz;

$$kT_c = 1.14 \ (\hbar\omega_c) \exp - \left(\frac{1}{N(o)V}\right) \qquad 1.3$$

enables the energy gap and T_c to be linked directly;

$$\Delta = 3.52 \ kT_c \text{ at } 0^{\circ}K \qquad 1.4$$

Fig 1.6 shows the extremely good agreement obtained between theory and experiment. Here the energy gap is plotted as a function of temperture for indium, tin and lead.

Table 1.1 gives values of the exponent β involved in the Isotope Effect; (which according to the B.C.S. theory should equal 0.5);

$$T_c \propto \frac{1}{M^{\beta}}$$

Here again agreement is found for many elements. However it is noticable that the transition metals are markedly different. Further, measurement of the critical magnetic field variation with temperature (Fig 1.7) shows large differences between the theory and experiment in the cases of lead and mercury. Experiments involving the tunneling of electron pairs through thin film junctions have been able to measure the ratio of the energy gap to T_c. According to the Bardeen, Cooper, Schrieffer theory $\frac{2\Delta}{k\,T_c} = 3.53$. Table 1.2 shows that there is apparently considerable deviation from this value in practice. Values below 3.53 have been successfully explained by experimental error (Claesen and Lundquist, 1974), however the large values found for lead and mercury again indicate some limitation to the theory.

The reason for these discrepancies is believed to lie in the assumptions made in the theory rather than in its basic premises. To ease the mathematical difficulties, Bardeen et al had assumed that the

FIG. 1.6. THE GAP PARAMETER VERSUS TEMPERATURE.

SEE CLARKSON ET AL 1974

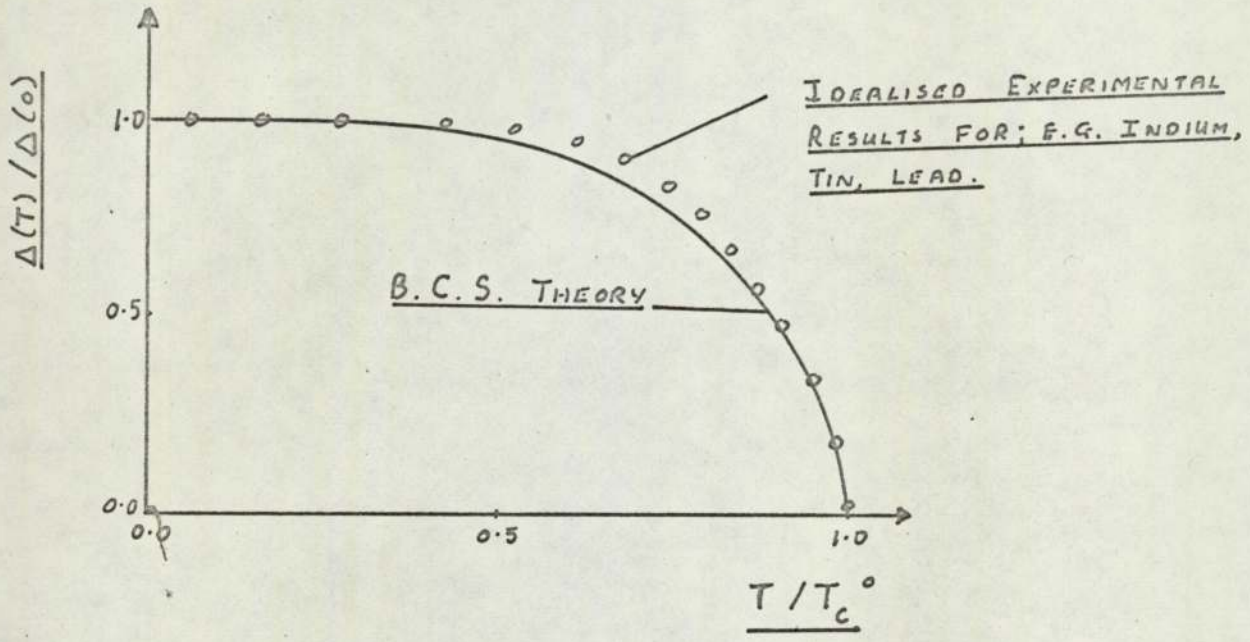

TABLE 1.1 EXPERIMENTAL VALUES FOR THE EXPONENT OF THE ISOTOPE EFFECT.

SUPERCONDUCTOR	β EXPERIMENTAL	β THEORETICAL
Hg	0.50	0.46
Mo	0.37	0.3
Os	0.23	0.25
Pb	0.48	0.47
Re	0.39	0.41
Ru	0.00	0.35
Sn	0.47	0.42
Tl	0.5	0.43
Zr	0.00	0.30

Note: The B.C.S. theory predicts $\beta = 0.5$ for all superconductors. The theoretical values of β given above are from the work of Morel and Anderson. (see, Claeson and Lundquist, 1974)

FIG. 1.7 THE NORMALISED CRITICAL MAGNETIC FIELD VERSUS TEMPERATURE

SEE CLAESON ET AL 1974

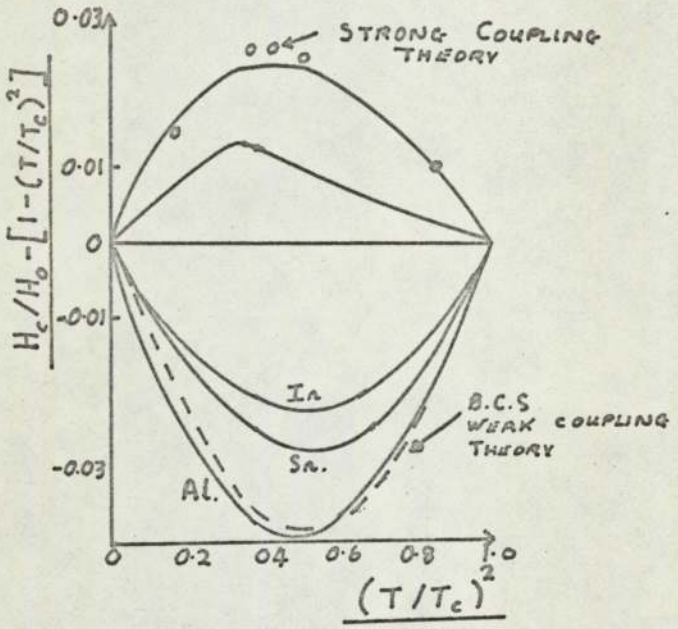

TABLE 1.2 MEASURED VALUES OF

$$\left(\frac{2\Delta(o)}{k_B T_c}\right)$$

SUPERCONDUCTOR	$2\Delta(o)/k_B T_c$ EXPERIMENTAL
Al	3.37
Cd	3.2
Hg	4.6
Nb	3.84
Pb	4.38
Sn	3.46
Ta	3.6
Th	3.47
V	3.4
Zn	3.2

(See, Claeson and Lundquist, 1974)

interaction parameter V was constant, isotropic and instantaneous. It has been suggested that in some superconductors the electron - phonon coupling is so strong that the attraction mediated by the heavy ions is retarded, that is that there is a delay between the emission and absorption of the virtual phonons. Furthermore, V can not be strictly isotropic, nor is it well described as a constant for electron energies below $\hbar\omega_c$, unless, as was assumed by Bardeen et al, the excitation energies, which are of the order of $k T_c$ are very much less than $\hbar\omega_c$. Since the latter equals $k \theta_D$ this criteria, which is termed the "weak - coupling limit" may be expressed as $T_c \ll \theta_D$. This does not hold for a number of superconductors and these are therefore termed "strong - coupled".

By removing the restrictions on V Morel and Anderson (1962) have been able to develop a "Strong - Coupling, B.C.S." theory which describes such superconductors more accurately. They introduced the expression $(\lambda - \mu^*)$ for $N(o)V$ into the Bardeen, Cooper, Schrieffer formulation, λ being the electron - phonon coupling constant and μ^* the Coulomb interaction parameter. The success of this extension to the theory is shown by the improved values for β in the Isotope Effect. (Table 1.1).

1.3 High T_c Superconductivity

1.3.1. Empirical Developments

It has been known from the earliest work on superconducting elements that there are strong correlations between the property of superconductivity and the periodic table. The qualitative behaviour is shown diagramatically in Fig 1.8. Matthias, Geballe and Compton (1963) have discussed these and other correlations in some detail. The empirical rules of superconductivity may be summarised as follows;

(i) Superconductivity is excluded from non - metals and from metals with less than two or more than eight electrons per atom.

(ii) High T_c's correspond to metallic elements with five or seven

FIG. 1.8 QUALITATIVE T_c THROUGHOUT PERIODIC TABLE

AFTER MATTHIAS 1969

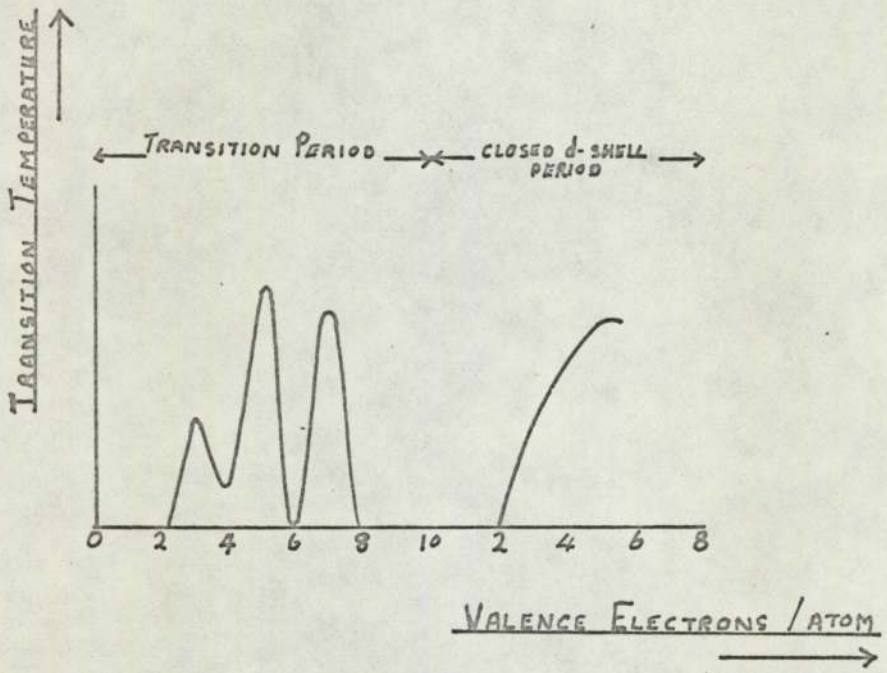

valence electrons per atom.

(iii) There are three crystal structures which are most favourable for superconductivity; a.) face, centred cubic, b). body centred cubic, c) Hexagonal close packed.

(iv) Transition elements tend to have the highest T_c's and their isotope effects are anomalous (Indeed the isotope effect is absent from Ru and Os).

Matthias has also analysed superconductivity in compounds and found that the T_c versus electrons per atom curves are identical to those of the elements, but with slight shifts of the peaks depending upon the crystal symmetry. Further, (Matthias, 1969) he has established a correlation between T_c and T_m, the melting point, which arises, he argues, since it is the electrons outside the closed shell which are involved in both phenomena.

Matthias's empirical rules have been extremely useful as a guide in the search for compounds with high transition temperatures. Table 1.3 lists a number of these and also emphasizes a further remarkable discovery. That is that all the compounds discovered so far with a transition temperature greater than $15^{o}K$. belong to one or other of two crystallographic groups. These are the group of compounds with the β - tungsten or A15 structure, typified by Nb_3Sn and the compounds related to NbN whose crystal structure is of the NaCl type.

Both of these groups of superconductors contain transition elements and share other remarkable properties. For example, Pessall, Gold and Johansen (1968), in their search for relationships amongst the transition metal carbides and oxides with high transition temperatures, have found striking correlations between T_c and valence electron density. (i.e. valence electrons per Å^3 rather than per atom as Matthias had suggested.) Similar correlations have been found among the β - tungsten group by Roberts (1964) (See Fig 1.9).

TABLE 1.3

SOME HIGH T_c SUPERCONDUCTORS

COMPOUND	T_c °K	CRYSTAL STRUCTURE TYPE
V_3Si	17.1	A.15 (β - Tungsten)
V_3Sn	8.3	"
Nb_3Al	18.9	"
Nb_3Ga	20.3	"
Nb_3Sn	18.3	"
Nb_3Au	11.5	"
Nb_3Ge	23.2	"
$Nb\ C_{0.977}$	11.1	Na Cl
$Ta\ C_{0.987}$	9.7	
$Nb\ N_{0.96}$	15.6	
$Nb\ C_{0.3}\ N_{0.7}$	21.8	
$(Nb\ N)_{0.8}\ (Ti\ C)_{0.2}$	18.0	

See; Matthias, Geballe and Compton (1963)

Testardi (1973)

Roberts (1969)

FIG. 1.9. T_c VERSUS ELECTRON DENSITY FOR THE β-W AND NbN HIGH T_c SUPERCONDUCTING GROUPS.

AFTER PESSALL ET AL 1968

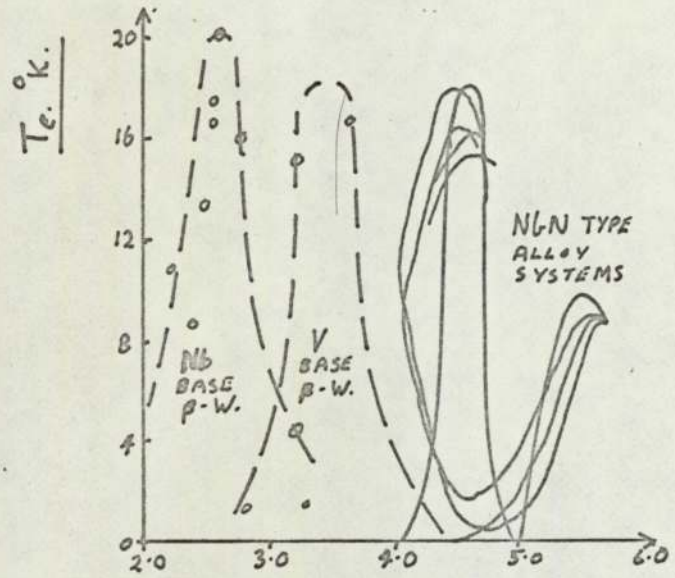

FIG. 1.10 T_c OF INTERSTITIAL COMPOUNDS AS A FUNCTION OF THE 'OD' RATIO R.

AFTER PESSALL ET AL 1968.

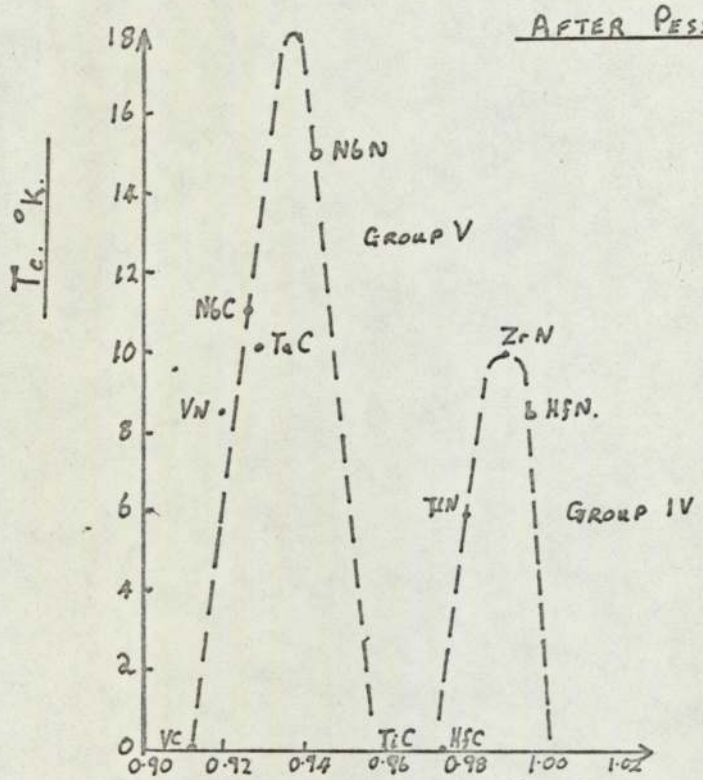

Perhaps the most surprising development however has been the realization that the β - tungsten and rocksalt structures are peculiar, in that they are among those which possess an intrinsic instability connected with an excess volume afforded to one constituent. Thus, Pessall et al (1968) Phillips (1972) and Zeller (1972) all find a significant correlation between T_c and relative volume available to the transition metal atoms in NbN and related compounds (see for example, Fig. 1.10), while Testardi (1972) working on the strain dependence of T_c in the β - tungsten alloys has emphasized the importance of volume per atom. It seems clear from this work that, as Hopfield (1969) remarked, there should be a viewpoint on superconductivity which reflects the dominance of atoms and their local environments in determining superconducting parameters.

1.3.2. Theoretical developments

Following the strong - coupling modifications to the Bardeen, Cooper, Schrieffer theory the importance of the phonon density of states began to be appreciated and it was mainly through the work of McMillan (1968) that these ideas developed theoretical foundations.

In the case of strong - coupling electron - phonon interaction, McMillan has derived a relation for the superconducting transition of the form;

$$T_c = \frac{\theta_D}{1.45} \exp.\left[\frac{-1.04\,(1+\lambda)}{\lambda - \mu^*\,(1+0.62\lambda)}\right] \qquad 1.5$$

Where μ^* = Coulomb coupling constant and the electron - phonon coupling constant, λ is defined through,

$$\lambda = 2\int_0^{\omega_0} \alpha^2(\omega)\, F^2(\omega)\, \frac{d\omega}{\omega} \qquad 1.6$$

Where ω_0 is the maximum phonon frequency, $F(\omega)$ is the phonon density of states, $\alpha^2(\omega)$ is an average electron - phonon interaction which, if constant, leads to;

$$\lambda = \frac{N(o)\langle J^2\rangle}{M\langle \omega^2\rangle} \qquad 1.7$$

Where $$\langle \omega^2\rangle = \langle \omega\rangle / \langle \omega^{-1}\rangle \qquad 1.8$$

N(o) is the electronic density of states at the Fermi level and $\langle J^2\rangle$ is the averaged electron - phonon matrix element (see McMillan, 1968).

A significant contribution from McMillan's work was his discovery that the purely electronic factor $N(o)\langle J^2\rangle$ could be a constant for a given class of materials e.g. $7eV/\text{Å}^2$, for the transition elements. For such a group of materials, $\lambda \propto \frac{1}{M\langle \omega^2\rangle}$ and therefore T_c would be essentially determined by the phonon frequencies and not by the electronic band structure.

These empirical findings were explained by Hopfield by considering the p-d electron overlap and he has extended the results to alloys having a high N(o) and Ef. Weber (1973) has since shown that for accuracy and particularly for the transition metal carbides the d-d electron overlap must also be included.

A remarkable feature of McMillan's theory is that he was able to derive an expression for the maximum transition temperature attainable within a given class of material, viz.

$$T_c/T_c \text{ MAX.} = \left(\frac{2}{\lambda}\right)^{\frac{1}{2}} \exp\left(\frac{1}{2} - \frac{1}{\lambda}\right) \qquad 1.9$$

Now in his assumption of a maximum T_c, (T_c MAX.) for a group of compounds, it is necessary that the average phonon frequency be capable of indefinite reduction. McMillan notes however that this is likely to drive a phonon mode unstable, resulting in lattice transformation before T_c MAX. can be attained.

Coincidentally it was at this time that experimentalists and in particular those associated with Matthias's group, began to realise that the compounds with predicted high T_c according to Matthias's rules would not form. The implication seemed to be that instability was an essential

prerequisite for high T_c superconductivity.

1.4 Lattice Instabilities in High T_c Superconductors.

The realization of the importance of lattice instabilities to superconductivity was initally very disturbing, since these lead to phase transformations. It was expected therefore, as appeared to be experimentally true, that compounds with theoretically predicted high transition temperatures would not form or would transform to a low T_c or even non-superconducting state.

The stability rules, which derive from the expression for the strain energy of a crystal (Born and Huang, 1954) are;

$$(C_{11} + 2C_{12}) \geqslant 0$$
$$(C_{11} - C_{12}) \geqslant 0$$
$$C_{44} \geqslant 0$$

These are connected with the velocities of sound in the crystal structure, i.e. with the initial slopes of the dispersion curves, and it was thought that as one of these modes tended towards zero, the corresponding phonons would enhance T_c tending towards a maximum as phonon velocity tended to zero.

Velocity of sound measurements have been used by Testardi (1967, 1970, 1971, 1972) in studying the β-W superconductors. He found considerable lattice softening upon cooling, for those with a high T_c, but the more normal lattice stiffening for those with low T_c, (Fig 1.11). Initially Testardi implied that the lattice softening affected T_c via its effect upon the electronic band structure, which required the involvement of low frequency phonons. However Shirane and Axe (1971) showed later, that it is the high frequency transverse acoustic (T.A.) modes that soften (see Ramakrishnan, (1973).). In later work Testardi showed that the large strain dependence of T_c that occured, was not a function of the band structure at all, but depended upon the phonon density of states and λ.

FIG. I.11. THE TEMPERATURE DEPENDANCE OF THE VELOCITY OF SOUND IN THE β-W COMPOUNDS.

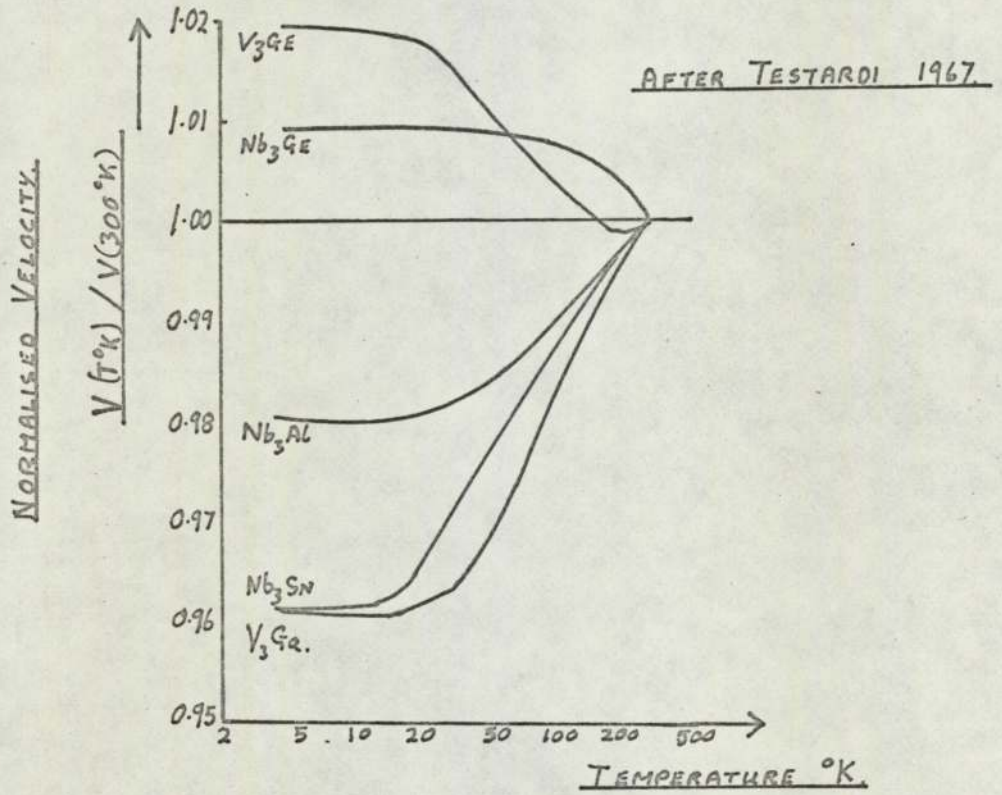

It was the neutron diffraction work which first established the presence of anomalies in the phonon density of states of the high T_c superconductors. Anomalies which are notably absent in low T_c superconductors. For example Nakagawa (1963) found that the T.A. mode goes soft in Nb ($T_c \sim 9^oK$) but Woods (1964) found that it does not in Ta. ($T_c \sim 5^oK$). Smith and Glaser (1970) have found identical results for Ta C ($T_c \sim 10^oK$) and HfC ($T_c \sim 1^oK$) which are shown in Fig 1.12.

Numerous workers have been engaged upon establishing the cause of the phonon anomalies. Phillips (1971) for example, suggested that they arise from overscreening of the ion - ion interaction by the electron - ion interactions, resulting in the ions vibrating more independently of one another. Lattice instability would result at normal ion - ion equilibrium separations, but crystal structure breakdown may be avoided by anharmonic forces, allowing alterations in the bond lengths. Phillips (1971, 1972) found striking correlations between anomalies in the lattice constant trends and high T_c's in the NbN family of superconductors (Fig 1.13). Further he remarks that the overscreening model explains Matthias's correlation between T_c and T_m, since both are functions of lattice instability.

Now a lower T_c would be expected from the reduction of the density of electronic states at the Fermi Energy, following transformation to a lower crystal symmetry (Phillips, (1971)). However, enhancement may occur if it correlates with lattice instability. Further the natural expansion of the lattice in the series NbX (X = C,N,O) raises T_c of this high T_c superconductor more than the contraction does in the low T_c series Zr X (Fig 1.13). Artificial compression of high T_c superconductors should therefore increase T_c by opposing the lattice transformation correcting mechanism, this driving the crystal towards high frequency instabilities. This appears to have been found experimentally (Smith (1970).).

FIG. 1.12 THE PHONON SPECTRA OF TaC. AND HfC.

SEE PHILLIPS 1972.

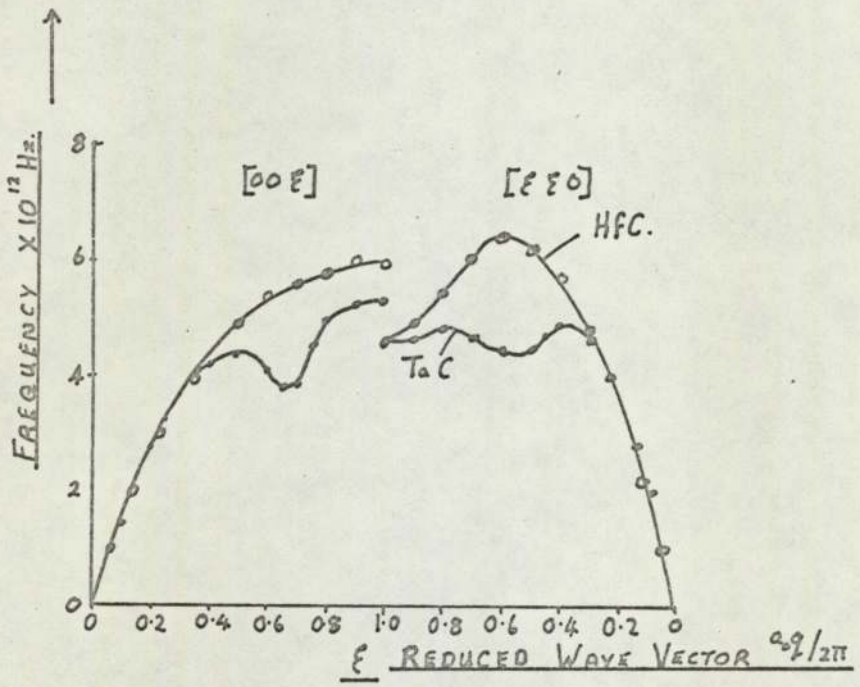

FIG. 1.13. HIGH T_c's AND LATTICE PARAMETERS IN THE NbN GROUP

AFTER PHILLIPS 1971.

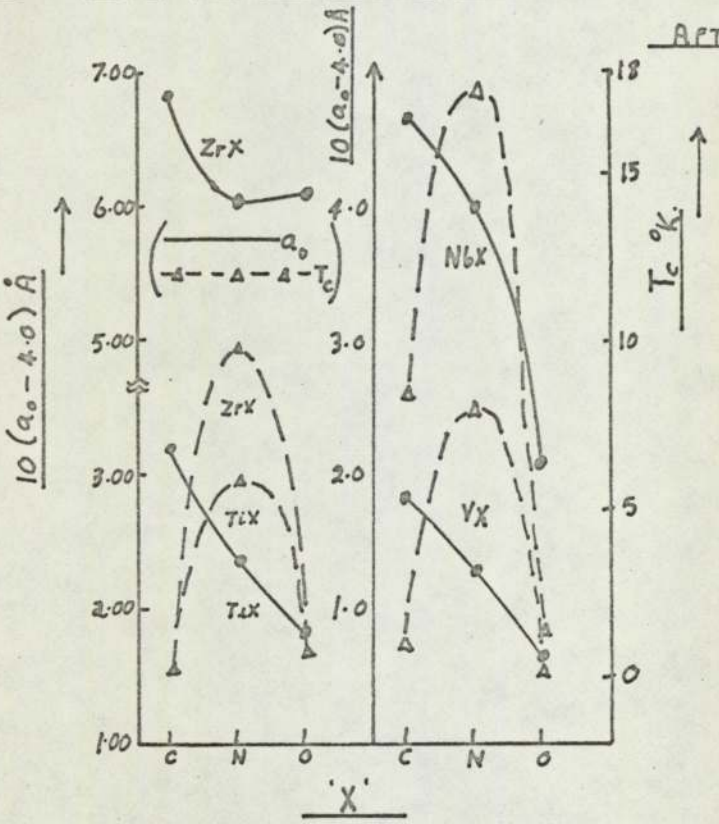

In a later paper Phillips (1972) extended his work on the NbN family of superconductors by analysing other chemical trends (e.g. heats of formation). He concluded that there is a lattice instability present in the high T_c members of the group which is largest for the highest T_c. Further he shows that appropriate generalization of McMillan's theories leads to the conclusion that the McMillan limit successfully predicts T_cMAX.

Other work on the reasons for high transition temperatures has been based upon the electronic properties. In particular, the model of Labbé and Friedel (1966, 1967.) correlates an extremely narrow d - band in the electronic density of states near the Fermi Energy, with the high T_c members of the β - tungsten group. (e.g. Nb_3 Sn.). This model has also been used to explain the occurance of very soft T.A. modes in these compounds as they tend to low temperature lattice transformations (Labbé et al 1967.). An important assumption is that the electron - phonon coupling does not change as the mode softens and changes in N(o) are solely responsible for both phenomena. However, as Ramakrishnan (1973) has pointed out the softening of the lattice at a phase change produces just those phonons (high frequency, T.A.) necessary for increased electron - phonon coupling and therefore enhanced T_c. Clearly lattice instability and high T_c can not be separated and the degree of dependance of T_c on N(o) is not absolute.

Ramakrishnan showed that the electron coupling by the T.A. mode in the β - tungsten high T_c compounds was considerably enhanced as this mode softened i.e. as the lattice tended towards instability. Further, he shows that a surprisingly large fraction ($\sim$20%) of the phonons contributing to the electron pairing phenomena are, in fact, from the T.A. mode and when this mode is as soft as possible (i.e. at transformation) there is little change in T_c. Thus in the Nb_3 Ge_{1-x} Sn_x system T_c saturates at the Nb_3 Sn end and this is close to the revised McMillan limit for the β - W group. (Hertz (1971), Cohen and Anderson (1972), Shen (1972)). Similarly for V_3 Si in the

$V_3 Ge_{1-x} Si_x$ system.

In contrast to Phillip's remarks about NbN, Ramakrishnan suggests an increase in lattice constant for $Nb_3 Sn$ should raise its T_c. This seeming contradiction arises because $Nb_3 Sn$ is not just near a lattice instability, it actually transforms. It is necessary to defer this transformation to a lower temperature in order to soften the lattice further and increase T_c. Thus NbN and $Nb_3 Sn$ must be considered from either side of a structural transition. In NbN the transformation is close and to move closer pressure must be applied to drive the crystal towards lattice instability. In $Nb_3 Sn$ the transition occurs and it is necessary to withdraw pressure to stabalise further instability. It is noted that both authors feel that the T_c's of NbN and $Nb_3 Sn$ represent the T_cMAX. of their respective families; only minor improvements are to be expected from increases in instability.

There have been other approaches towards defining the role of the lattice in the high T_c superconductors. Zeller (1972), for example has investigated tantalum carbide, TaC_x, using tunneling experiments. There is a lattice instability at stoichiometry and the composition dependence of T_c is solely a result of the composition dependence of the phonon spectrum's acoustic modes, (the optic modes contributing very little).

Gommersall and Gyorffy (1973), have investigated the nitrogen atom contribution to the electron - phonon coupling constant, λ in NbN. Using arguments based upon the "overscreening" model of Phillips, they conclude that the nitrogen would give rise to a large λ because of its low mass and associated large oscillations.

It seems clear, that one must conclude, that the phonons associated with high T_c superconductivity are high frequency acoustic phonons near the Brillouin Zone boundry. These contribute to a form of hydrostatic lattice instability which, in simple terms, is the cause of the McMillan limit on T_c for a given group of compounds. In order to increase T_cMAX by increasing the

electron - phonon coupling, an increase in the number of degrees of freedom seems essential. This is the origin of the new emphasis on materials based on a ternary system. (Matthias, 1968).

1.5 Superconductivity among compounds with the Spinel structure

1.5.1. Crystal Structure

The spinels are ternary compounds which tend to have a molecular formula of the form $A\,B_2\,X_4$ in which A and B are metal ions and X is an ion such as O^{2-}, S^{2-} or Se^{2-}. The crystal structures are related to that of the mineral Spinel, $Mg\,Al_2\,O_4$ and the cubic unit cell contains 8 molecular units.

In the simplest form of the crystal structure, called "normal spinel", the 32 anions of the unit cell are in approximately face - centred cubic arrangement specified in detail by a single parameter, u. Metal ions A then occupy 8 of the 64 possible tetrahedral interstices, while the B cations occupy 16 of the possible octahedral interstices (see Table 1.4). Different cation distributions among the available interstitial sites are also known however and the reader is refered to the review by Gorter (1954) for a more detailed discussion.

An important feature of this structure for the present work, discussed in more detail in section 1.5.2, concerns the symmetry of the octahedral or B-site. When u has the value 0.375 the anion packing is perfect and the octahedral interstitial hole has cubic symmetry. Deviations from the perfect packing are extremely common however and produce a distortion at the B-site with symmetry $\bar{3}m$ and a change of the nearest neighbour distance (Fig 1.14) according to;

$$p = a\,(3\delta^2 - \frac{\delta}{2} + \frac{1}{16})^{\frac{1}{2}} \qquad 1.10$$

Where a= cubic unit cell parameter and $\delta = u - 0.375$, The corresponding

TABLE 1.4 ATOMIC POSITIONS IN THE SPINEL STRUCTURE ACCORDING TO Fd $\bar{3}$m SYMMETRY

8 METAL IONS IN,

$0, 0, 0; \frac{1}{4}, \frac{1}{4}, \frac{1}{4};$

POINT SYMMETRY $\bar{4}$ 3m

16 METAL IONS IN,

$\frac{5}{8}, \frac{5}{8}, \frac{5}{8}; \frac{5}{8}, \frac{7}{8}, \frac{7}{8}; \frac{7}{8}, \frac{5}{8}, \frac{7}{8}; \frac{7}{8}, \frac{7}{8}, \frac{5}{8};$

POINT SYMMETRY $\bar{3}$ m

32 ANIONS IN,

$u, u, u; u, \bar{u}, \bar{u}; \frac{1}{4} - u, \frac{1}{4} - u, \frac{1}{4} - u; \frac{1}{4} - u, \frac{1}{4} + u, \frac{1}{4} + u;$

$\bar{u}, u, \bar{u}; \bar{u}, \bar{u}, u; \frac{1}{4} + u, \frac{1}{4} - u, \frac{1}{4} + u; \frac{1}{4} + u, \frac{1}{4} + u, \frac{1}{4} - u;$

POINT SYMMETRY 3m

WITH THE FACE CENTRED CUBIC TRANSLATIONS

$(0, 0, 0; 0, \frac{1}{2}, \frac{1}{2}; \frac{1}{2}, 0, \frac{1}{2}; \frac{1}{2}, \frac{1}{2}, 0).$

FIG. 1.14. THE UNIT CELL OF SPINEL : AB_2X_4

AFTER GORTER 1954.

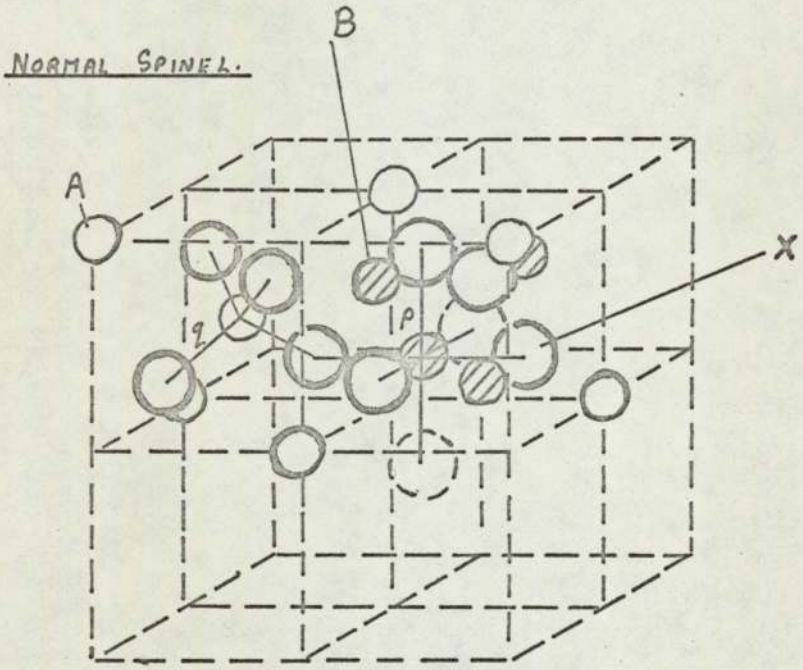

nearest neighbour separation for the A - site is;

$$q = a\,(\delta + \tfrac{1}{8})\sqrt{3} \qquad 1.11$$

1.5.2. Structural distortions

The above description of the crystal structure is a simplification, for there exist a group of spinel compounds whose members undergo transformation to a structure of tetragonal symmetry. The reason for this behaviour became more clear when Dunitz and Orgel (1957) drew attention to the presence of certain transition ions like Cu^{2+} and Mn^{3+} in the compounds concerned. These ions because of their particular electronic configurations, tend to produce instabilities when placed in a symmetrical environment, a phenomenon known as the Jahn - Teller effect. In the spinels they produce local distortions of the crystal structure which, at sufficiently low temperatures, can co-operate to give rise to an overall structural transformation.

The presence of such local distortions in the cubic phase of spinels containing Jahn - Teller ions was first revealed indirectly by the X-ray studies of Cervinka (1965) who found that the Debye- Waller factors of such compounds were generally somewhat higher than might be expected. Further supporting evidence has been found by Tanaka, Tokoro and Aiyama (1966) as a result of the Mössbauer investigation of the compounds $Fe\,V_2\,O_4$ and $Fe\,Cr_2\,O_4$. Also Brabers (1969) has observed changes in the infra - red absorption spectra in the spinel series $Mn_x\,Fe_{3-x}\,O_4$ which may be unambiguously attributed to the development of local structural distortions.

Now a cubic spinel such as $Mg\,Cr_x\,Al_{2-x}\,O_4$ in which Cr^{3+} occupies the octahedral site is expected to remain free from structural distortions since Cr^{3+} is not a Jahn - Teller ion. Indeed Lotgering (1962) has measured the magnetic susceptability of $Mg\,Cr_2\,O_4$ showing the Cr^{3+} ions to be without degeneracy. It was rather surprising therefore that Grimes and Hilleard (1970) should obtain substantial increases in Debye-Waller factor with

increasing Cr^{3+} concentration in $Mg\ Cr_x\ Al_{2-x}\ O_4$, implying the presence of appreciable distortion, in exact analogy with the observations of Cervinka on the Jahn - Teller series $Mn_x\ Fe_{3-x}\ O_4$.

Stahl - Brada and Low (1959) had found that an exceptionally strong trigonal field existed in $Mg\ Cr_x\ Al_{2-x}\ O_4$ from electron spin resonance studies and Lou and Ballentyne (1968) reached similar conclusions from their optical spectra studies. Further they found that the distortions increased with increasing Cr^{3+} content and that the Cr^{3+} ions occupied C_{3v} symmetry. This last observation rules out Fd3m space group in describing spinels with this distortion. $F\bar{4}3m$ symmetry however allows Cr^{3+} to have C_{3v} symmetry and Grimes and Collett (1971) used this to explain the complexity of the infra-red absorption spectra of $Mg\ (Cr_x\ Al_{2-x})\ O_4$. The displacements of the octahedral ions corresponding to the change of symmetry from Fd3m to $F\bar{4}3m$ are shown in Fig 1.15.

Electron diffraction experiments (Hwang, Heuer and Mitchell; 1973) have indicated that reflections of the type h,k,o with (h+k) = 4n+2, (i.e. 2,0,0; 4,2,0; etc.) are present in $Mg\ Al_2\ O_4$, $Mg\ Fe_2\ O_4$ and $Mn\ Fe_2\ O_4$. Such reflections are forbidden in Fd3m symmetry but would be expected for $F\bar{4}3m$.

The displacement of the octahedral ions proposed by Grimes (1971, 1972) is small, (less than 0.1 Å for Cr^{3+} in $Mg\ Cr_2\ O_4$) and this type of distortion is very reminiscent of the behaviour of small impurity ions in the alkali - halides (Diennes, 1968). For example Li^+ ions replacing K^+ in KCl suffer the same [1,1,1] directional distortion as does Cr^{3+} in $Mg\ Cr_2\ O_4$. The explanation is that the conventional lattice site is not a potential minimum. Large ions are held in position by the repulsive interactions with neigbouring ions. Smaller ions however may move off - centre. Evidence for the "off - centre" ions model for the spinels has been obtained by Grimes (1972) through an analysis of the extensive data on Debye - Waller factors of oxide, sulphide and selenide spinels. Indeed he has been able to point out those spinels most likely to contain the anomaly. The exceptions to this off -

FIG. 1.15. OCTAHEDRAL CATION DISPLACEMENT CORRESPONDING TO THE CHANGE $Fd3m$ TO $F\bar{4}3m$.

AFTER GRIMES 1973

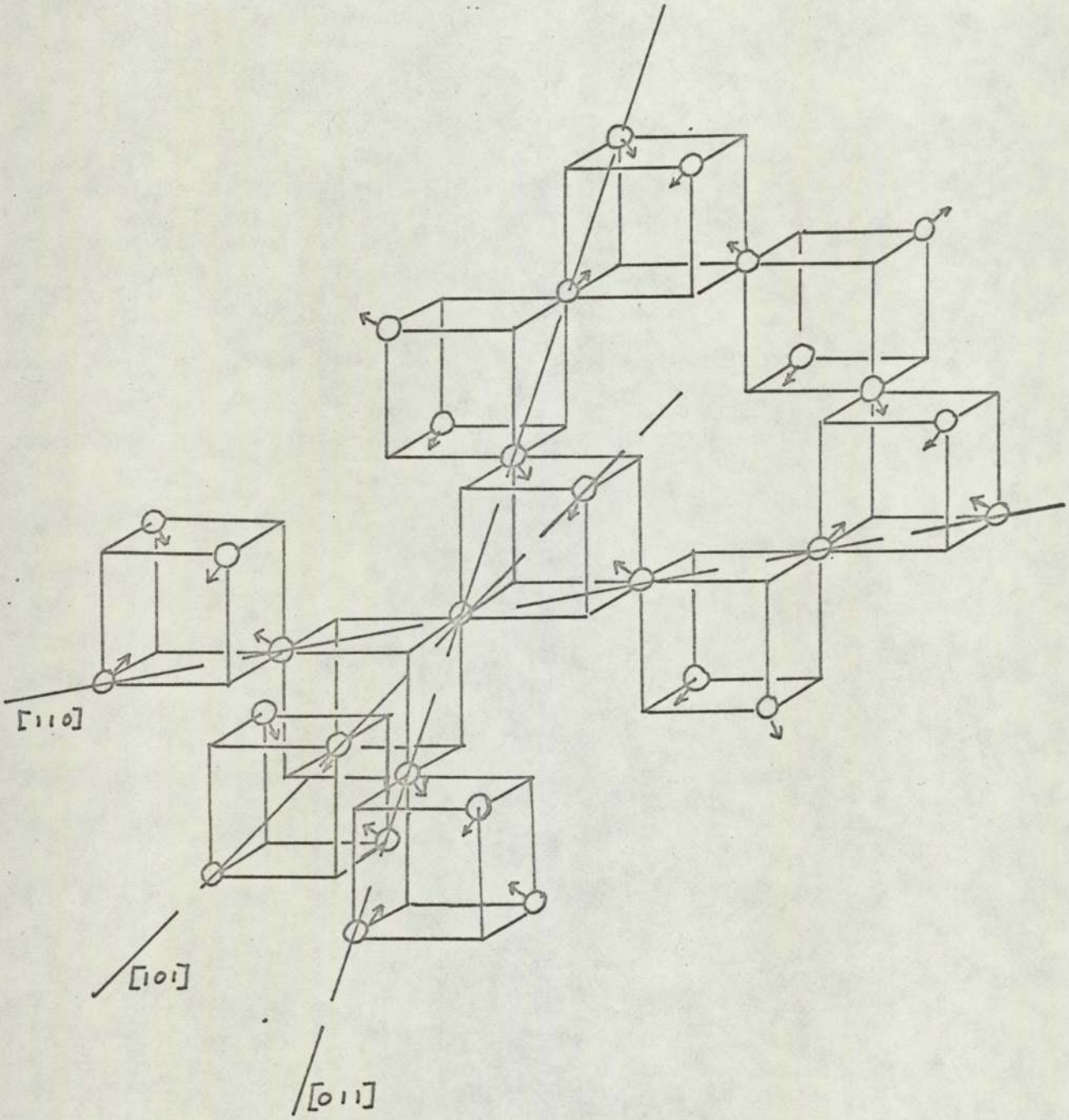

centre ion behaviour exist almost exclusively among the sulphide and selenide spinels and almost invariably the materials are metallic.

Cubic to tetragonal transitions occur in the high T_c superconducting families Nb_3 Sn and NbN and it is instructive to compare the results of experiments on these compounds with similar ones on spinels.

Pytte (1970), for example has investigated the structural transformation in Nb_3 Sn and V_3 Si and successfully explained them using a band analogue model of the Jahn - Teller effect. In this case it is the band structure that becomes degenerate rather than localised orbitals. Further Pytte, (1971) has shown that anomalous elastic constants would be expected from the interaction of the electronic system of the Jahn - Teller active spinels and the acoustic phonons. Kino, Lüthi and Mullen, (1972) investigating the Jahn - Teller system $Ni_x\ Zn_{1-x}\ Cr_2\ O_4$ determined the degree of $C_{11} - C_{12}$ softening, (this is the shear mode restoring force corresponding to tetragonal distortion) as it tends to a small non - zero value at the transition. Vieland, Cohen and Rowald (1971) using velocity of sound techniques have shown that this same mode relaxes to a non - zero value near the transition of Nb_3 Sn. The analogy is further strengthened when it is recalled that the NbN family belongs to the alkali halide crystallographic group, which provided the off - centre ion model for the spinels.

Of course, in the case of the metallic spinels off - centre ions can not exist and $Fd\bar{3}m$ symmetry would be expected. This has been found to be the case with $Cu\ Co_2\ S_4$ for example, (Williamson and Grimes (1974)). However a metallic spinel with a relatively small octahedral ion (or large octahedral volume) and the values of a_o and u that would produce distortions in an insulating spinel, could leave the octahedral ion anharmonically bound. It is perhaps significant that low temperature anharmonicity has recently been found in Nb_3 Sn. (Shier and Taylor 1967, 1968).

1.5.3. The Superconducting Spinels

Superconductivity in spinel compounds was discovered in 1967 by Van Maaren, Schaeffer and Lotgering and independantly by Robbins, Willens and Miller. Their results are given in Table 1.5 along with data from other authors. Before the discovery of the superconducting property, $Cu\ Rh_2\ Se_4$ $Cu\ Rh_2\ S_4$ and $Cu\ V_2\ S_4$ had been partially investigated in respect of their electrical and magnetic properties, but these results were usually incidental to the main research topic. For example Robbins, (1967) had examined the electrical properties of $Cu\ Rh_2\ Se_4$ during an investigation of $Cu\ Cr_2\ Se_4$. He found it to be a p - type metal with a carrier concentration of about $5 \times 10^{21}\ cm^{-3}$. Lotgering (1968), in work mainly concerned with a general study of copper containing sulphide and selenide spinels found $Cu\ Rh_2\ Se_4$ and $Cu\ Rh_2\ S_4$ to be paramagnetic, in comparison to $Cu\ Cr_2\ Se_4$ and $Cu\ Cr_2\ S_4$ which are strongly ferromagnetic. Robbins (1970) had also investigated $Cu\ V_2\ S_4$ but only as an end member of the series $Cu\ Cr_{2-x}\ V_x\ S_4$. Using crystallographic and magnetic experiments he looked at the delocalisation of the Vanadium d - electrons. The results are shown in Fig 1.16. He proposed that the d - electrons of Cr^{3+} are localised but those of V^{3+} are able to delocalise when x reaches 0.5. This explains why, despite the V^{3+} ion having a larger radius, the lattice parameter of $Cu\ Cr_2\ S_4$ is smaller than that of $Cu\ V_2\ S_4$. Note that this reduction in the effective ionic radius of V^{3+} is consistant with the model suggested for metallic spinels in which excess volume may be available at the octahedral sites.

With particular reference to superconductivity some of the above results may not be reliable. For example $Cu\ Rh_2\ Se_4$ has been found to be an n - type superconductor (Van Maaren and Harland, 1969) and not p - type as Robbins found for his sample. Indeed it may be significant that he has now indicated that his original sample was not superconducting. Moreover

TABLE 1.5 RESULTS FROM OTHER WORKERS

SPINEL	LATTICE PARAMETER a_o (Å)	T_c °K	ΔT °K	REFERENCE
$CuRh_2Se_4$	10.264 ± 0.001	3.5	0.1	ROBBINS ET AL (1967)
	10.34	3.49	0.2	VAN MAAREN ET AL (1967)
	-	3.48	-	SCHAEFFER ET AL (1968)
	10.259	-	-	ROBBINS ET AL (1967)
$CuRh_2S_4$	9.790 ± 0.01	4.35	0.3	ROBBINS ET AL (1967)
	9.78	4.8	0.5	VAN MAAREN ET AL (1967)
	9.72	-	-	BLASSE (1964)
	9.790 ± 0.001	4.37	-	SCHAEFFER (1968)
CuV_2S_4	9.82	4.45	1.3	VAN MAAREN ET AL (1967)
	9.824	-	-	HAHN ET AL (1956)
	9.805	-	-	ROBBINS ET AL (1970)

FIG. 1.16 LATTICE PARAMETER VERSUS COMPOSITION (x) FOR $CuV_xCr_{2-x}S_4$

AFTER ROBBINS ET AL. 1970

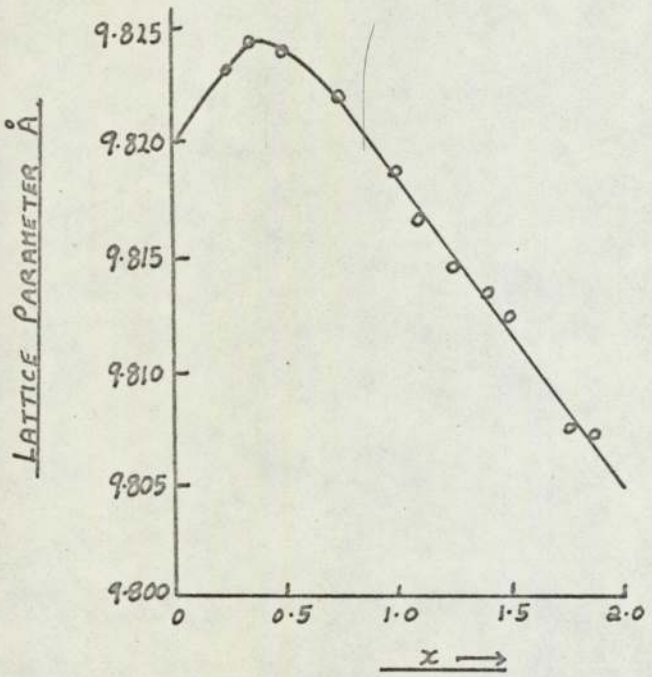

impurity levels were often detectable in many of the samples investigated but no detailed analysis was performed. Van Maaren et al (1967), for example found their superconducting Cu V_2 S_4 to be impure by upto 10% Cu_3 V S_4 and yet Robbins et al (1970) do not mention its presence in their samples.

Schaeffer and Van Maaren (1968) have made a detailed study of Cu Rh_2 S_4 and Cu Rh_2 Se_4, measuring various superconducting parameters. (Table 1.6). It was noted in particular, that these materials possess an exceptionally high density of states due to holes, at the Fermi Level, but it was apparently not possible to relate this to any current model of the band structure. In an attempt to fix the applicable model, an investigation of the series Cu Rh_{2-x} Sn_x Se_4 was made, (Van Maaren and Harland, 1969). Despite a positive thermoelectric effect, (implying holes as the majority carriers), he found a negative Hall Coefficient for $x \lesssim 0.15$, (see Fig. 1.17). The superconducting transition temperature, T_c decreased with increasing x until superconductivity disappeared at $\simeq 0.5$. The authors state that superconductivity correlates with the appearance of electrons in the band structure, despite the very much larger hole density of states.

In a second paper Van Maaren, Harland and Havinga, (1970) present the results of heat capacity measurements on Cu Rh_{2-x} Sn_x Se_4 (Fig. 1.18). For the case of a parabolic band shape the electronic heat capacity coefficient, γ is proportional to $n^{-\frac{1}{3}}$, where n is the number of current carriers per mole. However for strong - coupled superconductors, γ is increased by a factor $(1+\lambda)$, due to phonon enhancement. Since T_c and Θ_D were known from previous work, Van Maaren et al were able to calculate λ from the McMillan equation 1.5. Using an optimum value of μ^* the linear result shown was obtained, this being interpreted as meaning that the change in slope at $0.5 \lesssim x \lesssim 0.6$ is entirely due to strong electron - phonon coupling with the onset of superconductivity in this system.

The majority of the foregoing work was designed to establish a greater

TABLE 1.6 DETAILS OF THE RESULTS OF SCHAEFFER AND VAN MAAREN (1968)

	$Cu\,Rh_2\,S_4$	$Cu\,Rh_2\,Se_4$
T_c (^oK)	4.37	3.48
γ mJ mol^{-1} K^{-2}	30	27
α mJ mol^{-1} K^{-4}	1.13	1.32
$N(E_f)$ eV. mol^{-1}	12.6	11.3
θ_d (HEAT CAPACITY MEASUREMENT)	230	218
$C_{es}(T_c)/\gamma T_c$	2.50	2.44
(B.C.S. VALUE 2.43)		

NOTE: $C_{e.s}(T_c)$ = Heat capacity of superconducting electrons at T_c ^oK.

γ = Electronic heat capacity coefficient

α = Lattice heat capacity coefficient

FIG. 1.17 THE HALL COEFFICIENT AND T_c AS A FUNCTION OF COMPOSITION (x) FOR $CuRh_{2-x}Sn_xSe_4$

AFTER VAN MAAREN ET AL 1969

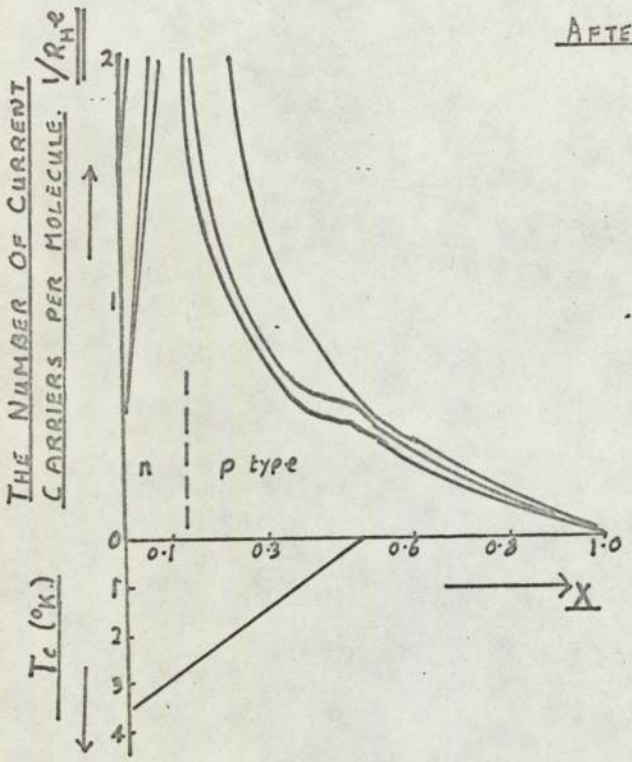

FIG. 1.18. THE ELECTRONIC HEAT CAPACITY COEFFICIENT OF $CuRh_{2-x}Sn_xSe_4$ WITH AND WITHOUT A PHONON ENHANCEMENT FACTOR.

AFTER VAN MAAREN ET AL 1970.

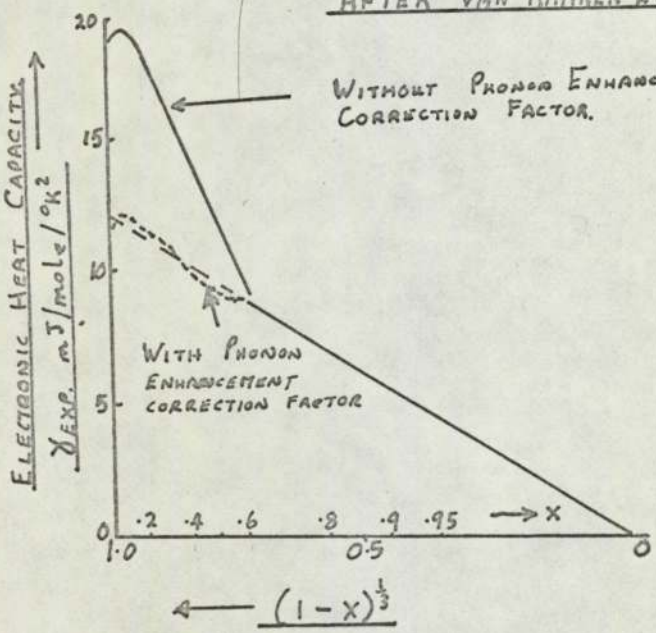

understanding of the spinel band structure. The phenomenological models that have been produced are due to two different approaches proposed by Lotgering, (see, for example Lotgering and Van Staple, 1967) and by Goodenough, (see, for example Goodenough, 1969). Both theories are rather complex and are based mainly upon magnetic measurements. Here only those models which apply to the superconducting spinels will be discussed.

Lotgering argues that tetrahedrally sited copper is monovalent, whilst Goodenough states that this is inconsistant with the periodic table and with experimental results on similar compounds. For his model he requires the copper ions to be divalent. However both theories arrive at a series of overlapping bands giving rise to the high hole density of states found experimentally. In Goodenough's model these bands arise from the overlap of the d - electron wave functions of the octahedral and tetrahedral ions; the Fermi level being near the top of the latter (Fig 1.19). Such a model is consistent with the experimental results of Robbins. Lotgering's band model (Fig 1.20) has been modified by Van Maaren and Harland (1969) (Fig. 1.21) to explain their results on the Hall and Thermoelectric effects in $Cu\ Rh_{2-x}\ Sn_x\ Se_4$, discussed earlier. Changes of the sign of the carriers in one of two conducting bands, accompanied by changes of mobility, are proposed. Schaeffer and Van Maaren, (1968) concluded that superconductivity arises from the presence of holes and electrons at the Fermi Level.

Whichever band model is correct, the similarities with those of the high T_c superconductors is striking. For example Clogsten and Jaccarino (1961) suggested that there is a very narrow d - band in the density of states of $Nb_3\ Sn$. Bachner, Goodenough and Gatos, (1967) have proposed the band structure of Fig 1.22 to explain the properties of $Nb_3\ Sn$ and it is notably similar to that of the superconducting spinels. Here the Fermi Level lies very near the top of a very narrow d - band and the high density of states is due to holes rather than electrons. Following the model of

FIG. 1.19. GOODENOUGH'S (1969) BAND MODEL FOR SUPERCONDUCTING CuV_2S_4

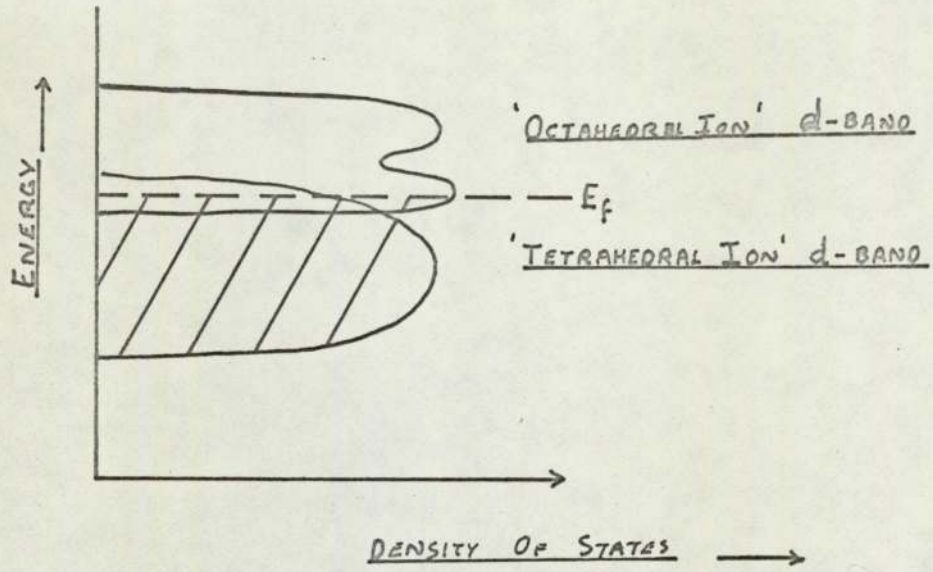

FIG. 1.20 LOTGERING AND VAN STAPELE'S BAND MODEL FOR THE SUPERCONDUCTING SPINELS 1968.

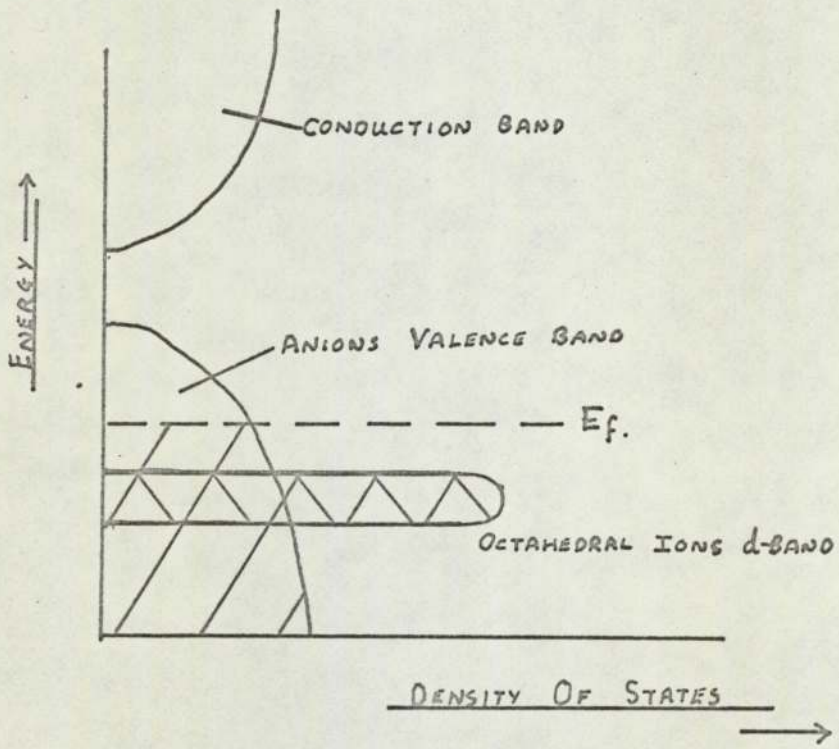

FIG. 1.21. SCHAEFFER AND VAN MAAREN'S (1968) BAND MODEL FOR THE SUPERCONDUCTING SPINELS.

(MODIFICATION OF THE BAND MODEL OF LOTGERING ET AL SEE FIG. 1.20.)

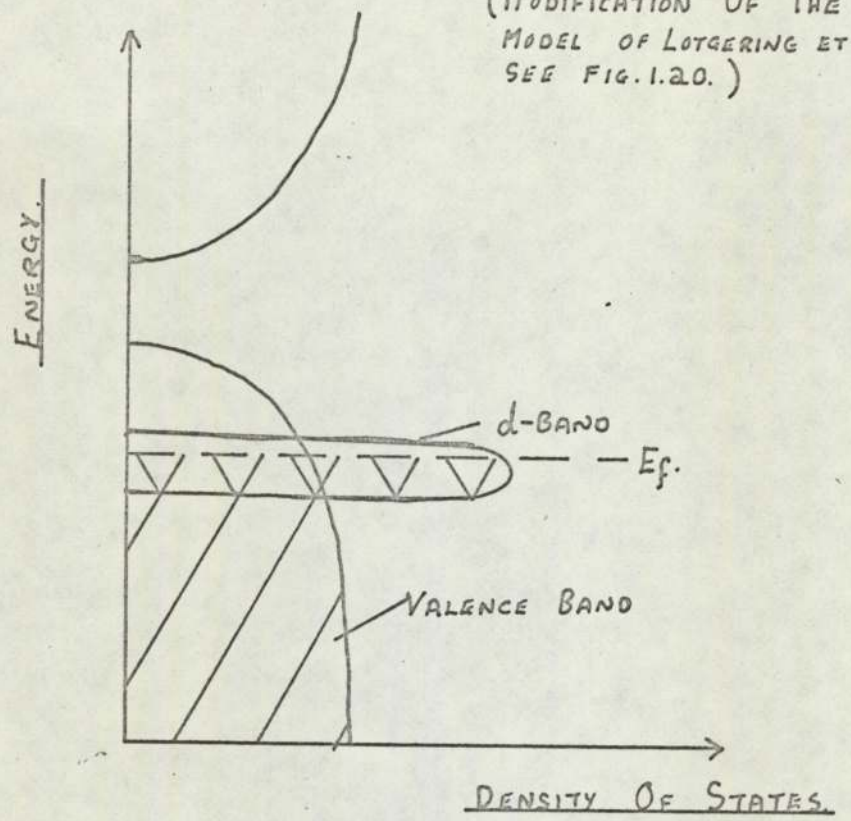

FIG. 1.22. THE BAND MODEL OF Nb_3Sn

AFTER BACHNER, GOODENOUGH AND CATOS (1967).

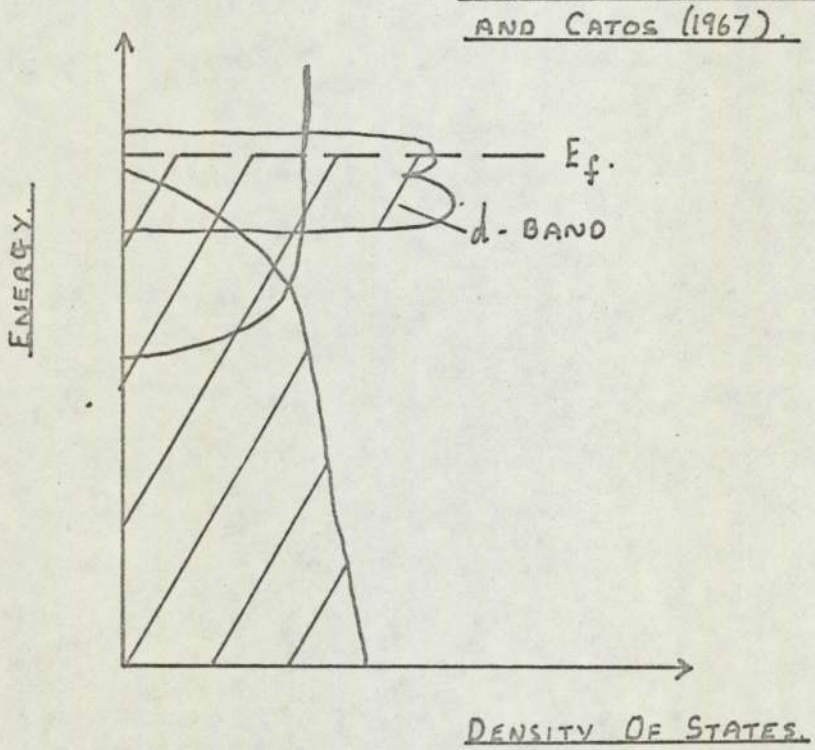

Labbé and Friedel (1967) to explain superconductivity in $Nb_3 Sn$, Cohen, Cody and Hall (1967) proposed a band model for the β - tungsten, high T_c group of compounds in which the density of states changes suddenly near the Fermi Level in a similar manner to that proposed for $Cu\ Rh_{2-x}\ Sn_x\ Se_4$.

1.6. Scope of the present work

The discovery of the remarkable structural instability, which arises in the octahedral sites in spinels, even in the absence of the Jahn - Teller effects and the subsequent discovery that structural distortions appear to be absent in metallic compounds and correlated with the occurence of superconductivity, has illuminated a number of striking similarities to those superconducting compounds known to have high transition temperatures. The possibility that the ternary superconducting spinels might show many of the technologically valuable properties of the β - tungsten and NbN compounds seemed worthy of further investigation and a suitable problem for a Ph. D. thesis.

In the work to be described, attention has been mainly concentrated upon the nature of the local bonding between the metal ion core and anion matrix at the octahedral site. In particular it seemed important to establish whether the harmonic approximation to the potential well was really reasonable or whether some degree of anharmonicity could be detected.

The spinel series $Cu\ Rh_{2-x}\ Sn_x\ Se_4$ and $Cu\ Rh_{2-x}\ Sn_x\ S_4$ were the subjects of the major part of the investigation, after preliminary X-ray work of the compounds $Cu\ Rh_2\ Se_4$, $Cu\ Rh_2\ S_4$ and $Cu\ V_2\ S_4$. Attempts were made to find entirely new superconducting spinels. The primary techniques employed, were X-ray diffraction to measure the important crystallographic parameters and assess the purity and stoichiometry of the prepared samples and Mössbauer spectroscopy to study the octahedral environment directly. The major results from these investigations are presented in Chapters 4 and 5 with a concluding discussion in Chapter 6.

CHAPTER 2: THE MÖSSBAUER EFFECT AND ITS SIGNIFICANCE FOR INVESTIGATIONS OF LATTICE VIBRATIONAL SPECTRA

"Although other techniques ..., may yield detailed information on the phonon frequency distribution, the Mössbauer Effect can give accurate measurements of certain integral moments of the frequency distribution, which are sensitive tests of harmonicity."

Johnson and Dash (1968)

2.1 The Mössbauer Effect, - Physical Principles

The emission of a gamma ray by a nucleus is a quantised phenomena, with an energy width at half peak height corresponding to the lifetime of the excited state, (Fig 2-1).

An isolated decaying nucleus, of mass M, will suffer recoil upon emitting a gamma-ray and providing its velocity, V, is much smaller than the velocity of light, c, classical mechanics may be used to calculate the energy and momentum changes.

If $(V+v)$ is the velocity of the nucleus after emission, then by the conservation of energy (Fig 2-2);

$$E + \frac{1}{2} M V^2 = E_\gamma + \frac{1}{2} M (V+v)^2$$

Where E is the energy of the nuclear transition and E_γ is the energy of the gamma ray.

$$\delta E = E - E_\gamma = \frac{1}{2} M v^2 + M v V \qquad 2\text{-}1$$

By the conservation of momentum;

$$M V = M (V+v) + (E_\gamma / c)$$

Hence,

$$v = - (E_\gamma / Mc) \qquad 2\text{-}2$$

The recoil energy of the nucleus,

$$E_r = \frac{1}{2} M v^2$$

may therefore be written as:

FIG. 2.1. GAMMA-RAY EMISSION FROM AN EXCITTED TIN NUCLEUS.

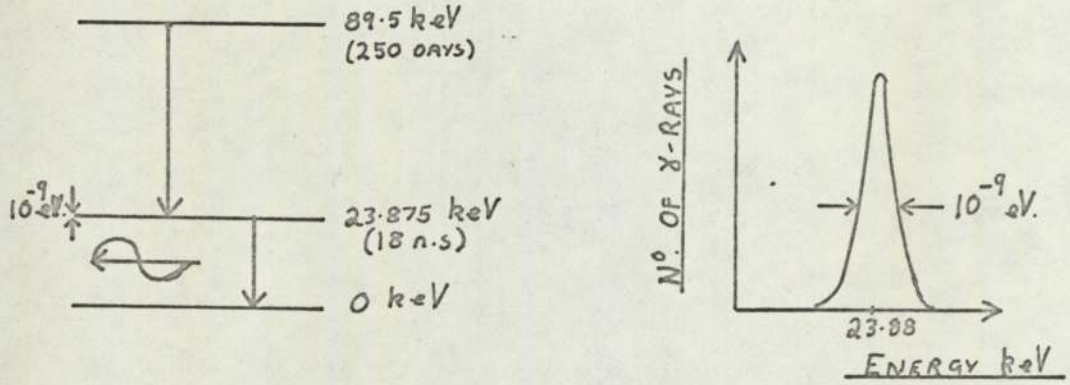

FIG. 2.2 'BILLIARD BALL' MODEL OF GAMMA-RAY EMISSION.

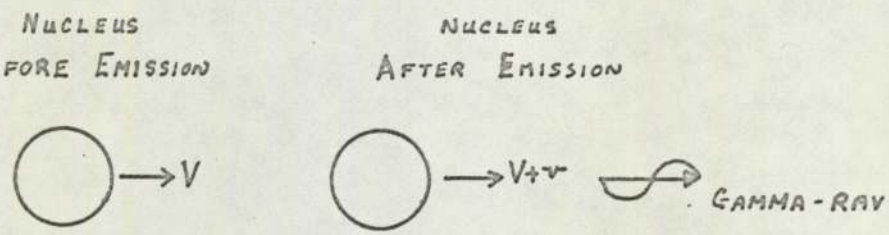

FIG. 2.3. THE EMISSION AND ABSORPTION LINES OF FREE NUCLEI FOR GAMMA-RAYS.

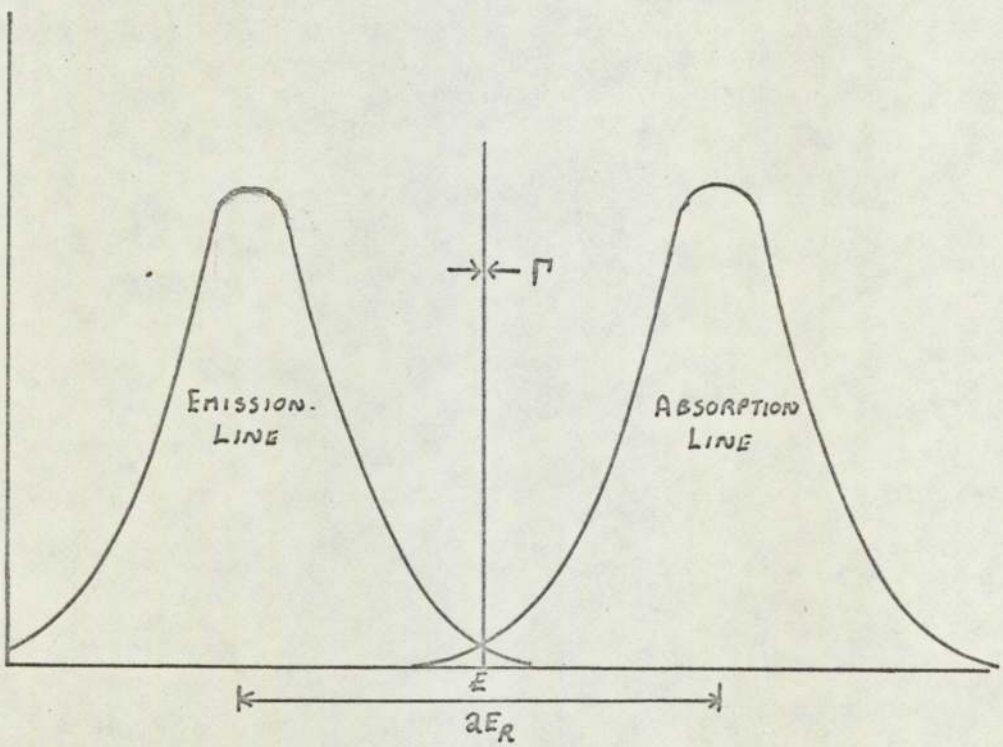

$$E_r = E_\gamma^2 / 2Mc^2 \qquad 2.3$$

Typically $E_r \lesssim 10^{-1}$ e.V.

The term $M\bar{v}V$ in δE represents the Doppler broadening of the emitted gamma-ray energy, (of the order of 1 e.V.). This is extremely large in comparison to the half - width (10^{-9} e.V.), as shown in Fig 2-3.

Exactly the same arguments apply to the absorption of a gamma-ray and the diagram also shows the absorption line. For those gamma-rays in the overlapping tails of the two distributions, resonance absorption is possible. This is exactly analogous to resonance fluoresence, observed with light photons emitted and absorbed by the electronic energy levels of an atom. However the recoil energy E_r in the case of nuclear resonance is so large, the resulting line overlap is not sufficient to make the phenomena observable. Moon (1950) found that by using very high speed rotors (upto 1600 m.p.h.), Doppler shifting of the emission line made it possible to compensate the gamma rays for E_r. In this way he observed resonance absorption.

Mössbauer (1958) discovered that E_r could be eliminated by effectively making M in equation 2-3 very large. This is achieved by fixing the emitting and absorbing nuclei rigidly in a lattice so that the recoil energy is taken up by the lattice as a whole. Even for small crystallites this means a reduction in E_r by at least 10^{14}.

Unfortunately atoms are not held rigidly within a lattice but are free to vibrate at quantised frequencies. Thus recoil energy may be taken up by the excitation of lattice phonons. However, there will still be a fraction, f, of gamma-rays which will be absorbed without recoil, since they will not be able to excite a phonon. The remaining fraction, (1-f), will transfer energy to the lattice; and Lipkin (1960) has shown that the average energy transfered per event is equal to E_r, the free atom recoil energy.

Experimentally the Mössbauer Effect is observed by utilizing the Doppler Effect, to adjust the effective energy of the gamma-rays relative to a stationary absorber and thereby reduce the resonance. This is achieved by moving the source relative to the absorber and recording the number of gamma-rays transmitted as a function of velocity. The resulting spectrum and the contributing factors are detailed in Fig 2-4.

It has been shown by Lipkin (1960) that the half-width of the spectrum for a thin absorber is just the sum of the half-widths of the emission and absorption spectra.

The shape of the Mössbauer spectrum is found to be Lorentzian for a thin absorber. However, distortions from this are found in practice and, particularly for thicker absorbers, a Gaussian or Voigt profile may become applicable.

Consider the absorption spectrum shown in Fig 2-4, at any source velocity v, the intensity recorded $I(v)$ will be given by:

$$I(v) = I(\infty)(1-f_s) + I(\infty) f_s + \int_{-\infty}^{+\infty} S(v) \exp\left(\frac{-T_A \sigma(v)}{\sigma(o)}\right) dv \qquad 2\text{-}4$$

O'Connor and Skyrme (1973)

Here;

f_s = Source recoil-free fraction.

$S(v)$ = Normalised source energy distribution.

T_A = Absorber thickness at its peak value.

$\sigma(v)$ = The nuclear absorption cross section.

$I(\infty)$= The intensity at infinite velocity.

and $$T_A = N\, t\, f_a \sigma(o) \qquad 2.4\ (a)$$

Where N is the density of resonant atoms in the absorber of thickness

FIG 2.4 CONSTITUENTS OF MÖSSBAUR ABSORPTION DIP.

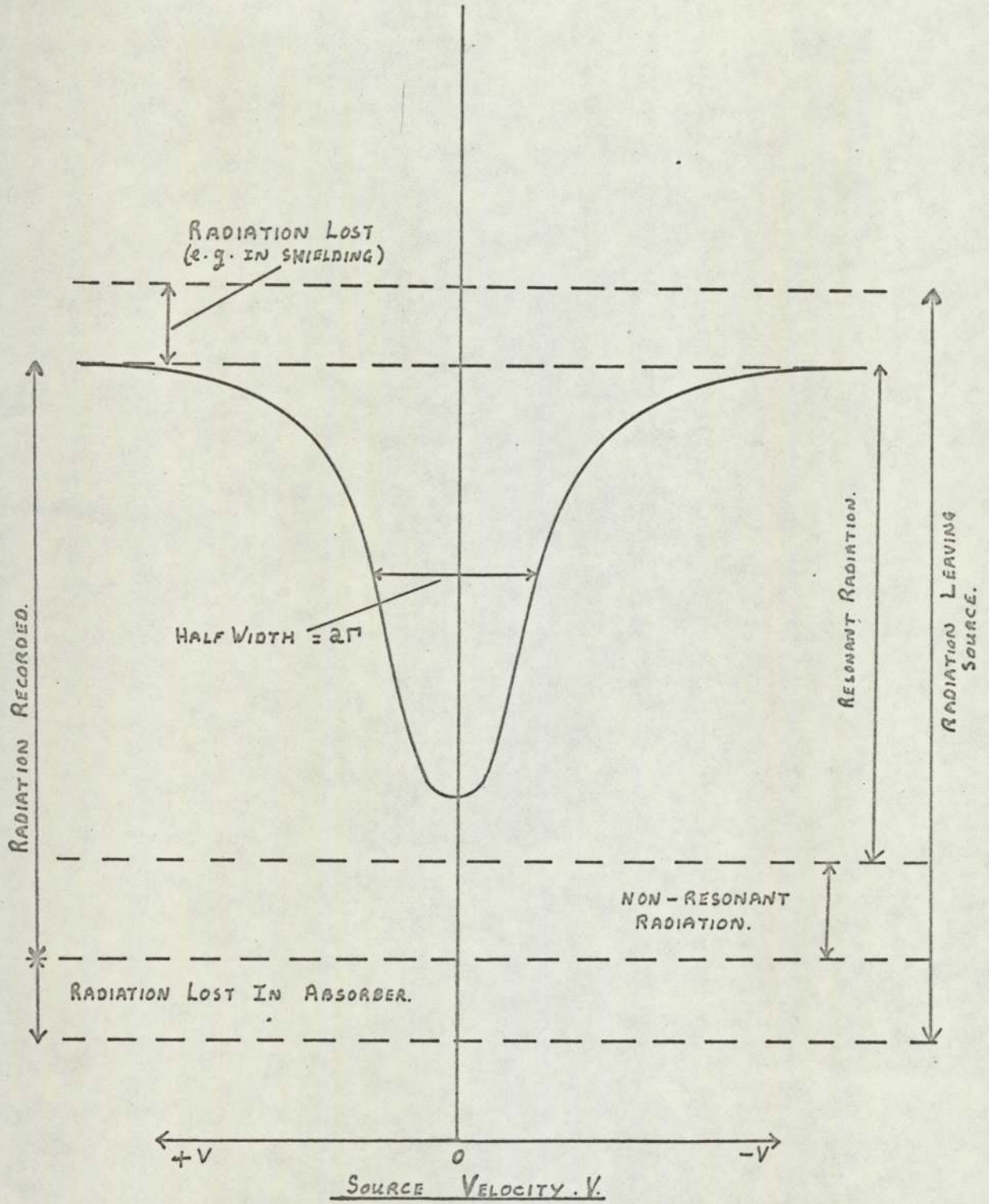

t and recoil-free fraction f_a.

Now, Lipkin (1960) has shown that the recoil free fraction, (that is the probability of not exciting a lattice phonon) is given by;

$$f = \exp\left(-K^2\langle x^2\rangle\right) \qquad 2.5$$

Where $K = \frac{2\pi}{\lambda}$, λ = the gamma-ray wavelength and $\langle x^2\rangle$ is the mean square displacement of the nucleus.

As will be explained later (section 2-3), equations 2-4 and 2-5 enable the calculation of the mean square displacement of suitable ions in crystals by measurement of the area of the absorption dip. The position of the minimum on the other hand allows the calculation of the mean square velocity again, for suitable ions in crystals.

There are several limitations on the type of nucleus which is suitable for Mössbauer work. The emitted gamma-ray energy, for example, must be above that which is strongly absorbed by a solid generally, (of the order of 10 k.e.V.) and yet still below that which would result in the gamma-ray dislodging an atom (of the order of 100 k.e.V.). The latter criterion rules out light elements of atomic weight less than 40. The cross section for resonant absorption or emission should be large compared with that of other processes. The recoil-free fraction must also be large, of course, so that the maximum number of gamma-rays having the full transition energy will be obtained, particularly in the case of the source when the absorber's recoil-free fraction is being measured. The half-life of the source must be large so that experimentation may proceed for several weeks without the activity falling to an unusable level. However the half-life of the excited state, that produces the resonant gamma ray, should be small (Fig 2-3), less than 100 n.s., so that the half-width will be narrow and only small source velocities will be required to remove resonance. On the other hand, it is difficult to define velocities sufficiently accurately if the excited state's

half-life is less than 1 n.s.

The most favourable Mössbauer isotopes have been found to be Fe^{57} and Sn^{119}, details of which are given in table 2-1.

A single Mossbauer absorption curve is not always obtained. Frequently the nuclei involved have split energy levels, which may be caused by several phenomena e.g. magnetic fields, crystalline electrostatic fields quadrapole coupling. Such splitting results in overlapping Mössbauer spectra due to resonance occuring at several source velocities. This phenomenon does not necessarily prevent the calculation of the mean square displacement, but somewhat complicates the mathematics. (see Johnson and Dash (1968)).

2.2 The Harmonic Approximation to Lattice Vibrational Spectra.

Although the dynamical behaviour of crystals is extremely complex, some aspects such as specific heat behaviour, may be accounted for on the simple assumption that the atoms vibrate independently of one another. This is the harmonic approximation and leads at once to an explanation for the Dulong and Petit empirical law that the molar heat capacity of simple solids at room temperature is approximately 25 joules /^{o}K. In order to explain the decrease in heat capacity below room temperature however, it is necessary to introduce the quantum theory and also to make some further assumptions concerning the distribution of vibrational frequencies.

In the simplest model, first introduced by Einstein, it is assumed that there exists a single characteristic angular frequency w_E which is the same for all atoms in a particular crystal (Fig 2-5). This accounts qualitatively for the decrease in heat capacity with decreasing temperature, but tends to zero too rapidly with temperature.

Born and Von Karman and Debye suggested that instead of considering each atom oscillating with the same frequency, a distribution of frequencies

TABLE 2.1

Details of Fe^{57} and Sn^{119} Mössbauer Isotopes

Stable Nucleus	Relative Abundance of Resonant Isotope	Gamma-Ray Energy k.	Half-life of Excited State	Γ (mM/s)	E_R ($\times 10^{-3}$)	σ (10^{-18} cm^{-2})
Fe^{57}	2.2%	14.4	100 nS	0.192	1.95	2.6
Sn^{119}	8.6%	24	18 nS	0.626	2.58	1.4

FIG. 2.5 EINSTEIN AND DEBYE FREQUENCY DISTRIBUTIONS

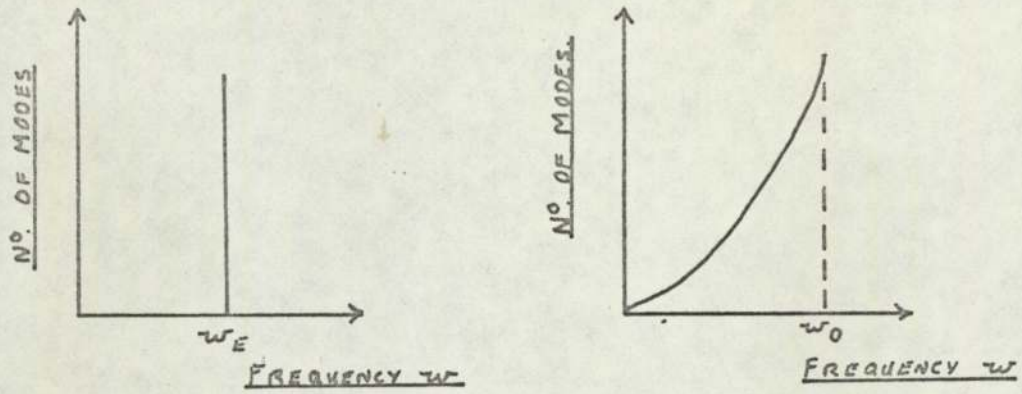

FIG. 2.6 PARABOLIC POTENTIAL WELL.

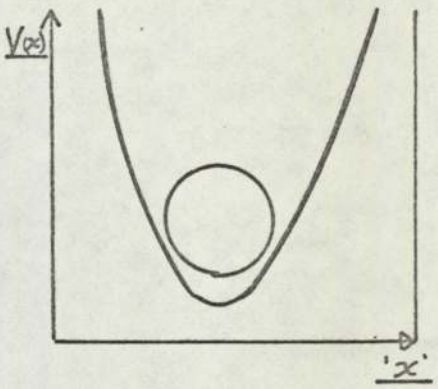

FIG. 2.7 POTENTIAL WELL MODEL FOR Ti IN $BaTiO_3$

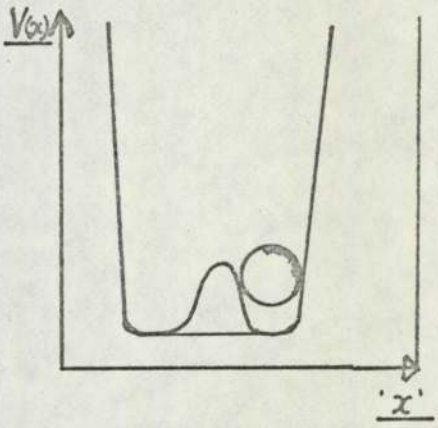

FIG. 2.8 POTENTIAL WELL MODEL FOR Sn. IN Nb_3Sn.

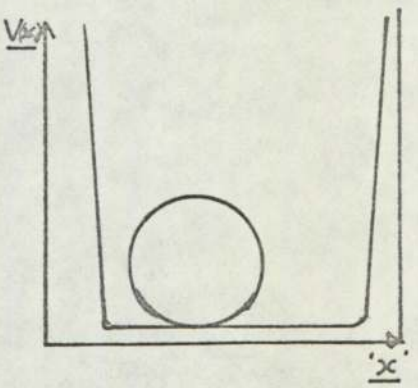

should be considered. These two proposals however, differ in a number of important respects. In the Debye theory for example, a crystal is regarded as a continuous isotropic elastic solid and this assumption leads to a frequency distribution of the form;

$$N(w)\,dw = \frac{1}{2\pi}\left(\frac{1}{C_l^3} + \frac{2}{C_t^3}\right) w^2\,dw.$$

Where C_l and C_t are the velocities of the waves for longitudinal and transverse vibrations. There is, moreover, a maximum or cut-off frequency w_D, determined by the number of independent modes of vibration that can exist with a given number of atoms. Thus the frequency distribution of each component (transverse or longitudinal) has the form illustrated in Fig 2-5.

The Debye theory gives such a successful account of specific heat behaviour that w_D, or rather the corresponding characteristic temperature θ_D, is often used as a basis for comparing different solid materials. There are, however, serious discrepancies with experiment at very low temperatures which are much better described when account is taken of the discontinuous structure of real solids. This is the approach adopted by Born and Von-Karman, who first showed that the total number of possible modes should more correctly be used to specify a cut-off wave vector, rather than a cut-off frequency. They distinguished between acoustic modes, (w tends to zero as wave vector $\underline{q}$ tends to zero) and optic modes, (w remains finite as $\underline{q}$ tends to zero) as well as between longitudinal and transverse polarization; and this recognition of the complexity of the vibrational spectrum is the real characteristic of the modern approach. Indeed, most recent experimental work has been directed at the investigation of individual modes, made possible through the development of the inelastic neutron scattering technique. Such work has uncovered the details of real vibrational spectra (see Fig 1-12)

and indicated the extent of the approximations involved in the Debye and and Einsten models.

Now it has been tacitly assumed in this review so far that the vibrational modes of a crystalline solid are simply those which may be deduced from a consideration of that solid as a whole. This is not quite complete, for it neglects the important aspects of the dynamics of a particular atom in a general harmonic solid. Such aspects are of considerable importance in certain circumstances and have been discussed within the harmonic approximation in some detail by Housley and Hess (1966) with particular reference to the interpretation of Mössbauer Spectroscopy. These authors have established that, for a homogeneous lattice, the mean square velocity and mean square displacement of the various atoms are given by;

$$\langle v^2 \rangle = \frac{kT}{M}\left[1 + \frac{1}{12}\left(\frac{\hbar}{kT}\right)^2 w^2(2) - \ldots\ldots\right] \qquad 2\text{-}6$$

$$\langle x^2 \rangle = \frac{kT}{M}\left[\frac{1}{w^2(-2)} + \frac{1}{12}\left(\frac{\hbar}{kT}\right)^2 - \frac{1}{720}\left(\frac{\hbar}{kT}\right)^4 w^2(2) \ldots\right] \qquad 2\text{-}7$$

and further that in the limit as T tends towards zero

$$\langle v^2 \rangle_o = \frac{\hbar}{2m} w(1) \qquad 2\text{-}8$$

$$\langle x^2 \rangle_o = \frac{\hbar}{2m} w(-1) \qquad 2\text{-}9$$

Here w (n) is a weighted mean frequency related to the maximum phonon frequency w_{MAX} by

$$w(n) = \left(\frac{m+1}{n+m+1}\right)^{\frac{1}{2}} w_{MAX}. \qquad 2\text{-}10$$

from which it follows that

$$w(2) > w(1) > w(-1) > w(-2).$$

The other symbols in these equations have their usual meanings.

Housley and Hess were able to establish two independent relationships between $\langle v^2 \rangle$ and $\langle x^2 \rangle$, since their intercepts and the high temperature slope of the latter are functions of the w (n):-

$$\langle x^2 \rangle_o \langle v^2 \rangle_o \gg \tfrac{1}{4}\left(\frac{\hbar^2}{M^2}\right) \qquad 2\text{-}11$$

$$\langle x^2 \rangle_T \geq \langle x^2 \rangle_o \left(\frac{4 M k T}{\hbar^2}\right) \qquad 2\text{-}12$$

Equation 2-11 is just Heisenberg's Uncertainty Principle. Equation 2-12, however, defines the limit on the possible values of $\langle x^2 \rangle_T$ for a given $\langle x^2 \rangle_o$ for an atom in a harmonic solid.

The equations 2-6 and 2-7 may be considerably simplified by restriction to the Einstein model. In this case there is only the single characteristic frequency, w_E.

$$\langle x^2 \rangle = \frac{k E_R}{K^2 \Theta_E} \operatorname{Coth}\left(\frac{\Theta_E}{2T}\right) \qquad 2\text{-}13$$

Here $K = \frac{2\pi}{\lambda}$, E_R is the recoil energy following the emission of a gamma-ray, and Θ_E is the characteristic Einstein temperature.

Similarly for the Debye model;

$$\langle x^2 \rangle = \frac{3\hbar^2}{4 M k \Theta_D} \left\{ 1 + \frac{2\pi^2 T^2}{3 \Theta_D^2} \right\} \qquad 2\text{-}14$$

2.3 The Application of the Mössbauer Effect.

2.3.1. The Recoil - Free Fraction.

Equation 2-4 relates the intensity of the Mössbauer spectrum at any velocity, v, of the source, to the properties of the source and absorber; in particular their recoil-free fractions. There are several methods which may be used to determine the latter from the Mössbauer spectrum, ("Double Absorber" technique, Johnson (1970), "Black Absorber" technique, Housley, Erikson, Dash (1964).). However, recently O'Connor and Skyrme (1973) have developed the so called "White Source" method, which has distinct advantages over the others. In particular there is no dependence upon the source line shape and also the dimensions and nuclear cross-section of the absorber need not be known.

The area of the absorption dip is given by

$$A = \int_{-\infty}^{+\infty} \frac{I(\infty) - I(v)}{I(\infty)} \, dv \qquad 2\text{-}15$$

(See Section 2-1 for the definition of terms).

Substituting into equation 2-4 yields

$$A = f_s \int_{-\infty}^{+\infty} \left\{1 - \exp\left[\frac{T_A \sigma(v)}{\sigma(o)}\right]\right\} dv \qquad 2\text{-}16$$

By averaging the spectrum over velocity limits $\pm$ V, (which are large enough to enable the errors caused by cutting off the tails of the Lorentzian absorption and emission spectra to be neglected), O'Connor and Skyrme have shown that, as V tends towards infinity;

$$\overline{I(v)} \longrightarrow I(\infty) - I(\infty)\frac{A}{2V} \qquad 2\text{-}17$$

Where $$\overline{I(v)} = \frac{1}{2V}\int_{-V}^{+V} I(v)\, dv \qquad 2\text{-}18$$

To a good approximation, at large V

$$\overline{I(v)} = I(\infty)\left(1 - \frac{A}{2V}\right) \qquad 2\text{-}19$$

Thus a graph of $\overline{I(v)}$ against $(2V)^{-1}$ yields a straight line (for large V) of slope $-(I(\infty)\, A)$ and intercept at $(2V)^{-1} = 0$ of $\overline{I(v)} = I(\infty)$ from which A may be found.

Providing $T_A \ll 1$ and $\sigma(v)$ may be assumed Lorentzian then,

$$\frac{A}{f_s} = T_A \pi \Gamma \qquad 2\text{-}20$$

Where f_s is the recoil-free fraction of the source and Γ is the half-width of the Lorentzian absorption dip.

Now for a harmonic lattice at high temperatures, (above the Debye Characteristic temperature) equation 2-7 may be written;

$$\ln f_a = -\frac{K^2 k_B T}{M}\left[\left(\frac{\hbar}{k_B \Theta(-2)}\right)^2 + \frac{1}{12}\frac{\hbar^2}{k_B^2 T^2} + \ldots\right] \qquad 2\text{-}21$$

Here, K is the wave vector of the gamma radiation and M is the mass of the absorbing nucleus. (Other terms have their usual meaning.). At low temperatures equation 2-21 becomes:

$$\ln f_a = \frac{-K^2 \hbar^2}{k_B M.2.\Theta(-1)} \qquad 2\text{-}22$$

Here $\Theta(n) = \frac{\hbar w(n)}{k_B}$, where w (n) are the weighted mean frequencies and Θ (n) are the related temperature factors.

Equation 2-21 may be rewritten to include T_A, (the factor determined experimentally) to give;

$$\ln T_A e^{\alpha} = \ln (T_A) + \frac{\hbar K^2}{12 M k_B T} = -\frac{\hbar^2 T K^2}{k_B M(\Theta(-2).)^2} + \ln Nt\sigma(o) \qquad 2\text{-}23$$

Thus a graph of the left hand side of equation 2-23 against temperature yields a straight line with intercept at T = 0^{o}K (extrapolated from high temperatures) of ln (Ntσ(o).). Using the equation 2-4 (a) values of f_a may be determined for each temperature. Similarly Θ (-1) and Θ (-2) may be determined from equations 2-22 and 2-23.

2.3.2. The Total Shift

If the source and absorber are identical then the Mössbauer absorption dip will be centered around zero velocity. When they are not equal, maximum resonance absorption occurs at a finite source velocity, the magnitude and sign of which is a function of the different electronic environments of the active nuclei and this is usually termed the 'Isomer Shift' or, more correctly the 'Total Shift'.

It can be shown, (see for example, Wertheim, 1968), by considering the electrostatic interaction between the nucleus and its surrounding electrons,

that the interaction energy E is given by;

$$E = C^1 \, |\psi(o)|^2 \int \rho r^2 \, d\tau \qquad 2\text{-}24$$

Where $C^1 = \frac{2\pi Z e^2}{5}$, $|\psi(o)|^2$ is the electron density at the nucleus, ρ is the charge density distribution at a distance r from the nucleus and $d\tau$ is a volume element. The energy change due to gamma emission in transition from an excited, (e) state to the ground, (g) state is then the difference between two similar terms,

$$\Delta E = C'' |\psi(o)|^2 \left[\langle r^2 \rangle_e - \langle r^2 \rangle_g \right] \qquad 2\text{-}25$$

and the isomer shift in energy is then;

$$\delta = C^{11} \left[|\psi(o)|_A^2 - |\psi(o)|_s^2 \right] \left[\langle r^2 \rangle_e - \langle r^2 \rangle_g \right] \qquad 2\text{-}26$$

Here,

$$\langle r^2 \rangle = \frac{\int \rho r \, d\tau}{\int r \, d\tau} \qquad 2\text{-}27$$

and 'A' and 'S' refer to absorber and source respectively.

Assuming that the charge density is constant over the nuclear volume, $\langle r^2 \rangle = R^2$ and hence,

$$\delta = C \left[|\psi(o)|_A^2 - |\psi(o)|_S^2 \right] \frac{\delta R}{R} \qquad 2\text{-}28$$

If one compares two absorbers with the same source, then the difference between their isomer shifts is;

$$\Delta\delta = C \left[|\psi(o)|_{A_1}^2 - |\psi(o)|_{A_2}^2 \right] \frac{\delta R}{R} \qquad 2\text{-}29$$

The factor $\delta R/R$ is derived from nuclear models. In the case of tin

it is well established that $\delta R/R$ is positive and of the order of $3x10^{-4}$ (Greenwood and Gibb, 1971).

Equation 2-29 permits the observation of differences between the electron density at the nucleus for similar absorbers, which can be related to differences in the S - electron density. In the cases of tin and iron compounds for example, excellent correlations between theory and experiment have been found. (Wertheim (1968), Greenwood and Gibb (1971).).

As well as the isomer shift there are contributions to the displacement of the Mössbauer peak arising from the temperature difference between the source and absorber. The most important arise from the second order term in the Doppler Effect and is called the Second Order Doppler shift, the Thermal Shift or sometimes the Red Shift. Although the mean velocity (v) averaged over the lifetime of the excited state (10^{-12} secs.) is negligible, (since positive and negative terms will occur with equal probability) this is not true of the mean square velocity ($\langle v^2 \rangle$), which will be different for source and absorber. This gives rise to a further energy difference between the states of the emitting and absorbing nuclei. The Thermal Shift as a function of absorber temperature is directly related to $\langle v^2 \rangle$ by

$$\delta_T = \frac{\langle v^2 \rangle_T}{2c} \qquad 2\text{-}30$$

Here

$$\langle v^2 \rangle = \sum_{\alpha=1}^{3} \langle v_\alpha^2 \rangle_T \qquad 2\text{-}31$$

for the three degrees of freedom.

For an isotropic solid:

$$\delta_T = \frac{3\langle v^2 \rangle_T}{2c} \qquad 2\text{-}32$$

By combining this equation with equations 2-6 and 2-8 the weighted mean frequencies w (1) and w (2) and the corresponding characteristic temperatures θ (1) and θ (2) may be determined from measurements of the thermal shift.

The expansion of the lattice upon heating causes a change in the electron density at the nucleus. This effect, which would be proportional to temperature (Shier and Taylor (1968).)is often ignored and indeed in many cases has been found to be negligable, (Johnson and Dash (1968), Housley and Hess (1967).). However the work of Shier and Taylor (1968) on Nb_3Sn has shown that there is an appreciable contribution to the Total Shift due to the temperature dependence of the electron density at the tin nucleus.

To sum up then, the shift of the Mössbauer absorption dip, δ, is given by;

$$\delta = \delta_1 + \delta_2 (v^2) + \delta_3 (T) \qquad 2\text{-}33$$

δ_1 = Isomer Shift. $\propto \Delta |\psi^2|$

$\delta_2(v^2)$ = Thermal Shift. $\propto \Delta \langle v^2 \rangle$

$\delta_3(T)$ = Temperature dependence of Isomer Shift.

If the term $\delta_3(T)$ is assumed negligible and the source is maintained at a constant temperature then, writing $\delta\langle v^2\rangle$ as the Thermal Shift for the absorber only;

$$\delta = \delta_o + \delta\langle v^2 \rangle \qquad 2\text{-}34$$

Where δ_o is a constant.

Measurement of δ can yield information about both the electron density at the nucleus and the mean square velocity of the active nuclei in the absorber.

2.4 Anharmonicity and the recoil-free fraction

2.4.1. Local atomic potential wells

The potential well at a particular atomic location is thought to arise essentially from two components. These are, a long-range component, which arises from forces which are primarily attractive and a short - range

component which arises from the repulsive interaction between the outer electron shell of the atom concerned and the corresponding shells of the nearest adjacent atoms. The effect of adding these components is believed to be a potential function of approximately parabolic shape (Fig 2-6) i.e. V (x) proportional to x^2.

In fact, if the potential wells were exactly parabolic the harmonic model for the solid state would also be exact and properties such as thermal conductivity and thermal expansion could not exist. In reality the potential wells are not so ideal and deviate from the parabolic model in a manner and to an extent which depends upon the nature of the atomic interactions involved.

2.4.2. High temperature anharmonicity.

It is assumed that for simple solids the parabolic approximation is a good one in the neighbourhood of the low temperature equilibrium atomic separation. At higher temperatures significant deviations are to be expected and these may be represented by writing:

$$V(x) = A x^2 + B x^3 + C x^4 + \ldots.$$

Where A,B,C are coefficients which become successively smaller in magnitude. This type of anharmonicity arises from the basic assymmetry in the nature of atomic interactions, that it is easier, generally, to increase rather than decrease the separation between atoms.

2.4.3. Low temperature anharmonicity.

The situation described in 2.4.2. is not the only one leading to anharmonicity. There are in fact a number of classes of materials for which the harmonic approximation is actually rather poor even at low temperatures and these have recently been reviewed by Dash, Johnson and Vischer (1968). These materials include ferroelectrics such as Ba Ti O_3 in which the Ti ions occupy wells with off centre valleys (Fig 2-7) and high transition

temperature superconductors like Nb_3 Sn in which the tin atoms are thought to occupy flat-bottomed wells (Fig 2-8).

The Mössbauer effect is a most suitable technique for the investigation of local potential conditions and the expression for the recoil-free fraction,

$$f = \exp\ (-K^2 \langle x^2 \rangle)$$

which is exact for harmonic systems, has been shown to remain a good approximation even in the presence of considerable anharmonicity (Maradudin and Flinn, (1963); Dash et al, (1968).).

A particularly important result obtained by Dash et al, is that at high temperatures, and under certain conditions at low temperatures, the recoil-free fraction is a simple product of harmonic and anharmonic components, i.e.

$$f = f_H \ f_{AN} \qquad 2\text{-}35$$

where f_H is the harmonic contribution to the recoil-free fraction and f_{AN} is the anharmonic contribution.

The restriction at low temperatures is that the Mössbauer atom must be much lighter or much heavier than the other atoms of the structure; this has been assumed to hold for Fe in $Fe\ Cl_2$ by Johnson and Dash (1968) and for Sn in Nb_3 Sn by Shier and Taylor (1967, 1968). As the later authors have pointed out, the high temperature behaviour of an harmonic 'f' must extrapolate to 1 at absolute zero, which enables a crude estimate of f_{AN} by extrapolating experimental date to absolute zero. The radius of the flat portion of the potential well (assuming this to be the cause of the anharmonicity) may be related to the f_{AN} by

$$\ln f_{AN} \simeq \tfrac{1}{3}\ K^2\ R^2 \qquad 2\text{-}36$$

where K is the wave vector of the emitted photon (This formula is a good approximation provided $K^2\ R^2 \leqslant \pi/2$).

Thus an estimate of the potential well flat-region radius is possible, enabling comparisons between materials of the same anharmonic group.

In practice the recognition of the presence of anharmonicity depends upon the relationship given in equation 2-12, which, by use of equation 2-5

FIG. 2.9. THE NATURAL LOG. OF THE RECOIL-FREE FRACTION VERSUS TEMPERATURE.

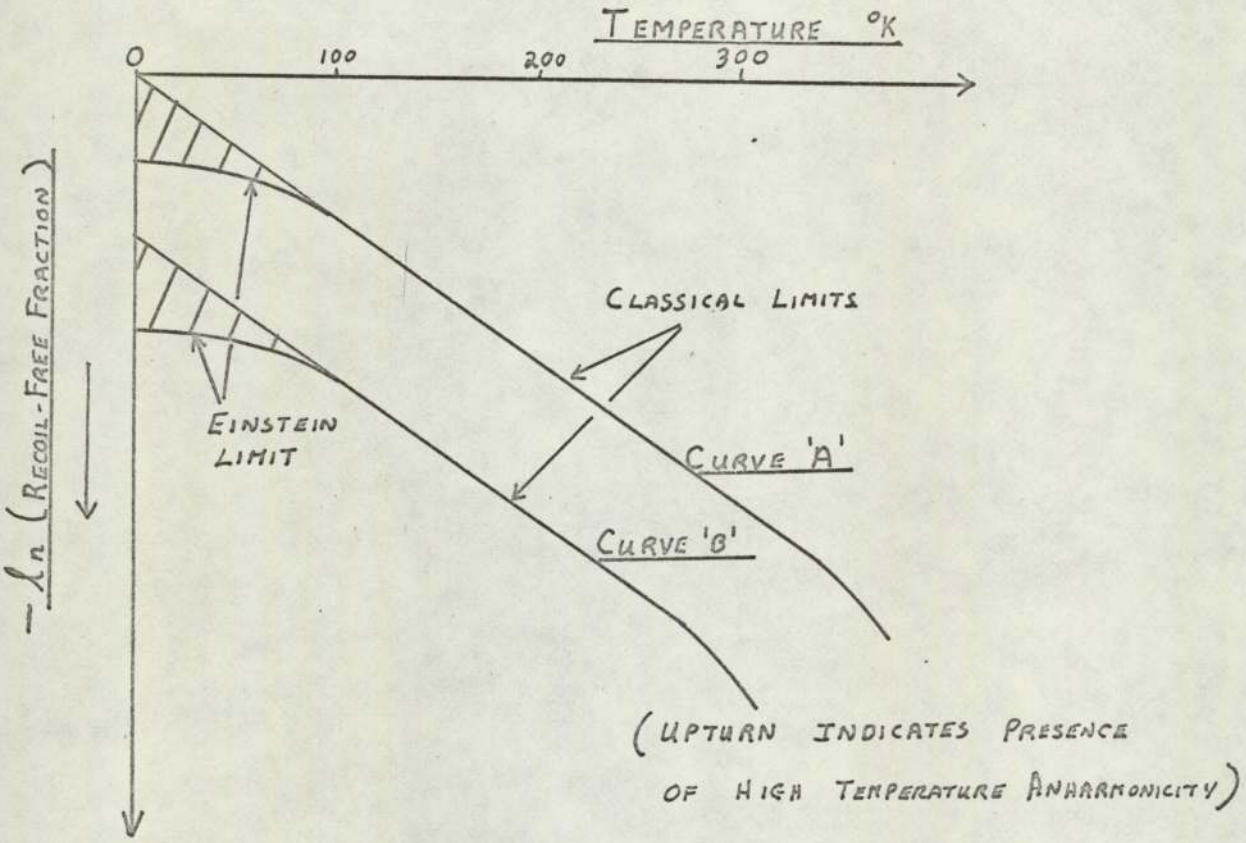

CURVE 'A' LOW-TEMPERATURE ANHARMONICITY ABSENT.

CURVE 'B' LOW-TEMPERATURE ANHARMONICITY PRESENT.

/ / / REGION OF ALLOWABLE RECOIL-FREE FRACTIONS FOR A HARMONIC FREQUENCY SPECTRUM.

may be rewritten as;

$$- \ln f(T) \leqslant \frac{2kT}{E_R} \left[\ln f(o) \right]^2 \qquad 2\text{-}37$$

where E_R = recoil energy and f (o) = recoil-free fraction at $0^{\circ}K$.

This equation must be satisfied in the harmonic approximation for any frequency spectrum, according to Housley and Hess, which places an upper limit on the value of ln f (T) provided ln f(o) can be found experimentally. Fig 2-9 (A) shows a possible curve of ln f (T), the linear portion of which corresponds to classical behaviour, whilst the shaded region shows the allowable values of ln f (T), limited finally by the Einstein Model. Curve (B) shows the affect of the presence of low temperature anharmonicity on the basis of equation 2.35. The harmonic curve is displaced by an amount approximately proportional to the square of the radius of the flat region of the potential well.

CHAPTER 3: EXPERIMENTAL TECHNIQUES

"When a theory predicts a superconductor and you try and make it, it won't form."

B. T. Matthias (1968)

3-1 Preparation of Samples

The formation of stoichiometric polycrystalline samples of spinels may be approached in two ways, both of which are primarily concerned with ensuring that the reacting constituents are homogeneously mixed. For example consider the reaction:

$$MgO + Al_2O_3 \rightarrow MgAl_2O_4$$

This is a relatively slow diffusion process, the completeness of which depends upon homogeneity of the reactant 'mix', as well as the temperature.

The 'wet' method of preparation is to mix a solution of the constituent nitrates, hence obtaining perfect homogeneity, evaporate to dryness and then to decompose the dry mixture to the oxides, before finally firing to derive the spinel phase.

A homogenous mixture may also be obtained by milling the basic reactants, MgO and Al_2O_3 together. However the degree of homogeneity in this case will be, by no means, as good as the 'wet' method.

Having obtained a satisfactory mix the reactants must be brought close together to ensure that diffusion takes place. This is done by compressing the mixture under several kilogrammes producing a hard dense pellet. The temperature at which the reactants are then fired is extremely important, since spinels will decompose if the temperature is too high and the diffusion process will not start at too low a temperature. Compressing and firing of the reactants is refered to as sintering.

Finally the atmosphere in which the reaction takes place must be considered, in order to maintain stoichiometry and exclude impurities.

For the oxide spinels it is possible to fire the reactants in an atmosphere of pure oxygen, which may be continually replaced, thus flushing the reactants. For the sulphide and selenide spinels however, it is difficult to obtain the corresponding continuously flushed atmosphere. Also, there are frequently competing reactions, which means that careful control is necessary if the spinel phase is to be the only product of the reaction. Indeed one of the difficulties in preparing such spinels is that there is a tendency for decomposition to occur before the temperature for a complete reaction is reached. The reactants are therefore sealed in evacuable tubes, both to constrain the gaseous elements and to isolate them from the atmosphere.

Lack of stoichiometry and the impurity phases which arise from this may be removed in some cases, particularly the oxide, by repeated milling, compressing and firing. It is important to realise that the initial reactant mix is stoichiometric and the term 'impurity' refers to the development of a foreign phase because of a competing reaction.

During this work several 'wet' methods of preparing the sulphide and selenide spinels were tried and although these produced good results, the final products were very fine grained with very broad X-ray diffraction lines. Since crystalite size also effects transition temperatures (T_c), pelletising and refiring at high temperatures was necessary to produce large crystallites. There was also the necessity to dry and clean the product prior to firing.

Typical examples of the effect of purity, stoichiometry and crystalite size upon T_c are the spinels under investigation. Cu V_2 S_4 has not been prepared without at least 5% Cu_3 V S_4 the competing product in the reaction. Despite a reported T_c of 4.5°K (Van Maaren et al, 1967) no superconductivity above 1.5°K was found in any of the samples prepared. Cu Rh_2 S_4 was found to have a T_c of 4.8°K by these authors but of 4.35°K by Robbins et al (1967).

The breadth of the transitions being 0.5°K and 0.3°K respectively. Yet both authors obtain 3.5°K for the transition temperature of Cu Rh_2 Se_4. These discrepencies are undoubtedly due to differences in the preparation of the samples.

The most satisfactory method of preparation found was to fire a stoichiometric mixture of the elements. These were all fine powders (less than 100 micrometres) of high purity, (better than 99.9%) (Supplier KOCH - LIGHT + CO.). Weighing was done to an accuracy of better than 0.05%, except in the case of very small additions when it was better than 1%. Transfer of the elements was kept to a minimum. They were mixed using a mortar and pestle until there was no visible trace of the seperate constituents. The mixture was pelletised using a steel press with 15mM. diameter polished dies. (PLATE 3-I)which was cleaned with acetone and greased very sparingly with dimethyl polysiloxone release agent. Average pellet weights were of the order of 2 GMS. More than 1,000 KGMS. was necessary to produce a hard pellet and pressures upto 10,000 KGMS did not cause cracking. Such high pressures however were not found to improve the purity of the final product and a pressure of three thousand KGMS. was used as standard throughout this work.

For the sintering, the pellets were sealed in separate evacuable silica tube (Fig 3-1), the pressure was reduced to below 1×10^{-5} Torr and the system was flushed thoroughly with pure argon. (99.99%). The tubes were then immediately sealed off. Calculation were made to ensure that the total vapour pressure of the elements did not over stress the silica tubes at the high temperatures.

It was found that a residual pressure of argon or helium removed the impurity in Cu Rh_2 Se_4. A residual pressure of 100 Torr of argon was therefore used as standard in all samples which were later investigated in detail. No difference in lattice parameter or transition temperature was

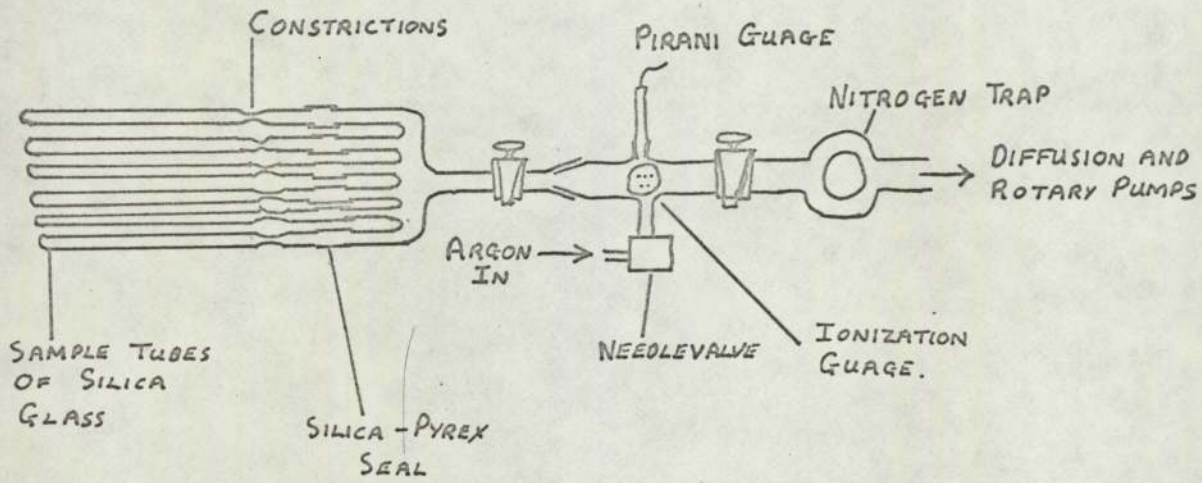

FIG. 3-1 SCHEMATIC DIAGRAM ILLUSTRATING SAMPLE TUBE SYSTEM

detectable between samples prepared with and without argon or helium. This indicated little or no inclusion of the gas in the spinel lattice.

After careful optimization of the reaction parameters it was found possible to avoid separate deposits of sulphur or selenium within the tube.

Tubular furnaces having 5" flat zones were used with alumina packing around the silica tube. Temperature control was to within $\pm$ 5°C, with a four to five hour build-up time to 800°C. Firing temperatures were found to be very critical particularly in the case of Cu Rh_2 S_4, but not so the time spent at temperature. The literature suggested temperatures of 800°C for 48 hrs. at least. It was found that the reactions were complete within 24 hrs. and did not appear to be affected by continued heating. In general the reactions were incomplete below 450°C, (which ruled out the use of pyrex tubing). Extensive investigation of ideal conditions could not be carried out because of the cost of rhodium but nevertheless it was found that temperatures around 600°C gave good purity results and an optimum transition temperature for Cu Rh_2 Se_4, whilst 550°C was found to be necessary to produce the optimum transition temperature in Cu Rh_2 S_4.

Although some authors found it possible, regrinding and repressing of the product did not produce hard pellets. They either cracked under pressure, or powdered whilst being transfered to the silica tube. Refiring did not improve the purity and in some cases actually destroyed the superconductivity.

The substitution of various elements for rhodium in Cu Rh_2 S_4 and Cu Rh_2 Se_4 was integral part of the programme. Typically the series Cu $(Rh/Co)_2$ Se_4 was examined to study the effect of, supposedly, not changing the electron atom ratio, one of Matthias's criteria for superconducting behaviour. However the impurity, of the (Rh/Co) Se_2 type, increased in concentration with increasing Cobalt. Very high temperatures (1200°C) and quenching down to liquid nitrogen temperature failed to produce even trace amounts of Cu Co_2 Se_4.

In order to study the binding of the octahedrally co-ordinated metal atom it was necessary to replace some rhodium with a Mössbauer atom. Ideally this would be Iridum, however the latter is extremely expensive and the more usual tin Mössbauer atoms were therefore used. It has been found (Fig 3-2) that superconductivity is retained in Cu Rh_{2-x} Sn_x Se_4 below X=0.5, so this series was particularly interesting. However in order to obtain adequate counting statistics it was necessary to use tin enriched in the 119 isotope (84% enriched tin, 119, supplied by U.K.A.E.A.).

Generally these series were manufactured at temperatures between 600°C and 650°C to obtain maximum purity and retain superconductivity. Further preparation details are given with the results.

3: 2 X-Ray Diffraction Analysis

3-2-1 General Remarks

The X-ray diffraction technique was used to:

(i) Identify the prepared samples as spinel and assess their purity.

(ii) Determine the crystal structure parameters of the superconducting spinels prepared.

The apparatus used was a Philips automatic powder diffractometer (Plate 3-II), shown in schematic form by Fig 3-3. This system included:

(i) Facilities for automatic continuous scanning across a range of angles in 2θ (θ = Bragg Angle), with output to a chart recorder. These were used to identify the samples and assess purities.

(ii) Facilities for automatic fixed - time step scanning across selected diffraction line profiles at intervals of 0.01, 0.02, or 0.05° (2 θ), with simultaneous output to a printer and tape punch to record intensities. These were used for the determination of crystal structure parameters.

PLATE 3.II PHILIPS DIFFRACTOMETER

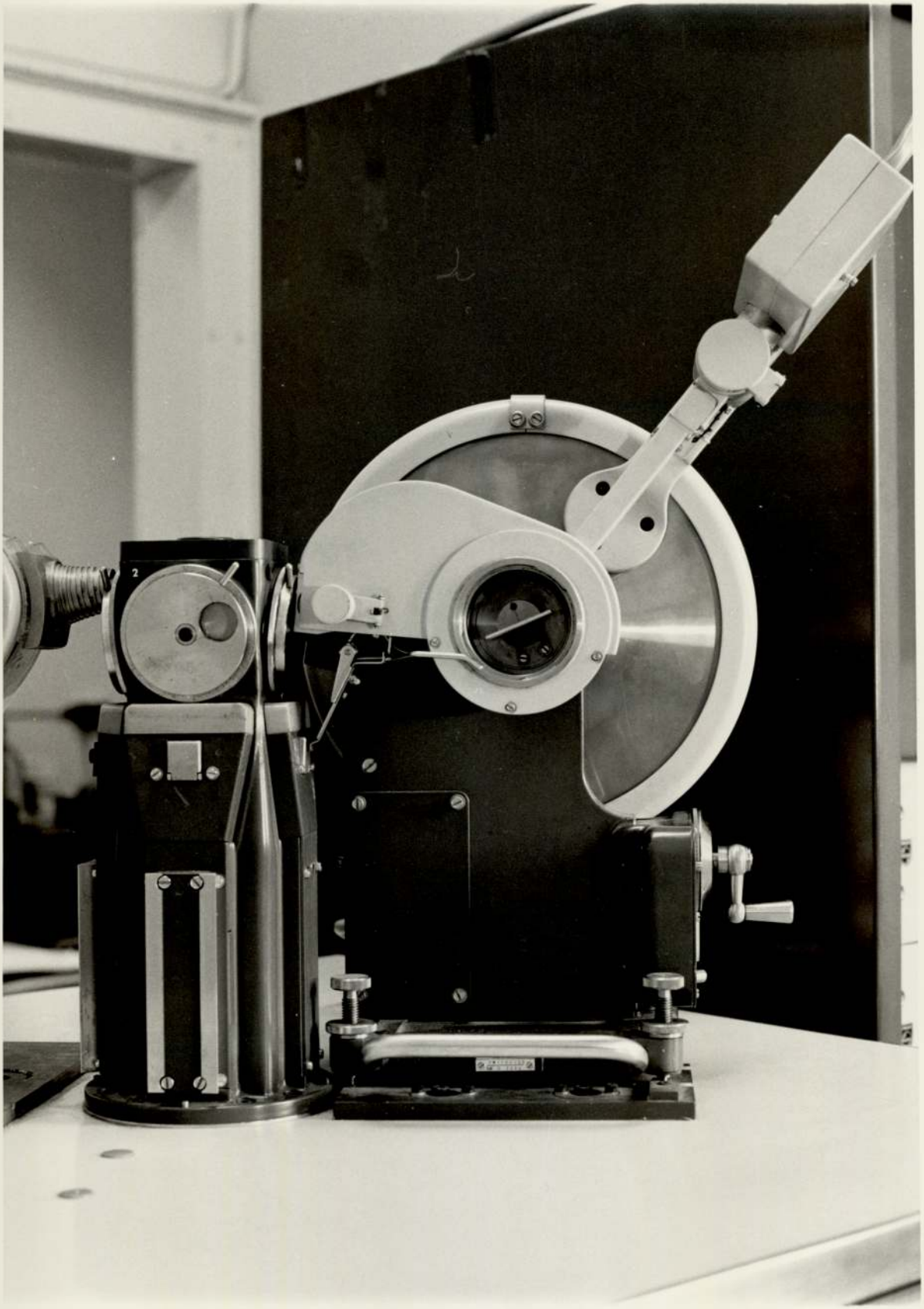

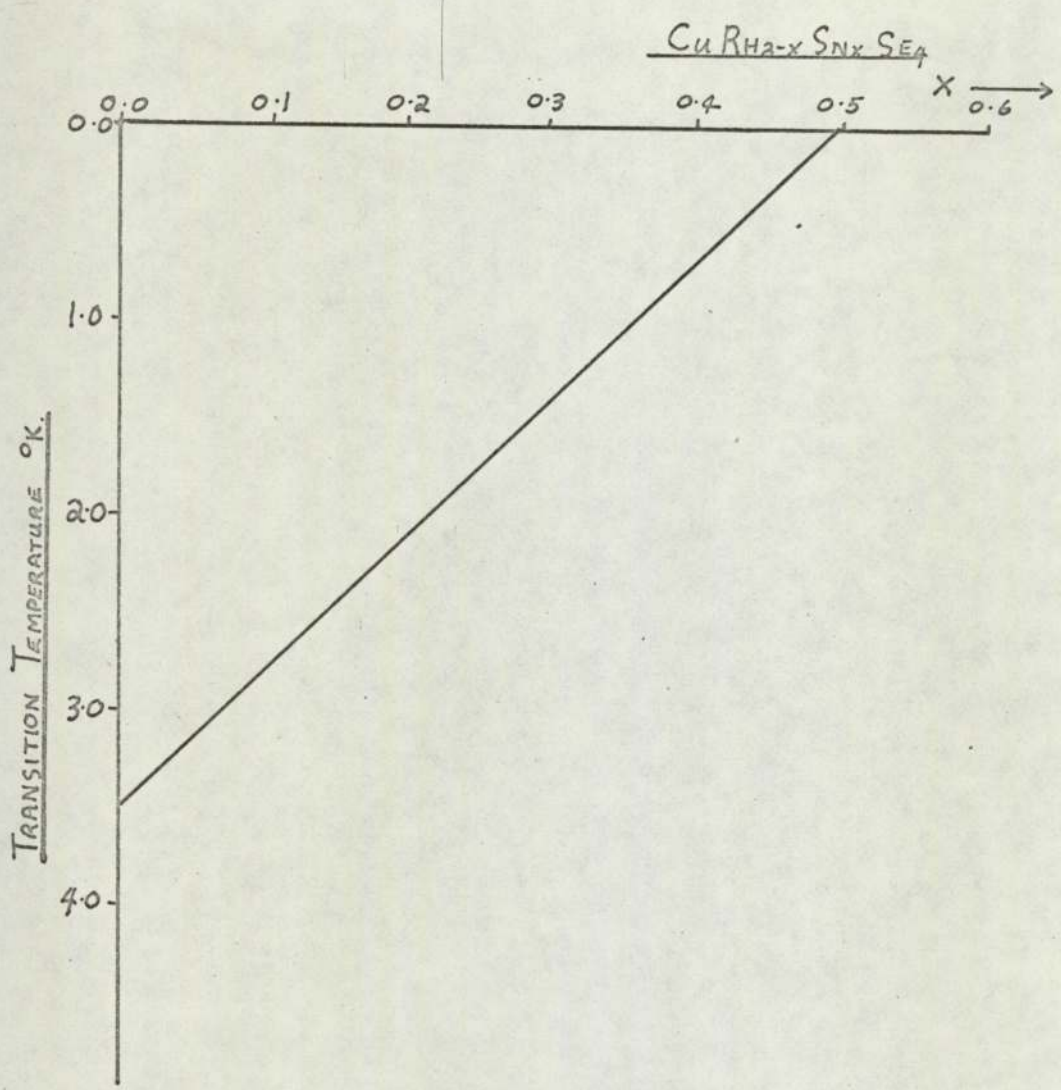

FIG. 3-2 TRANSITION TEMPERATURE VERSUS COMPOSITION

AFTER M. H. VAN MAAREN AND H. B. HARLAND (1969)

FIG. 3.3 SCHEMATIC DIAGRAM OF PHILLIPS DIFFRACTOMETER.

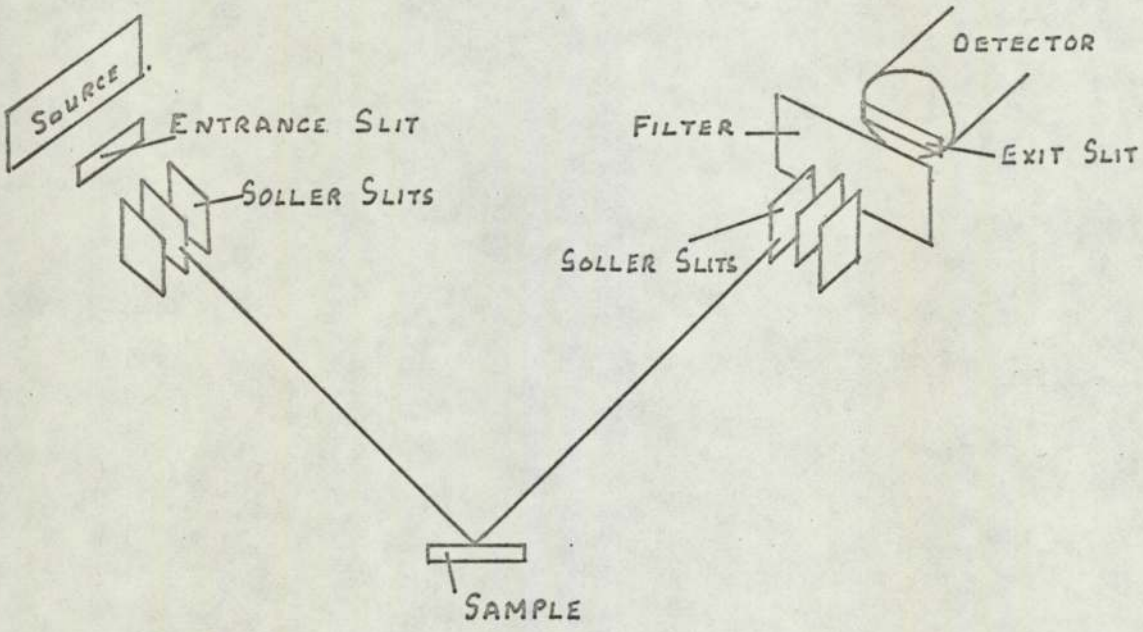

3-2-2 Diffractometer Alignment

The procedures for alignment of the source, sample, slits, filters and detector are described in the handbooks supplied by the manufacturers (Philips Ltd.) and also in some detail by Parrish (1965). A standard lithium fluoride sample enabled regular checks to be made on the calibration. The pulse height discrimination system was optimised using the Li F sample. (See relevant handbook for details). Only Cu Kα rediation was used, with the appropriate Ni filters to remove the Cu Kβ interference. The full experimental diffractometer conditions are given in Table 3-1. The samples were ground and sieved to smaller than 65 micrometers particle size and this powder was placed into the appropriate target holder and carefully pressed flat using a glass slide.

3-2-3 Measurement of Crystal Structure Parameters

A detailed analysis of a powder diffraction pattern involves the determination of a number of diffraction line positions and their integrated intensities. These are subject to numerous aberrations the effect of which may be minimised or in some cases completely eliminated by the use of modern techniques of analysis. For example Wilson (1963) has shown that there are considerable advantages to the use of the centroid as a measure of the diffraction line position rather than the peak. Similarly the background intensity to the diffraction line may be determined accurately from variance versus range curve, (Langford, 1968).

Considerable expertise has been developed in these techniques at Aston University including detailed computer programmes and full use was made of this, (See for example, Ph.D. theses by Hilleard (1973) and Cheary (1971).)

Initial chart recordings, made from 10 to 140° 2θ at $\frac{1}{4}$°/MIN. were analysed for spinel and impurity diffraction lines. Samples of particular interest were further examined using the step scanning technique, usually at

TABLE 3-1

EXPERIMENTAL CONDITIONS OF THE X-RAY DIFFRACTOMETER

Radiation	Cu Kα - Nickel filter
X-Ray tube supply	40 k.V, 20 mA.
Take-off angle	6°
Divergence slit	1°
X-Ray source size	1.6 mMs. X 12 mMs.
Sample size	20 mM X 10 mM X mM
Aperture of Sollerslits	2.25°
Receiving slit	0.1 mM.
Source of sample distance	173 mM.
Antiscatter slits	1°
X-Ray counter	Xenon proportional counter
Displacement of receiving slit from focussing circle	< 1 mM.
Inclination of specimen plane to goniometer axis	Unknown, but small
Angular mis-setting of 2:1 ratio	Unknown, but small
Displacement of goniometer outside focussing circle	0.025 mM
Angular mis-setting of receiving slit	Unknown, but small
Angular mis-setting of centroid of X-Ray beam	Probably $< \frac{1}{4}^{\circ}$

400 S./0.02° (2θ), through each line. The information, collected on punched tape, was then, with the relevant computer programmes, used to determine centroid and variance versus range plots. The Universities I.C.L. 1905 E computer was used for this with multiple on-line programming (M.O.P.) The latter enabled the main programmes to be stored in binary form and accessed repeatedly, considerably reducing 'turn-round' time. Modifications to the existing programmes were necessary, linking them so as to handle large amounts of data quickly, producing graphical output and executing several cross checks of the results.

3-2-3 (1) The Lattice Parameter

Accurate lattice parameters were determined from the centroid of the spinel lines, using a mean value for the Cu Kα radiation wavelength, since at present this is not known accurately, Cheary (1971) has described the effect of the Cu Kα satelite lines on the centroid at high ranges and these corrections were also made in this work (Fig 3-4)

Corrections to the calculated centroids due to physical and geometrical aberrations fall into two groups. (See Wilson (1967) and Cheary (1971).). The first must be calculated for each centroid and added or subtracted directly. The second group may be removed by extrapolation techniques. However it has been found that the corrections of the first kind cancel at high angles. (Approximately 2 θ = 100° upto 150°) and the extrapolation terms for the second kind (i.e. $\text{Cot}^2\ \theta$ and Cos θ Cot θ) tend to zero at high angles. Thus, for the spinel peaks which occur at approximately 130° (2θ), the geometrical and physical aberrations are negligible in comparison to possible errors in measuring the angle (Fig 3-5 shows the aberration variations with 2θ). This enabled an accurate and relatively rapid measurement of lattice parameter to be made from the centroid of the most intense line near 130° (2 θ), i.e. 12,0,0 line for $Cu\ Rh_2\ Se_4$. Naturally the same line

FIG. 3-4 . TYPICAL CENTROID VERSUS RANGE PLOT.

12,0,0 LINE $CuRh_2Se_4$

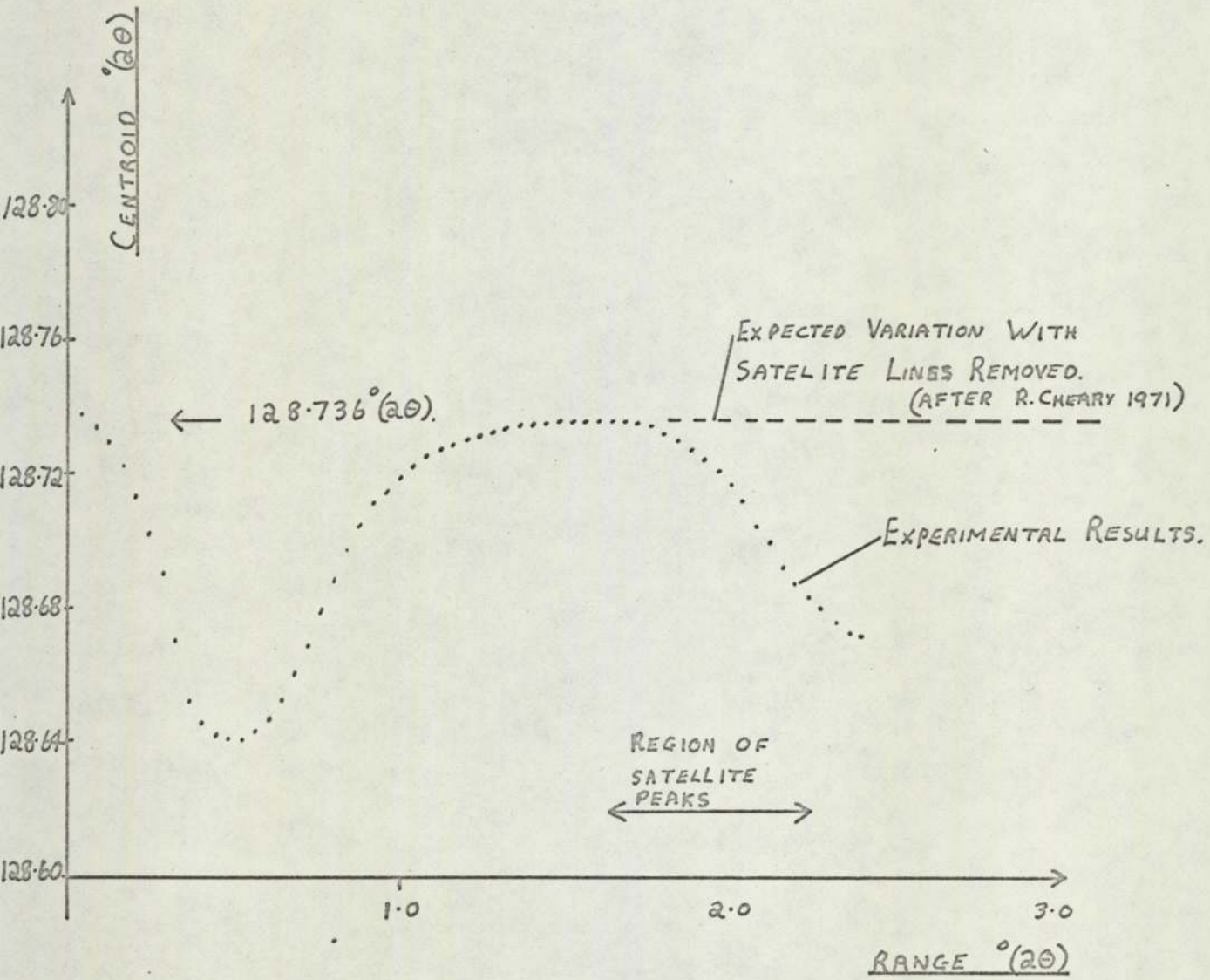

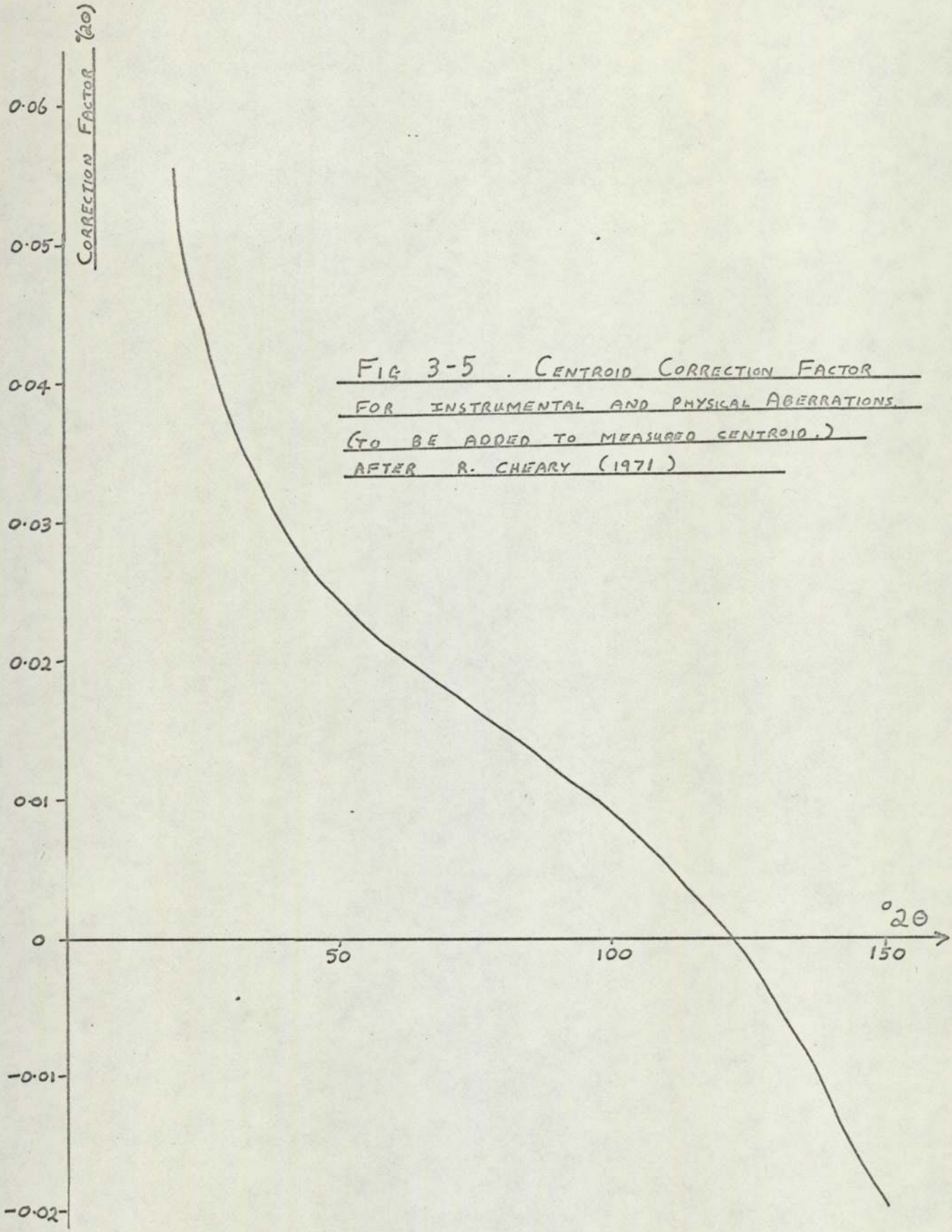

FIG 3-5 . CENTROID CORRECTION FACTOR FOR INSTRUMENTAL AND PHYSICAL ABERRATIONS. (TO BE ADDED TO MEASURED CENTROID.) AFTER R. CHEARY (1971)

was used for samples that were to be compared. The wavelength used in these calculations was the weighted mean wavelength for the $K\alpha_1$ and $K\alpha_2$ lines, as suggested by Wilson (1967).

3-2-3 (ii) The Background Correction to the Integrated Intensity

The variance-range function mentioned earlier enables the accurate determination of the diffraction line background and hence of the true integrated intensity for a diffraction line. With the correct value of background chosen, the variance becomes a linear function of range (Fig 3-6), above a range of the order of the doublet separation or the half-width of a single line. For large intensity peaks this method proved to be very satisfactory, however for those of low intensity the errors were large and it was difficult to determine the linear region. Now, the general trend of background with (2θ) is well known to be high at low angles, falling rapidly to an approximately constant value until high angles where it rises slightly. Bearing this in mind background levels for the low intensity peaks were estimated to ensure that they fell on the general trend outlined by the large intensity peak.

3-3 The Measurement of Superconducting Transition Temperatures

In the present work, superconductivity was invariably detected by exploiting the Meissner effect (Chap 1.) i.e. the exclusion of magnetic flux from the body of a superconducting sample.

The powder under investigation was placed within a glass tube 3 cms. long with 1cm bore (Fig 3-8 a,b) one end of which was sealed. Only sufficient powder was included to give an adequately strong reading of T_c and to cover the thermocouple. This was to ensure that the registered temperature and the transition corresponded to the same part of the powder. Around the tube were three layers of silk covered nickel wire (40 s.w.g.) of approximately 1000 ohms. held rigidly in araldite. This inductor formed one arm of a

FIG. 3·6 TYPICAL VARIANCE VERSUS RANGE PLOT.

4,4,0 LINE $CuRh_2Se_4$.

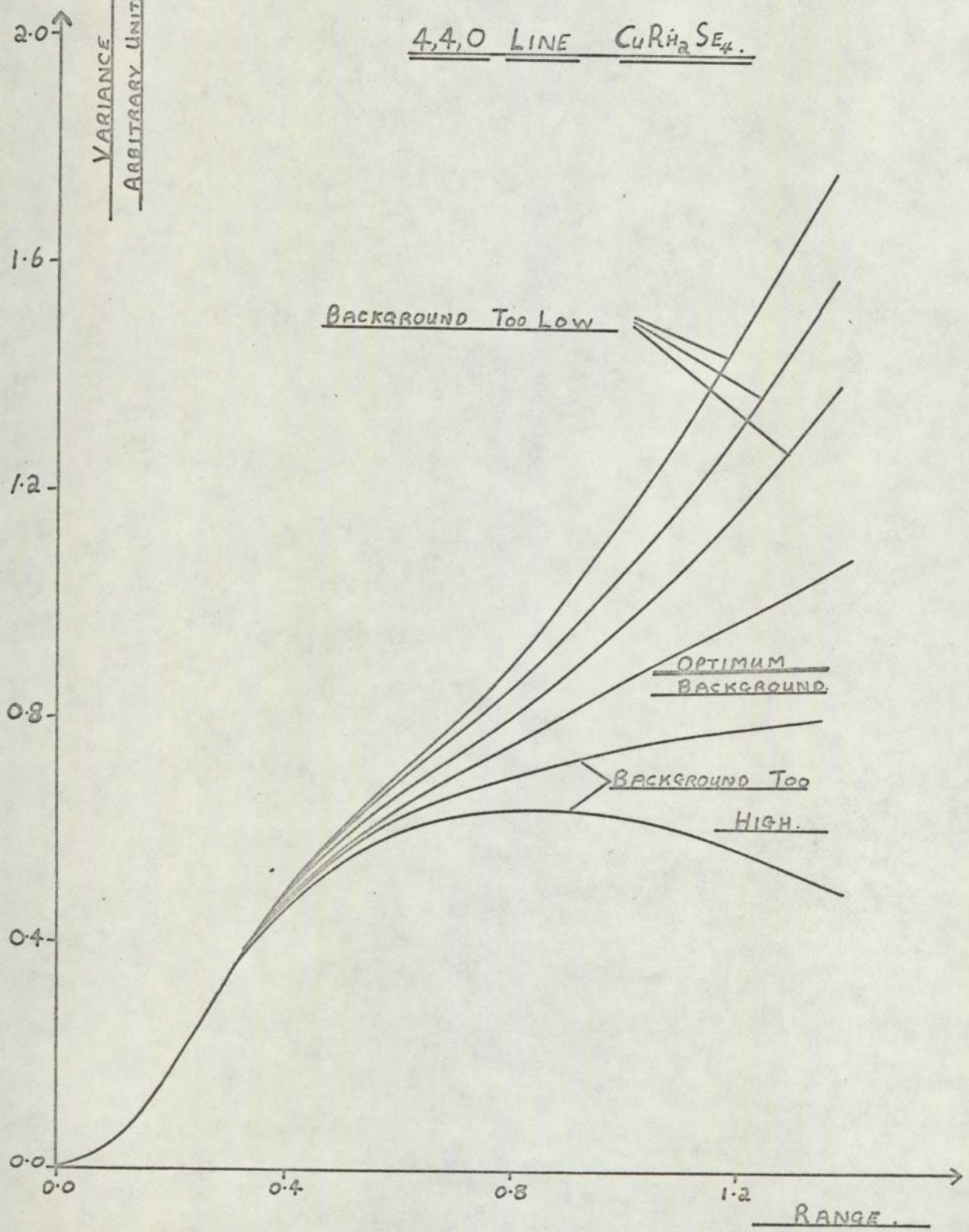

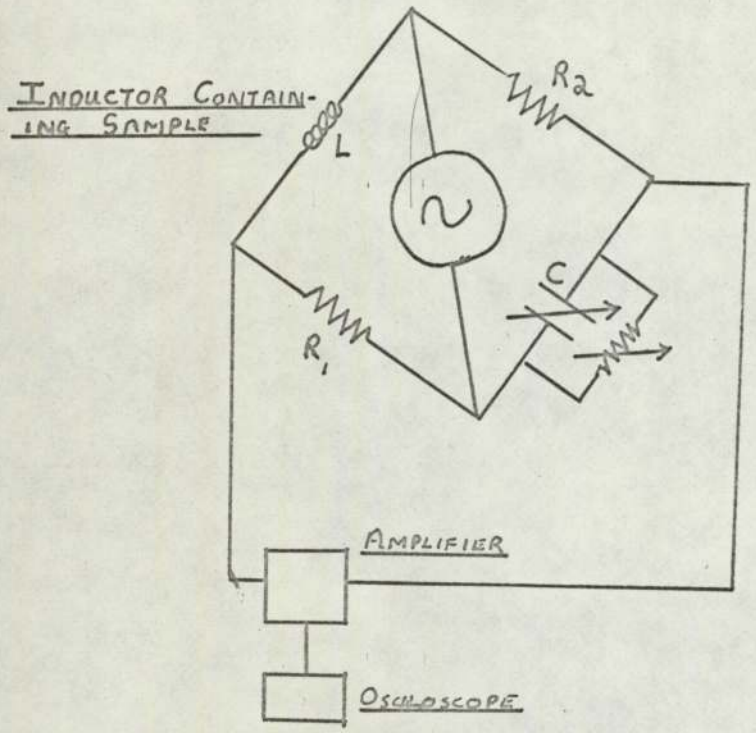

FIG 3·7 SUPERCONDUCTING TRANSITION DETECTION SYSTEM.

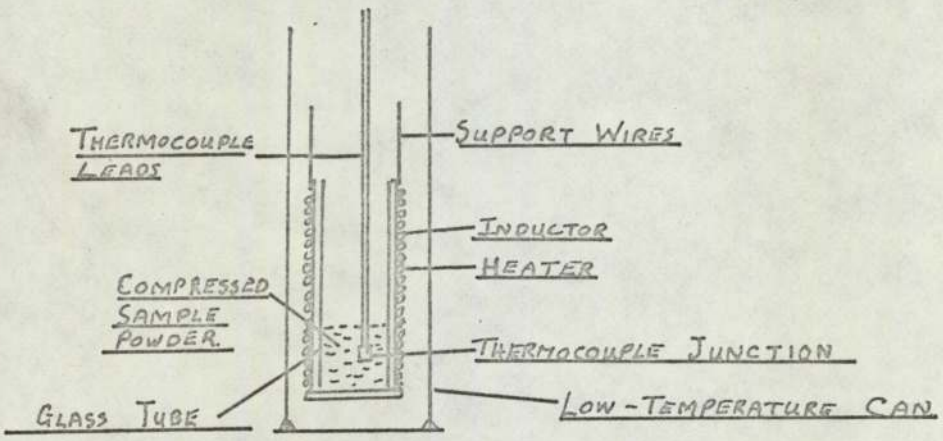

FIG. 3-8.a. THE SAMPLE HOLDER.

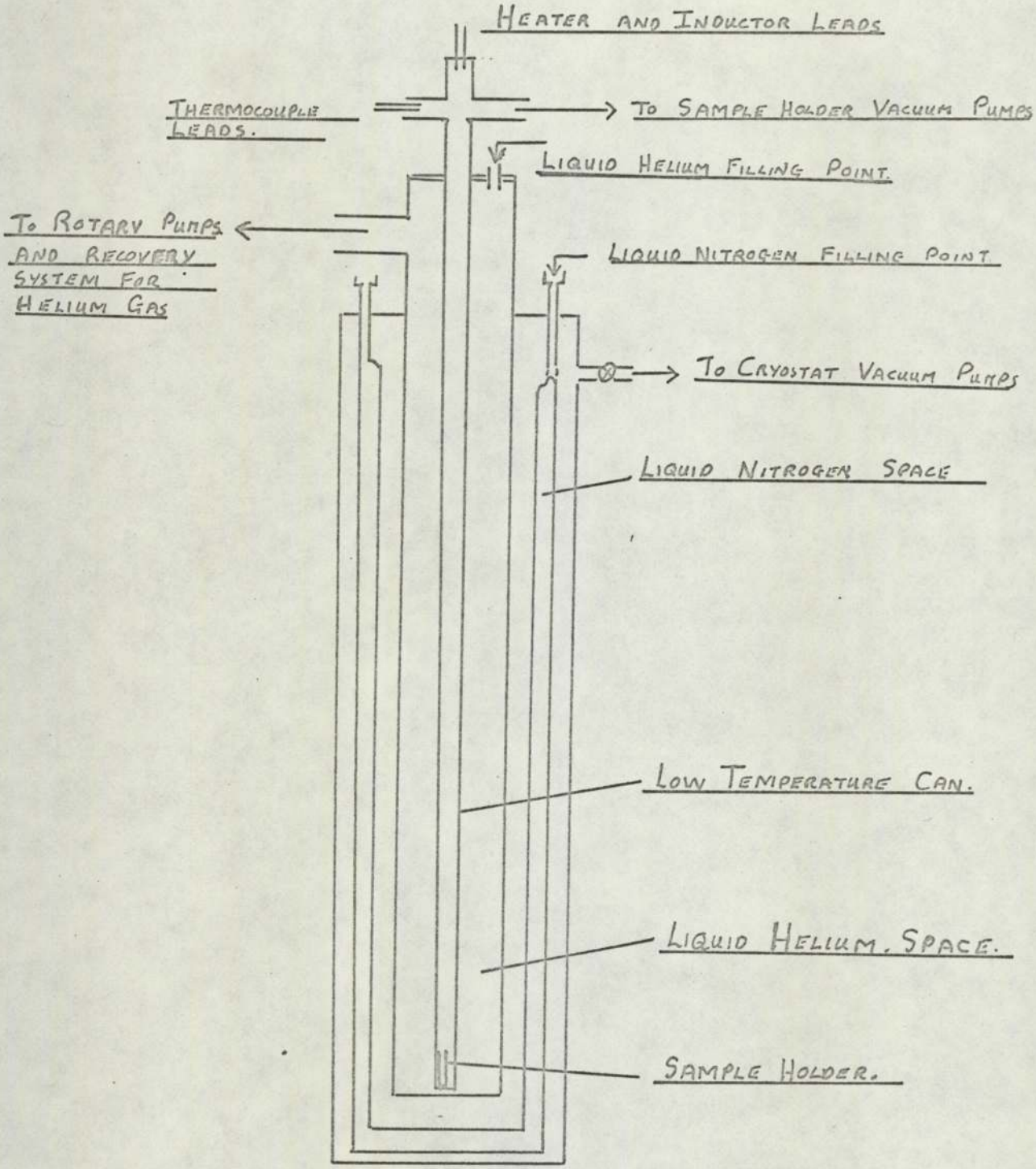

FIG. 3-8.6 CRYOSTAT AND SAMPLE HOLDER

bridge network, Fig 3-7 its inductance being given by $L = R^2C$ at balance. When the sample under test became superconducting the change of inductance of the coil, produced by the Meissner Effect, was detected by change in the balance value of the capacitor. The change of resistance of the coil over the temperature range of the transition was neglible. Phase sensitive detection, which had been used by previous workers. (Robbins et al (1967).) was found to produce little improvement in sensitivity for a great deal of added complexity.

A gold 3% iron versus chromel thermocouple was used, with a liquid nitrogen reference point, having an accuracy of $\pm$ 0.05°K. Calibration tables were checked against the transitions of tin, lead and niobium powder. To further prevent temperature gradients along the sample giving a false reading, the thermocouple junction was wrapped in a strip of copper sheet and each temperature was held for at least three minutes whilst helium exchange gas was maintained at a pressure of approximately 0.15 torr within the sample holder.

Temperatures down to 1.5°K were obtained by pumping over the liquid helium. Temperatures above 4.2°K were reached by means of a heater wrapped around the sample holder. Readings of inductance were made with the temperature rising and also with the temperature falling, the same temperature not necessarily being obtained at the same indicated reading of pressure over the helium. (The pressure indicator was not accurate.) There was no discrepancy outside the experimental errors.

All wires leading to the sample holder were of as large a guage as possible to minimise heat flows.

Fig 3-9 shows a typical result for the superconducting transition of $Cu\ Rh_2\ Se_4$. As has been pointed out in chapter one, the definition of the transition point is the temperature at which half the resistance of the normal state remains. However usually authors quote the temperature at which the transition commences as being the transition temperature T_c (Matthias,

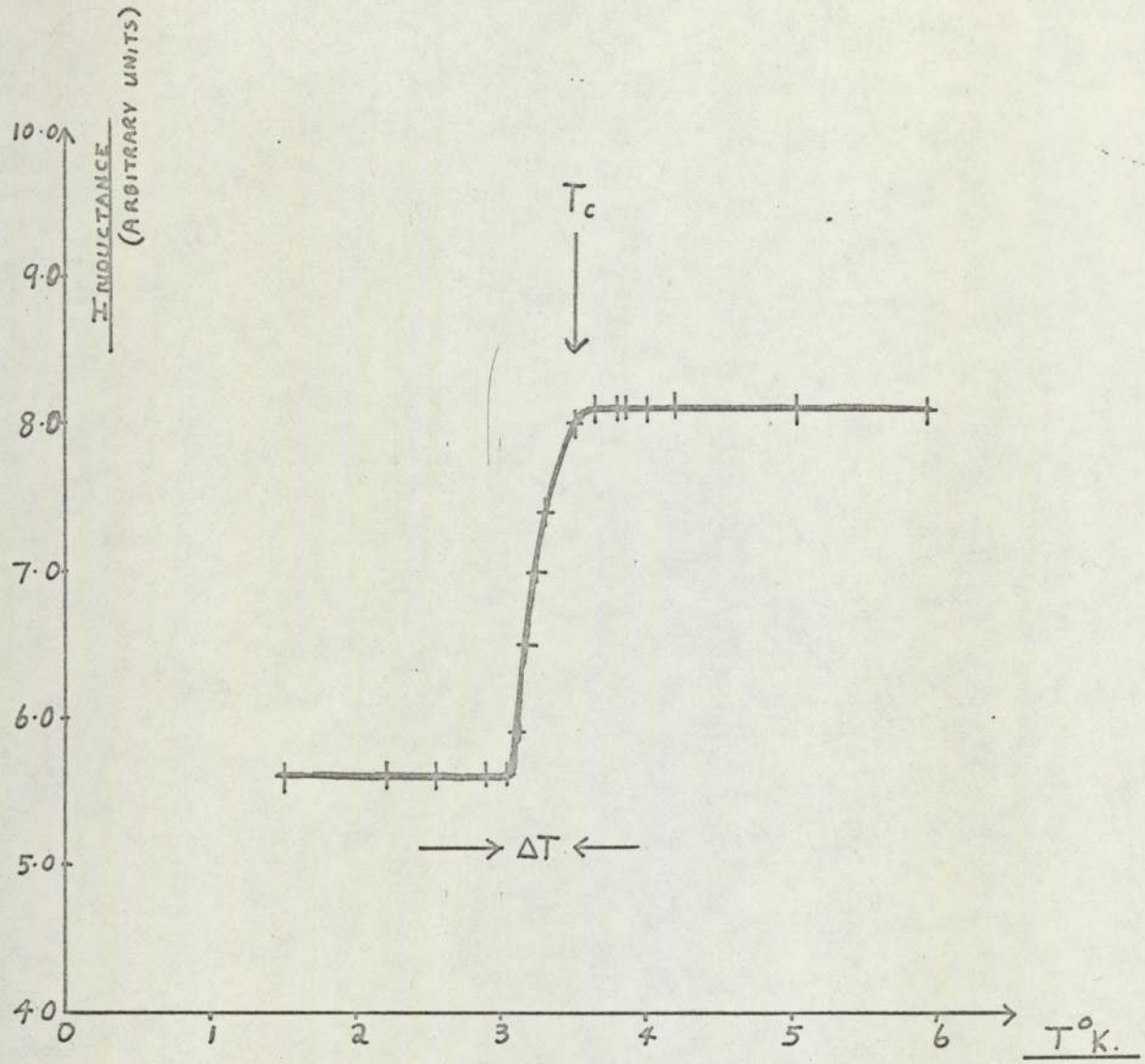

FIG. 3-9 THE SUPERCONDUCTING TRANSITION OF $CuRh_2Se_4$.

Geballe, Geller and Corenzwit, (1954) (Nb_3 Sn); Matthias, Geballe and Compton, (1963).). No doubt this is because it is at this temperature that superconductivity begins. The breadths of the transitions obtained with the spinel compounds under investigation made it difficult to determine the latter; both are given in the results along with approximate values for the widths.

3-4 Electrical Measurements and their Results

Considerable expertise existed within the department in electrical and optical measurements using thin films (less than 1,000 Å thick). Tunneling experiments may yield information about the phonon density of states, in particular the low frequency modes exhibiting strong electron-phonon coupling, as has been used by Zeller (1972). Also, details of the band structure may be determined from Hall Effect and Resistivity measurements. Optical measurements on thin films, particularly in the infra-red region, are capable of yielding information of considerable relevance to superconductivity (e.g. the electron-phonon coupling constant) as has been resently emphasised by Hopfield (1973).

To investigate the electrical properties of the superconducting spinels, thin films were prepared using radio-frequency sputtering, a technique which does not cause dissociation of the molecules. Since previous experiments had shown Cu Rh_2 Se_4 to be the least sensitive to purity and particle size and easy to prepare as a superconductor several films were manufactured (approximately 80) using samples of this spinel.

3-4-1 Thin Films:

Radio-frequency sputtering and in particular the system used in this work, has been described in detail elsewhere, (Jackson (1970), Newman (1973).) Only the more important practical details will be discussed. The basic system is shown in Plate 3-111 and fig 3-10. The Cu Rh_2 Se_4 target was made

PLATE 3.III THIN FILM SPUTTERING RIG.

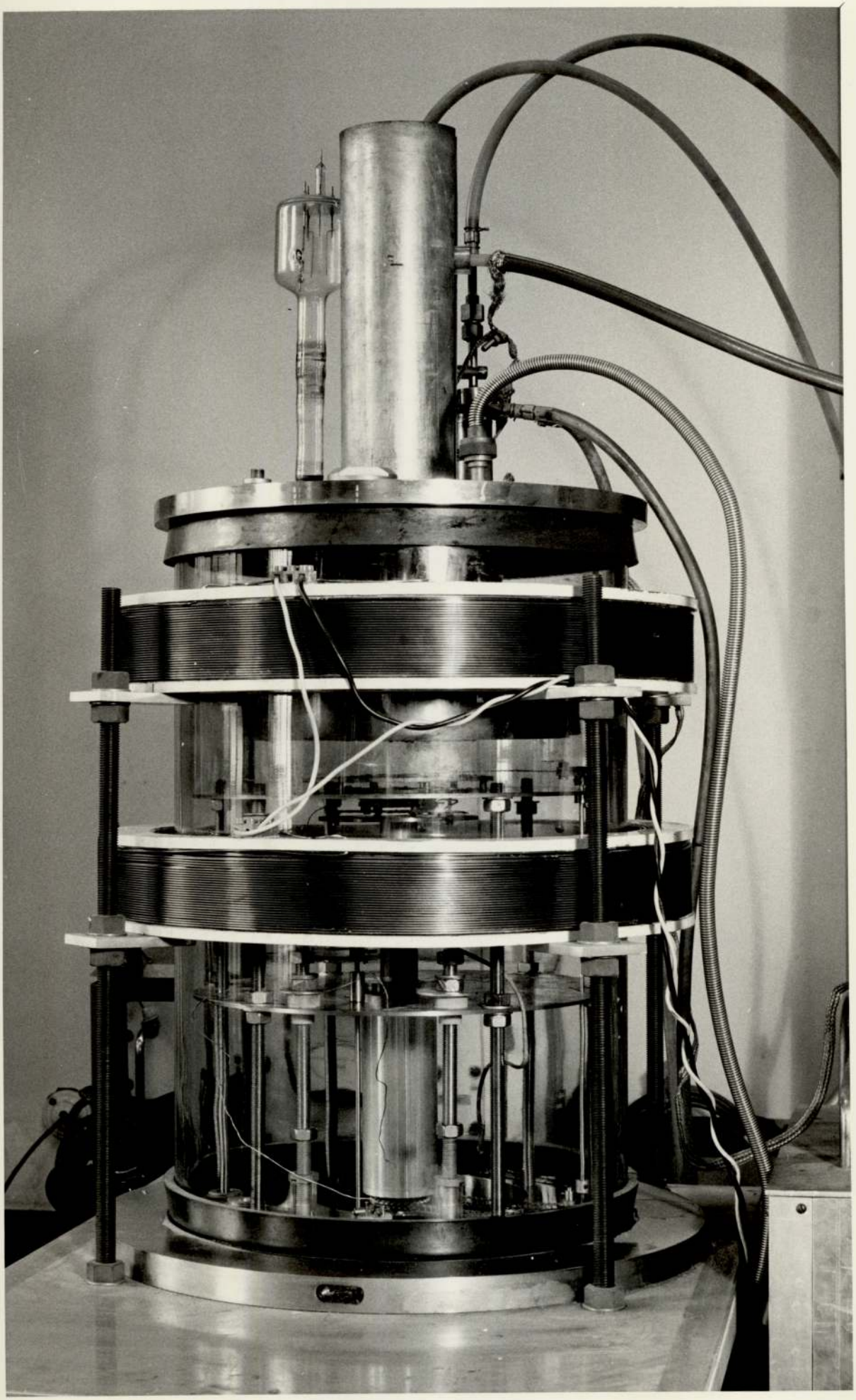

FIG 3·10 NON-GROUNDED DIODE SPUTTERING SYSTEM.

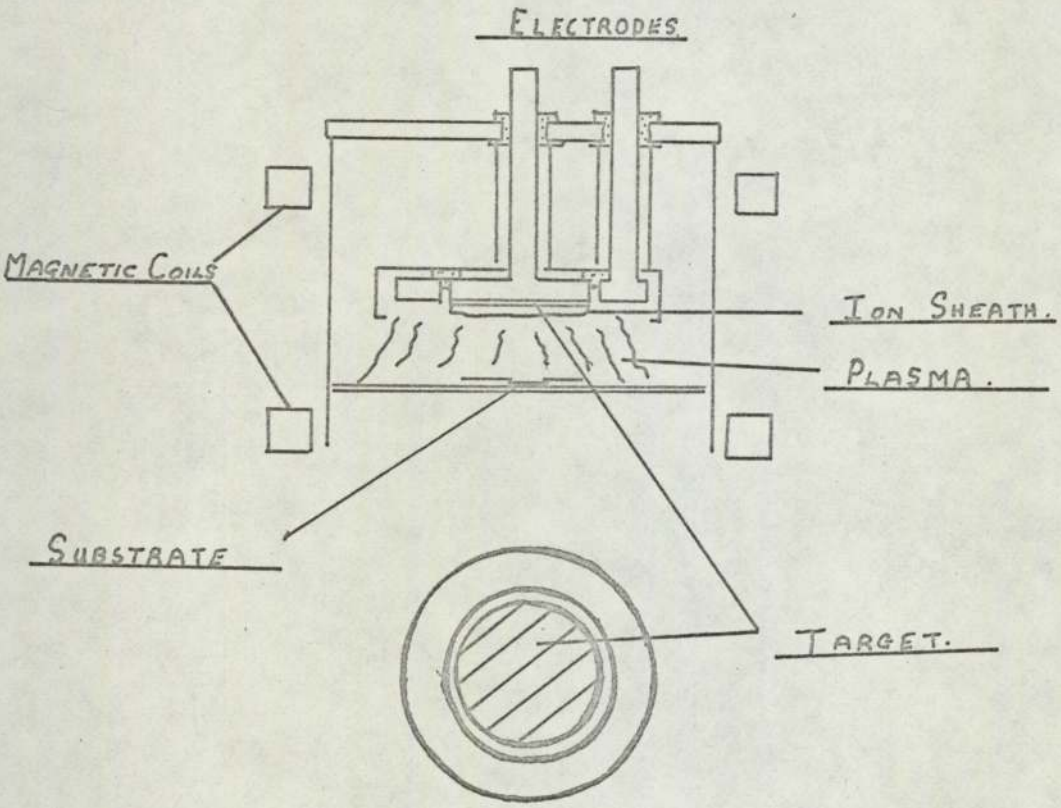

by suspending the powder in glycerine and coating the holder with this suspension. Slow evaporation of the glycerine left a dry powder clinging to the holder and ultra-sonic shaking failed to remove a significant amount. The normal precautions used in preparing thin films were observed (Jackson (1970).). In particular, prolonged sputtering before exposing the substrate, in order to reduce the oxygen content of the films. A range of film thicknesses was produced using plain and 'Van der Pauw' (1958) shaped masks (See Plate 3-IV.)

Electron diffraction through the films gave diffuse rings showing that the sputtered films were very polycrystaline, but nevertheless Cu Rh_2 Se_4. This is the first report that spinels have been prepared directly into thin films.

None of the films showed superconductivity above 1.5°K but the resistivity did fall with temperature indicating the metallic nature of the material. The lack of superconductivity was possibly due to impurity content (long sputtering times (2hrs.) were necessary for thick films of the order of 2,000 Å) or particle size. A range of substrates (e.g. Glass, Na Cl, CdS.) and substrate temperatures were tried, in order to induce epitaxial growth, without success. Heating of the substrate and film, after sputtering, in sealed evacuated silica tubes produced small pools of material and a resulting increase of electrical resistance.

Despite the polycrystaline nature of the films it should be possible to detect the Hall Effect and deduce the electron/molecule ratio (Putley (1960), Van Maaren and Harland (1969).). The phase sensitive detection apparatus shown in Fig 3-11 was used with Van der Pauw shaped sputtered samples. Calibration with zinc, copper and aluminium films showed that the system worked accurately. However none of the spinel samples exhibited a measureable Hall Effect despite complex noise screening allowing detection to below $\pm$ 1 microvolt. Calculations showed that this implied an R_H of $< 10^{-3}$ cm^3. C^{-1} that is an electron/molecule for Cu Rh_2 Se_4 of $>$ 1 electron or hole /

PLATE 3.IV VARIOUS PRESSES AND THIN FILM MASKS

NIMONIC 75 HOT PRESS AND POLISHED DIES WITH HEATER BARS.

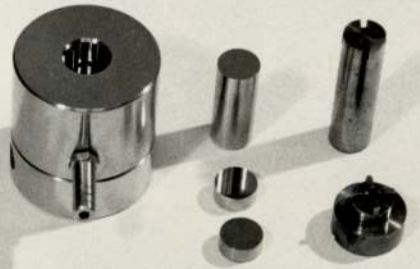

SAMPLE PREPARATION PRESS AND POLISHED DIES. (STAINLESS STEEL)

'VAN DER PAUW' SHAPED DIES. (SILVER STEEL)

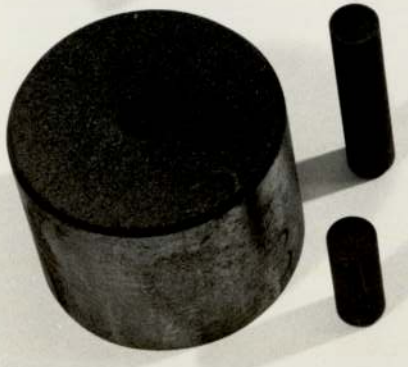

CARBON HOT PRESS.

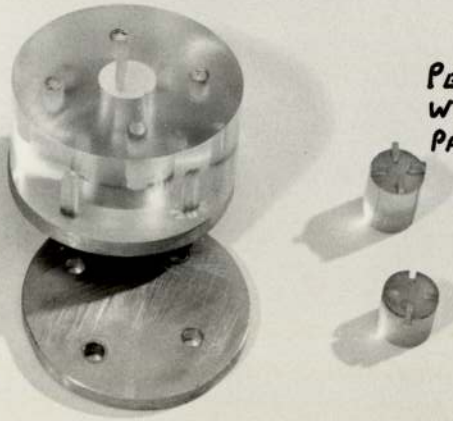

PERSPEX PRESS WITH 'VAN DER PAUW' SHAPED DIES

ALUMINIUM OVERLAY MASK.

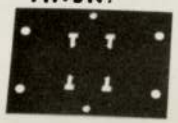

VAN DER PAUW MASK.

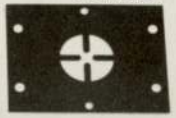

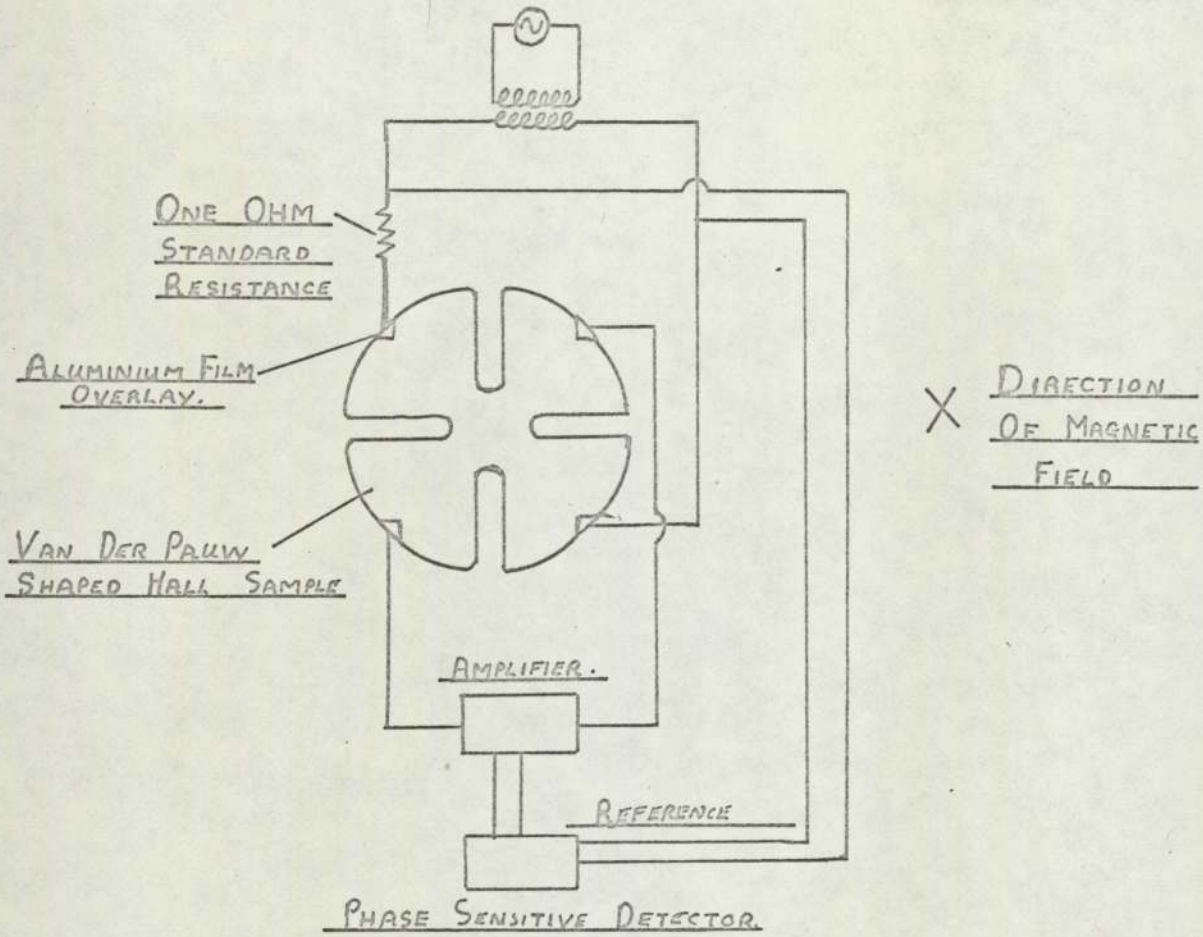

FIG. 3-11 SCHEMATIC DIAGRAM OF HALL EFFECT DETECTOR.

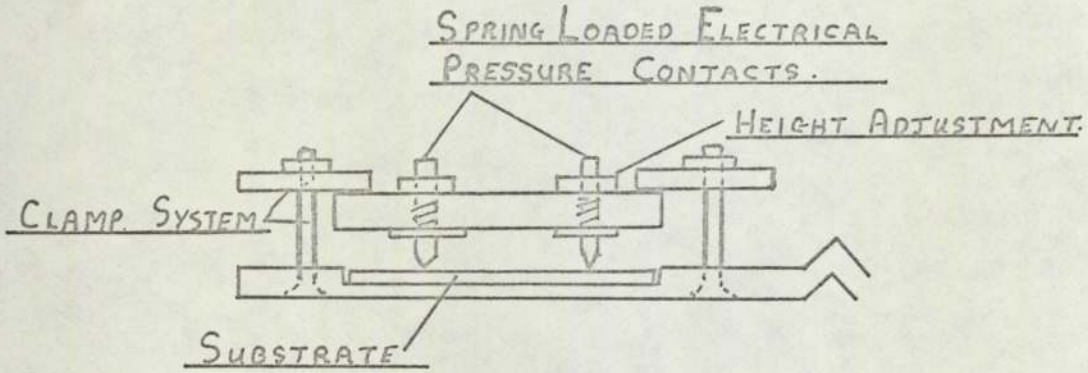

DIAGRAM OF SAMPLE HOLDER.

(NOT TO SCALE)

molecule. Film thickness (500 to 2,000 Å) were measured using multiple beam interfrometric techniques, after overlaying with an aluminium strip. Magnetic fields were measured by a Hall Effect probe and the current through the film was calculated from the voltage drop accross a standard one ohm resistance, measured, using the p.s.d. equipment. These results imply a slightly larger value of the current carriers/molecule than that found by Van Maaren and Harland (1969).

The failure to detect a Hall Voltage in the sputtered films could possibly have been due to the small particle size giving rise to an unusually large amount of grain boundry scattering of the carriers. To increase the grain size sintered compacts were investigated as were used in the work of Van Maaren et al (1967).

3-4-2 Sintered Pellets

Despite the use of various pressures and grinding the spinel powder to different sizes it was not found possible to produce an uncracked, hard spinel pellet which could then be fired in the normal way. It was not possible to use a normal binder since it was desired to make electrical measurements. The British Ceramic Research Association was contacted and agreed to hot press six samples in non-evacuable graphite dies. These were fired at 600°C for 20 mins. at a pressure of about 3,500 KGMS. Five of the samples were elemental mixtures which did not react sufficiently to produce the spinel phase. The other pellet, $Cu\ Rh_2\ Se_4$ was found to be cracked on removal from the die. Although this was still spinel, it was no longer superconducting above 1.5°K, probably due to a loss of selenium or to impurity inclusion.

To reduce cost and to enable complete control of the procedures a stainless steel (Nimonic 75) and a graphite die were purchased from B.C.R.A. (Plate 3-IV). These were not evacuable. High temperatures were obtained using two 1KW. heater bars wrapped around the die. (Again pressures of the order of 3,500 KGMS. were used). The press was protected from the heat by

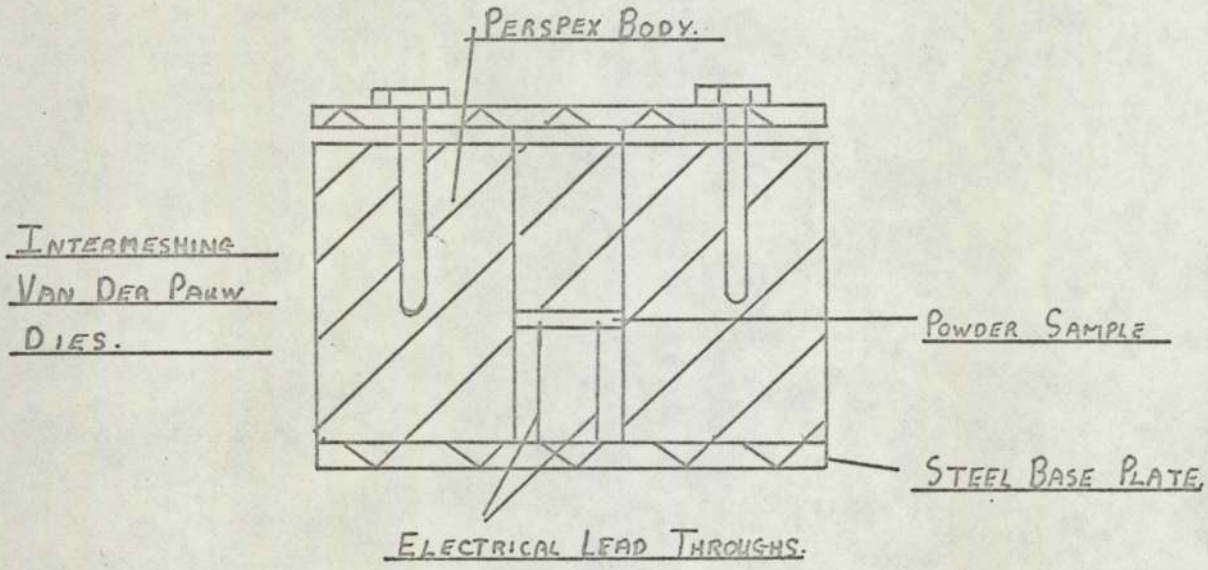

FIG. 3-12. SECTION THROUGH PERSPEX HALL PRESS.

two internally water cooled copper discs and various shieldings. Graphite and fibre spacers were used to wipe the bore of the die clean and avoid jamming.

A relatively hard disc of $Cu\ Rh_2\ Se_4$ was obtained by hot pressing for 30 mins. at 450°C after a build-up time of 1½ hrs. with a pressure of 3,500 KGMS. Constant supervision of the pressure was necessary to prevent it from relaxing.

Hall Effect measurements on this pellet gave similar results to the thin film measurements i.e. $R_H < 10^{-3} cm^3\ C^{-1}$

When the sintering temperature was raised significant chemical reaction took place between the powder (Selenium) and the die (Stainless Steel) causing serious corrosion of the die wall and jamming of the plungers.

Experimentation showed that it was possible to measure the Hall Effect on thin Van der Pauw shaped carbon discs. This work was extended to measure the Effect on a powder whilst it was held in compression. (The apparatus shown in Fig 3-12 and Plate 3-IV was made for this work) The powder was compressed in the perspex die to approximately 1,000 KGMS. the pressure being maintained by the two brass plates. Whilst the results for carbon powder were encouraging, no Hall Effect could be detected for the spinel powder. Eventually the die fractured under the loading.

3-5 Mössbauer Spectroscopy

3-5-1 General Remarks

The Mössbauer apparatus shown in Plate 3-V and schematically in Fig 3-13 was loaned by Birmingham University, where the experiments were performed. The system consists of an oscillating source, an absorber held in a cryostat and a detector linked to a multichannel analyser. (Note that the detector shown in Plate 3-V is a proportional counter and in this work a Na I / photomultiplier was actually used.) Both the recoil-free

PLATE 3V THE MOSSBAUER CRYOSTAT

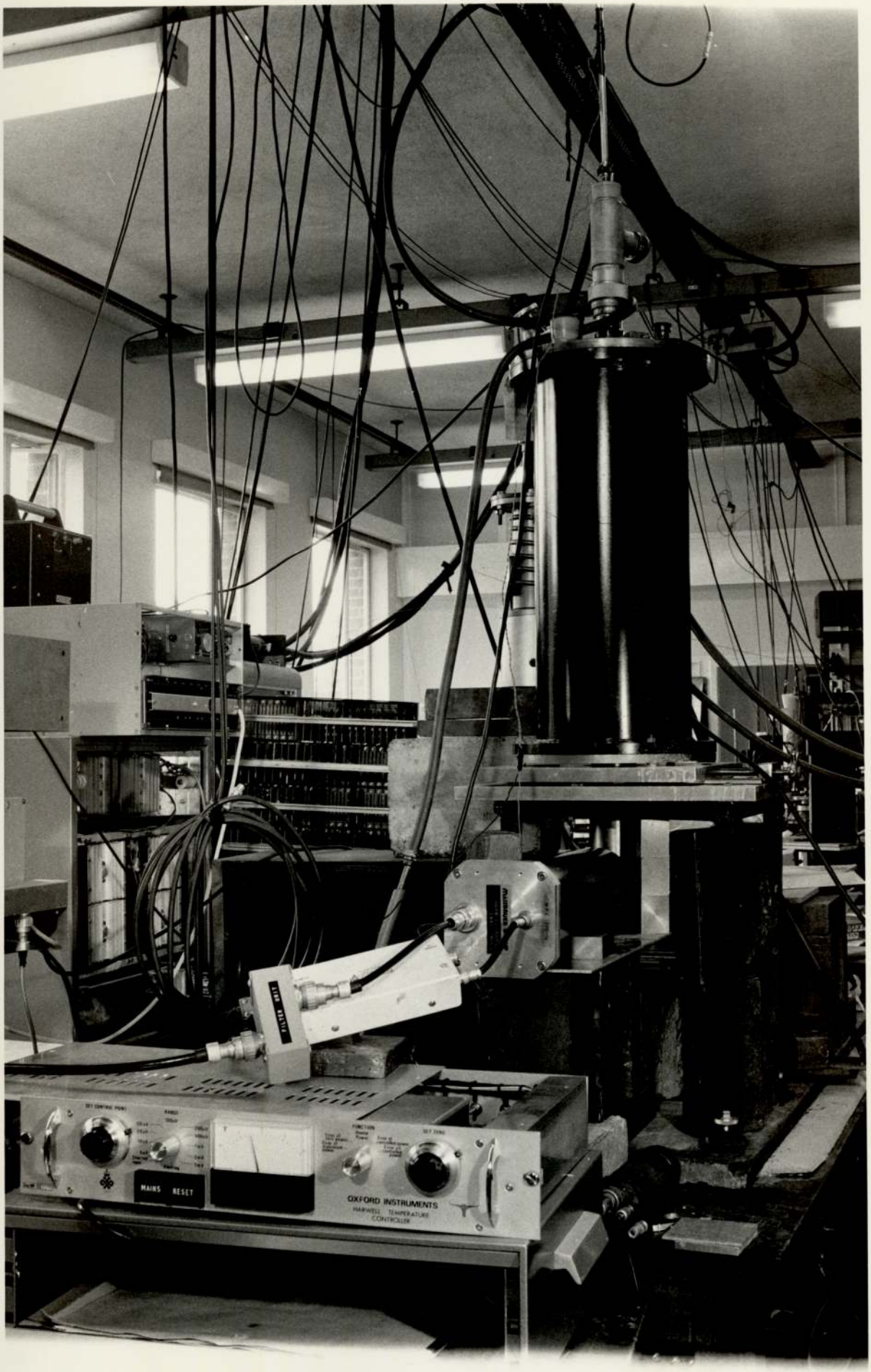

fraction and the total shifts were determined from the same experimental results and the apparatus was set up to give the optimum accuracy.

3-5-2 The Apparatus.

The diagrams, Fig 3-13 and 3-14 illustrate the link between the oscillating source and the abscissae of the multi-channel annalyser. At any instant in time the counts measured are amplified, analysed, (pulse height analysis) and switched into the appropriate channel of the multi-channel analyser. This channel is selected by dividing the velocity spectrum of the 'constant acceleration' source into discrete units, (250 in this case) using each one to define a channel, the velocity difference between each channel being a constant.

Two Sn^{119} gamma-ray sources were used in this work, held at constant temperature ($300^{o}K$). For the first sample ($Cu\ Rh_{2-x}\ Sn_{x}\ Se_{4}$ $x=0.05$) only a relatively weak $Ba\ Sn\ O_{3}$ source was available. This had the disadvantage that a considerable time was required (approximately 24 hrs.) to collect sufficient information, resulting in large errors. A much stronger source (10 microcuries) of $Ca\ Sn\ O_{3}$ was used to study the other absorbers.

The spinel samples were in powder form (less than 60 micrometers) and it was necessary to support them in the gamma-ray beam. The first sample was suspended in Canada Balsam, between two sheets of aluminium foil. Several faults with this method of absorber preparation became apparent. For example:

(i) It was difficult to dry out the Balsam sufficiently to prevent bubbling when the sample holder was evacuated.

(ii) Cracking of the compact occured after temperature cycling to liquid helium.

All other absorbers were prepared by mixing the powder with a small amount of wax binder and pressing into a thin disc (approximately 10,000 KGMS

FIG 3-13 SCHEMATIC DIAGRAM OF MÖSSBAUER SPECTROMETER.

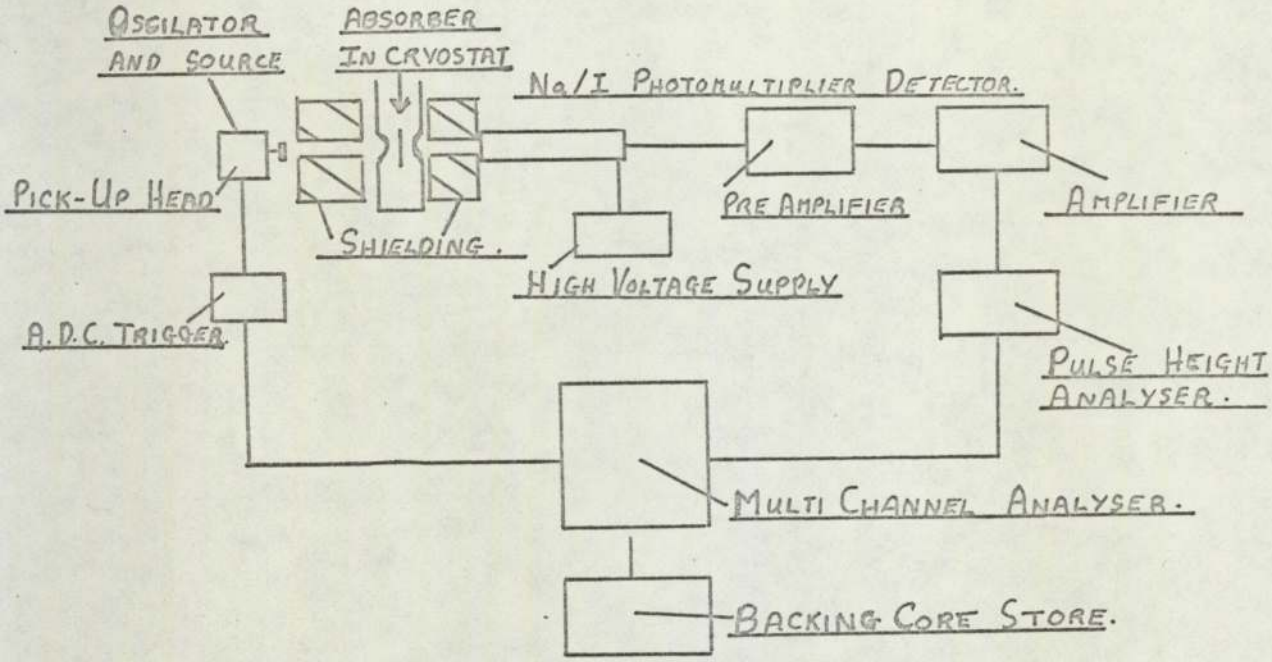

FIG. 3-14 ILLUSTRATION OF VELOCITY CHANNEL SELECTION.

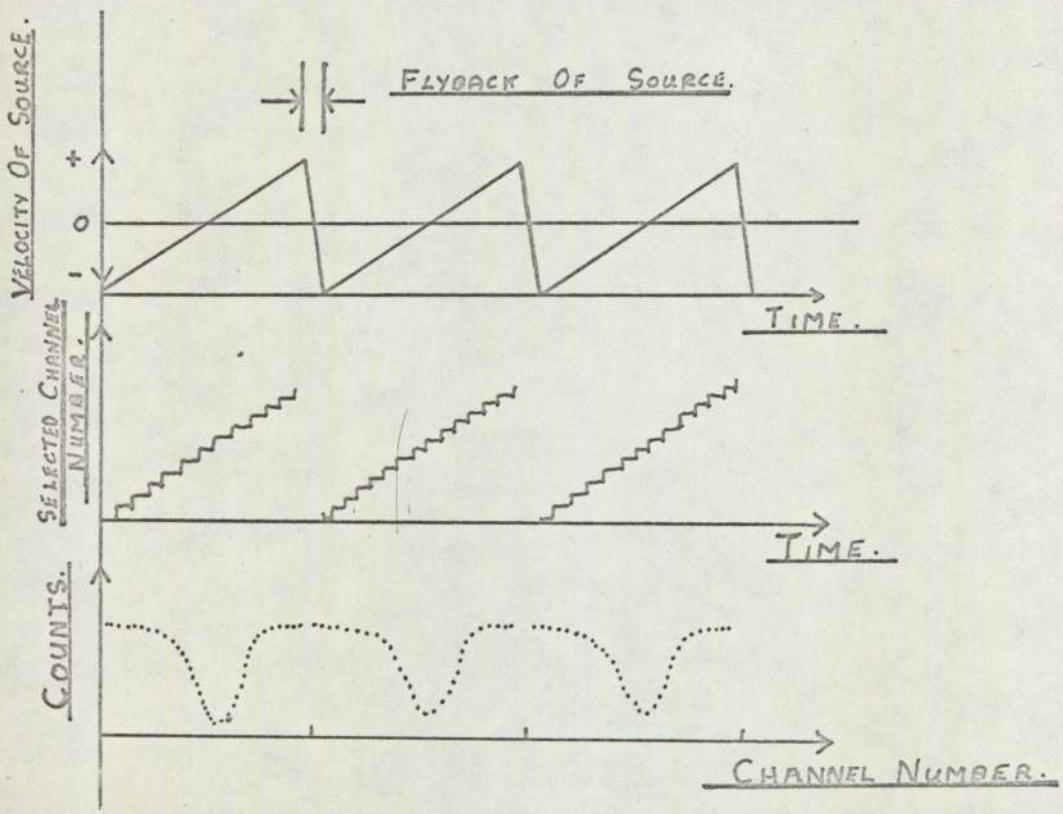

was used). It was not necessary to obtain uniform disribution of the powder but this was attempted in order to optimise the required counting time. The effect of shrinkage on the absorbers cross section as the temperature was lowered, was assumed to be negligable throughout this work.

The cryostat Fig 3-15 was made by the Harwell Mössbauer Group and is designed to hold 3 litres of liquid helium for 3 days. Radiation (heat) shielding of aluminised mylar is used to achieve this, with an initial vacuum of better than 10^{-7} torr.

The sample holder is shown in Fig 3-16 and in Plate 3-VI. The sample and two aluminuim radiation shields were trapped by a brass ring which fitted closely within the heater mounting. A small groove in the ring enabled the thermocouple to be clamped upon the sample without obstructing the beam. The heater wire was silk covered 40 s.w.g. copper of 300 ohms. total resistance, which was wound into the groove and held by araldite. In order to reduce heat loss, the sample support and heater were suspended from a stainless steel framework by cotton threads (See Plate 3-VI). However to enable the rapid cooling of the sample to liquid helium temperature it was necessary to introduce a removable heat leak. This consisted of a thin copper strip which, by means of a bellows unit, (Fig 3-15) could be engaged or disengaged from the brass heater ring. There were problems with leak sealing of the bellows, ensuring that the connecting cable ran smoothly and also ensuring good thermal contact between the strip and the heater ring.

When the stronger source was introduced, it was possible to leave a residual pressure of helium (less than 0.15 torr) in the sample holder to act as a heat exchange gas. This had the disadvantage of increasing the liquid helium boil-off rate at temperatures above $4.2^{\circ}K$, but since the counting time was reduced by a factor of ten when using the Ca Sn O_3 source this method of temperature equalization was to be preferred. The exchange gas was also used to ensure that there were no temperature gradients across the absorbers,

FIG. 3-15 CRYOSTAT WITH SAMPLE HOLDER CAN

NOT TO SCALE.

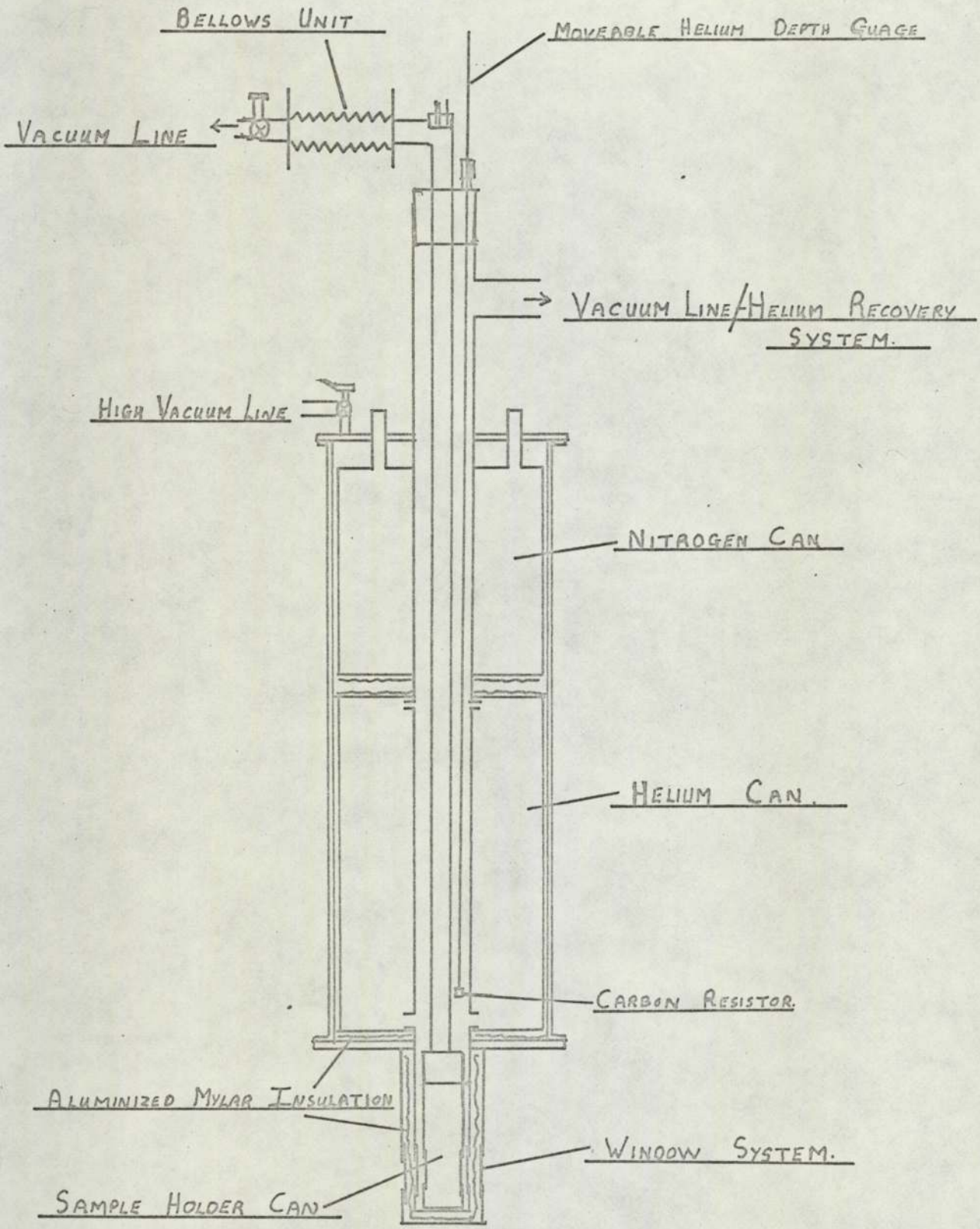

FIG 3·16 SAMPLE HOLDER AND LOW TEMPERATURE CAN (NOT TO SCALE.)

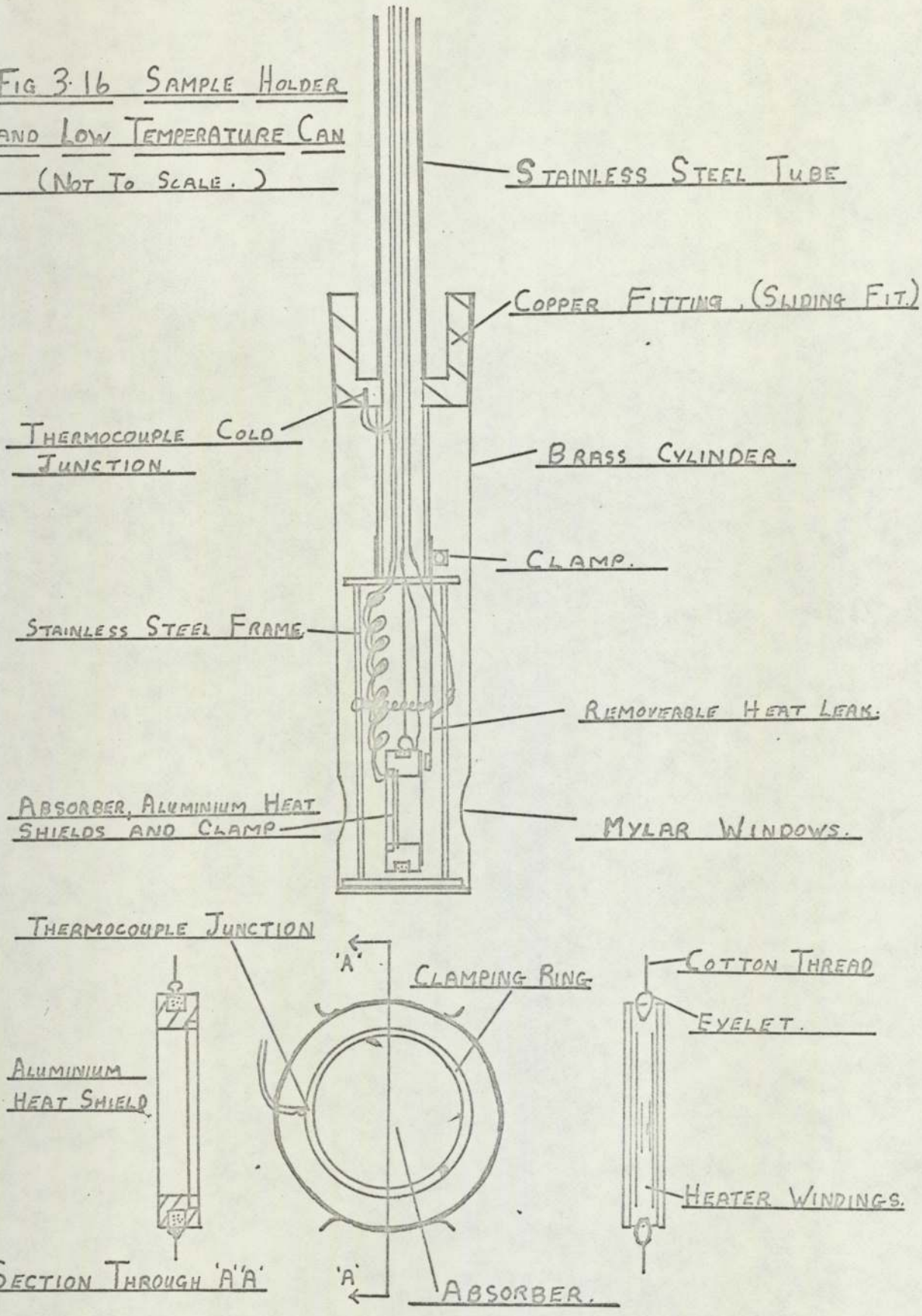

SAMPLE HOLDER.

PLATE 3VI MÖSSBAUER SAMPLE HOLDER

particularly after the introduction of the stronger source. Extra radiation shielding was included around the stainless steel framework and also around the sample support and heater. A check on the presence of such temperature gradients was made by running the whole system at room temperature (293°K) and then at 300°K relative to the nitrogen bath. The results were identical within the experimental error.

An Oxford Instruments 'Harwell' temperature controller was used with temperature control of better than $\pm$ 0.05°K. The gold 3% iron versus chromel thermocouple used, was calibrated at liquid helium and liquid nitrogen temperatures.

3-5-3 Data Handling

The data collected by the multi channel annalyser was punched out onto tape, converted to cards and fed into an existing computer programme in order to annalyse the spectrum. Details of this programme are given in the Ph.D. thesis of M. J. Evans (1971).

A Lorentzian curve was fitted to the data for each temperature (Fig 3-17), corrected for inverse square effect and the values of best fit for the fractional effect, half-width, line position, isomer shift and the counts at infinite velocity I (∞) were calculated by the computer. In fitting a Lorentzian, the assumption is made that the source and absorber are thin, neglecting the naturation effects which can cause line broadening. It has been shown (Shenoy (1974), O'Connor (1963).) that providing $T_a \leq 1$, as is the case here, the error introduced is negligable. The Lorentzians fitted were always within two standard deviations of the experimental points and other possible curves for a Mössbauer Absorption Spectrum (i.e. Gaussian, Voigt) did not give a better fit to the data.

A plot of I (N) versus $\frac{1}{(2N + 1)V}$ (where N is the channel number and V the velocity/channel) in steps of 5 channels produced a straight line at high velocity (O'Connor and Skyrme 1973) which was extrapolated to infinite

FIG. 3-17 MÖSSBAUER ABSORPTION CURVE.

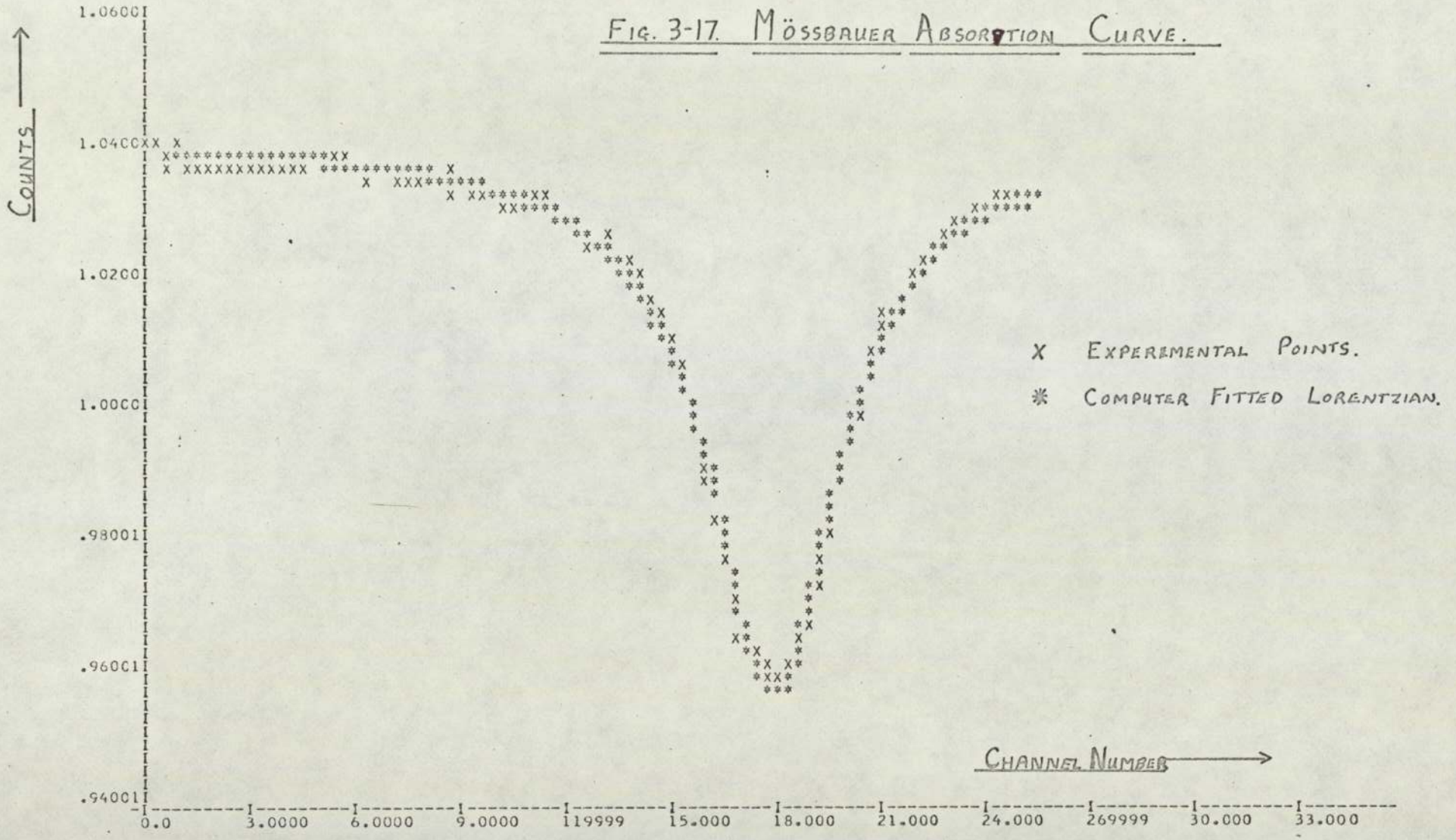

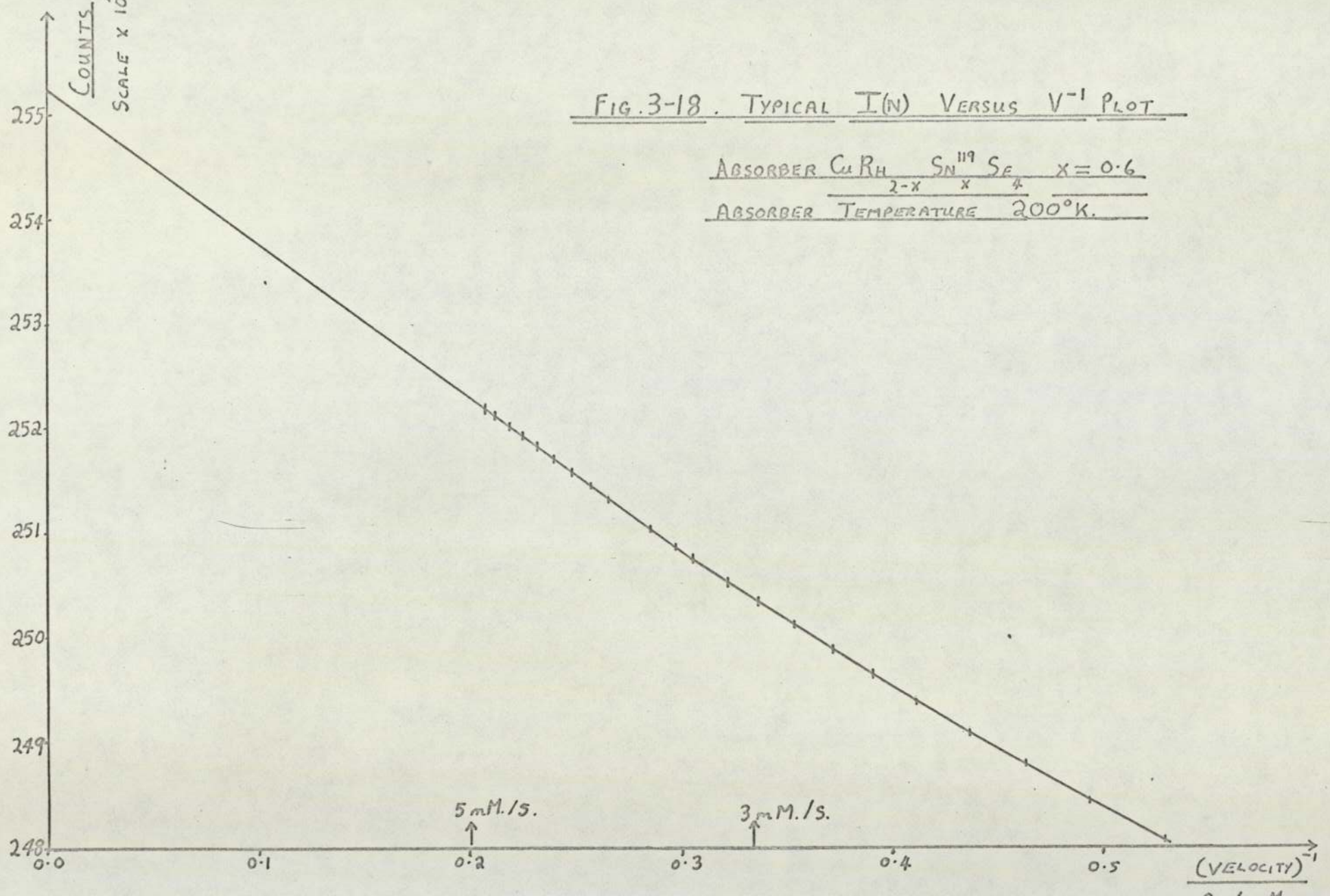

FIG. 3-18. TYPICAL I(N) VERSUS V^{-1} PLOT

ABSORBER $Cu\,Rh_{2-x}\,Sn^{119}_{x}\,Se_{4}$ $x = 0.6$

ABSORBER TEMPERATURE 200°K.

velocity giving accurate values of I (∞) and slope (Fig 3-18). Owing to the large total shift of these absorbers it was necessary, for high accuracy, to assume a symetric Mössbauer spectrum and use values of I (N) from one side only. From I (∞) and the lines' slope the area under the absorption curve was calculated for each temperature and hence T_a. A plot of T_a^{α} versus temperature then gave $Nt\sigma(o)$ for each absorber and hence the absolute recoil-free fractions as a function of temperature. The graphs of T_a exp$^{\alpha}$ versus temperature are given in the results section.

3-5-4 Analysis of the Data

There are a great number of corrections necessary to the observed count rate due to phenomena such as self-absorption and inelastic scattering of X-rays and reference is given to Housley (1965) for a theoretical treatment of these. Nassbaum, Howard, Nees, Stern (1968) and Sitek (1974) have analysed them experimentally and it is clear that other errors in this work are of far greater magnitude. Nassbaum, for example was measuring recoil-free fractions to better than 0.7% accuracy. The following is a list of the major contributions to experimental error considered.

(i) The effect of absorber granularity on the Mössbauer Effect is often ignored, but it has been shown that it can be appreciable when using dispersed powder absorbers. (See Bowman, Kankeleit and Persson (1967). These authors have evaluated the fractional effect and line width for granular absorbers for a range of total resonant thickness and grain thickness, with and without the effects of non-resonant absorbtion being taken into consideration. They find that the fractional effect is a decreasing function of granular thickness and non-resonant absorbtion, whilst the line width is an increasing function of them both. Granular absorbers were used throughout this work and using the somewhat complex

treatment of Bowman et al the relevant factors were calculated approximately. It was concluded that the effects of granularity could be neglected in this work, basically because T_a, the resonant absorption thickness, was so small throughout.

(ii) The recoil free fractions of the sources were measured using the 'Two - Resonant Absorbers' technique of Johnson (1970). This does not require special absorbers as does the 'Black Absorber' technique of Housley, Erikson and Dash (1964) and is independent of source line shape, absorber line shape and velocity independent instrumental broadening effects. For these measurements a Li - drifted silicon detector, and associated electronics, was used in order to separate the tin X-ray peaks, at approximately 24 k eV from the tin gamma-ray peak at 23.8 k eV. By displaying the source radiation spectrum, discriminator levels could be set and the background reduced to a negligible level. It did not matter that some of the X-ray tail was removed (approximately 2% of peak area) since neither Johnson's nor O'Connor and Skyrme's methods are functions of line shape.

A palladium filter could have been used throughout this work to reduce the intensity, from the X-ray peaks, which entered the Na I photomultiplier detector. However this produced X-rays of the same energy as the Sn^{119} gamma-rays and detailed measurements are necessary in order to determine the optimum thichness and position (Sitek (1974).).

The majority of the remaining background radiation, in the source recoil-free fraction measurements, is due to high energy x-rays degraded by Compton scattering and falling into

the 23.8 K.eV window of the detector. The error due to such background has been found to be less than 1% by Sitek (1974). The precautions, such as a constant geometry, suggested by Johnson (1970) were used in this work.

It was found that the strong Ca Sn O_3 source used had a recoil free fraction of 0.51 ± 0.02 in excellent agreement with the Ba Sn O_3 source of Sitek of 0.52 ± 0.01. The weaker Ba Sn O_3 source used in this work initially, was found to have a recoil-free fraction of 0.64 ± 0.02 by a previous worker and comparisons with the Ca Sn O_3 absorber using Johnson's method supported this value. Presumably the difference between the Ba Sn O_3 sources is due to different geometries of the active material. (See Housley, 1965 for details of corrections to recoil-free fraction measurements due to geometrical factors.

(iii) By measuring the recoil-free fraction of the absorbers investigated with both the Li-drifted silicon detector system and the Na I photomultiplier system, the background correction factor for the measured line area was found to be 2.478 with negligible error.

(iv) There are several sources of error in the calculated absorber recoil-free fractions and a discussion of the errors quoted is presented:

1. An error of ± 2% was taken for the recoil-free fraction of the Ca Sn O_3 source.
2. The error in the background correction was assumed negligible.
3. The error in the half-width, from the curve fitting programme was estimated to be less than ± 0.5%.
4. The errors in O'Connor and Skyrmes method can be made very small and these are mainly in the determination of $I(\infty)$ and the high

velocity slope of I (v). A least squares analysis on the linear portion of these curves was made in every case and the maximum error, in the area of the absorption dip, was estimated from the sum of the squares of the deviations from the mean line. This error never exceeded $\pm$ 0.05%.

As it was intended to measure the change in total shift with temperature for an absorber and also between absorbers, it was necessary to compromise between the low velocity per channel required for accurate shift measurement and the relatively high velocity per channel for accurate recoil-free fraction measurements, since there was a large isomer shift between source and absorber. It was apparent from experiments at high velocities/channel that the spectrums obtained were symetrical and therefore a low velocity/channel could be used, with only half the spectrum providing sufficient information to determine the linear region in I (v). In practice it was found that the velocity/channel chosen was adequate to allow the full spectrum obtained to be used, the required linear region being reached, just within the maximum source velocity used.

5. The foregoing sources of error in the source's recoil-free fraction (f_s) produce errors in the values of $Nt\sigma(o)$ causing additional error in the absorbers recoil-free fractions (f_a). Fortunately an error of + 2% in f_s produces an error of only + 1% in f_a via $Nt\sigma(o)$. This must be added to the -2% error in f_a produced directly. The error in f_a due to the error in f_s is therefore half the latter. However the error in the value of T_a produced by the error in f_s is the same as the

error in f_s.

The largest total error in $Nt\sigma(o)$ estimated from a least squares analysis of ln (T_a exp.α) versus temperature was found to be approximately 5% for the first absorber (Cu Rh_{2-x} Sn_x Se_4, x = 0.05), but the stronger source reduced this to less than 2.5% for the others.

The total error in the calculated absorber recoil-free fractions was $\pm$ 5% for the first absorber and $\pm$ 2.5% for the remaining.

6. The absorption curve is not strictly Lorentzian, but it is clear from the literature (O'Connor and Skyrme (1973).) that the error in assuming such a curve is small, particularly when $T_a < 1$ (i.e. when the half-width is twice the natural half-width of the emission line.).

The error in assuming $\sigma(v)$ to be Lorentzian is not known, but this is unlikely to be appreciable with $T_a < 1$. (See O'Connor and Skyrme (1973).).

(v) The errors in the measured total shifts were taken from the standard deviation in the counts given by the Lorentzian curve fitting programme.

CHAPTER 4 RESULTS FROM CRYSTAL STRUCTURE INVESTIGATIONS AND MEASUREMENTS OF TRANSITION TEMPERATURES

"Our work with these compounds, (binary metallics) leads us to conclude that the only genuine hope of going to even higher temperatures (T_c's) lies in turning our attention to ternary systems."

B. T. Matthias (1971)

4.1 The Superconducting Spinels; $Cu\ Rh_2\ Se_4$, $Cu\ Rh_2\ S_4$, $Cu\ V_2\ S_4$

4.1.1. Stoichiometry of Samples

The samples of $Cu\ Rh_2\ Se_4$ prepared and investigated showed no impurity lines in their X-ray diffraction patterns. The limit of detection, for the diffractometer in step scanning mode, is approximately 1% and traces of an impurity found in certain samples were of this magnitude. This impurity was of the $Rh\ Se_{2+x}$ type ($|x| \leqslant 1$), the largest peak (3,1,1) occuring close to the strong 4,4,0 spinel line, whilst the next largest (2,1,0 and 2,1,1) occur in the tails of the strong 4,0,0 spinel line. Samples prepared without flushing the silica tubes with argon, showed upto 10% $Rh\ Se_{2+x}$ concentrations.

Lattice parameters for samples of $Cu\ Rh_2\ Se_4$, prepared with and without residual argon gas within the sealed silica tubes, were identical within the experimental error. This indicates that argon was not being trapped within the spinel lattice. However the presence of argon reduced the impurity $Rh\ Se_{2+x}$ to below detectable limits. Now, according to Dalton's Law of Partial Pressures, the argon would not prevent the escape of selenium gas from the pellet. The most probable explanation therefore is that the thorough flushing with argon removes residual oxygen and thus prevents the formation of copper oxide and maintains stoichiometry. The strongest lines of copper oxide would be hidden by those of the spinel lines, to which they are all close. The cost of rhodium powder prevented extensive investigation of the development of alternative phases. However it was found that the use of argon gas gave consistent purity and crystallographic results.

In the case of $Cu\ Rh_2\ S_4$ spinel, the impurity concentration remained approximately constant despite the use of argon. The foreign diffraction lines bore the same relationship to $Cu\ Rh_2\ S_4$ as $Rh\ Se_{2+x}$ did to $Cu\ Rh_2\ Se_4$ and the presence of an analogous sulphide phase was therefore inferred.

Sulvanite, $Cu_3\ V\ S_4$ was always present in $Cu\ V_2\ S_4$ spinel, despite attempts by many different methods of preparation. In the samples investigated the sulvanite lines were close to the spinel lines and consequently the errors in the derived crystallographic parameters are relatively large. The replacement of some vanadium by small concentrations of tin (~2%) does help to suppress competing reaction leading to the formation of sulvanite.

The precise stoichiometry of the spinels investigated is difficult to establish. For example in the case of $Cu\ Rh_2\ Se_4$, where $Rh\ Se_{2+x}$ was present there may have been corresponding amounts of undetected copper/rhodium selenides which left the spinel phase completely stoichiometric Table 4.1 sumarises the preparation details for the samples investigated. These spinels will form over a range of temperatures, but those stated gave the minimum impurity content. The length of time at the preparation temperature was not found to be critical. Twenty-four hours appeared sufficient in most cases, but seventy-two hours was used as standard. Re-sintering was not found to be possible, as discussed in chapter 3, since the pellets of spinel powdered, after removal from the press.

4.1.2 Determination of Average Crystal Structures

Samples with optimum purity were analysed to determine their crystallographic parameters using the diffractometer in step scanning mode. Values of lattice parameter were calculated using the centroid versus range technique outlined in chapter 3. The Variance-Range technique enabled the calculation of the background intensity correction to the integrated line intensity.

TABLE 4.1

PREPARATION DETAILS OF THE SUPERCONDUCTING SPINELS

SPINEL	TEMP (^{o}K)	TIME (DAYS)	ARGON PRESS. (TORR)	IMPURITY (%)
$Cu\ Rh_2\ Se_4$	600	3	100	$<$ 1% $Rh\ Se_{2+x}$
$Cu\ Rh_2\ S_4$	600	3	100	$\sim$ 1% $Rh\ S_2/Cu\ S$
$Cu\ V_2\ S_4$	500 TO 800	3	100	$\sim$ 8% $Cu_3\ V\ S_4$

According to the theory of X-ray diffraction from powders in the form of thick slabs, the integrated intensity I_{obs} of an (h,k,l) profile, corrected for angular and multiplicity factors is given by;

$$I_{obs} = K/F_{hkl}^{2}/ \exp.\left(\frac{-2B \sin^2\theta}{\lambda}\right) \qquad 4.1$$

(James, 1948)

Where, K is a constant of proportionality $/F_{hkl}/$ is the modulus of (h,k,l) structure factor. (Note, that the real and imaginary corrections to the atomic scattering factors were necessary in this work).

B is the Debye Waller factor, related to a characteristic Debye temperature, θ_D by,

$$B = \frac{6h^2}{mk\theta_D}\left\{\frac{1}{4} + \frac{\phi(x)}{x}\right\} \qquad 4.2$$

Here $x = \frac{\theta_D}{T}$ and $\phi(x)$ is the Debye function

Now for any sample equation 4.1 may be written;

$$\ln\left\{\frac{I_{obs}}{I_{calc}}\right\} = \ln K^1 - \frac{2B \sin^2\theta}{\lambda} \qquad 4.3$$

$$I_{calc} = m.\ LP.\ /F_{hkl}^{2}/ \qquad 4.4$$

m = Multiplicity factor, LP = Lorentz Polarization factor.

Since the spinels are cubic,

$$\ln\left(\frac{I_{obs}}{I_{calc}}\right) = \ln K^1 - \frac{BN}{2a_o^2} \qquad 4.5$$

Where a_o is the lattice parameter

and $N = h^2 + k^2 + l^2$

Thus a plot of $\ln\left\{\frac{I_{obs}}{I_{calc}}\right\}$ versus N gives a straight line for the optimum u-parameter, from which B and hence θ_D may be calculated.

Plots of $\ln (I_{obs}/I_{calc})$ versus N are shown in Figs. 4.1, 4.2, 4.3, using their optimum u-parameters, for the spinels $Cu\ Rh_2\ Se_4$, $Cu\ Rh_2\ S_4$, $Cu\ V_2\ S_4$. The structure factors were calculated using an existing computer

PLOTS OF $LN(I_{OBS.}/I_{CALC})$ VERSUS N FOR THE SUPERCONDUCTING SPINELS

$CuRh_2S_4$ FIG 4.1

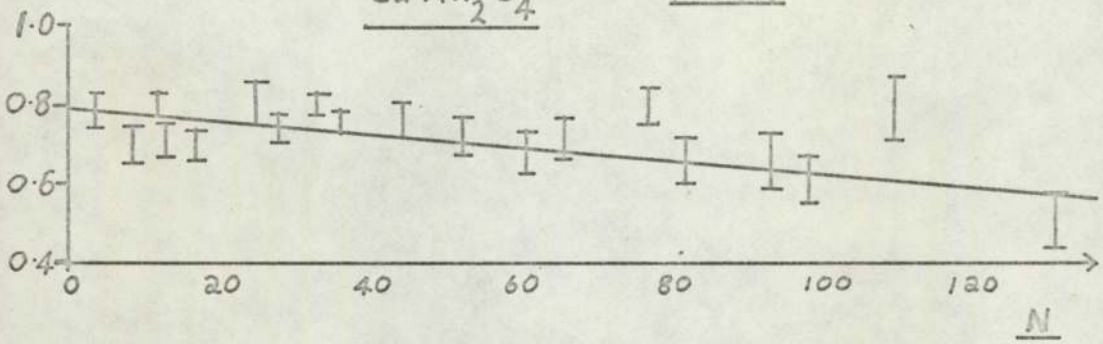

$LN.(I_{OBS.}/I_{CALC.})$

$CuRh_2Se_4$. FIG 4-2

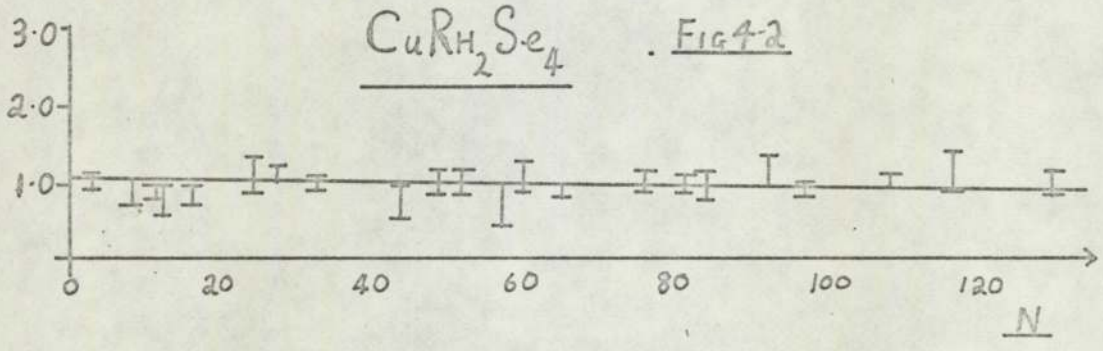

CuV_2S_4 FIG 4-3

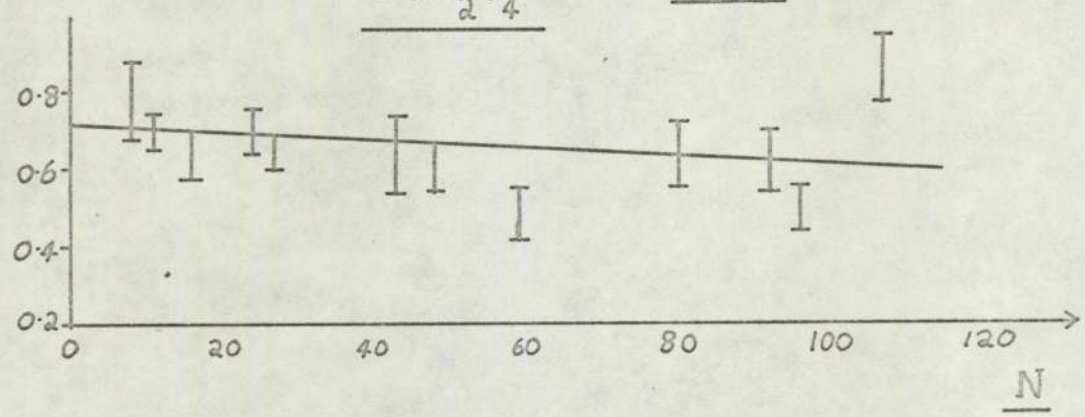

programme modified to make both the real and imaginary dispersion corrections. This programme enabled the calculation of structure factors for both Fd 3m and F$\bar{4}$3m crystal symetries with predetermined amounts of inversion between the octahedral and tetrahedral sites. For all the spinels investigated no amount of inversion was found and the structures were satisfactorily fitted by Fd 3m symmetry. Now, it has been pointed out in chapter one that considerable work has been done detailing those spinels which do not show Fd 3m symmetry and that the question of whether the structure is distorted to F$\bar{4}$3m is important for the mechanism of superconductivity. Therefore the linearity of Figs. 4.1 and 4.2 is striking evidence for the applicability of Fd 3m symmetry.

No corrections were made in this work for Thermal Diffuse Scattering (Willis, 1969), which would not be appreciable, except at very high angles, as the Debye-Waller factors are all very small. It is also to be noted that the exponential absorption correction term in the intensity formula 4.1, is a constant to a good approximation, since the absorption in these spinels is very strong.

Table 4.2 summarises the values of lattice parameter, Debye Waller factor and Characteristic Temperature for the spinels Cu Rh_2 Se_4 and Cu Rh_2 S_4 and Cu V_2 S_4. Table 4.3 records the values of F_{calc} and F_{obs} for Cu Rh_2 Se_4 and Cu Rh_2 S_4 with their residual factors. F_{calc} is in absolute electron units and F_{obs} has been scaled to F_{calc} using K^1 calculated from equation 4.5 and the appropriate Debye-Waller factor.

The errors shown in Figs. 4.1, 4.2, 4.3 are mainly due to the necessity to estimate backgrounds for some diffraction peaks. For high intensity peaks a standard deviation error is given. Large errors are recorded where adjustment has been made to allow for overlapping foreign phase lines. The results for Cu V_2 S_4 contain relatively large errors because of the large impurity content and since it was also not found to be superconducting, a

TABLE 4.2

X-RAY RESULTS FOR THE SUPERCONDUCTING SPINELS

SPINEL	PARTICLE SIZE (Å) ± 500 Å	LATTICE PARAMETER (Å) AT 25°K ± 0.0005	u ± 0.001	B ($Å^2$) ± 0.1	Θ_0 (°K) ± 50°K
$CuRh_2Se_4$	5,500	10.2603	0.384	0.1	675
$CuRh_2S_4$	2,750	9.7877	0.384	0.2	550
CuV_2S_4	6,000	9.795 (± 0.001)	0.382	-	-

TABLE 4.3

THE RESIDUAL FACTORS FOR $Cu\ Rh_2\ Se_4$ AND $Cu\ Rh_2\ S_4$

	$Cu\ Rh_2\ Se_4$			$Cu\ Rh_2\ S_4$		
h,k,l	F_{calc}	F_{obs}	$/F_{calc}-F_{obs}/$	F_{calc}	F_{obs}	$/F_{calc}-F_{obs}/$
111	273.0	272.6	0.4	229.6	224.5	5.1
220	195.3	184.7	10.6	187.8	176.5	11.3
311	400.9	376.6	24.4	410.4	404.5	5.9
222	254.6	225.4	29.2	214.5	204.4	10.1
400	1,205	1,115	90	741	698	43.5
422	149.3	159.2	9.9	152	153.5	1.5
440	1,341	1,353	12.0	923.6	928.5	4.9
531	205.8	251	45.0	169.3	169.2	0.1
533	322	286	36.0	321.5	323	2.5
444	933	951	17.8	577.5	585.6	8.1
551/711	330	340	9.6	236.9	237.4	0.5
642	147.3	132.3	15.0	-	-	-
800	1,085	1,050	35.0	767	778	11.0
840	781	803	22.0	509.4	512.2	2.8
931	364.7	418	43.6	301.7	310.2	8.5
844	924.3	933	8.4	668.0	694.9	26.9
953	284.4	281	32.5	-	-	-
880	845.6	892	46.0	595.5	589.5	6.0
	Residual Factor = 4.9%			Residual Factor = 2.2%		

detailed analysis of this spinel was not carried out.

4.1.3 Particle Size

An approximate measure of particle size is possible from the breadth of the diffraction lines(International Critical Tables (1965).). Assuming that other forms of broadening (e.g. strain) are negligible, then the Integral Breadth (D) due to particle size is related to the average particle dimensions in units of interplanar spacing (Ld) by;

$$B = \frac{\lambda}{Ld \cos \theta}$$

B is defined as the total integrated intensity divided by the peak intensity. For integral multiples of h,k,l, $\frac{B \cos \theta}{\lambda}$ is a constant if only particle size broadening is present.

The Variance-range function may be used to measure the particle size very accurately. However, in this work only an order of magnitude figure was necessary to indicate any possible influence of particle size on T_c. Therefore the more rapid Integral Breadth technique was used.

The results of particle size calculation are given in table 4.2. It appeared to be the major source of line broadening.

4.1.4. Transition Temperatures

The transition temperatures were measured by the technique outlined in section 3.3, where a typical transition for a Cu Rh_2 Se_4 sample is shown (Fig. 3.9). Table 4.4 lists the results for Cu Rh_2 Se_4, Cu Rh_2 S_4 and Cu V_2 S_4 along with the results of other authors.

Note, that the Cu Rh_2 S_4 sample has a lower T_c than that found by other authors and also that the transition width ΔT_c is large. This may be due to impurity content or poor stoichiometry or the relatively low particle size for Cu Rh_2 S_4 (Table 4.2). Particle size effect are indeed well known (Salter, (1973).) but normally occur only below the order of hundreds of Ångstroms

TABLE 4.4

T_c RESULTS AND COMPARISON WITH OTHER WORKERS

SPINEL	MEAN TRANSITION TEMPERATURE T_m (^oK)	ΔT_c (^oK)	T_c FOR INITIAL ONSET OF SUPERCONDUCTIVITY (^oK)			
			PRESENT WORK	VAN MAAREN (1967)	ROBBINS ET AL (1967)	SCHAEFFER ET AL (1968)
$CuRh_2Se_4$	3.25	0.5	3.5	3.49	3.50	3.48
$CuRh_2S_4$	3.7	0.7	4.1	4.80	4.35	4.37
CuV_2S_4	-	-	<1.5	4.45	-	-

NOTE: The T_c values given by Schaeffer et al (1968) arise from heat capacity measurements. The other results are from experiments utilizing the Meissner and Oschenfield phenomena.

and therefore this explanation is not likely to apply here. A later sample of $Cu\ Rh_2\ S_4$ had a T_c of 4.7^oK and ΔT_c of 0.4^oK. There was no apparent reason for this as there was no discernable change in preparation technique or crystallographic parameters.

Neither preparation temperature (between 550^oC to 1000^oC.) nor impurity content (upto 10% investigated) had any effect upon T_c or ΔT_c for $Cu\ Rh_2\ Se_4$. However they varied markedly (upto $\pm\ 0.7^oK$ and $\pm\ 0.2^oK$ respectively) between samples of $Cu\ Rh_2\ S_4$ in a manner which could not be related to the variables being controlled.

4.1.5 Discussion

The comparisons in table 4.5 indicate a wide variation in the experimental T_c's found for $Cu\ Rh_2\ S_4$ and this presumably is associated with its sensitivity to preparation. There is a marked contrast for example with the relative consistancy of the observed T_c for $Cu\ Rh_2\ Se_4$.

Further there is a large difference between the Characteristic Temperatures (θ_D) measured by heat capacity experiments and from these X-Ray Diffraction Experiments. θ_D is also larger for the selenide than the sulphide according to the latter, whilst the opposite is true according to the former experiments. These apparently ambiguous results are, in fact, rather informative. Large X-ray θ_D values imply high phonon frequencies and a relatively rigid lattice, since X-rays measure an average over the whole lattice, which mainly consists of the anion cages. The X-ray results therefore imply rigid anion cages. On the other hand the heat capacity results imply low phonon frequencies, which in conjunction with the X-ray results, indicates that the cations must be relatively loosely bound within the rigid anion cages. For $Cu\ Rh_2\ S_4$, the results imply that the cage is less rigid and the cations more loosely bound than for $Cu\ Rh_2\ Se_4$. That is to say that the $Cu\ Rh_2\ S_4$ is less stable. Indeed $Cu\ Rh_2\ S_4$ is more difficult to prepare and, it must be noted, also has the higher T_c.

TABLE 4.5

SUMMARY OF CRYSTALLOGRAPHIC PARAMETERS

	$Cu\ Co_2\ S_4$	$Cu\ Rh_2\ S_4$	$Cu\ Rh_2\ Se_4$
T_c (^oK)	NONE ABOVE 0.5^oK	4.07 ± 0.05	3.50 ± 0.05
LATTICE PARAMETER a_o (Å) AT 25^oC	9.478 ± 0.001	9.7877 ± 0.0005	10.2603 ± 0.004
'u' PARAMETER	0.388 ± 0.001	0.384 ± 0.001	0.384 ± 0.001
OCTAHEDRAL SITE NEAREST NEIGHBOUR DISTANCE 'P' (Å)	2.253	2.362	2.476
IONIC RADIUS OF OCTAHEDRAL ION. (Å) AHERNS (1952)	0.63	0.68	0.68
IONIC RADIUS OF ANION (Å) AHERNS (1952)	1.84	1.98	1.98
'P' USING IONIC RADII (Å)	2.47	2.52	2.66
θ_D (X-RAY) (^oK)	-	550 ± 50	675 ± 50
θ_D (HEAT CAPACITY) (^oK) SCHAEFFER ET AL (1968)	-	230^oK	218

NOTE: $Cu\ Co_2\ S_4$ details from Williamson and Grimes (1974) and Van Maaren et al (1967)

It has been pointed out that many spinels have structural distortions associated with the octahedral sites and that these spinels are fitted by the $F\bar{4}3m$ symmetry. The superconducting spinels however have been easily accounted for on the basis of Fd 3m symmetry. Presumably the potential conditions at the octahedral sites have been modified by good electrical conductivity. This lack of structural distortion coupled with the Characteristic Temperature observations indicate that instability may be located at the octahedral sites. Unfortunately, relative ionic radii are not able to determine the "space available" at the octahedral site (Table 4.5). The situation is clearly more complicated than a 'hard sphere' model allows. However it is striking that the metallic non-superconducting spinel $Cu\ Co_2\ S_4$ has a relatively small octahedral volume, in fact its lattice parameter is amongst the smallest known for sulphide spinels. Its lack of superconductivity is possibly correlated with this fact.

Now, Van Maaren et al (1970) have shown that the spinel superconductors are best described as strong-coupled and since the mechanism responsible for superconductivity in these compounds appears so similar to that of the β-W and NbN groups, it is reasonable to conclude that the spinels are the first truly ternary compounds for which the high T_c mechanism holds. We may therefore use McMillan's formula (Equation 1.9) to calculate λ, the electron phonon coupling constant for $Cu\ Rh_2\ Se_4$, since $\mu^* = 0.13$, (Van Maaren et al (1970).) and Θ (specific heat) = 218°K (Schaeffer (1968).) may be used as the average phonon temperature. This gives $\lambda = 0.63$ and hence T_c MAX for the spinel group of compounds of 13°K, which is nearly three times as high as $Cu\ Rh_2\ Se_4$ (Dawes and Grimes (1975).). It must be noted that in McMillans equation for T_c, the phonon term (Θ) is a dominant factor in the exponent. This may not be generally true and the extra degree of freedom available in the ternary spinels may relax the restrictions on T_c MAX inherent in simpler systems. That is to say, that the average phonon frequency may possibly be reduced far further in the spinels before

instability forces it to change its crystal structure.

These predictions are born out by the recent discovery by Johnston, Zacharrasen and Viswanathan (1973) that the spinel $Li_{1+x}\ Ti_{2-x}\ O_4$ ($-0.2 < x < 0.33$) becomes superconducting as x tends towards zero, with a range of T_c's from 7^oK upto a maximum of 13.7^oK. This is not only by far the highest temperature superconducting oxide known, but also the lowest density superconductor in existance.

4.2. Experiments on Related Compound Series

4.2.1 General remarks

The indication that the spinel's octahedral site may provide the same mechanism for superconductivity as that which is present in the NbN and β-W systems, led to attempts to study this site using X-ray diffractometry. Now, Matthias had indicated the importance of the electron/atom ratio in deciding whether a material is a superconductor or not and therefore initial experiments were designed to maintain the existing electron/atom ratio by substituting Cobalt for Rhodium. Several spinels and spinel series were prepared and analysed but all of them suffered from contamination by competing phases, with resultant impurity and stoichiometry problems.

4.2.2. Results from Investigated Series

$$Cu\ Rh_{2-x}\ Co_x\ S_4$$

Despite the ease of preparation of the end members of this series, intermediate compounds were invariably contaminated with a Co/Rh S_2 phase. Within the limits of detection (1.5^oK), superconductivity disappeared for $x \geqslant 0.1$.

$$Cu\ Rh_{2-x}\ Co_x\ Se_4$$

For $x < 0.5$ this series retained superconductivity (above 1.5^oK) and was relatively free from impurity phases and therefore presumably close to stoichiometry. For $x = 0.75$ the impurity phase concentration rose to $\sim 25\%$.

Despite many different preparation techniques, (including, high ($\sim$1200°C) and low ($\sim$ 400°C) temperatures, quenching experiments (e.g. 1200°C down to liquid nitrogen) and hot pressing), the series end member Cu Co_2 Se_4 would not form Co Se_2 being the only product. The impurity phase of this series was Co/Rh Se_{2+x}, the diffraction lines shifting from those of Rh Se_{2+x} at $x = o$ to those of Co Se_2 for x = 2.0.

For the region in which the concentration of impurity phase was less than 10% (i.e. x=0.5) lattice parameters were determined using the centroid versus range technique. Fig. 4.4 shows the change of transition temperature with lattice parameter for these compounds. A small change of inductance in the x = 0.4 sample at about 1.8°K indicated a possible transition below the 1.5°K experimental limit.

Preliminary investigations indicated that the Debye-Waller factors of these compounds were similar to that of Cu Rh_2 Se_4, but detailed investigation was not attempted because of the strong impurity phase and the resulting lack of reliability in the stoichiometry of the spinel phase. It was also not possible to determine whether the cobalt was substituting for rhodium or displacing copper, since copper and cobalt have nearly equal scattering factors and the concentration of cobalt was very small relative to the rhodium:

$$\underline{Cu\ Rh_2\ Se_{4-x}\ S_x}$$

This series was investigated briefly and the results are shown in table 4.6. Impurity phases were very low (less than 5%) compared to other series and were of the Rh $(Se/S)_{2+x}$ type. The lattice parameters do not appear to obey Vegard's law (Fig. 4.5). The large errors are due to the calculation of the lattice parameters from chart recordings rather than step-scanning and the centroid range technique. These samples were prepared at a relatively early stage in this work and the lack of superconductivity in some samples is probably not significant.

FIG. 4-4 T_c VERSUS a_o $CuRh_{2-x}Co_xSe_4$.

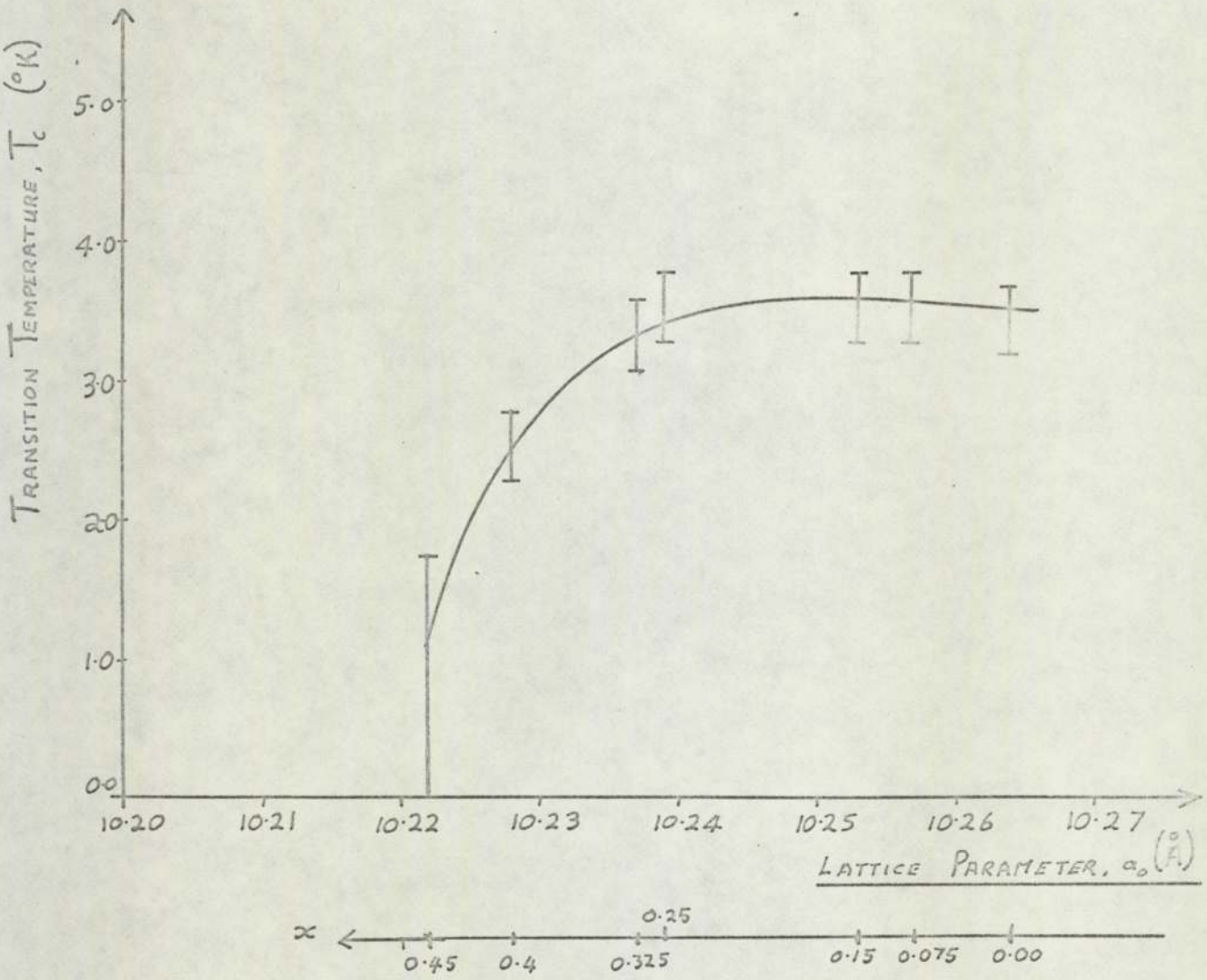

TABLE 4.6

RESULTS FOR $Cu\ Rh_2\ Se_{4-x}\ S_x$

x	LATTICE PARAMETER a_o (Å)	T_c (^oK)
	± 0.05	± 0.25
0.0	10.263 ± 0.005	3.5
0.25	10.15	3.45
0.5	10.02	2.0
1.0	10.00	3.6
1.5	9.58	1.5
2.0	9.54	3.17
4.0	9.787 ± 0.005	3.95

NOTE: The samples for x = 0.0 and x = 4.0 are not those that were used in experiments which produced the results in table 4.2. Note also the large errors, (See text).

FIG. 4-5 a_o VERSUS X

$CuRh_{H_2}.S_{\mathbb{Z}_{4-X}}S_X$.

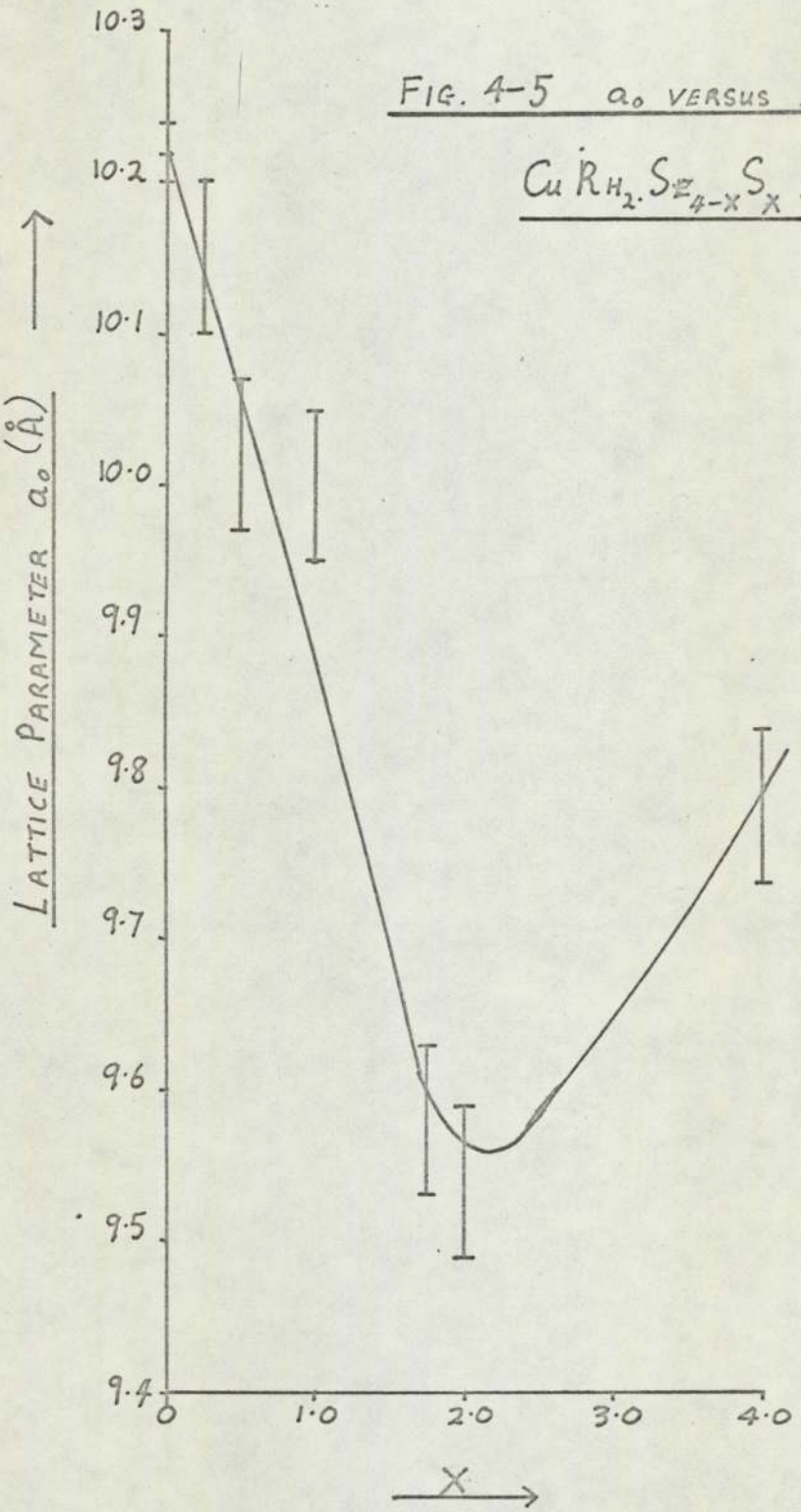

TABLE 4.7

DETAILS OF OTHER SPINELS PREPARED

SPINEL	T_c (°K)	PURITY
$CuIr_2Se_4$	NONE OBSERVED ABOVE 1.5°K	NO IMPURITY PHASE DETECTED
$CuRh_{2-x}Ir_xSe_4$ $x = 0.1$	3.6°K BROAD TRANSITION	UNIDENTIFIED PHASE ~2%
$CuRh_2Te_4$	COULD NOT BE PRODUCED	
CuV_2Te_4		
$CuNb_2S_4$		
CuV_2Se_4		
$Cu_{1-x}Ag_xRh_2Se_4$ $x = 0.1$	NONE OBSERVED ABOVE 1.5°K	NO IMPURITY PHASE DETECTED
$Cu_{1-x}Au_xRh_2Se_4$ $x = 0.1$	NONE OBSERVED ABOVE 1.5°K	NO IMPURITY PHASE DETECTED

4.2.3. Other Spinels

Table 4.7 gives brief details of other spinels prepared and analysed during the course of this work.

4.2.4. Some Conclusions

The poor purity and the associated lack of stoichiometry make it difficult to draw sharp conclusions from the samples investigated. The indications are however that $Cu\ Rh_2\ Se_4$ will allow a certain amount of alteration in its octahedral site occupant (Rhodium) without loss of superconductivity or stoichiometry.

The problem of ascertaining the position of substituted atoms was highlighted. Indeed retention of superconductivity in the series $Cu\ Rh_{2-x}\ Co_x\ Se_4$ may have been because cobalt was replacing copper rather than rhodium. That is that the spinel phase formed could have been $Cu_{1-x}\ Co_x\ Rh_2\ Se_4$. However the series $Cu_{1-x}\ Ag_x\ Rh_2\ Se_4$ and $Cu_{1-x}\ Au_x\ Rh_2\ Se_4$ lost superconductivity at $x = 0.1$, indicating the importance of tetrahedrally positioned copper to superconductivity.

The preparation problems found, further serve to illustrate the instability of these compounds.

4.3 X-Ray Diffraction Data for Samples Investigated By Mössbauer Spectrometry

4.3.1 Introduction

Following the work described in the preceeding sections, which had indicated the possible presence of a lattice instability at the octahedral sites, more direct information was desirable. It was decided to use Mössbauer Spectrometery since this allows the study of atoms in specific crystal sites. However the crystallography of the Mössbauer absorbers had to be examined in some detail in order to establish that:

(i) The Mössbauer atom was in the correct site.

(ii) There were no other tin containing phases present.

(iii) The spinels prepared were superconductors.

It was also valuable to gain as much information as possible about the absorbers using X-ray diffraction.

The most suitable Mössbauer atom for this work was tin, since the series Cu Rh_{2-x} Sn_x Se_4 had already been investigated by Van Maaren (1969) and found to retain superconductivity below x = 0.5. Iridium could also have been used but it is extremely expensive and a source was not readily available. Iron could also have been used since cobalt is the precursor, but the impurity phases present in Cu Rh_{2-x} Co_x Se_4 and the uncertainty regarding the position of the cobalt made this a less satisfactory experiment.

4.3.2 Crystallographic Data and T_c's.

The two series Cu Rh_{2-x} Sn_x Se_4 and Cu Rh_{2-x} Sn_x S_4 were prepared, using tin enriched in the 119 isotope, for Mössbauer investigation of the octahedral site. X-ray diffraction and T_c results are given in Table 4.8. A typical plot of inductance versus temperature is shown in Fig 4.6. Lattice parameters were calculated using the centroid-range technique, however the accuracy was not as high as the earlier work owing to lower count rates. A plot of a_o versus x (Fig. 4.7) shows slight deviation from Vegard's Law. Fig 4.6 shows a plot of T_c versus composition for Cu Rh_{2-x} Sn_x Se_4. Figs. 4.8 to 4.13 show plots of ln (I_{obs}/ I_{calc}) versus N for all the samples investigated. Debye-Waller factors (B) and Characteristic temperatures (θ_D) were calculated. Here the large errors in these quantities are again due to the low value of gradients. Table 4.9 shows preparation details. Impurities, where present, were of the same type as appeared in Cu Rh_2 Se_4 and Cu Rh_2 S_4, but percentages were very low.

By deliberately preparing samples at too low a temperature for complete reaction it was possible to identify tin impurity lines, but the large amount of impurity and the low tin concentrations prevented accurate determination. The very small amounts of impurities present in the samples investigated could not be fitted to any known tin compounds. (Note the improved purity for

TABLE 4.8

RESULTS FOR $Cu\ Rh_{2-x}\ Sn_x\ Se_4$

	CRYSTALLOGRAPHIC PARAMETERS						ELECTRICAL RESULTS			
X	a_o (Å) ±0.001	u	B (Å^2) ± 0.1	Θ_a (°K) ± 50	L* (Å) ±500	p(Å)	T_c(°K) ± 0.3	ΔT_c(°K) ±0.3	T_m(°K) ± 0.1	T_c** ± 0.1
0.00	10.260	0.384	0.1	680	5,500	2.473	3.5	0.5	3.3	3.5
0.05	10.276	0.384	0.2	470	5,000	2,477	2.7	1.0	2.3	3.25
0.10	10.284	0.384	0.2	470	2,250	2,478	3.3	0.5	3.1	2.9
0.175	10.330	0.383	0.25	400	3,000	2,500	2.35	1.0	2.0	2.3
0.60	10.575	0.382	0.4	320	3,750	2,570	1.5	-	-	0.0
0.10	10.284	-	-	-	-	-	1.5	-	-	2.9
0.2	10.385	-	-	-	-	-	1.5	-	-	2.0

NOTE: * L = Average particle size

** T_c from the results of Van Maaren and Harland, (1969)

RESULTS FOR $Cu\ Rh_{2-x}\ Sn_x\ S_4$

	CRYSTALLOGRAPHIC PARAMETERS						ELECTRICAL RESULTS		
X	a_o (Å) ± 0.001	u	B (Å^2) ± 0.1	Θ_a (°K) ± 50	L (Å) ± 500	p(Å)	T_c(°K)	ΔT_c(°K)	T_m(°K)
0.00	9.788	0.384	0.2	550	2,750	2.359	4.1	0.7	3.80
0.05	9.799	0.382	0.2	550	1,750	2.381	4.7	1.5	3.85
0.10	9.908	0.382	0.25	500	4,000	2.408	1.5	-	-

FIG. 4-6 TRANSITION TEMPERATURE

$Cu\ R_{H_{1.95}} : S_{N_{0.05}}^{119}\ S_4$

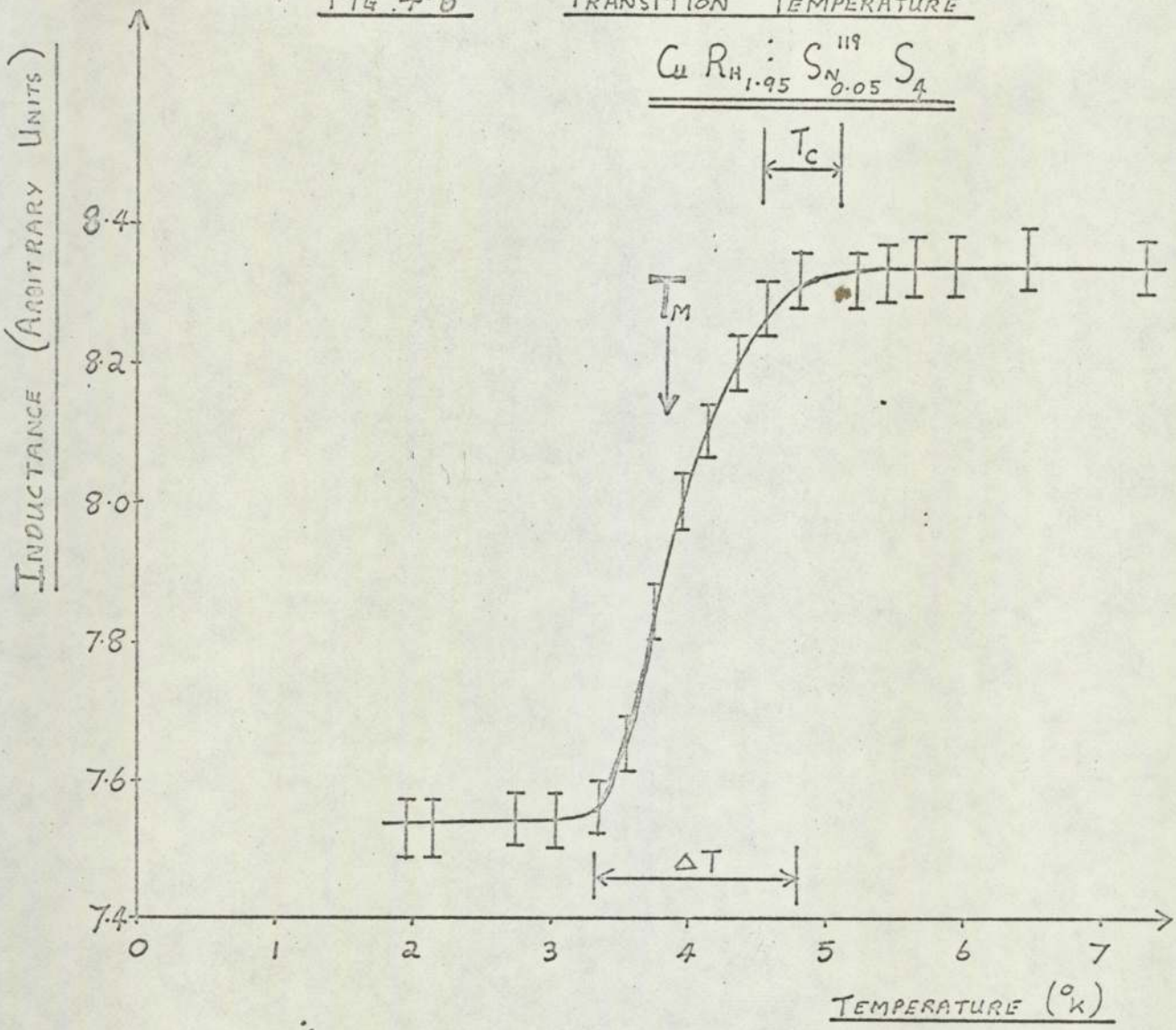

FIG 4-7 a_o VERSUS x : $Cu\,R_{H_{2-x}}Sn_x^{119}Se_4$

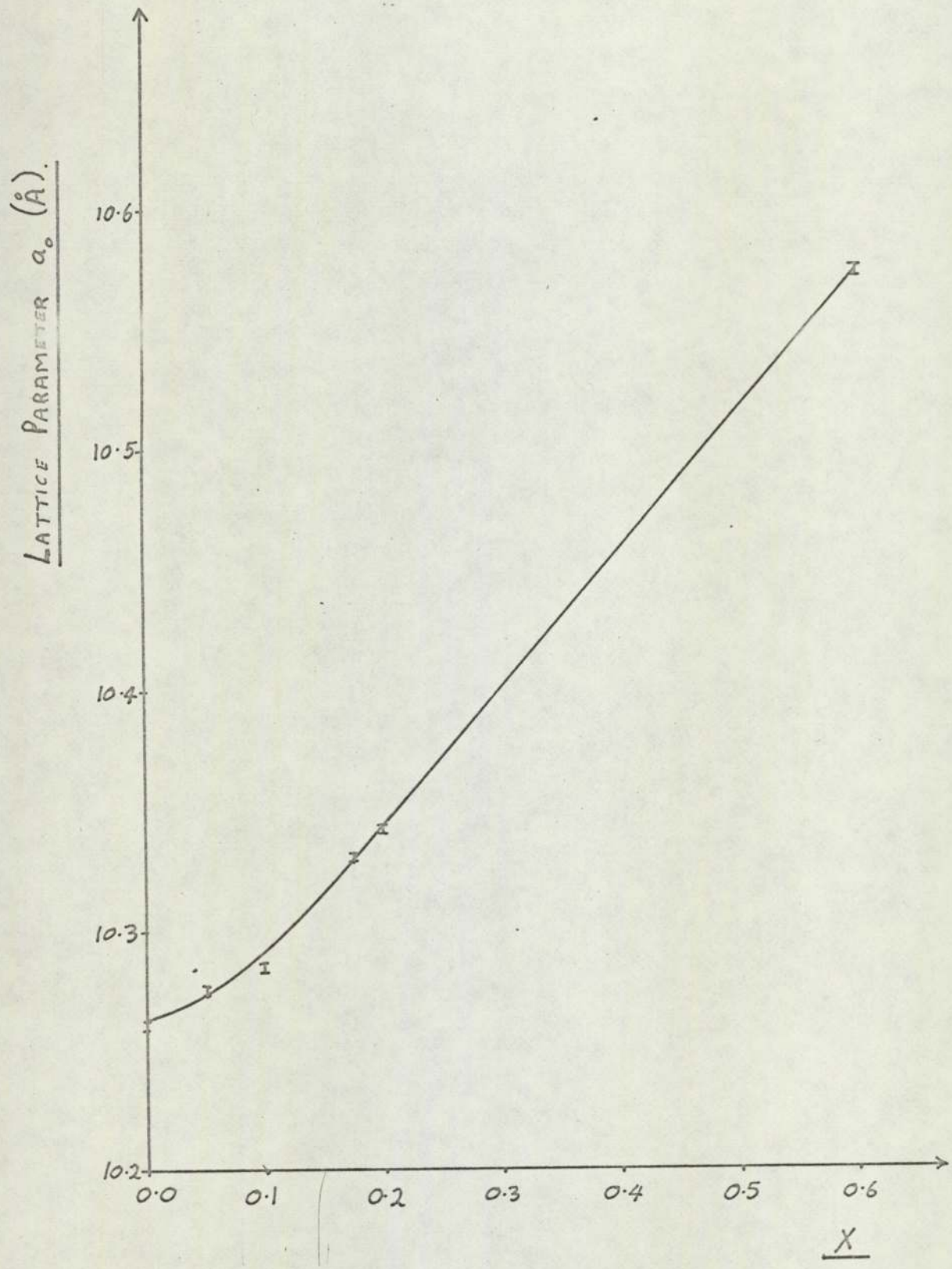

FIG. 4-8 $Cu\,R_{H_{2-x}}\,Sn_x^{119}\,Se_4$ $x = 0.05$

$u = 0.384$ $B = 0.21$

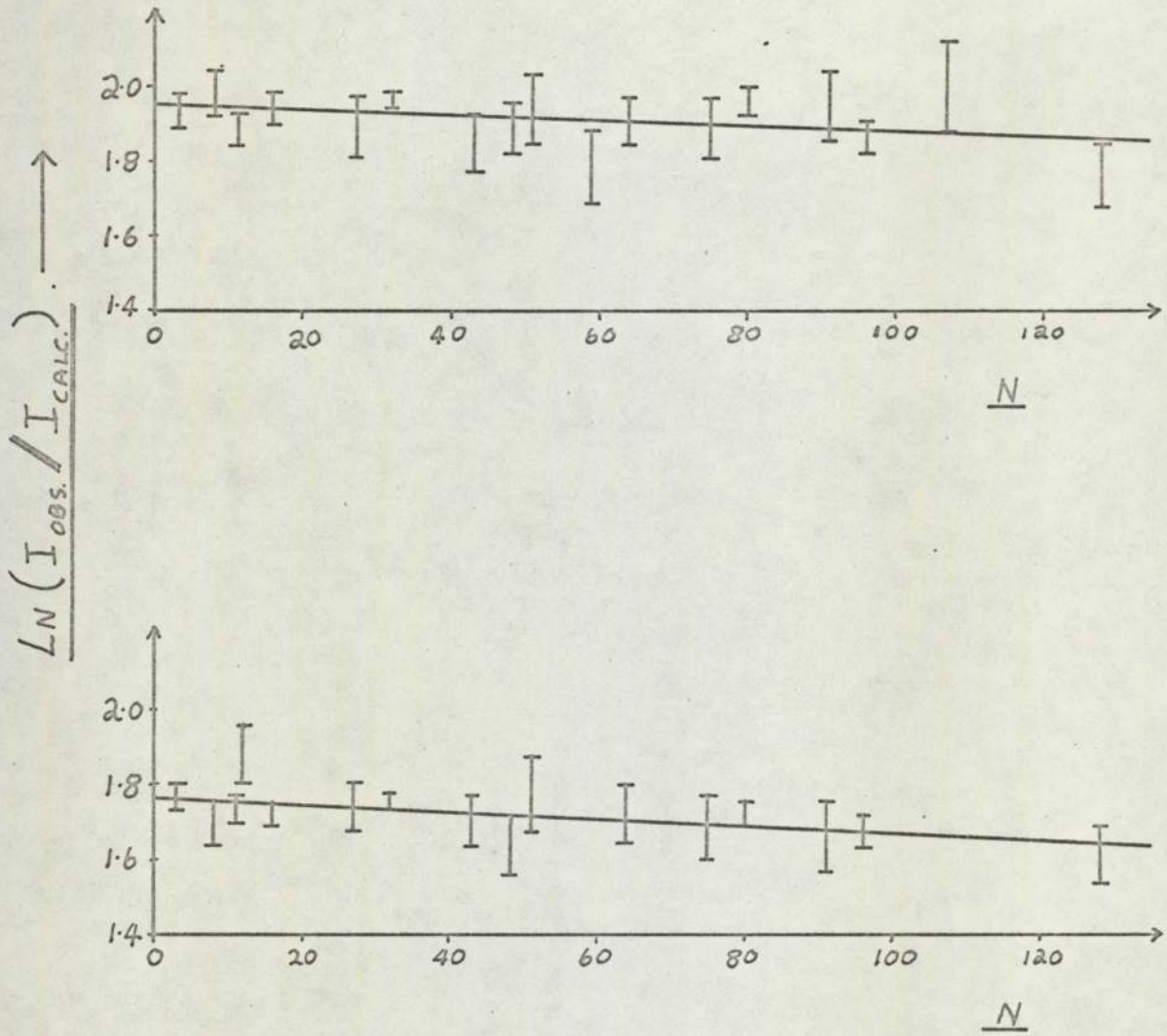

FIG. 4-9 $Cu\,R_{H_{2-x}}\,Sn_x^{119}\,Se_4$ $x = 0.10$

$u = 0.384$ $B = 0.19$

FIG. 4-10 $CuRh_{2-x}Sn_x^{119}Se_4$ $x = 0.175$

$u = 0.383$ $B = 0.25$

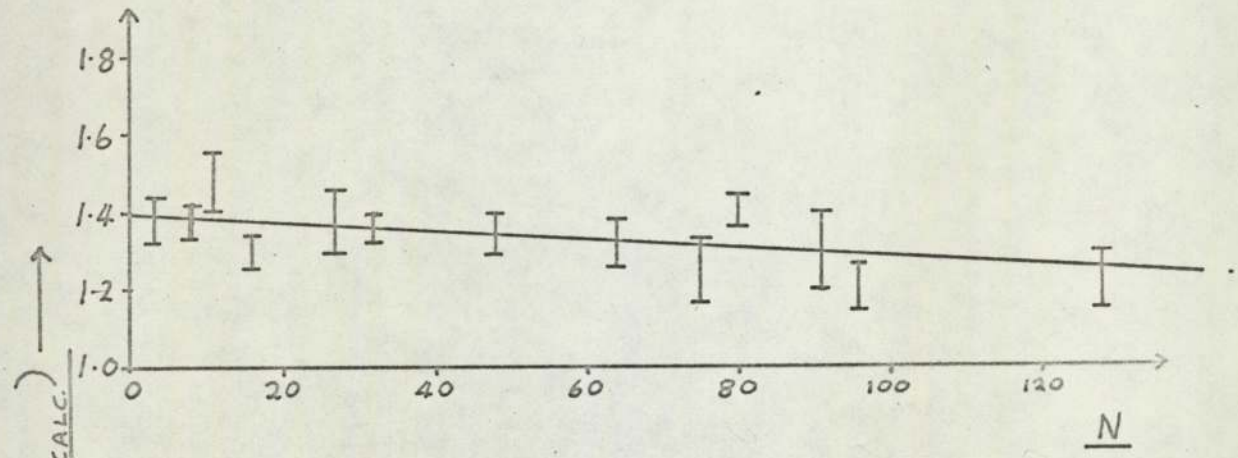

$Ln\ (I_{OBS.} / I_{CALC.})$ ⟶

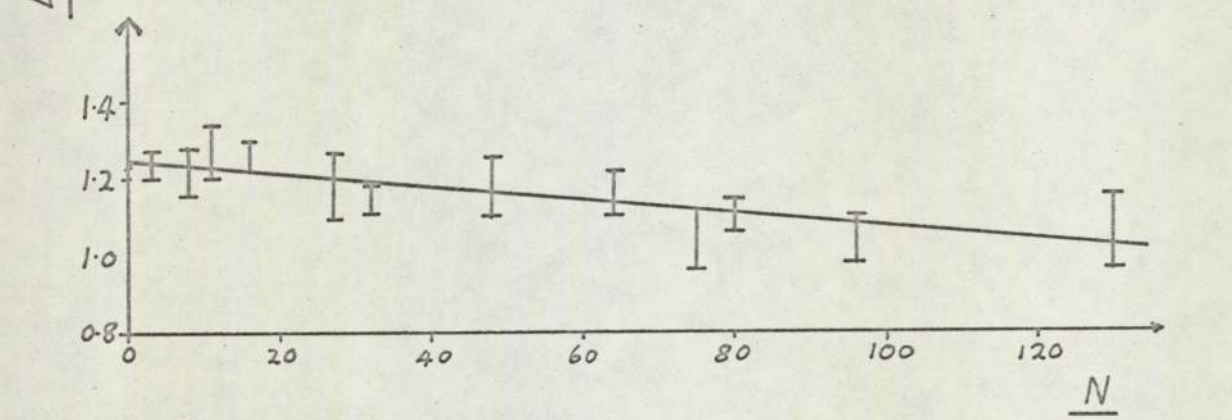

FIG 4-11 $CuRh_{2-x}Sn_x^{119}Se_4$ $x = 0.6$

$u = 0.382$ $B = 0.4$

FIG. 4-12. $CuRH_{2-x}Sn_x^{119}S_4$ $x = 0.05$

$u = 0.382$ $B = 0.2$

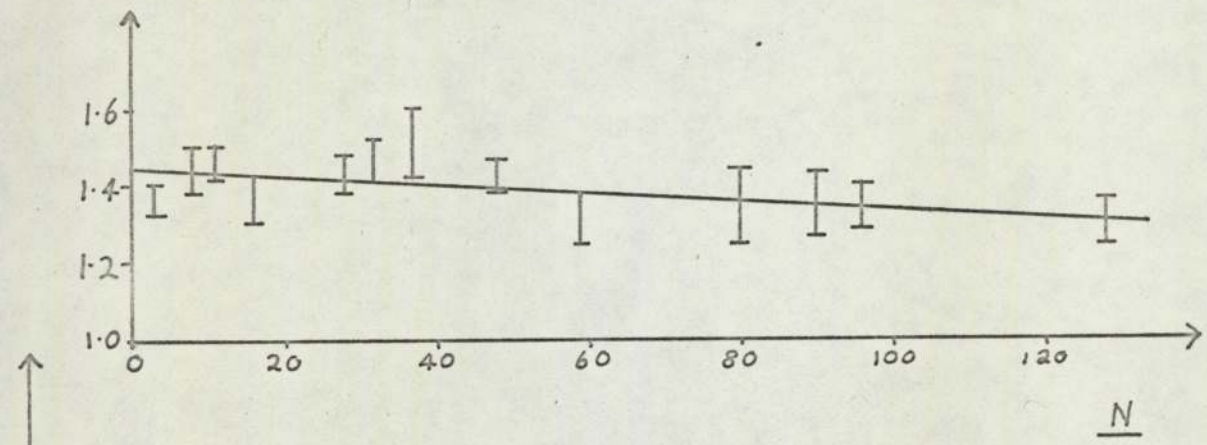

$LN\ (I_{OBS}/I_{CALC})$

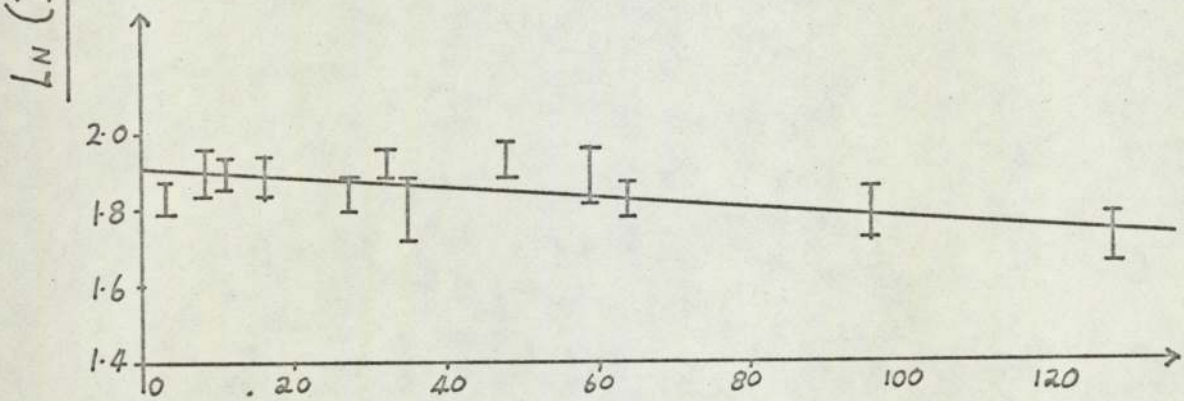

FIG 4-13 $CuRH_{2-x}Sn_x^{119}S_4$ $x = 0.10$

$u = 0.382$ $B = 0.25$

TABLE 4.9

PREPARATION DETAILS

$Cu\ Rh_{2-x}\ Sn_x\ Se_4$

X	FIRING TEMP. (^{o}K)	FIRING TIME (DAYS)	% IMPURITY AND TYPE
0.00	600 ± 10	3	NONE DETECTED
0.05	600	3	NONE DETECTED
0.10	600	3	~2% $Rh\ Se_{2+x}$
0.175	625	3	NONE DETECTED
0.60	600	3	~4% $Rh\ Se_{2+x}$
0.1	640	3	NONE DETECTED
0.2	640	3	NONE DETECTED

$Cu\ Rh_{2-x}\ Sn_x\ S_4$

X	FIRING TEMP. (^{o}K)	FIRING TIME (DAYS)	% IMPURITY AND TYPE
0.00	600 ± 10	3	~1% Cu S
0.05	600	3	~1% Cu S
0.10	600	3	~2% Cu/Rh.S

$x = 0.175$ was achieved by slightly raising the preparation temperature). Samples of $Cu\ Rh_{2-x}\ Sn_x\ Se_4$ with $x = 0.1$ and $x = 0.2$ were also prepared at the higher temperature (640°C) but despite the absence of impurities there was no detectable superconducting transition for these samples above 1.5°K.

$Cu\ Sn_2\ Se_4$ and $Cu\ Sn_2\ S_4$ could not be formed by any method used and further intermediate compounds were not investigated.

4.3.3. Concluding Remarks.

In order to establish that the tin is substituting for rhodium, it would normally be necessary to consider those h,k,l reflections which receive no contributions from the tetrahedral site atoms and those which receive non from the octahedral atoms, e.g. respectively 2,2,2 and 2,2,0 lines. Unfortunately in this work such reflections are relatively weak and close to stronger lines. With the small amounts of tin used as well, it is impossible to be accurate, although the trend indicates octahedral site occupation by the tin atoms. Of a more conclusive nature is the use of average tin/rhodium scattering factors for the octahedral site atom and the resulting linearity of the $\ln (I_{obs}/ I_{calc})$ versus N curves. Tin has a scattering factor of nearly twice that of copper it would therefore be impossible to achieve such linearity if the tin was displacing copper. As there were no identifiable tin compounds present as impurities, it was concluded that the tin atoms occupy octahedral sites in the spinel lattice. (This was later verified by the Mössbauer technique,(chapter 5) since the absorption dips were all single Lorentzians). Approximate values of particle size are given in Table 4.8, the effects of which were assumed negligable since there is no correlation with T_c.

The T_c's found by Van Maaren and Harland (1969) are reproduced in Table 4.8. (Also T_m the mid-point of the observed transitions are recorded.) Comparison of these results illustrated in Fig 4.8 shows that there is appreciable discrepancy in certain cases. The breadth of the transitions

measured in this work, indicates that these values of T_c may be somewhat inaccurate and for later detailed calculations the T_c values of Van Maaren have been used.

CHAPTER 5. RESULTS FROM MÖSSBAUER SPECTROMETRY

5.1 Introduction

In order to exploit the Mössbauer Effect to investigate low temperature anharmonicity the chemical composition of samples had to include a suitable Mössbauer nucleus. It was essential however, that the presence of such substitutional atoms did not completely destroy the superconducting property (with which a connection was sought) or substantially interfere with the development of the spinel phase (see section 3.1).

The range of compositions suitable for the experiments to be described was therefore very restricted. Firstly, investigations were limited to the series $Cu\ Rh_{2-x}\ Sn_x\ Se_4$ and $Cu\ Rh_{2-x}\ Sn_x\ S_4$ for the former of which Van Maaren and Harland (1969) had discovered that superconductivity was retained within the range $0 \leq x \leq 0.5$. Further restrictions emerged however since the counting statistics became very poor for $x < 0.05$ and, in the case of the sulphide series, through difficulties connected with stoichiometry and the problem of retaining superconductivity.

Ultimately extensive investigations were only carried out on four samples from the selenide compositional range and two samples from the corresponding sulphide series. The results are described and analysed in section 5.2.

Preliminary observations of the Mössbauer resonant absorption dips obtained showed them all to be single unbroadened Lorentzian lines. This indicated the absence of tin based impurities in the absorbers and also that the tin lies only in the octahedral sites.

5.2 The Application of the Method of O'Connor and Skyrme

5.2.1 The recoil-free fraction

The theory and the experimental details for the determination of the area of a Mössbauer resonant absorption dip by the method of O'Connor and Skyrme (1973) have been described in chapter 2 and in section 3.5. The

results of applying this technique to the present series of selenide and sulphide absorbers are presented in columns, 2,3 and 4 of tables 5.1 to 5.6. However, the possible presence of anharmonicity requires a modification to the method of analysis previously outlined for the derivation of the corresponding values of recoil-free fraction.

If it may be assumed, following the work of Dash, Johnson and Visscher (1968), (see also section 2.4.3), that the recoil-free fraction may be expressed as the product of harmonic and anharmonic components.

$$\text{i.e. } f = f_H \cdot f_{AN} \cdot \qquad 2.35$$

then in the high temperature region the effective absorption thickness, T_a depends upon temperature as;

$$\ln T_a + \frac{\hbar K^2}{12\, Mk\, T} = -\frac{\hbar^2 K^2 T}{Mk\, \theta^2 (-2)} + \ln (Nt\sigma(o)\, f_{AN}) \qquad 5.1$$

Where K is the wave vector of the gamma ray.

Using $\alpha = \frac{\hbar K^2}{12\, MkT}$ this equation may be rewritten as.

$$\ln T_a e^{\alpha} = -\frac{\hbar^2 K^2 T}{Mk\, \theta^2 (-2)} + \ln (Nt\sigma(o)\, f_{AN}) \qquad 5.2$$

Assuming the anharmonic factor to be only weakly temperature dependant then a plot of the left hand side of equation 5.2 against temperature yields the value of the -2 moment of the harmonic frequency distribution, θ (-2), (See, Figs 5.1a to 5.6a). The intercept yields the value of $Nt\,\sigma(o)\, f_{AN}$ and hence f_H may be found from; (see Table 5.7.)

$$f_H = \frac{T_a}{Nt\,\sigma(o)\, f_{AN}} \qquad 5.3$$

Values of f_H versus temperature are presented in columns 6 and 7 of tables 5.1 to 5.6 and are plotted in Figs 5.1b to 5.6b.

Similarly by fitting the experimental data in the neighbourhood of $T=0^{\circ}K$, where $\ln f_H$ tends towards the limit, (see section 2.3)

TABLE 5.1

RESULTS FOR $Cu\,Rh_{2-x}\,Sn_x\,Se_4$, $x = 0.05$

ABSORBER NO.1

TEMP. T. °K ± 0.1	HALF WIDTH $\Gamma/2$ mm/s	AREA OF DIP, A mm/s	T_a mm	$-\ln T_a e^{\alpha}$ ± 0.05	f_H	$-\ln f_H$ ± 0.1	TOTAL SHIFT mm/s. δ. ± 0.005
300	39.7	0.5844	0.00730	4.901	0.113	2.180	1.728
275	41.4	0.6855	0.00823	4.782	0.127	2.064	1.733
250	37.5	0.8167	0.01083	4.506	0.167	1.790	1.714
200	37.5	1.0669	0.01417	4.232	0.218	1.523	1.717
100	37.8	1.5784	0.02083	-	0.320	1.139	1.741
78	40.65	2.5610	0.0313	-	0.482	0.730	1.768
40	44.65	3.9720	0.0442	-	0.680	0.386	1.791
26	37.5	2.8208	0.0371	-	0.571	0.560	1.798
4.2	44.1	3.9199	0.0442	-	0.685	0.378	1.810

ABSORBER NO.2

250	43.0	0.7713	0.00892	4.700	0.178	1.724	1.782
225	42.1	0.9055	0.01070	4.516	0.214	1.542	1.774
200	36.0	0.9008	0.01245	4.362	0.250	1.386	1.724
175	41.0	1.1410	0.01380	4.255	0.276	1.287	1.755
150	40.0	1.3804	0.01716	4.003	0.325	1.124	1.769
85	41.7	1.6583	0.01980	-	0.396	0.926	1.796
78	46.7	1.5757	0.01680	-	0.376	0.978	1.760
78	37.1	1.6116	0.0217	-	0.434	0.835	1.769
57	33.7	1.7935	0.0265	-	0.530	0.635	1.744
15	39.3	2.2627	0.0286	-	0.572	0.559	1.769
4.2	38.5	2.2910	0.0296	-	0.592	0.524	1.806

NOTE: 1. Two absorbers were examined (see section 3.5)
2. The errors are detailed in section 3.5.4.

TABLE 5.2

RESULTS FOR $Cu\ Rh_{2-x}\ Sn_x\ Se_4$ $x = 0.1$

T °K	Γ 10^{-2} mm/s	A mm/s	T_a mm	$-\ln T_a e^{\alpha}$ (± 0.02)	f_H	$-\ln f_H$ ± 0.05	δ mm/s ± 0.002
300	46.9	3.979	0.0519	2.941	0.273	1.397	1.682
293	47.7	4.247	0.0545	2.893	0.288	1.254	1.681
275	45.4	4.329	0.0584	2.823	0.306	1.185	1.691
275	47.1	4.620	0.0601	2.795	0.314	1.157	1.693
250	47.0	4.585	0.0597	2.800	0.314	1.095	1.706
225	48.9	5.565	0.0696	2.643	0.364	1.009	1.700
200	49.6	6.418	0.0793	2.513	0.415	0.879	1.715
175	49.7	7.516	0.0925	2.350	0.481	0.732	1.712
150	49.1	7.299	0.0910	2.365	0.476	0.741	1.719
78	55.3	10.657	0.1180	-	0.618	0.482	1.734
78	54.5	11.020	0.1237	-	0.651	0.429	1.734
55	52.7	11.089	0.1287	-	0.677	0.389	1.740
35	53.0	10.962	0.1266	-	0.666	0.406	1.746
15	54.7	11.283	0.1263	-	0.665	0.408	1.750
4.2	53.7	11.185	0.1275	-	0.671	0.399	1.751
2.35	52.8	10.950	0.1269	-	0.668	0.403	1.755

NOTE: Note the improved accuracy of these results compared with those of table 5.1 (see section 3.5.4.). The errors in the following tables are identical.

TABLE 5.3

RESULTS FOR $Cu\ Rh_{2-x}\ Sn_x\ Se_4$ $x = 0.175$

T °K	Γ 10^{-2} mm/s	A mm/s	T_a mm	$-\ln T_a e^{\alpha}$ ± 0.02	f_H	$-\ln f_H$ ± 0.05	δ mm/s ± 0.002
325	43.68	5.8744	0.0714	2.6449	0.3188	1.1433	1.7021
300	43.09	6.0870	0.0750	2.5745	0.3340	1.0940	1.6975
293	44.56	5.8857	0.0808	2.4995	0.3610	1.0190	1.6980
275	46.61	6.2948	0.0827	2.4754	0.3690	0.9969	1.7048
265	44.22	6.9552	0.0963	2.4651	0.4298	0.8444	1.7078
250	51.26	7.1563	0.0855	2.4404	0.3815	0.9636	1.7015
225	45.34	7.7959	0.1053	2.2298	0.4699	0.7553	1.7167
200	45.49	8.0838	0.1088	2.1945	0.4856	0.7223	1.7183
150	49.15	9.2393	0.1151	-	0.5138	0.6658	1.7272
100	48.87	10.5806	0.1325	-	0.5916	0.5248	1.7372
78	48.98	11.3690	0.1421	-	0.6346	0.4552	1.7458
40	48.35	13.9252	0.1596	-	0.7123	0.3392	1.7492
10	48.34	13.8163	0.1583	-	0.7068	0.3470	1.7545
4.2	48.33	13.5647	0.1554	-	0.6941	0.3653	1.7533

TABLE 5.4

RESULTS FOR $Cu\ Rh_{2-x}\ Sn_x\ Se_4$ $x = 0.6$

T ^{o}K	Γ 10^{-2} mm/s	A mm/s	T_a mm	$-\ln T_a e^{\alpha}$ $\pm$ 0.02	f_H	$-\ln f_H$	δ mm/s $\pm$ 0.002
300	47.48	8.5057	0.1103	2.2104	0.4880	0.7173	1.6497
293	48.10	8.5571	0.1089	2.2010	0.4819	0.7299	1.6541
275	48.55	9.6522	0.1083	2.2055	0.4792	0.7356	1.6740
265	47.99	9.3119	0.1188	2.1305	0.5255	0.6433	1.6637
250	48.42	9.6980	0.1226	2.0794	0.5425	0.6116	1.6605
225	49.00	10.7254	0.1340	1.9906	0.5872	0.5324	1.6699
200	49.80	10.6973	0.1308	2.0099	0.5788	0.5469	1.6756
150	50.80	13.0563	0.1603	1.7982	0.7093	0.3435	1.6883
100	53.06	14.0119	0.1616	1.7749	0.7150	0.3354	1.7021
78	52.04	14.9339	0.1757	-	0.7773	0.2520	1.7080
78	52.77	15.3297	0.1778	-	0.7867	0.2399	1.7080
55	53.56	15.3584	0.1755	-	0.7765	0.2529	1.7026
45	53.22	15.7849	0.1816	-	0.8035	0.2187	1.7107
35	53.51	16.1006	0.1842	-	0.8150	0.2045	1.7096
15	53.90	16.5699	0.1882	-	0.8327	0.1830	1.7067
10	54.40	16.5410	0.1861	-	0.8234	0.1942	1.7174
4.2	53.28	16.6112	0.1908	-	0.8442	0.1693	1.7096

TABLE 5.5

RESULTS FOR $Cu\ Rh_{2-x}\ Sn_x\ S_4$ $x = 0.05$

T °K	Γ 10^{-2} mm/s	A mm/s	T_a mm	$-\ln (T_a e^{\alpha})$ ± 0.02	f_H	$-\ln f_H$ ± 0.05	δ mm/s ± 0.02
300	43.00	7.899	0.1124	2.1692	0.614	0.4878	1.4102
293	43.06	8.168	0.1155	2.1422	0.631	0.4612	1.4171
275	43.06	8.025	0.1141	2.1533	0.623	0.4732	1.4232
250	44.00	8.867	0.1234	2.0733	0.674	0.3945	1.4302
225	45.03	9.066	0.1232	2.0720	0.673	0.3960	1.4378
210	44.53	8.910	0.1225	2.0768	0.669	0.4020	1.4402
200	44.46	9.371	0.1290	2.0239	0.706	0.3481	1.4402
150	47.40	10.990	0.1493	1.9202	0.712	0.3397	1.4534
78	48.70	11.373	0.1480	-	0.809	0.2119	1.4691
50	49.67	11.223	0.1489	-	0.814	0.2058	1.4815
15	50.42	11.330	0.1495	-	0.817	0.2021	1.4866
10	51.81	14.529	0.1508	-	0.824	0.1936	1.4850
4.2	50.72	11.612	0.1507	-	0.823	0.1948	1.4826

TABLE 5.6

RESULTS FOR $Cu\ Rh_{2-x}\ Sn_x\ S_4$ $x = 0.1$

T ^{o}K	Γ 10^{-2} mm/s	A mm/s	T_a mm	$-\ln (T_a e^{\alpha})$ ± 0.02	f_H	$-\ln f_H$ ± 0.05	δ mm/s ± 0.02
300	40.27	7.3286	0.1113	2.1795	0.5250	0.6444	1.4229
293	40.60	7.3983	0.1115	2.1774	0.5262	0.6421	1.4162
275	40.90	7.6660	0.1147	2.1482	0.5410	0.6143	1.4256
250	39.33	8.2586	0.1284	2.0333	0.6057	0.5014	1.4302
225	41.40	8.6094	0.1272	2.0410	0.6000	0.5108	1.4350
200	40.85	9.2839	0.1390	1.9498	0.6557	0.4221	1.4399
150	42.69	10.5709	0.1515	1.8553	0.7146	0.3360	1.4577
100	43.50	10.7491	0.1513	-	0.7135	0.3376	1.4726
78	43.93	11.0581	0.1540	-	0.7264	0.3197	1.4693
40	43.36	11.9393	0.1685	-	0.7948	0.2297	1.4766
20	44.94	12.4510	0.1695	-	0.7995	0.2238	1.4753
10	45.61	12.4896	0.1676	-	0.7096	0.2350	1.4809
4.2	45.43	12.1861	0.1641	-	0.7774	0.2518	1.4742

TABLE 5.7

VALUES OF THE INTERCEPT, $(Nt\sigma(o)\, f_{AN})$ FROM $-\ln (T_a e^{\alpha})$ VERSUS T.°K.

$Cu\ Rh_{2-x}\ Sn_x\ Se_4$

X	$Nt\sigma(o)\, f_{AN}$	
0.05	0.065	ABSORBER No. 1
0.05	0.050	ABSORBER No. 2
0.10	0.188	
0.175	0.224	
0.6	0.227	

$Cu\ Rh_{2-x}\ Sn_x\ S_4$

0.05	0.183
0.10	0.212

$-\ln(T_A e^{\alpha})$ VERSUS T°K.

FIG. 5.1a. $CuRh_{2-x}Sn_xSe_4$ $x=0.05$

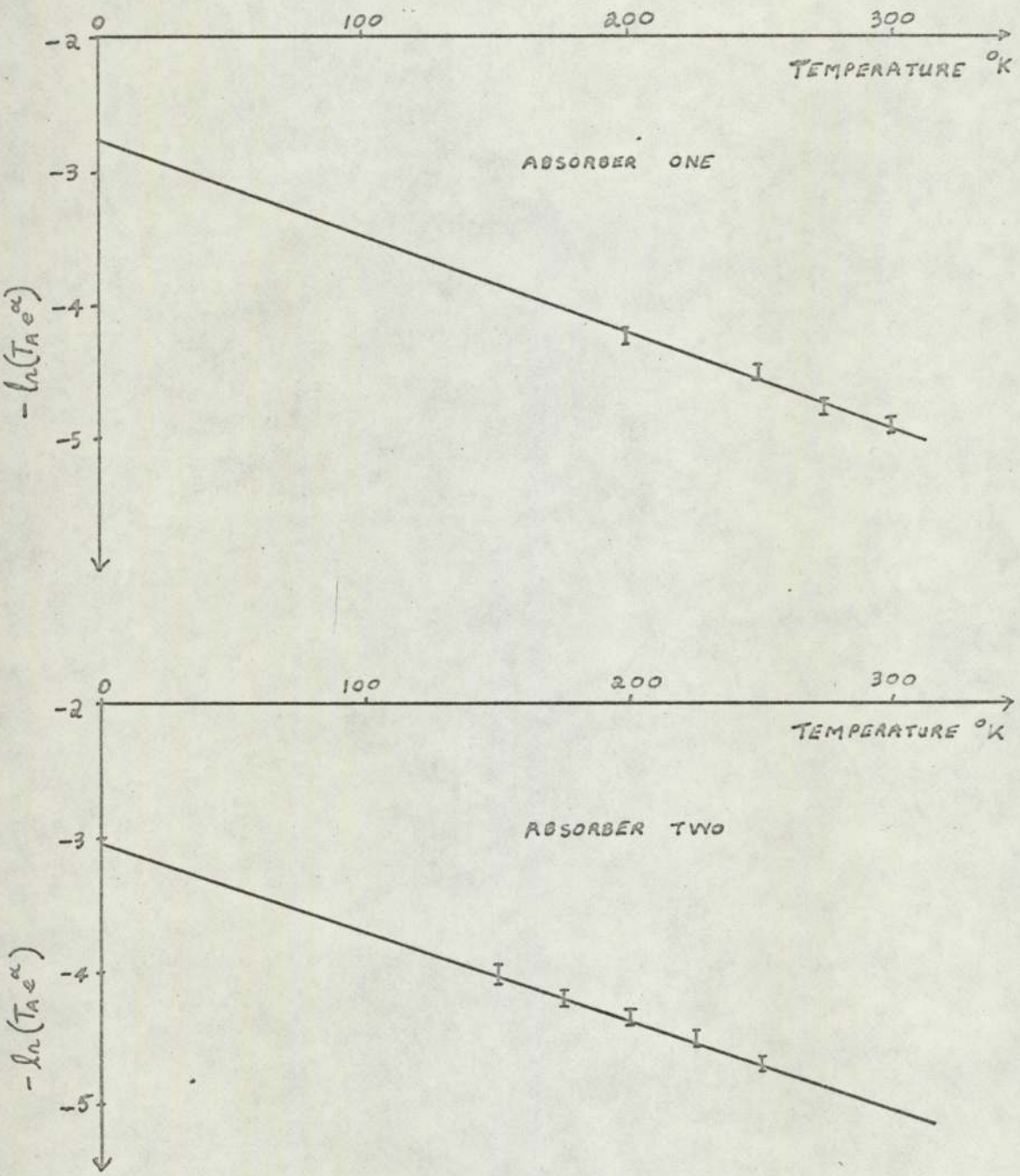

FIG. 5.1b. $-\ln(f)$ VERSUS T°K.

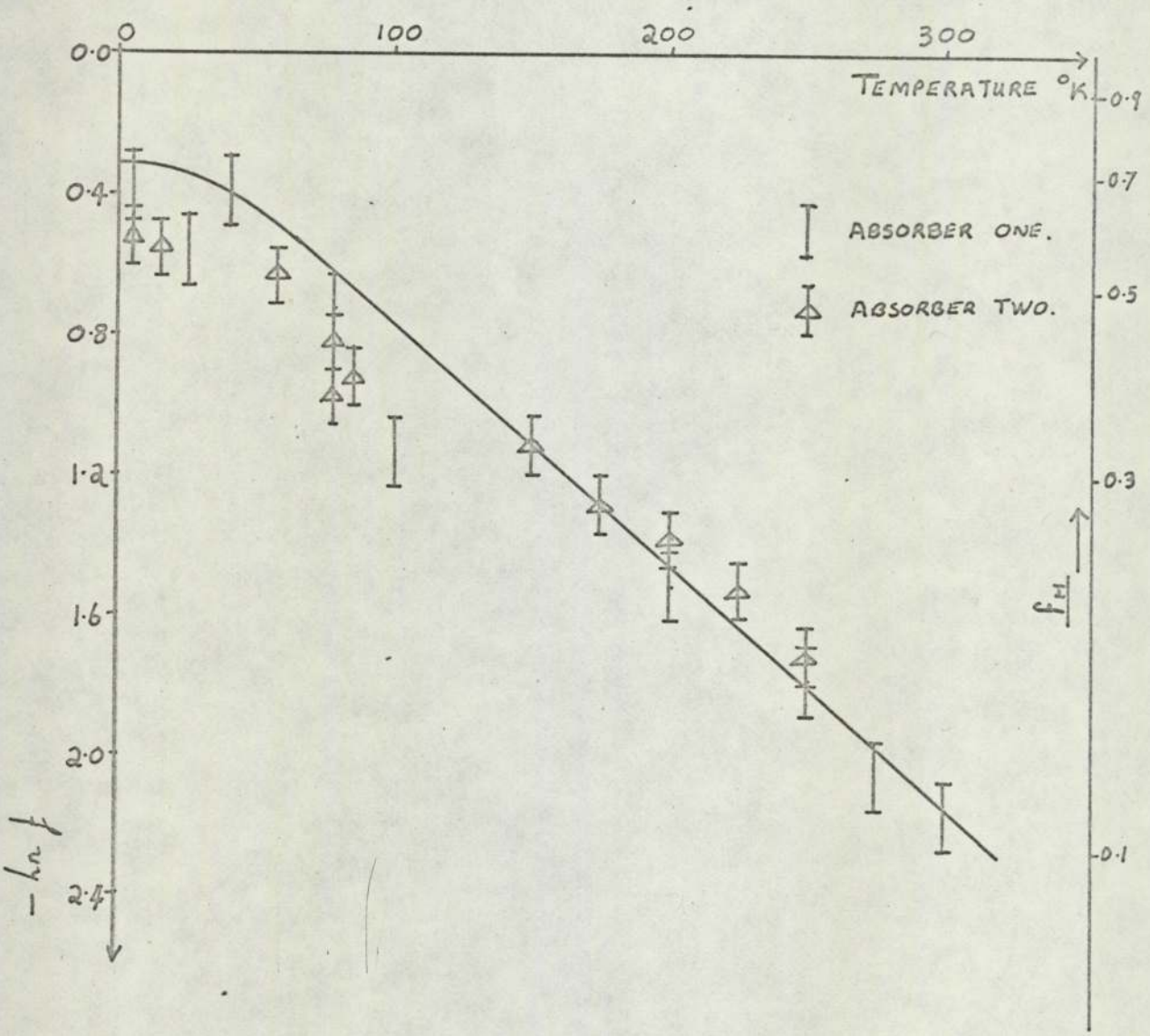

FIG. 5.2 a. $-\ln(T_A e^{\alpha})$ VERSUS T °K.

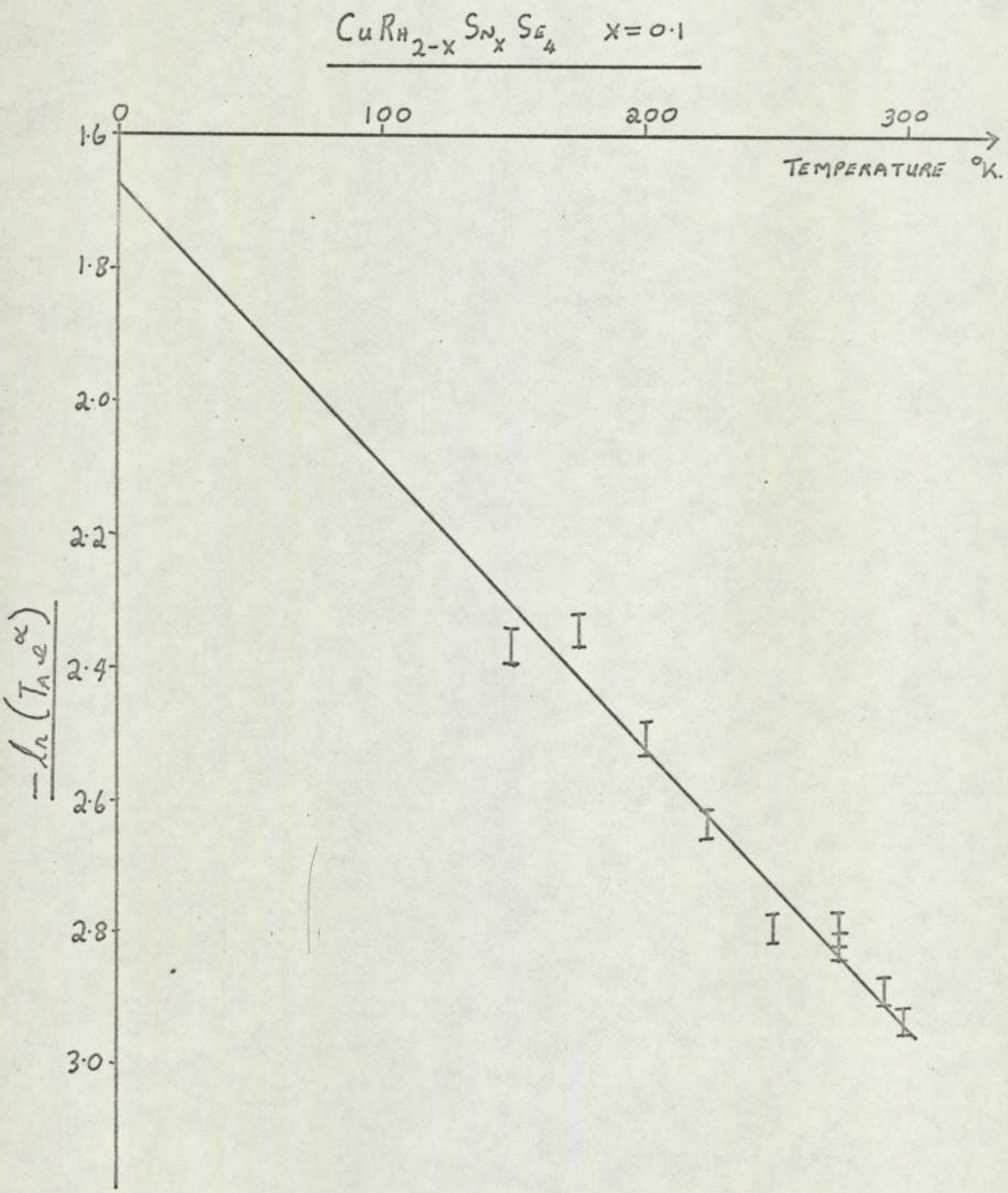

FIG. 5.2b $-\ln(f_H)$ VERSUS T°K

$CuRh_{2-x}Sn_xSe_4$ $x = 0.1$

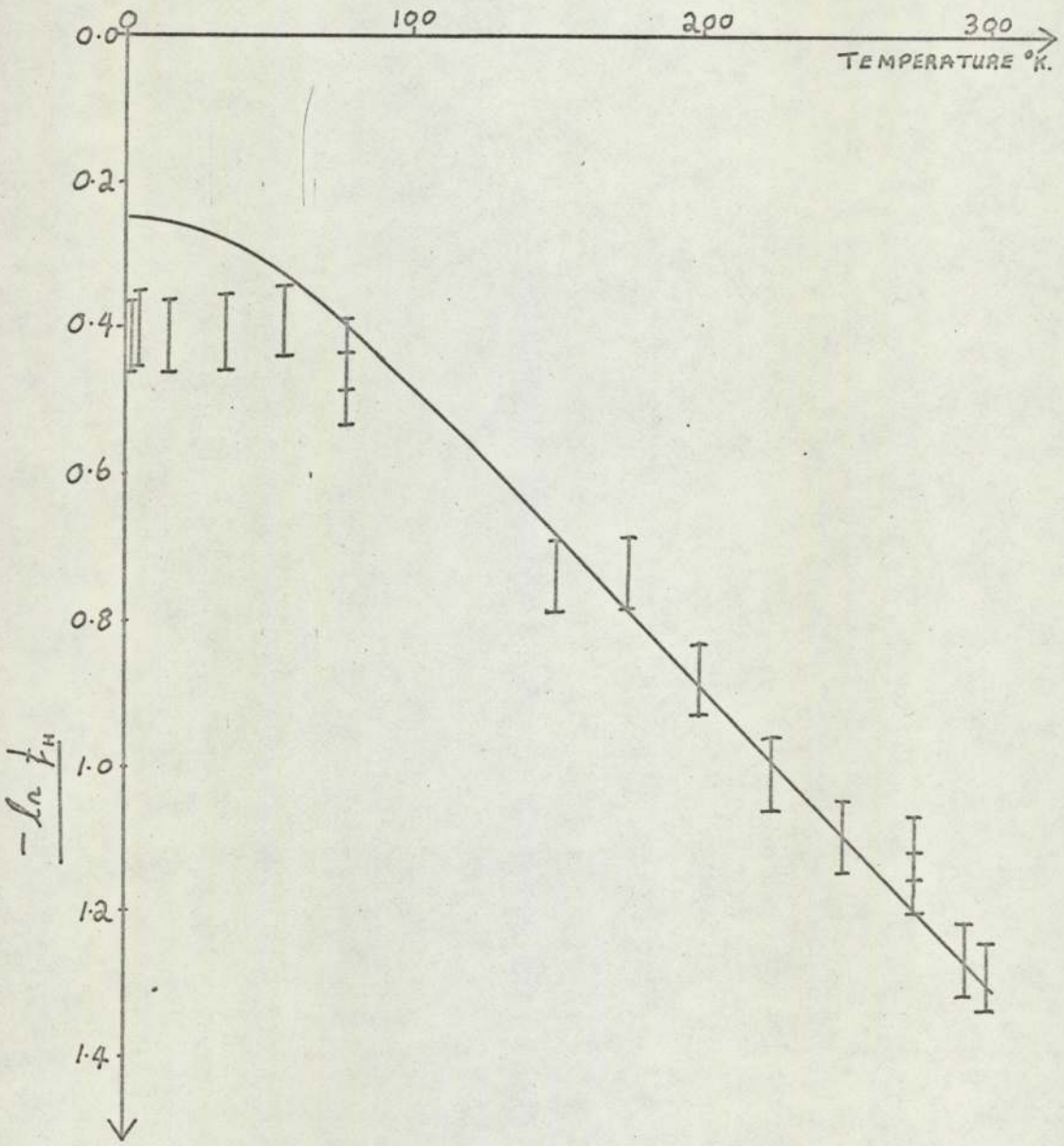

FIG. 5.3 a. $-\ln(T_A e^{\alpha})$ VERSUS T°K.

$CuRh_{2-x}Sn_xSe_4$ $x = 0.175$

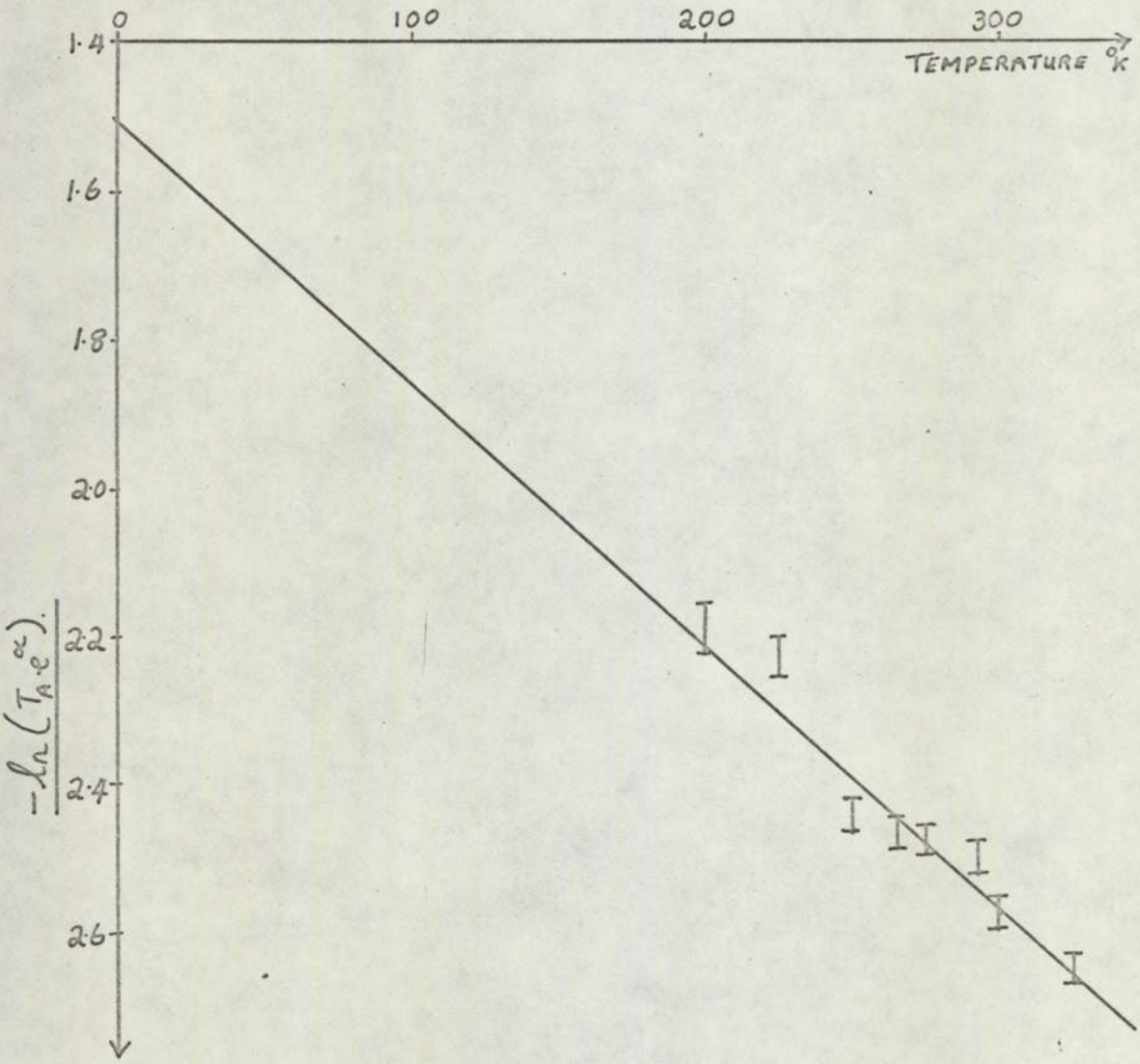

FIG 5.3b $-\ln(f_H)$ VERSUS T°K.

$CuRH_{2-x}Sn_xSe_4$. $x = 0.175$

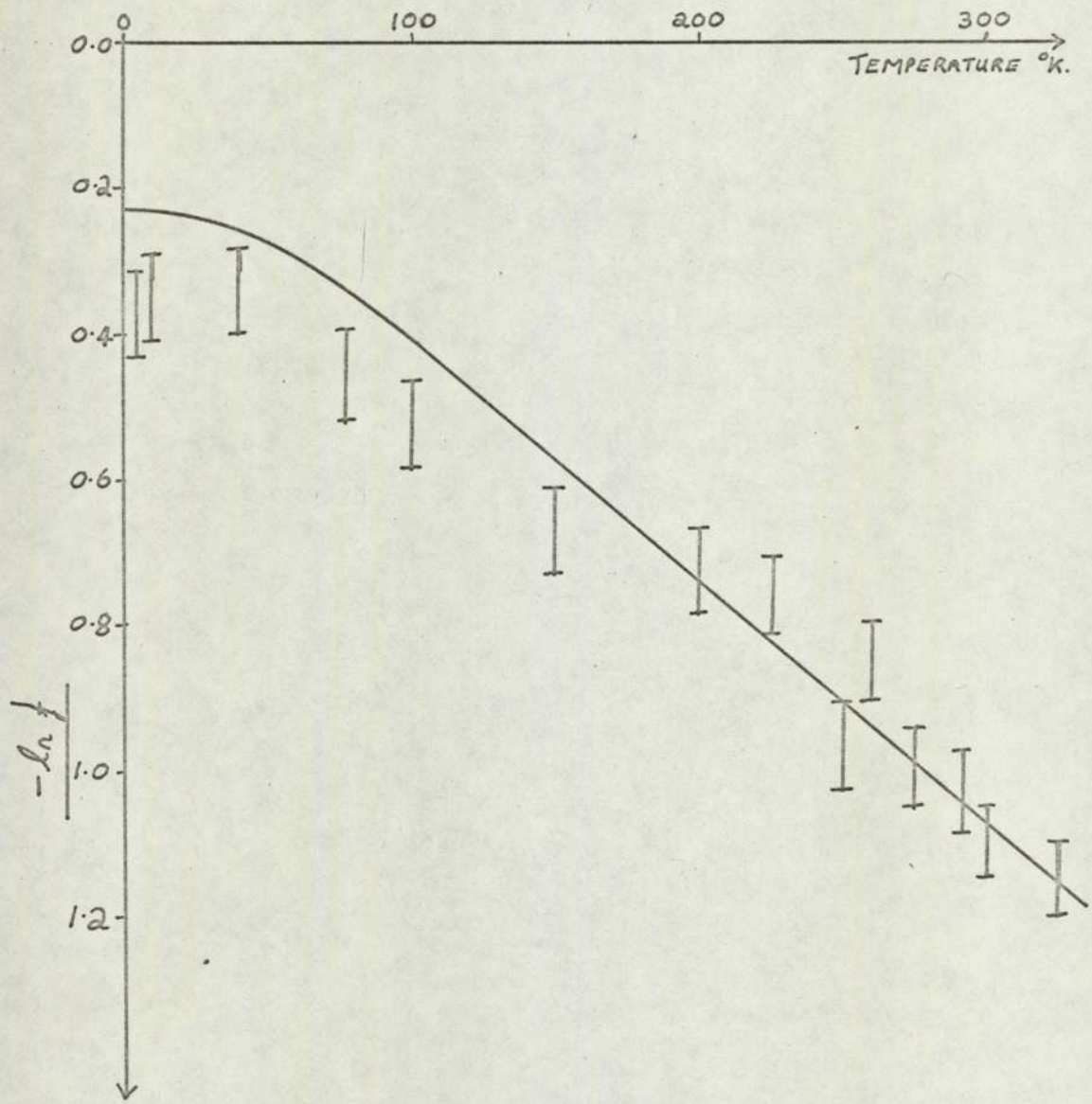

FIG. 5.4a. $-\ln(T_A e^{\alpha})$ VERSUS T°K.

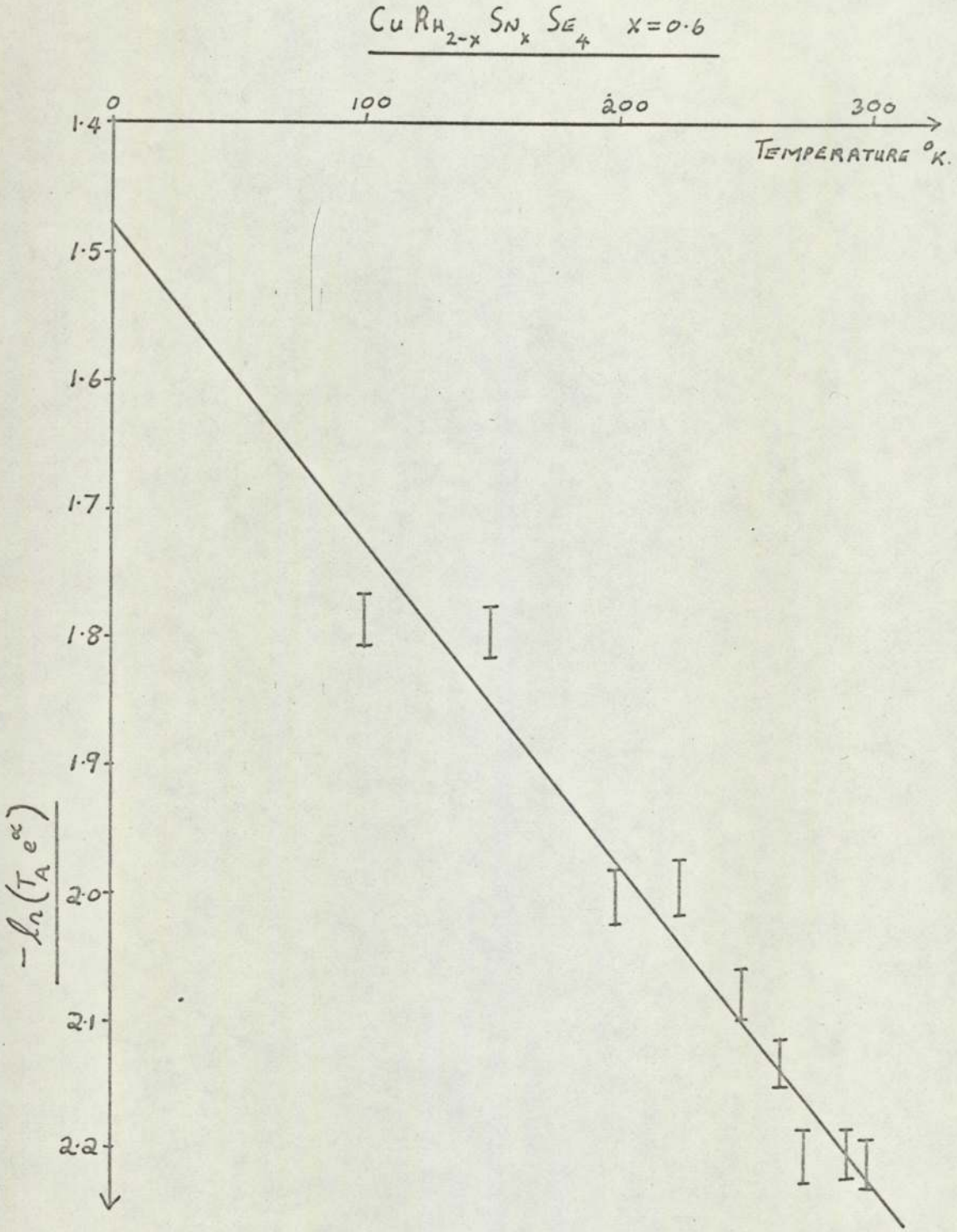

FIG 5.4b $-\ln(f_H)$ VERSUS T°K.

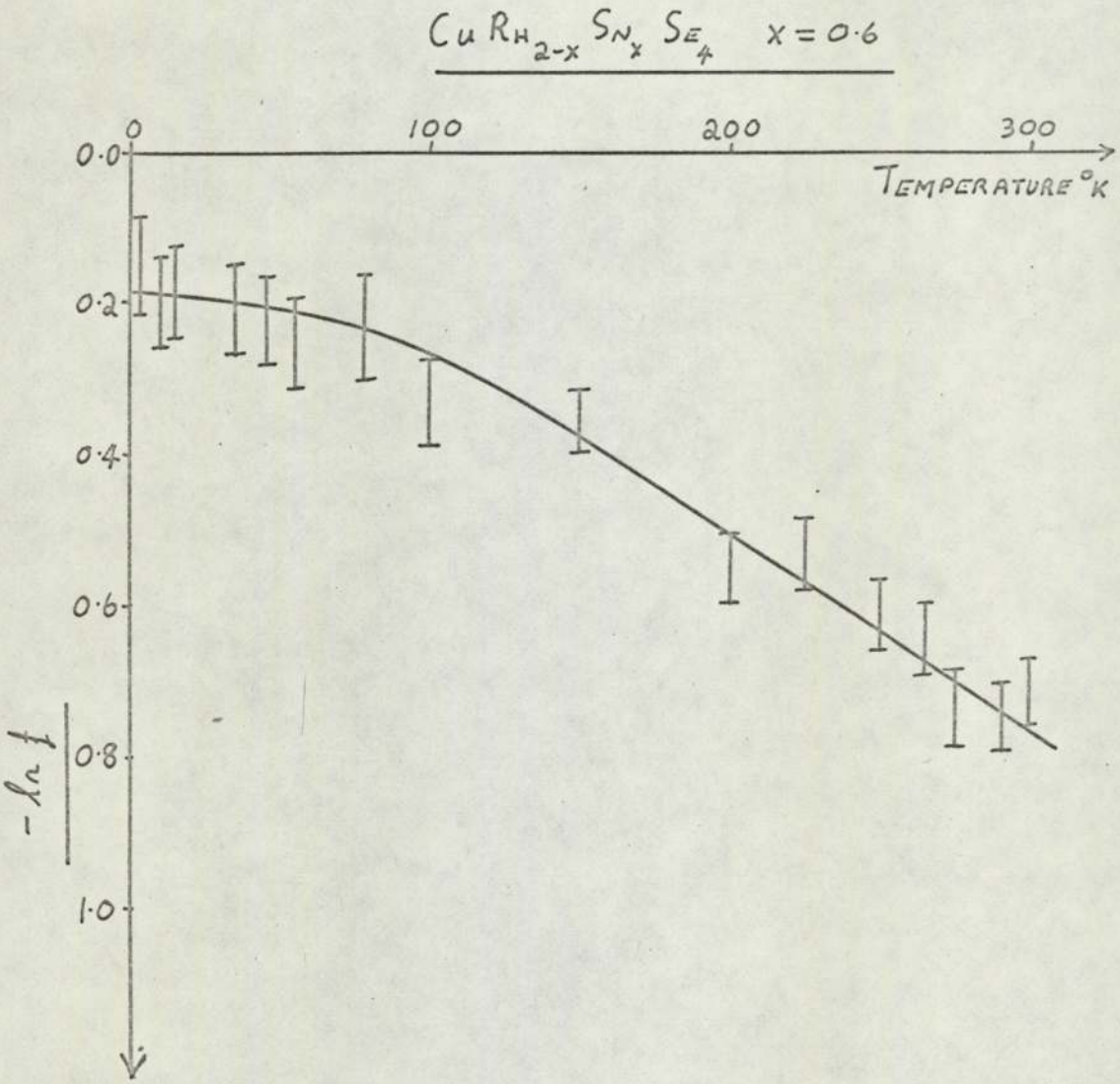

FIG. 5.5a $-\ln(T_A e^{\alpha})$ VERSUS T°K.

$CuRh_{2-x}Sn_xS_4$ $x = 0.05$

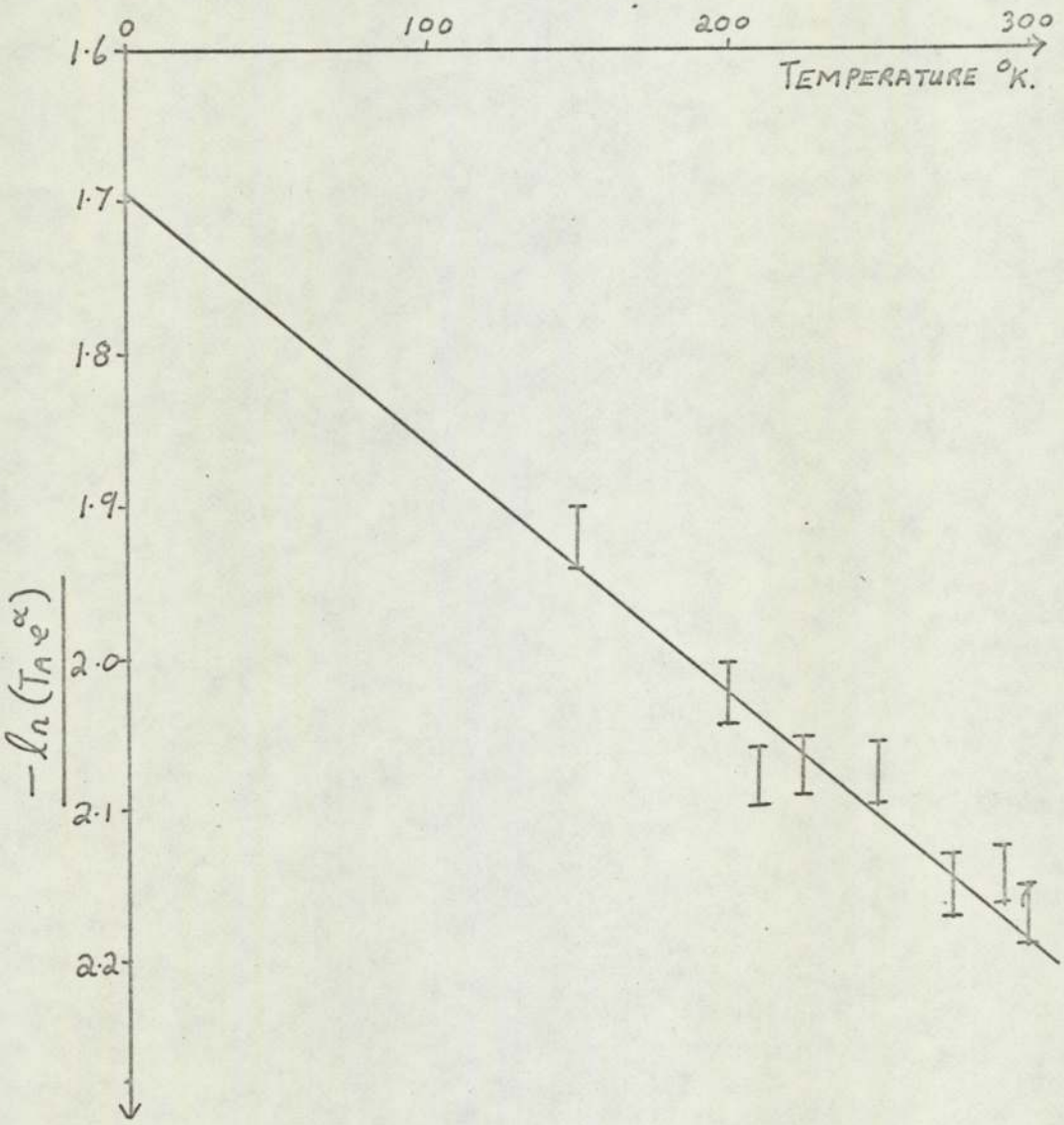

FIG 5.5b $-\ln(f_N)$ VERSUS T°K.

$CuRH_{2-x}Sn_xS_4$ $x=0.05$

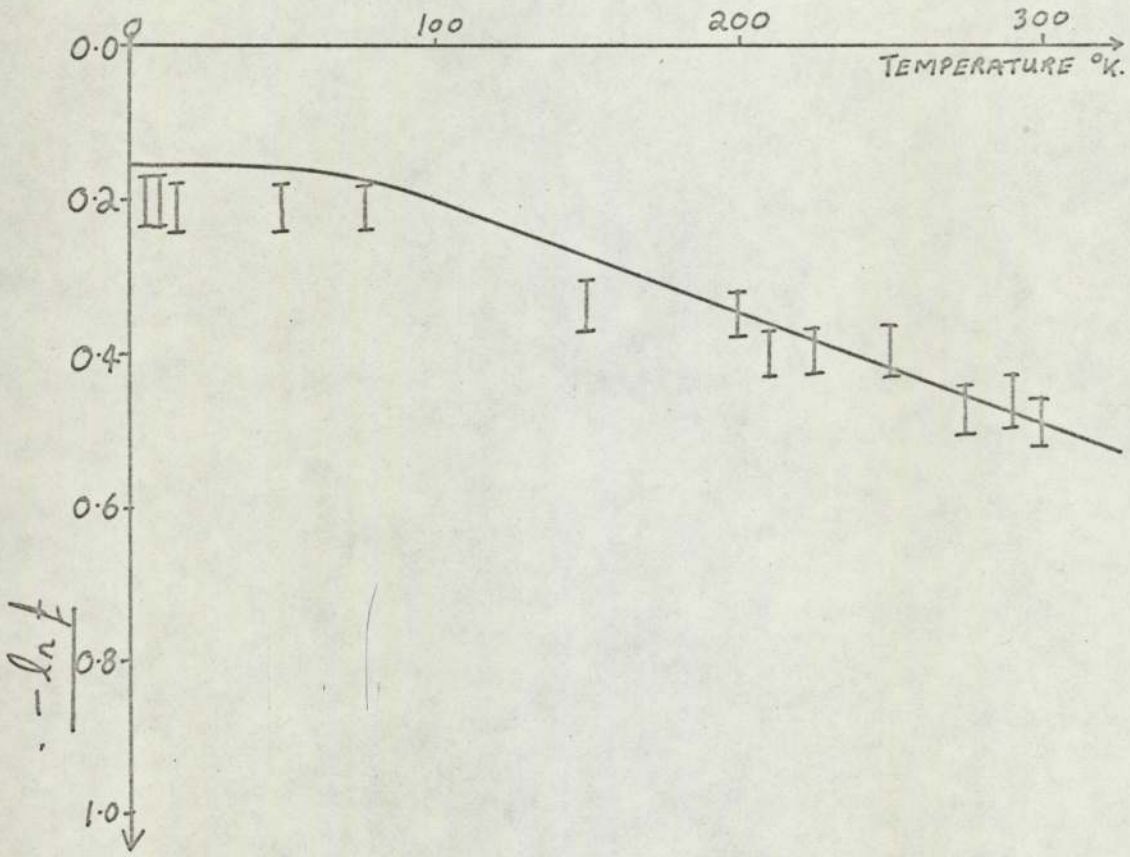

FIG. 5. 6a $-\ln(T_A e^{\alpha})$ VERSUS T°K.

$CuRh_{2-x}Sn_xS_4$ $x=0.1$

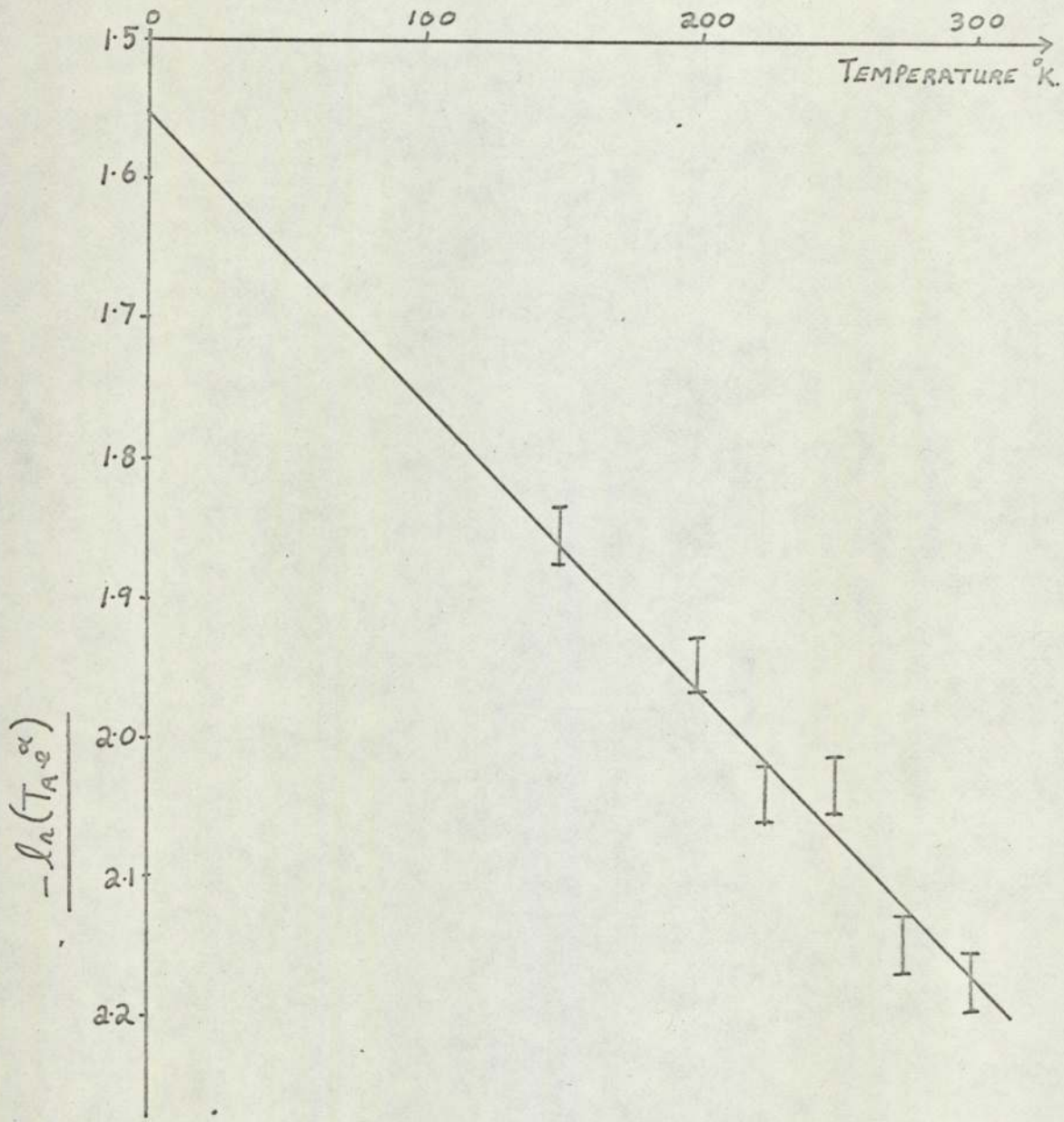

FIG 5.6.b. $-\ln(f_H)$ VERSUS T°K.

$CuRh_{2-x}Sn_xS_4$ $x=0.1$

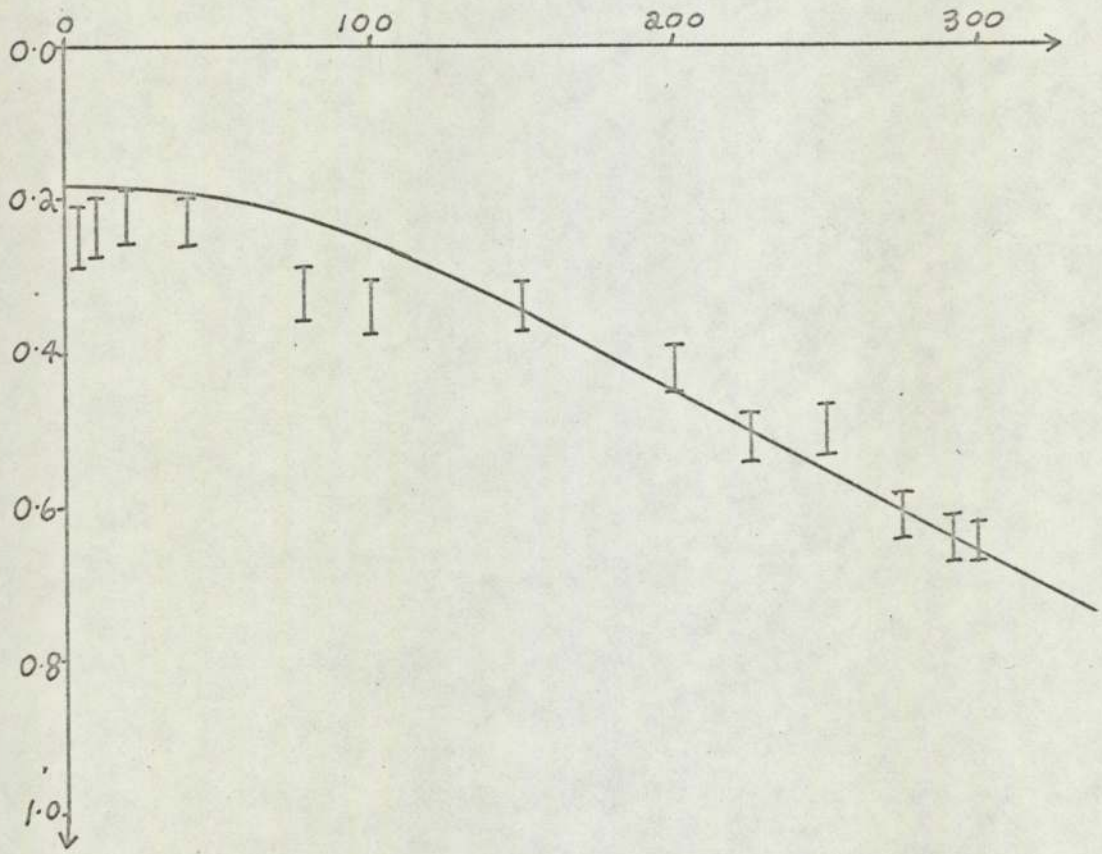

$$\ln f_H = \frac{-K^2 \hbar^2}{2 Mk \Theta (-1)} \qquad 5.4$$

the value of the -1 moment, Θ (-1) may be obtained. The sources of errors shown in the tables of results and the graphs, are detailed in subsection 3.5.4.

5.2.2 The characteristic temperatures

The characteristic temperatures Θ (-1) and Θ (-2) are significant for the recognition of the presence of anharmonicity, for as explained in section 2.2 the moments of the harmonic frequency distribution must obey the relationship Θ (-2) $\leq \Theta$ (-1). The limit Θ (-2) = Θ (-1) corresponds to the Einstein model Θ (n) = Θ_E for which solid curves have been drawn in the Figs 5.1b to 5.6b, after fitting in the high temperature region, (see Table 5.8.)

Comparison of the low temperature experimental data for recoil-free fraction with these limiting curves reveals immediately that for all the superconducting spinels investigated Θ (-2) $>$ Θ (-1) and therefore that the results cannot be explained on the basis of a temperature-independent harmonic frequency distribution. Indeed, according to Dash et al (1968) and Johnson and Dash (1968) it must be concluded that below approximately 100°K there must be an extra temperature dependent anharmonic contribution to the frequency distribution which results in the lowering of Θ (-1).

Such behaviour was first observed in superconductors by Shier and Taylor (1967, 1968) with the compound Nb_3Sn. In this case the anomalous region of ln f versus temperature developed below 85°K and was believed to be associated with the crystallographic phase change from cubic to tetragonal symmetry first observed by Mailfert, Battermann and Hanak (1969). Such transformations are correlated with the development of a soft mode and are now thought to have considerable importance for the strong coupling mechanism of superconductivity (see for example, Testardi, 1972 and also section 1.4). However, whether the same conclusions may be drawn for the spinel superconductors is more

TABLE 5.8

MÖSSBAUER CHARACTERISTIC TEMPERATURE

X	$\omega(-1) \times 10^{12}$ Hz $\pm 1 \times 10^{12}$	θ (-1) ^{o}K ± 6	$\omega(-2) \times 10^{12}$ Hz $\pm 0.5 \times 10^{12}$	θ (-2) ^{o}K ± 2
$Cu\ Rh_{2-x}\ Sn_x\ Se_4$				
0.05	8.6	65.4	12.0	92.0
0.10	9.6	73.6	15.4	117.9
0.175	11.0	84.1	16.8	128.5
0.6	19.3	147.1	20.2	154.5
$Cu\ Rh_{2-x}\ Sn_x\ S_4$				
0.05	19.3	147.1	24.6	187.9
0.10	15.4	117.7	22.1	168.7

difficult to say at the present time.

Two further observations of possible importance are the small temperature dependence of the recoil-free fraction and its decrease with increasing tin concentration, (f is particularly low in the case of the sulphides.). Thus the tin ions become more tightly bound at all temperatures as the tin concentration increases. The magnitude of the room temperature recoil-free fractions reaches 0.6 in the case of the sulphide as compared with 0.3 for anharmonically bound tin in Nb_3Sn (Shier and Taylor, 1967, 1968) and 0.7 for anharmonically bound Fe^{57} in Cu-host lattices (Naussbaum, Howard, Nees and Steen, 1968).

The fact that the temperature dependence of f above 100°K reduces as the tin concentration increases means a reducing temperature dependence of the mean square displacement with increasing tin concentration. This is to be expected as the tin ion is larger than that of rhodium. Expansion of the spinel lattice with temperature would not allow the tin ions as much volume as their concentration increased, (see section 5.3 for further discussion of this point.)

It is possible to determine the characteristic temperatures θ (1) and θ (2) from the following relationships (due to Housley and Hess, 1966) and either θ (-1) or θ (-2);

$$w(n) = \left(\frac{3}{n+3}\right)^{\frac{1}{n}} \frac{k\theta_o}{t} \qquad 5.5$$

Here θ_o is a characteristic temperature obtained from experimental low temperature specific heat measurements, assuming a T^3 law.

At first site this equation should enable the calculation of θ (1) and θ (2) from either θ (-1) or θ (-2), but the presence of low temperature anharmonicity clearly rules out the use of θ (-1). Using θ (-2) and the following relationships derived from equation 5.5, the results of table 5.9 were obtained for θ (1) and θ (2);

TABLE 5.9

HARMONIC MODEL RELATED MÖSSBAUER TEMPERATURES

X	θ (2) ^{o}K	ω(2) x 10^{12} Hz	θ (1) ^{o}K	ω(1) x 10^{12} Hz
$Cu\ Rh_{2-x}\ Sn_x\ Se_4$				
0.05	123	16.0	119.5	15.6
0.10	158	20.5	153.2	20.0
0.175	172	22.4	167.0	21.8
0.6	207	26.9	201.5	26.4
$Cu\ Rh_{2-x}\ Sn_x\ Se_4$				
0.05	251.5	32.7	244	32.0
0.10	226	29.4	219.5	28.7

$\Theta(2) = 1.34\,\Theta(-2)$, $\Theta(1) = 1.3\,\Theta(-2)$

(Values of $\Theta(1)$ and $\Theta(2)$ may also be determined from the total shift results, see section 5.5). Now it is well known that Θ_D may be described as a temperature dependent characteristic temperature in a quasi-harmonic approximation, (see for example Deckor, 1967) and presumably so may $\Theta(-2)$. Therefore the use of a high temperature $\Theta(-2)$ would be expected to make a derived Θ_o too high and therefore a derived $\Theta(1)$ and $\Theta(2)$ too high.

The harmonically related $\Theta(1)$ and $\Theta(2)$ from Mössbauer $\Theta(-2)$ may be compared with the corresponding averages from known infra-red absorption spectra of other sulphide and selenide spinels. The four principle infra-red absorption bands of some examples are given in table 5.10. If one halves these frequencies according to the two phonon assumption of Grimes (1972) and then calculates;

$$w(1) = \langle w \rangle \text{ and } w(2) = \langle w^2 \rangle^{\frac{1}{2}}$$

the results of table 5.11 follow. Clearly the order of magnitude of the results for the harmonically related $\Theta(1)$ and $\Theta(2)$ are correct, (table 5.9). Also, it is interesting to note that the $\Theta(1)$ and $\Theta(2)$ are lower for selenium than for sulphur, from both the infra-red work and this Mössbauer work.

5.2.3 Determination of the potential well flat-zone radius

An important derivative of the approach developed by Dash, Johnson and Visscher (1968) is that an estimate may be made of the radius of the flat-zone of the potential well. The argument follows immediately from the expression of the recoil-free fraction as a product of harmonic and anharmonic components, for in this circumstance,

$$\ln f = \ln f_H + \ln f_{AN} \qquad 5.5$$

Where $\ln f_H$ must lie between zero and the Einstein curve in the low temperature limit. The discrepancy between the experimental values for recoil-free fraction and the Einstein harmonic limit at $0^\circ K$. (see Figs 5.1b to 5.6b)

TABLE 5.10

THE PRINCIPLE INFRA-RED ABSORPTION BANDS OF SOME SULPHIDE AND SELENIDE SPINELS

SPINEL	ABSORPTION BANDS CM^{-1}
$Co\ Cr_2\ S_4$	388, 330, 258, 120
$Zn\ Cr_2\ S_4$	392, 344, 246, 115
$Zn\ Cr_2\ Se_4$	300, 281, 202, 86
$Hg\ Cr_2\ Se_4$	289, 275, 171, 59

REFERENCES: Lutz and Feher (1971)

Wakamura et al (1973)

TABLE 5.11

$\omega(1)$ AND $\theta(1)$ CALCULATED FROM INFRA-RED ABSORPTION SPECTRA TABLE 5.10

SPINEL	$\omega(1) \times 10^{12}$ Hz	$\theta(1)$ °K	$\omega(2) \times 10^{12}$ Hz	$\theta(2)$ °K
$CuCr_2S_4$	25.8	197	27.5	210
$ZnCr_2S_4$	25.9	198	27.7	212
$ZnCr_2Se_4$	20.5	156	22.0	168
$HgCr_2Se_4$	18.7	143	20.6	157

is therefore a measure of the minimum anharmonic contribution to total recoil-free fraction.

According to Dash et al, (see also Shier and Taylor, 1968) this anharmonic contribution may be related to the radius, R of the flat-zone through;

$$\ln f_{AN} \simeq \tfrac{1}{3} K^2 R^2 \qquad 5.6$$

a form of result which was originally a product of harmonic theory. However, it seems that the anharmonic corrections are small provided that $K^2 R^2 \leq \frac{\pi}{2}$ (Maradudin and Flynn, 1963). The latter condition is easily satisfied in the present experiments and it was therefore possible to investigate the correlation of flat-zone radius with superconducting transition temperature, T_c.

The results from these calculations for the spinels investigated are summarized in table 5.12. Unfortunately as explained in section 5.1, it was impossible to retain superconductivity in the sulphide series at resonable tin concentrations. Nevertheless, Fig. 5.7 shows that for the series $Cu\ Rh_{2-x}\ Sn_x\ Se_4$ there appears to be an approximately linear relationship between T_c and flat-zone radius over the range $0.05 \leq x \leq 0.175$ and also, if the same characteristics were appropriate for the sulphide series, (corresponding members having the same electron-atom ratio), that an R of 0.03 Å would correspond to a transition temperature below 1.5°K, the lower level of detection of superconductivity in these experiments. The apparent absence of superconductivity in the compound $Cu\ Rh_{2-x}\ Sn_x\ S_4$, $x = 0.05$, would then be consistant with the results found for the selenide series. (Note that in Fig 5.7 the values of T_c found by Van Maaren et al, (1969) have been used.)

The natural extrapolation of Fig 5.7 suggests the conclusion that an increase in R, whilst holding other factors, such as electron-atom ratio, constant would increase T_c. Now an increase in R, that is an increase in

TABLE 5.12

T_c, (^oK) VERSUS POTENTIAL WELL RADIUS, R (Å) AT 0^oK

$Cu\ Rh_{2-x}\ Sn_x\ Se_4$

X	R Å	T_c ^oK	T_c* ^oK
0.0	-	3.5	3.5
0.05	0.065 ± 0.003	2.7	3.25
0.10	0.065 ± 0.001	3.1	2.9
0.175	0.05 ± 0.001	2.35	2.3
0.6	0.00 ± 0.001	< 1.5	0.0

*These values of T_c are from Van Maaren et al (1969)

$Cu\ Rh_{2-x}\ Sn_x\ S_4$

0.00	-	4.1
0.05	0.03 ± 0.01	4.7
0.10	0.00 ± 0.01	-

FIG. 5.7. PLOT OF T_c VERSUS EFFECTIVE OCTAHEDRAL WELL RADIUS FOR $CuRh_{2-x}Sn_xSe_4$.

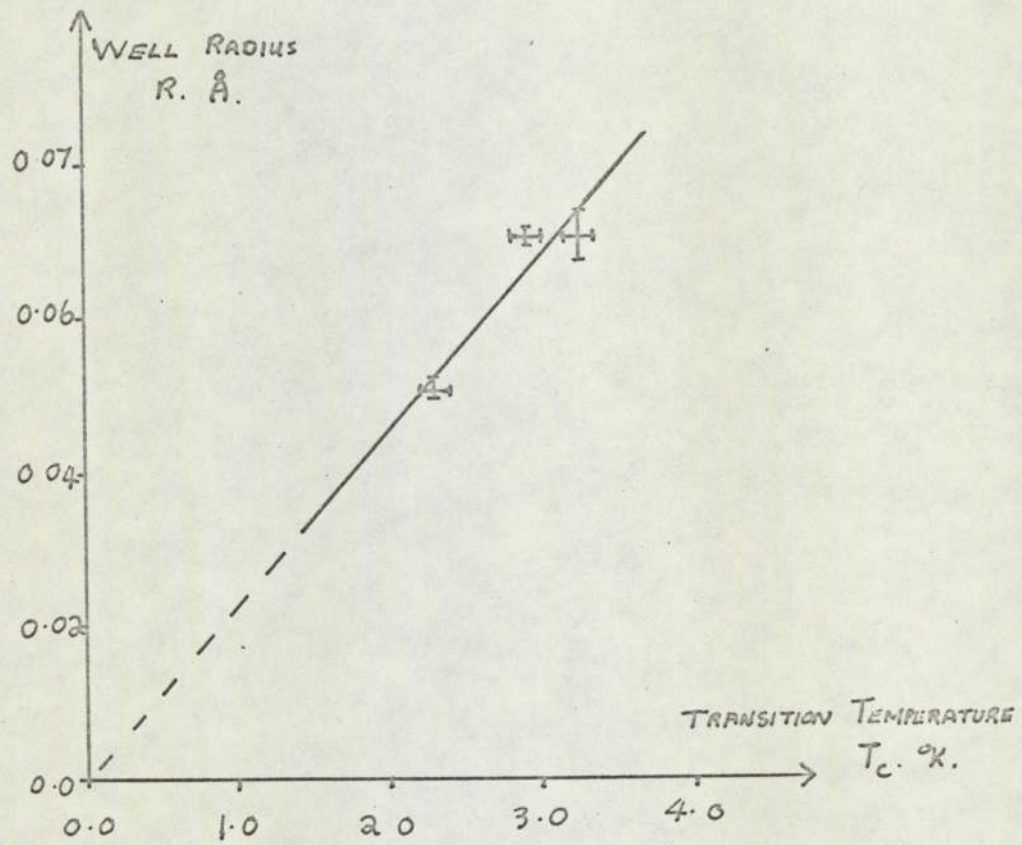

the region of negligable force constant, would presumably also increase the compressibility, β. On the other hand, since;

$$\frac{1}{\beta} = \frac{C_{11} + 2\,C_{12}}{3}$$

there would simultaneously arise an increasing instability corresponding to the approach of the Born limit $(C_{11} + 2\,C_{12}) > 0$ (see section 1.4).

Thus the present results, though few, reinforce yet again the impression derived by so many other workers, (with NbN and β-tungsten compounds, see section 1.3) that instability in these high T_c systems is important for their form of superconductivity; and also that this instability is hydrostatic in character. Moreover, the similarities between the ternary spinel system and the binary NbN and β-tungsten systems are once again quite striking.

5.3 Correlation of the X-ray and Mössbauer results

The X-ray results show that the nearest neighbour separation for the octahedral ion (p) is increasing with increasing tin replacement of rhodium for both the sulphide and selenide spinels, (see table 5.13). The change is small $\lesssim 0.02$ Å per 5% tin, as would be expected, since p is fixed by the more numerous selenium and rhodium ions. Further the root mean square displacement calculated from the X-ray Debye Waller factor B increase by ~ 0.015 Å per 5% tin. The Mössbauer results on the other hand, show that the root mean square displacement of the tin ion on the octahedral site (and the potential well in which the ion is situated), is decreasing as the concentration of tin increases in the selenide, but increases with tin concentration in the sulphide.

Thus for the selenide series whilst the average octahedral hole size is increasing with tin concentration, the Mössbauer root mean square displacement of the occupying tin ions is decreasing. It follows therefore that either the effective radius of the tin atom is increasing with tin concentration or the octahedral sites occupied by tin atoms are being preferentially reduced

TABLE 5.13

COMPARISON OF X-RAY AND MÖSSBAUER RESULTS

$Cu\ Rh_{2-x}\ Sn_x\ Se_4$

X	p (Å) AT 293°K	$\langle x^2 \rangle^{\frac{1}{2}}$ (Å) FROM B AT 293°K	$\langle x^2 \rangle^{\frac{1}{2}}$ (Å) FROM MÖSSBAUER AT 293°K
0.0	2.474	0.062	-
0.05	2.477	0.087	0.120
0.10	2.478	0.087	0.094
0.175	2.500	0.097	0.085
0.6	2.570	0.123	0.072

$Cu\ Rh_{2-x}\ Sn_x\ Se_4$

0.0	2.359	0.087	-
0.05	2.381	0.087	0.058
0.10	2.408	0.097	0.067

in size. The latter is unlikely, since the rhodium ion is smaller than that of tin. The former is possible, however and may arise either from electron localization or from orbital expansion. Both of these effects could produce an increase in effective tin radius with increasing tin concentration, but would be difficult to distinguish.

Very similar results have been found by Nassbaum, Howard, Nees and Steen, (1968) for anharmonically bound Fe^{57} in copper and nickel host lattices. The ratio of nearest neighbour separation in α- Fe compared with that of pure copper is 0.97 whilst relative to pure nickel it is 1.00. Yet the rate of change of lattice parameter with iron concentration is positive for both the copper and nickel hosts. Nassbaum et al were concerned with the anomalously large anharmonicity of the iron impurity and this ion core size was a side issue. Nevertheless, for the present context it is interesting to note that they consider that in their case the overlap of the outer electron wave functions is involved. Further they remark that this is possibly the cause of the anharmonicity.

A particularly pertinant example of unusual involvement of outer electron wave functions in the spinel structure, is the electron localization around vanadium ions in Cu Cr_{2-x} V_x S_4, at low vanadium concentrations, (Robbins et al, 1970. See section 1.5.3 for a discussion of this work). This phenomena is demonstrated by the marked increase in lattice parameter for $0 < x < 0.5$, followed by a decrease to that of Cu V_2 S_4 as the electrons delocalise, (see Fig 1.16).

Now the Isomer Shift constituent of the Total Shift, (see section 2.3.2) is a function of the electron density at the nucleus and the latter will be affected by outer orbital expansion; increasing if electron localization takes place. Precision measurements are required for a quantitative analysis but a qualitative picture is available from the total shift results of this work presented in Tables 5.1 to 5.6.

In section 2.3.2 it was shown that the total shift will increase with decreasing temperature, since the thermal shift contribution decreases with decreasing temperature. This enables the direction of increasing total shift to be determined. Now at a fixed temperature an increase in the total shift with tin concentration will be due solely to an increase in the electron density at the nucleus. Table 5.14 shows the results obtained, the direction of increasing shift being to higher velocities. (The isomer shift for the tin nucleus is positive, see section 2.3.2). The isomer shift results for the absorber Cu Rh_{2-x} Sn_x Se_4, x = 0.05 are not reliable, due to the weak source used (see section 3.5) and are not reproduced here.

Clearly there is no simple relationship between electron density and tin concentration. There are however several phenomena which could be responsible for this complexity. For example recent work has indicated (Moller and Mössbauer, 1967), that the isomer shift for tin decreases with decreasing volume. Apparently the increased p-electron shielding overcomes the tendency for an increase in S-electron density at the nucleus. Thus as the octahedral sites expand with increasing tin, the tin ions' outer orbitals are able to expand and take-up the available space, resulting in a decrease in the root mean square displacement and producing an increase (due to reduced p shielding) in S-electron density at the nucleus.

If the hypothesis is made that electron localization at the tin ion sites takes place, then this two would be affected by the increased tin concentration directly and also by the resulting orbital expansion. If in a similar manner to Cu Cr_{2-x} V_x S_4, the electron localization reduced with increasing tin concentration the combined effect of this and the orbital expansion could well account for the total shift changes, as a function of tin concentration.

The order of magnitude of the isomer shift changes in 0.03 mm/sec per 5% tin, compared with shifts of the order of 3 mm/sec between di- and

TABLE 5.14

TOTAL SHIFT VERSUS TIN CONCENTRATION X

$Cu\ Rh_{2-x}\ Sn_x\ Se_4$

X	TOTAL SHIFT (AT 293°K) mm/sec. ± 0.002
0.05	-
0.10	1.683
0.175	1.692
0.6	1.647

$Cu\ Rh_{2-x}\ Sn_x\ S_4$

0.05	1.412
0.10	1.412

NOTE: These results are taken from Figs. 5.8 to 5.12

trivalent tin (Mössbauer Effect Data Index, 1965). Thus changes of electron density of the order of a few hundreths of an electron per atom correlate with changes in ionic radius of a few hundreths of an Ångstrom. This was also found to be the case by Shier and Taylor (1967, 1968) from experiments on Nb_3 Sn.

In the case of the sulphide spinel series, there is little or no isomer shift change with tin concentration. Here however the increase in octahedral hole size correlates with an increase in the root mean square displacement and therefore it appears that no unusual electronic behaviour is taking place. It is to be noted however that in these compounds superconductivity disappears very rapidly with increasing tin concentration.

In conclusion it is striking that the changes in both anharmonicity and superconductivity are correlated with changes in electron orbital occupation and size. The implication is that the superconductivity in the spinels, like the anharmonicity is connected with a localized phenomena.

5.4 The Total Shift Results

5.4.1 General remarks

In the tables 5.1 to 5.6 the total shifts for all the absorbers are recorded as a function of temperature. Figs 5.8 to 5.12 present these results graphically. The results for the selenide Cu Rh_{2-x} Sn_x Se_4, x = 0.05 are not drawn because of the inherent errors discussed previously (see section 3.5).

The solid lines in each graph represent the limiting harmonic curves for the thermal shifts, fitted to the high temperature data and the estimated shift at 10°K. These curves are not optimised fits because the data indicates that the high temperature limiting slope of 3 k T/M (see section 2.2), has not been reached much below 300°K. It must also be remembered that the materials under investigation are anharmonic and also

FIG. 5.8 TOTAL SHIFT VERSUS TEMPERATURE.

$CuRh_{2-x}Sn_xSe_4$ $x = 0.10$

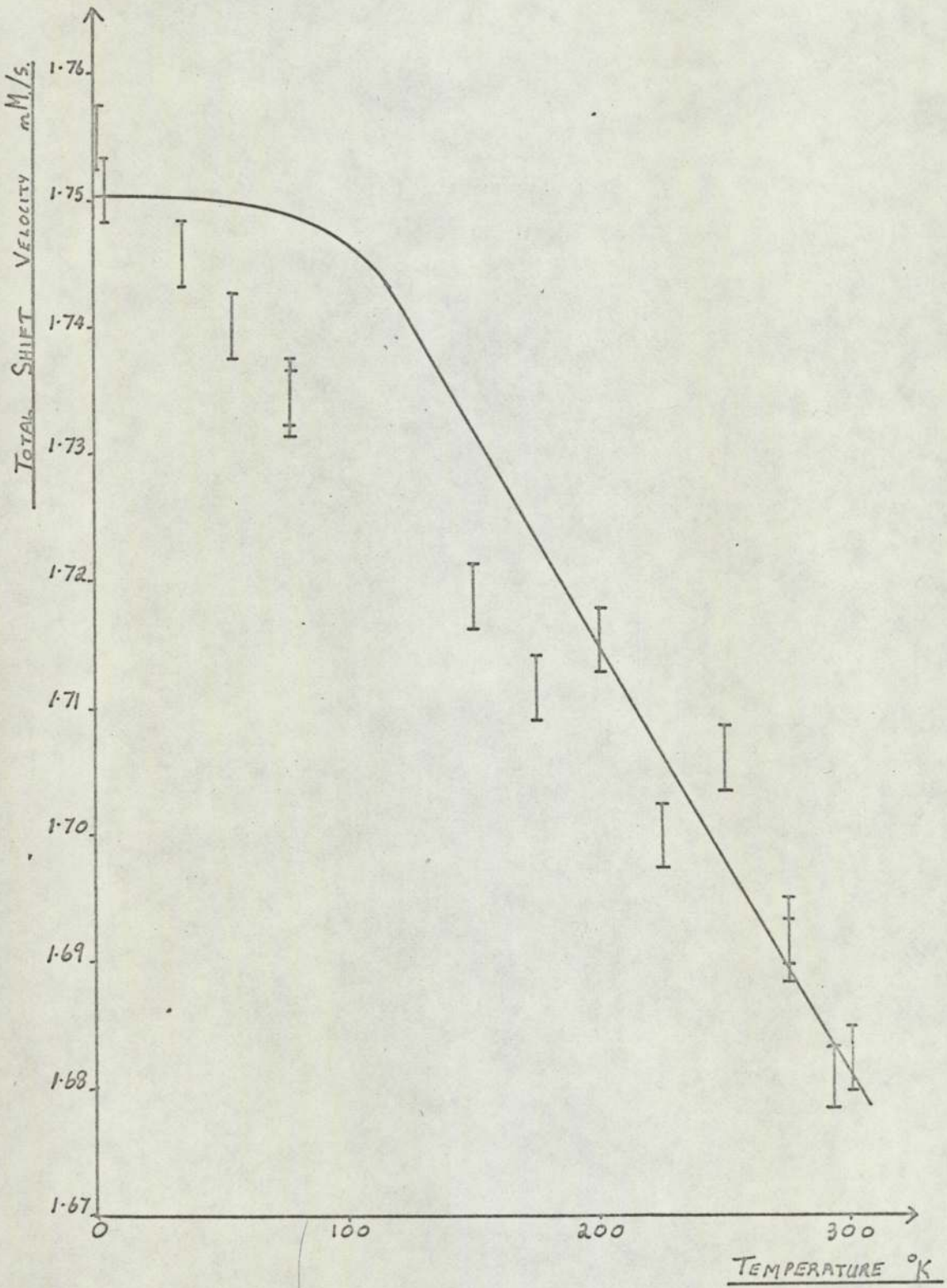

FIG. 5.9 TOTAL SHIFT VERSUS TEMPERATURE

$CuRh_{2-x}Sn_xSe_4$ $x = 0.175$

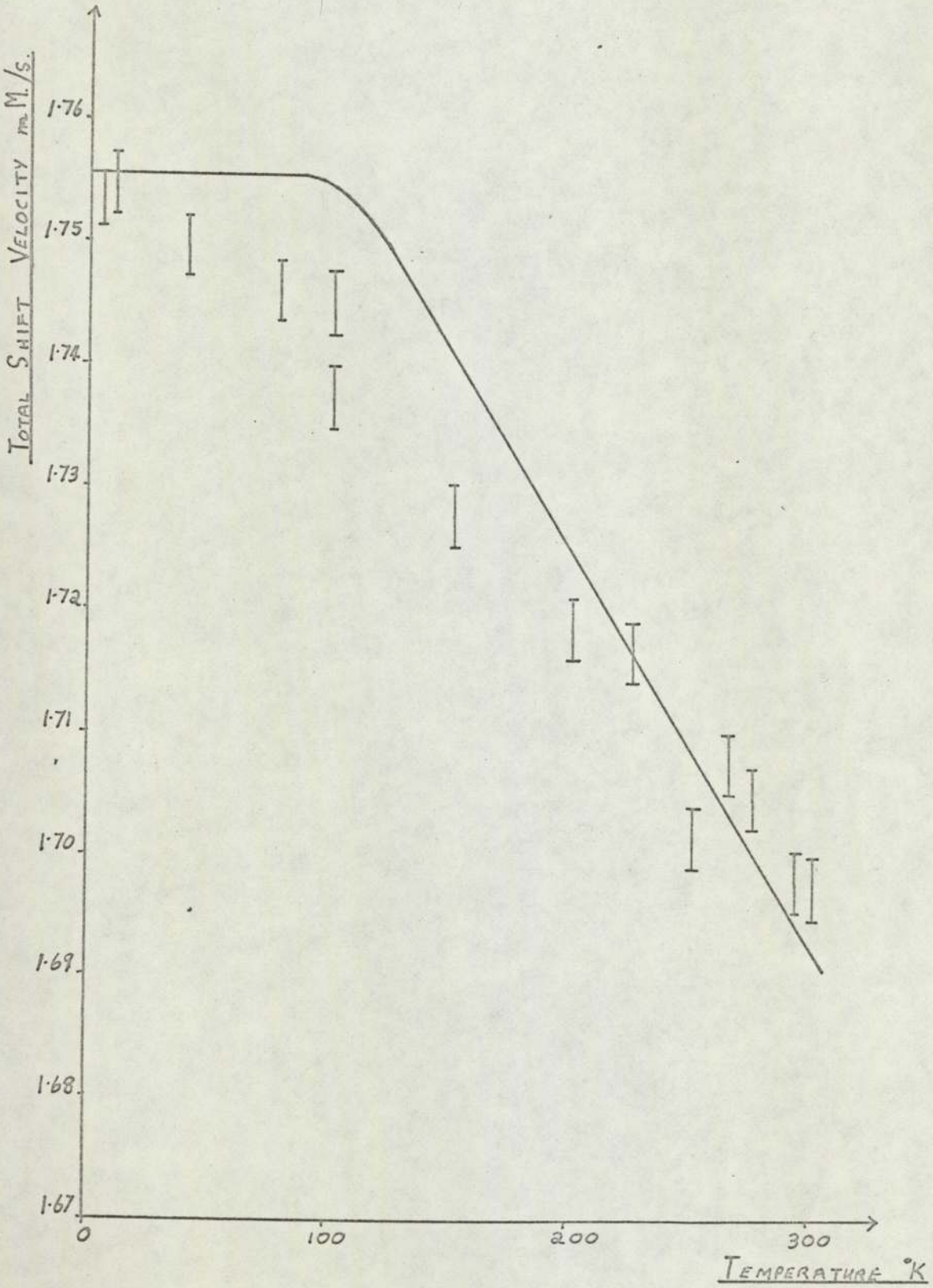

FIG. 5.10 TOTAL SHIFT VERSUS TEMPERATURE

$CuRh_{2-x}Sn_xSe_4$ $x=0.60$

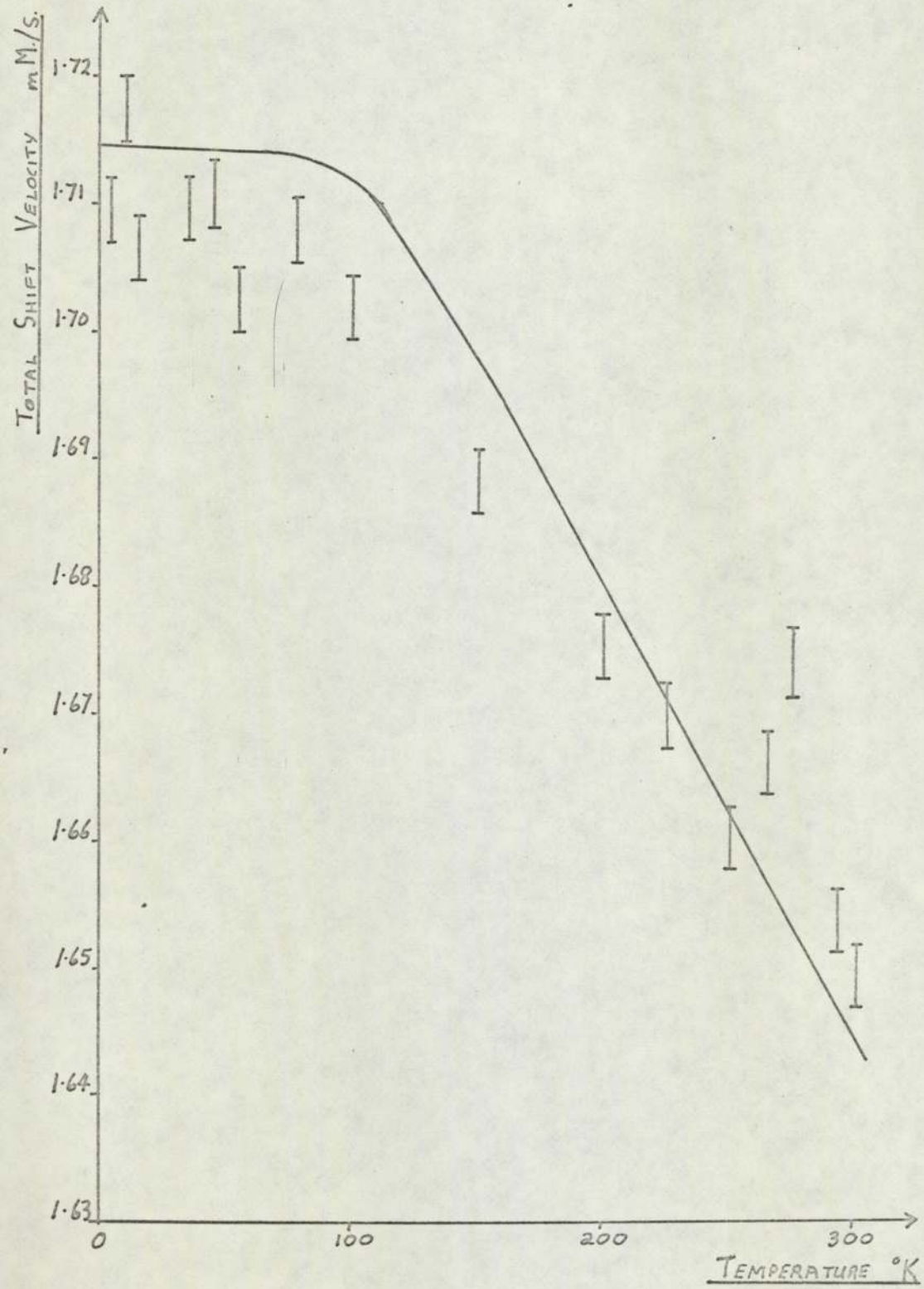

FIG. 5.11. TOTAL SHIFT VERSUS TEMPERATURE

$CuRh_{2-x}Sn_xS_4$ $x = 0.05$

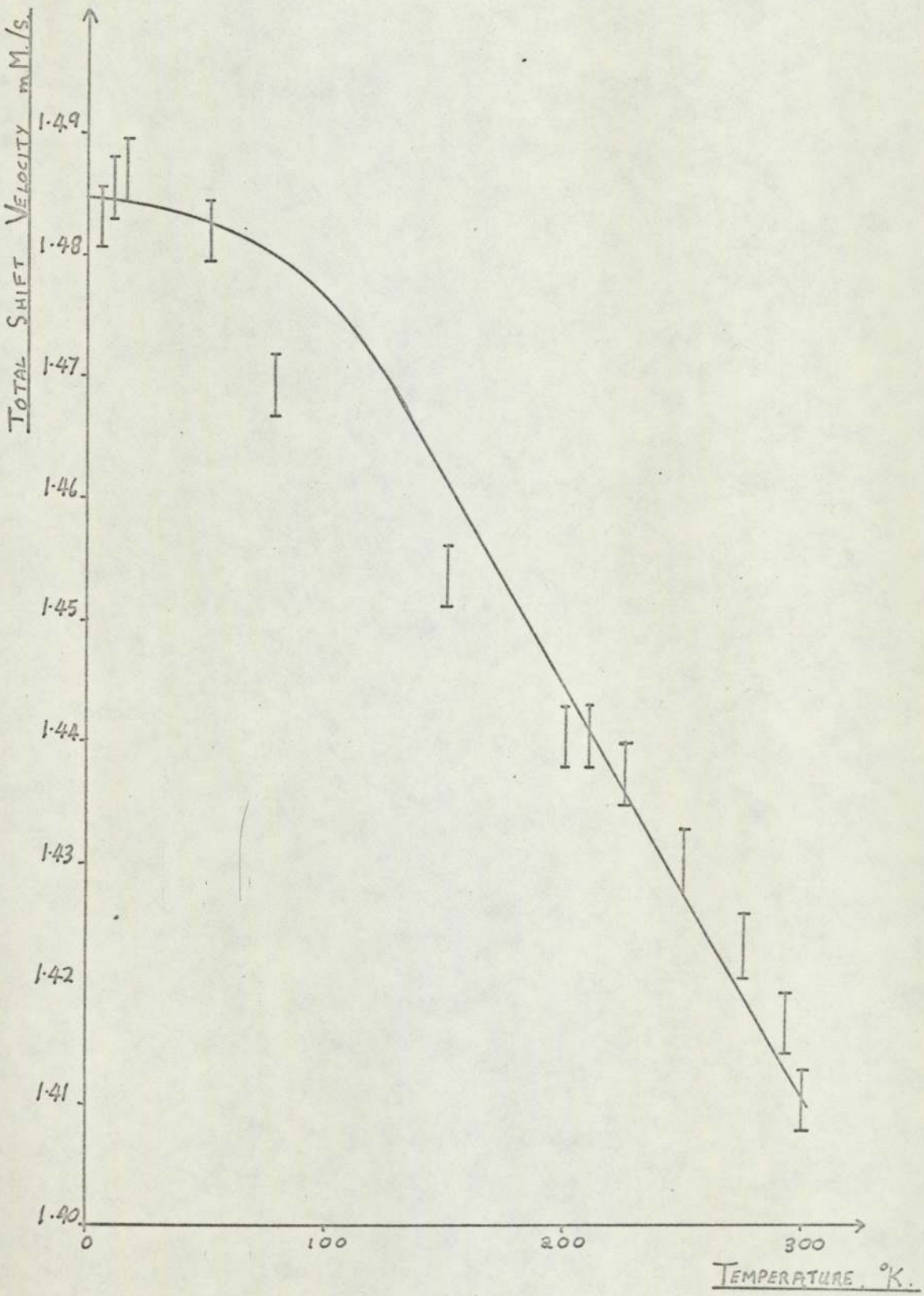

FIG. 5.12 TOTAL SHIFT VERSUS TEMPERATURE

$CuRh_{2-x}Sn_xS_4$ $x = 0.10$

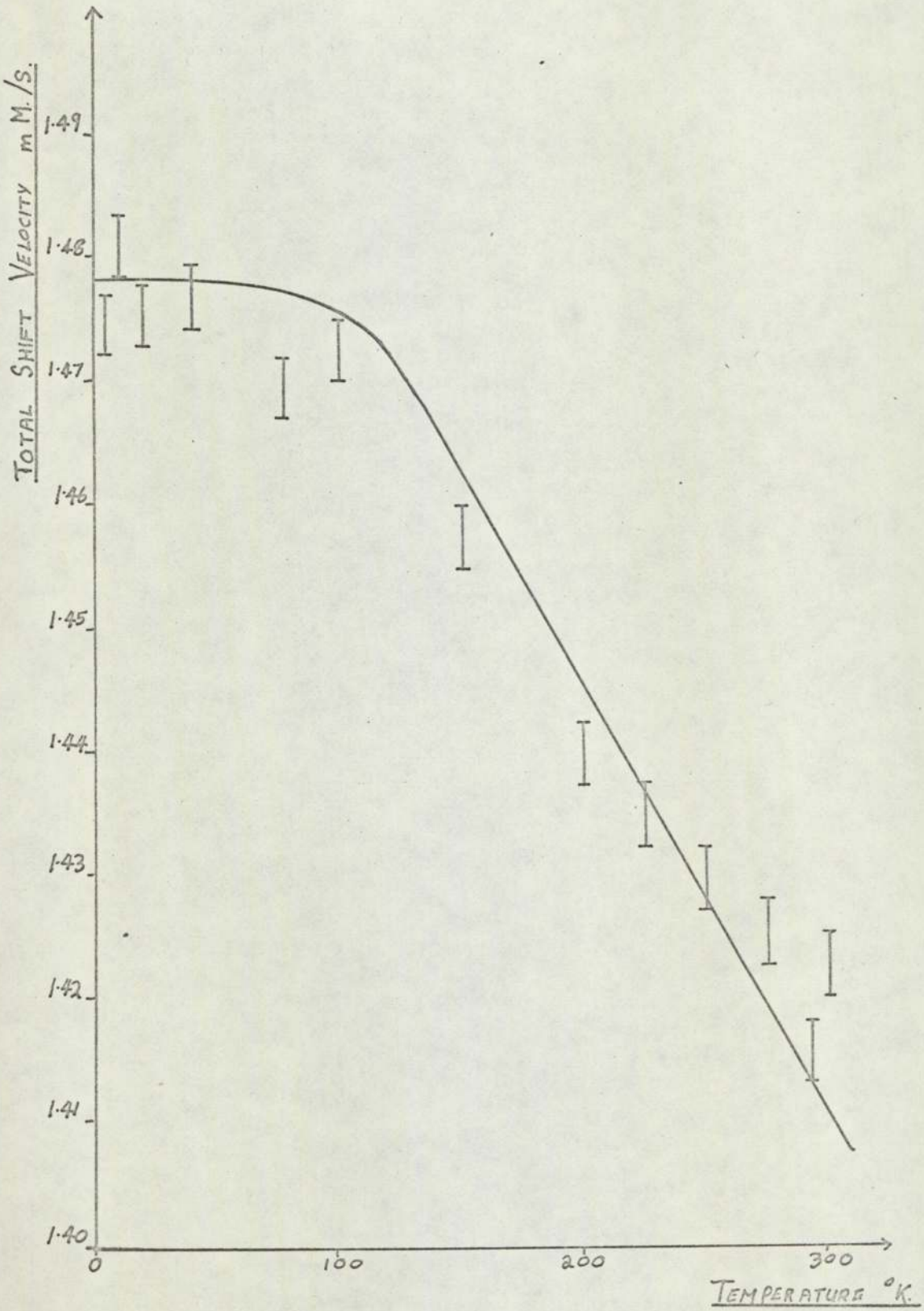

that there is a small, but finite contribution to the total shift from the temperature dependence of the isomer shift, via thermal expansion.

Despite these points, the results of table 5.15 for the first and second moments of the frequency spectrum, (derived from the curve fitting procedure and the $0^{o}K$ intercept) are close to those predicted in table 5.9 from the (-2) moment. Moreover as explained in section 5.2.2. the latter results were expected to be high due to the failure to allow for the temperature dependence of θ (-2).

The most striking feature of the data is the strong temperature dependence of the total shift at low temperatures. Indeed the data lie on straight lines. It is necessary to consider the sign of the shift in order to analyse this anomaly further.

Now, since the source was at room temperature its thermal shift, δ (thermal, source), will be greater than that of the absorber at low temperature, δ(thermal, absorber). Using equation 2.34 the total shift, δ, at low absorber temperature is given by;

$$\delta = \delta_{o} + / \delta(\text{thermal}) /$$

Where δ_{o} is the isomer shift and δ(thermal) = δ(thermal, absorber) - δ(thermal, source). The total shift was always large, indicating that if δ_{o} is negative, it is much greater in magnitude than the thermal shift. However, as the absorber temperature increases / δ(thermal) / decreases, requiring, /δ/ to increase if δ_{o} is negative. It is concluded therefore that the isomer shift is large and positive for the absorber / source ($Ba\ Sn\ O_{3}$ and $Ca\ Sn\ O_{3}$), combination used in this work.

As the temperature rises from $0^{o}K$ there is required, either a decrease in the isomer shift or an increase in the thermal shift to explain the total shift's strong temperature dependence at low temperature. An increase in thermal shift with temperature implies a change in crystal structure which would allow the octahedral ions to vibrate at larger velocities as the

TABLE 5.15

VALUES OF θ (1), θ (2) AND THE TIN FORCE CONSTANT

X	δ_o mm/s	$\omega(2) \times 10^{12}$ Hz	θ (2) ^{o}K	$\omega(1) \times 10^{12}$ Hz	θ (1)	K x 10^2 Newtons/metre
$Cu\ Rh_{2-x}\ Sn_x\ Se_4$						
0.05	-	-	-	-	-	-
0.10	1.785	14	104	26	201	0.39
0.175	1.795	16	120	30	229	0.50
0.6	1.750	14	107	28	212	0.39
$Cu\ Rh_{2-x}\ Sn_x\ Se_4$						
0.05	1.515	12	96	23	172	0.285
0.10	1.515	14	107	28	212	0.39

temperature rises than would normally occur in the temperature region below 100°K. A change in the thermal shift would be accompanied by an appreciable heat capacity (Wertheim, 1971) which would render this explanation open to investigation. However the changes in the crystal structure would also have an appreciable effect upon the S-electron density and thus the isomer shift. This combination of effects would therefore be expected to produce rather more complex total shift versus temperature results than those obtained. A change in thermal shift as an explatation of the anomaly therefore seems unlikely. However structural distortions in the spinels are well known, (see section 1.5.2) and this explanation can not be ruled out until low temperature heat capacity measurements are made.

A rather more straight forward explanation of the anomaly uses changes in the occupation of the electronic levels in the band structure. Consider the band model discussed in section 1.5.3. A narrow band occupied by holes and sharply decreasing above the Fermi level will provide holes for an upper band, having s-state admixture, as the temperature rises. This will produce a decrease in the S-electron density and therefore, in the isomer shift as the temperature rises. Thus the observed anomaly lends support to the theory of Schaeffer and Van Maaren, (1968) that the superconducting spinels have a narrow d-band at the Fermi level occupied by holes. It was pointed out in chapter 1 that the spinel band structure is very similar to the high transition temperature β-tungsten group of which Nb_3Sn is typical. That exactly the same anomaly should occur in Nb_3Sn, as observed by Shier and Taylor, (1967, 1968) would therefore be expected. Their arguments for the band structure explanation are very similar to those presented here and in addition they were able to exclude possible thermal shift effects, as no corresponding heat capacity anomaly has been observed.

As with the present results, the total shift results of Shier and Taylor do not reach the high temperature classical limit. They suggest that

this arises from the high temperature contribution to the isomer shift from thermal expansion. They also point out that changes in the electron density could be related to the structural transition known to occur in Nb_3Sn. However it would be expected that quadropole line splitting (Wertheim, 1971) would result from such structural transition, with consequent Mössbauer line broadening. It is interesting to note that no unusual line broadening occurs in either Nb_3Sn or the spinel absorbers, implying that the structural transformations, if any, are only minor and that the cause of both the anharmonicity and the total shift anomaly is more likely to be related to changes in the electronic band structure. The latter is also supported by the analysis of section 5.3, where the X-ray and Mössbauer results were correlated.

It is also important to note that for the non-superconducting spinels the anomaly in the total shift is much smaller, suggesting a connection between the anomaly and superconductivity, (e.g. compare Fig 5.8 and Fig 5.10). Possibly the energy band gap increases with tin concentration and thus prevents the holes from populating the upper band, thereby also influencing the isomer shift.

5.4.2 Derivation of the force constants of tin

As was first pointed out by Housley and Hess (1966) the determination of the characteristic frequencies $\omega(2)$ from the thermal shift permits the derivation of a simple average over the force constants, K for the Mössbauer atom (see also Johnson and Dash,1968). The relationship derived by them is:

$$K = \frac{1}{3} \sum_{\alpha=1}^{3} K^{\alpha\alpha} = M\omega^2 (2) \qquad 5.7$$

and thus K for the tin atom may be obtained.

Applying this simple relation to the spinel data leads to the results included in table 5.15. As expected, the values for K are low. They may be

compared for example, with those of Grimes and Collett, (1971) obtained from the analysis of the infra-red absorption spectra of $Mg\ Al_2\ O_4$ and $Mg\ Cr_2\ O_4$. In these ionic compounds it seems that Al - O and Cr - O bands are best characterised by;

$$K = 0.59 \times 10^2 \quad \text{Newtons/metre}$$

i.e. some 20% or so higher than the values of table 5.15. On the other hand, similar low values were found with $Fe\ Cl_2$ and $Sn\ S_2$ by Johnson and Dash, (1968) and are believed to provide additional evidence for the presence of a local flat-zone potential well.

5.5 Investigation of the validity of the McMillan Hypothesis for the spinels

5.5.1 Introduction

In 1968 Taylor and Craig discovered that for a variety of Mössbauer systems, including the superconductor $Nb_3\ Sn$, ln f is approximately linearly related to the total shift. This observation led them to suggest that it might be possible to characterise different materials through a parameter 'S' which they defined by the relationship;

$$S = \frac{\ln f}{\delta} = \frac{2c^2 K^2 \langle x^2 \rangle}{\langle v^2 \rangle} \qquad 5.8$$

(See also Kitchens, Craig and Taylor, 1970). Where $K = E/\hbar c$ and E is the energy of the gamma-radiation. δ is the relative gamma-ray energy shift, (i.e. $\delta(E)/E$, see, Taylor and Craig, 1968) obtained from the measured velocity shift by dividing by the velocity of light. The major contribution to the total shift as a function of temperature is, of course, the thermal shift and it is assumed to be the only contribution of significance within the experimental errors. (see secton 2.3.2.). Whilst this approximation has been shown to be poor at low temperatures (see section 5.4) the value of S is determined mainly by the high temperature measurements.

In the harmonic limit equation 5.8 may be written as;

$$S = \frac{2c^2 K^2}{3} \frac{\langle \omega^{-1} \rangle}{\langle \omega \rangle} \qquad 5.9$$

(using equation 2.8 and 2.9). So that for an Einstein model S would be a constant, independant of temperature. On the Debye model however, S is found to be constant only for temperatures greater than $\sim 0.3\ \Theta_D$ and decreases by a factor upto $\frac{2}{3}$ at lower temperatures so that $S\ (0^\circ K) \geqslant \frac{2}{3} S$, (Taylor and Craig, 1968). Further these authors have found that using the known phonon spectrum for metallic Fe a computed ln f versus δ curve does show this low temperature upturn, with a final slope of 0.699S (c.f. 0.667S on the Debye model). The experimental results on Sn Te, presented by these authors, also show this upturn, (the magnitude of which supports the $\frac{2}{3}$ coefficient) despite the known presence of a large degree of anharmonicity.

Ln.f versus δ is plotted in Fig 5.13 to 5.18 from the results shown in tables 5.1 to 5.6. The total shift is shown in both mm/sec. and as the relative energy shift. Values of absolute temperature at which the parameters were measured are also shown. The accuracy of the measurements, particularly for Cu Rh_{2-x} Sn_x Se_4, x = 0.05, precludes comment on the curvature at low temperatures, but reasonable estimates of the S parameter are possible. These are presented in table 5.16.

Taylor and Craig, (1968) define a characteristic temperature, γ, by;

$$\gamma = \frac{E}{k} \left(\frac{2}{S}\right)^{\frac{1}{2}} \qquad 5.10$$

Their measurements show γ to be in good agreement with Θ_D, the Debye characteristic temperature, found from heat capacity experiments on Nb_3 Sn and on Fe^{57} in a range of host lattices.

They also defined the zero point velocity by;

$$v_{zp} = c \left\{\frac{-3 \ln f_o}{S}\right\}^{\frac{1}{2}} \qquad 5.11$$

Where f_o refers to the recoil free fraction at absolute zero. This quantity v_{zp} is not accessible by any other type of experiment at present.

Finally Taylor and Craig defined a dimensionless zero-point parameter "zp";

$$zp = (x_{zp})\ (m\ v_{zp})\ /\hbar \qquad 5.12$$

FIG 5.13 $-\ln(I_H)$ VERSUS TOTAL SHIFT

$Cu\,Rh_{2-x}\,Sn_x\,Se_4$ $x = 0.05$

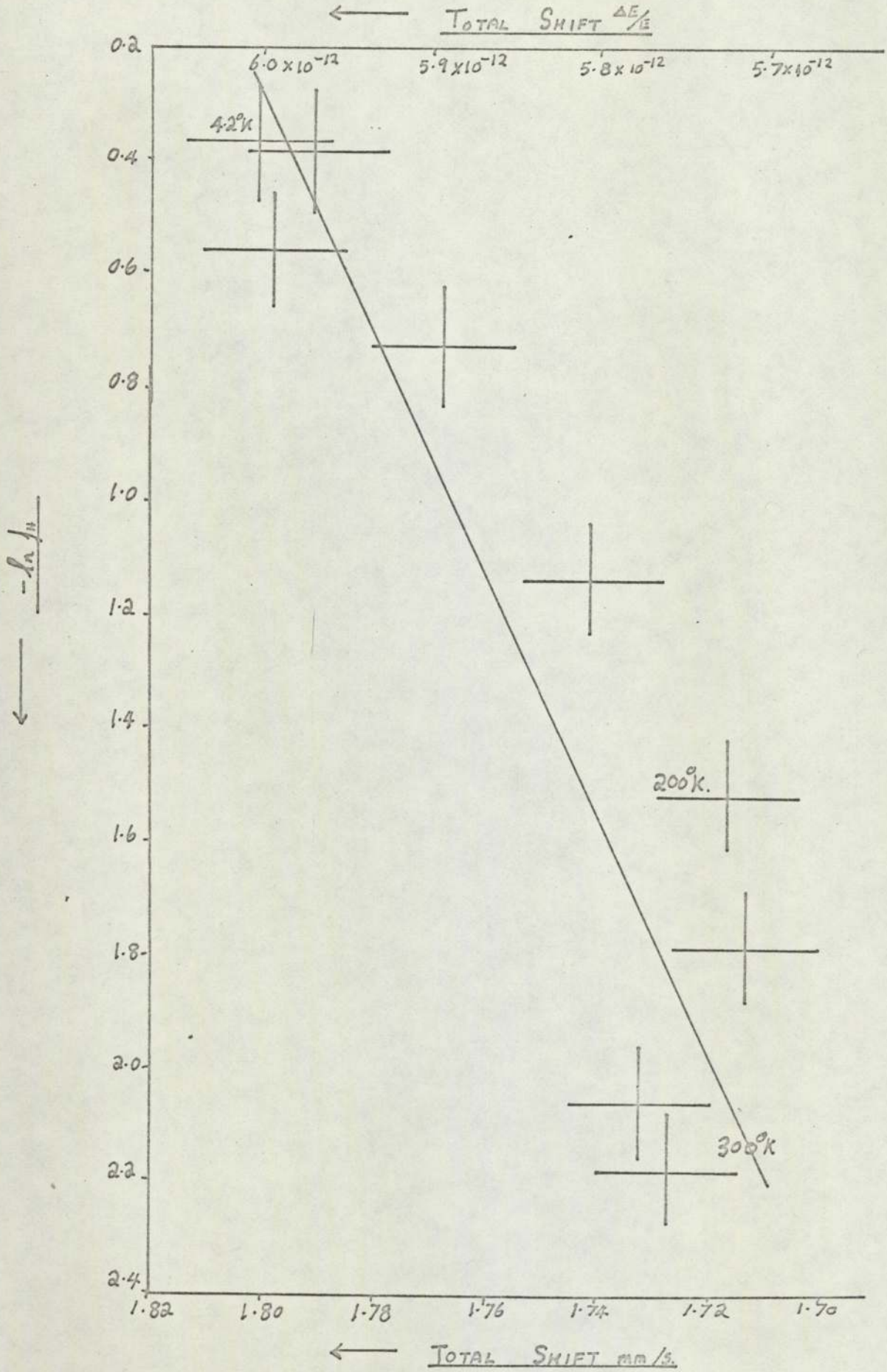

FIG. 5.14 $\ln I$ VERSUS TOTAL SHIFT.

$CuRh_{2-x}Sn_xSe_4$ $x = 0.1$

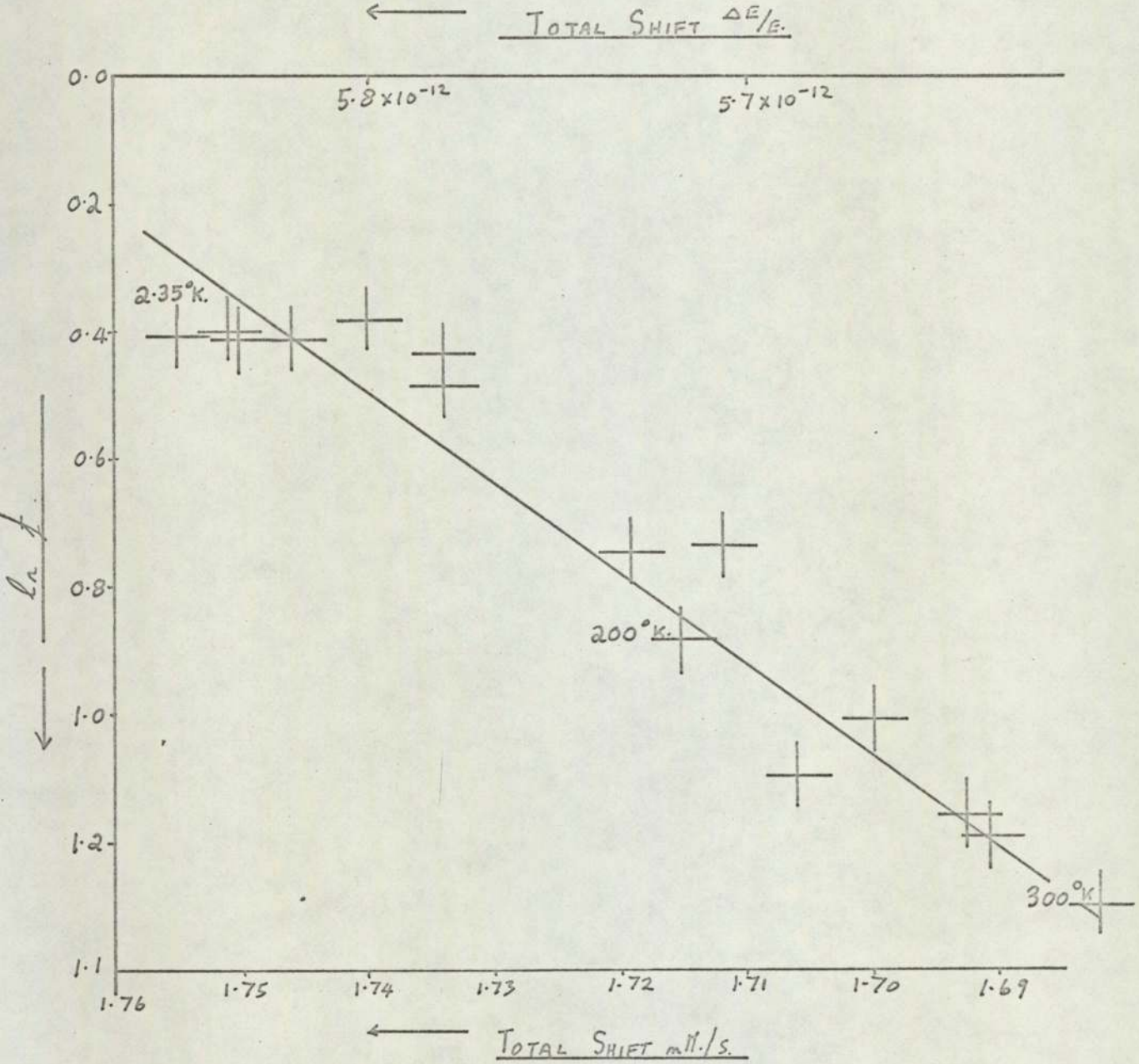

FIG. 5.15 $\ln f$ VERSUS TOTAL SHIFT.

$CuRh_{2-x}Sn_xSe_4$ $x = 0.175$

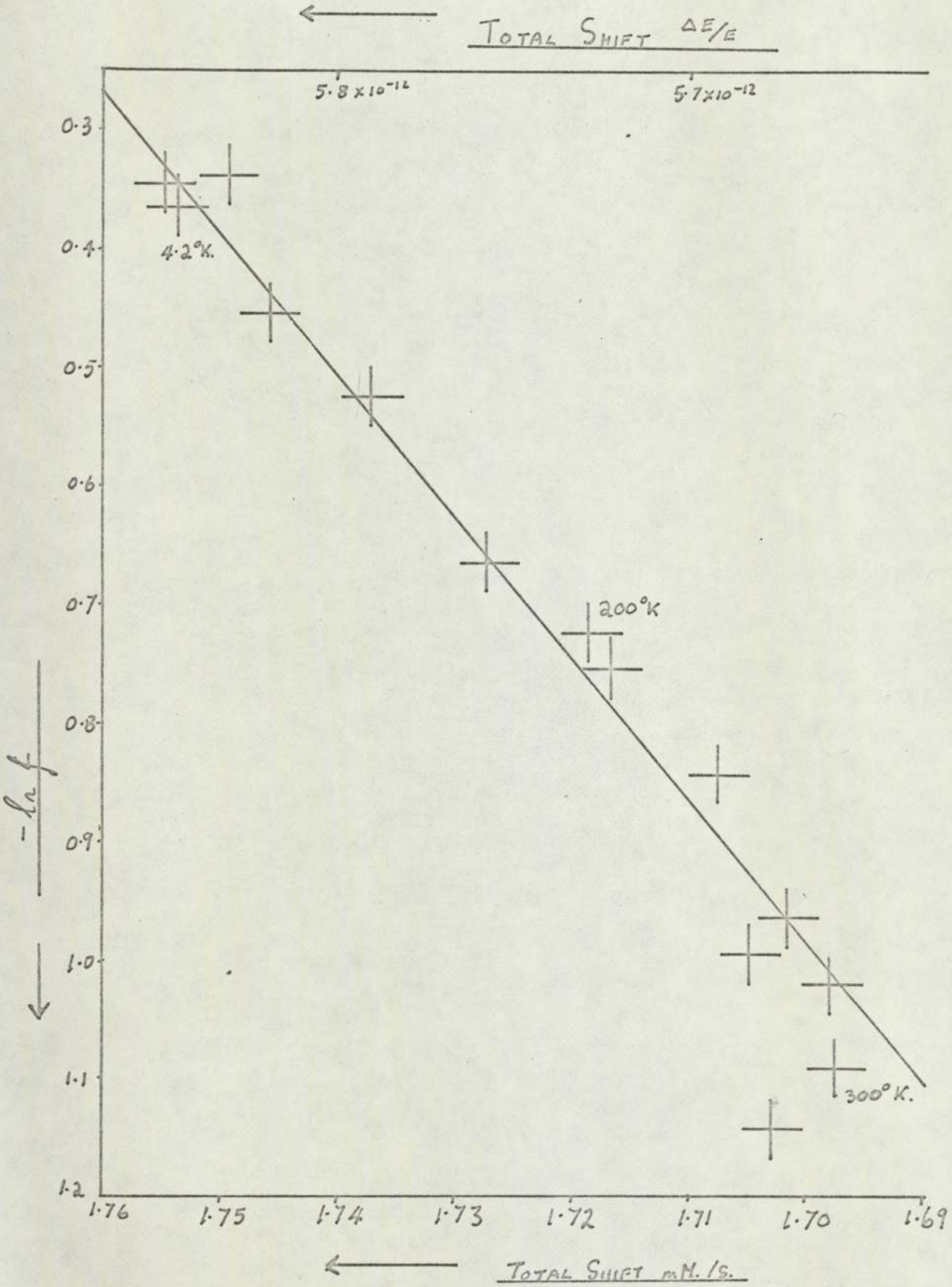

FIG 5.16 $\ln f$. VERSUS TOTAL SHIFT.

$CuR_{H_{2-x}}S_{N_x}S_{E_4}$ $x = 0.6$

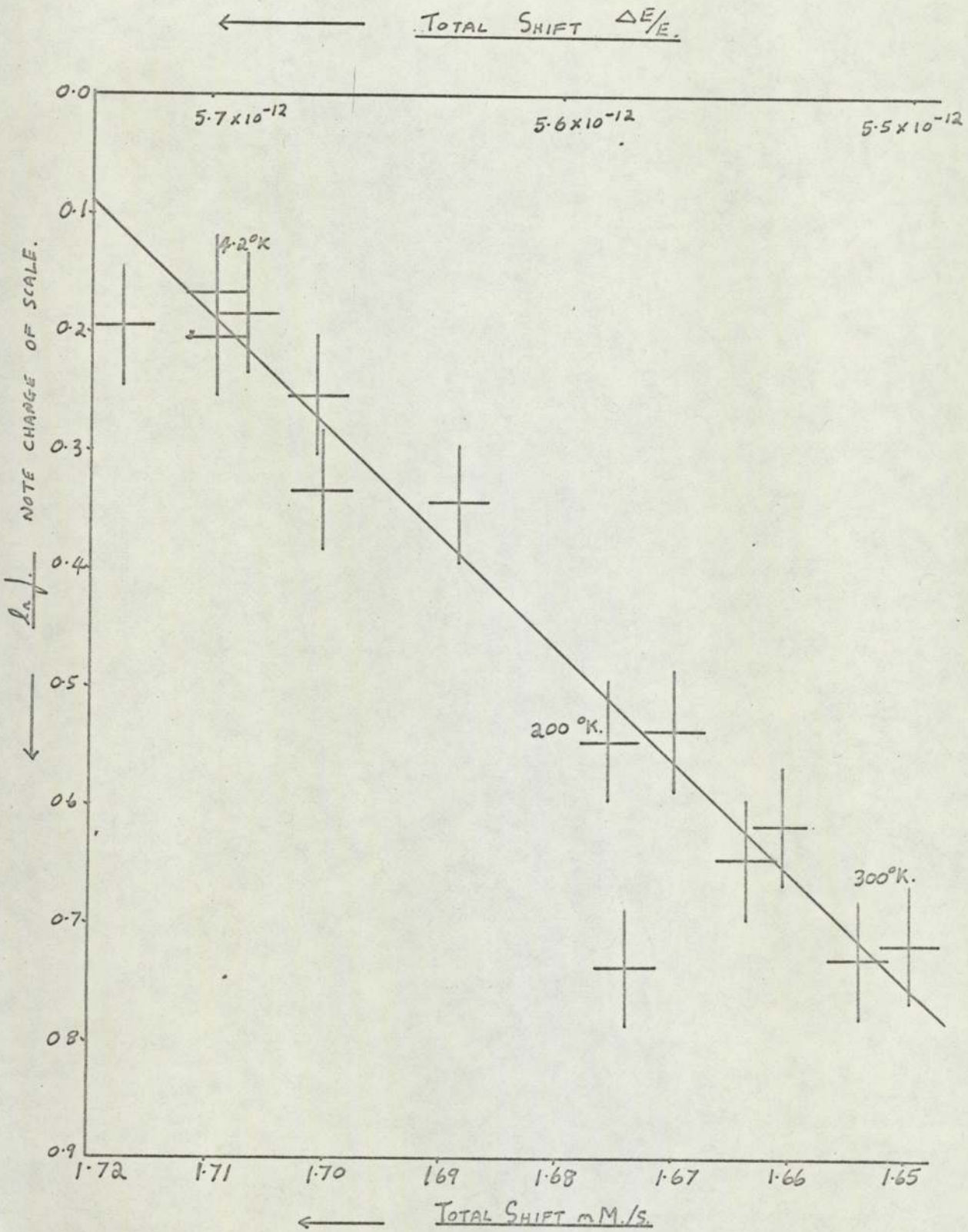

FIG 5.17. $\ln(f)$ VERSUS TOTAL SHIFT

$Cu\ R_{H_{2-x}}\ Sn_x\ S_4.\quad x = 0.05$

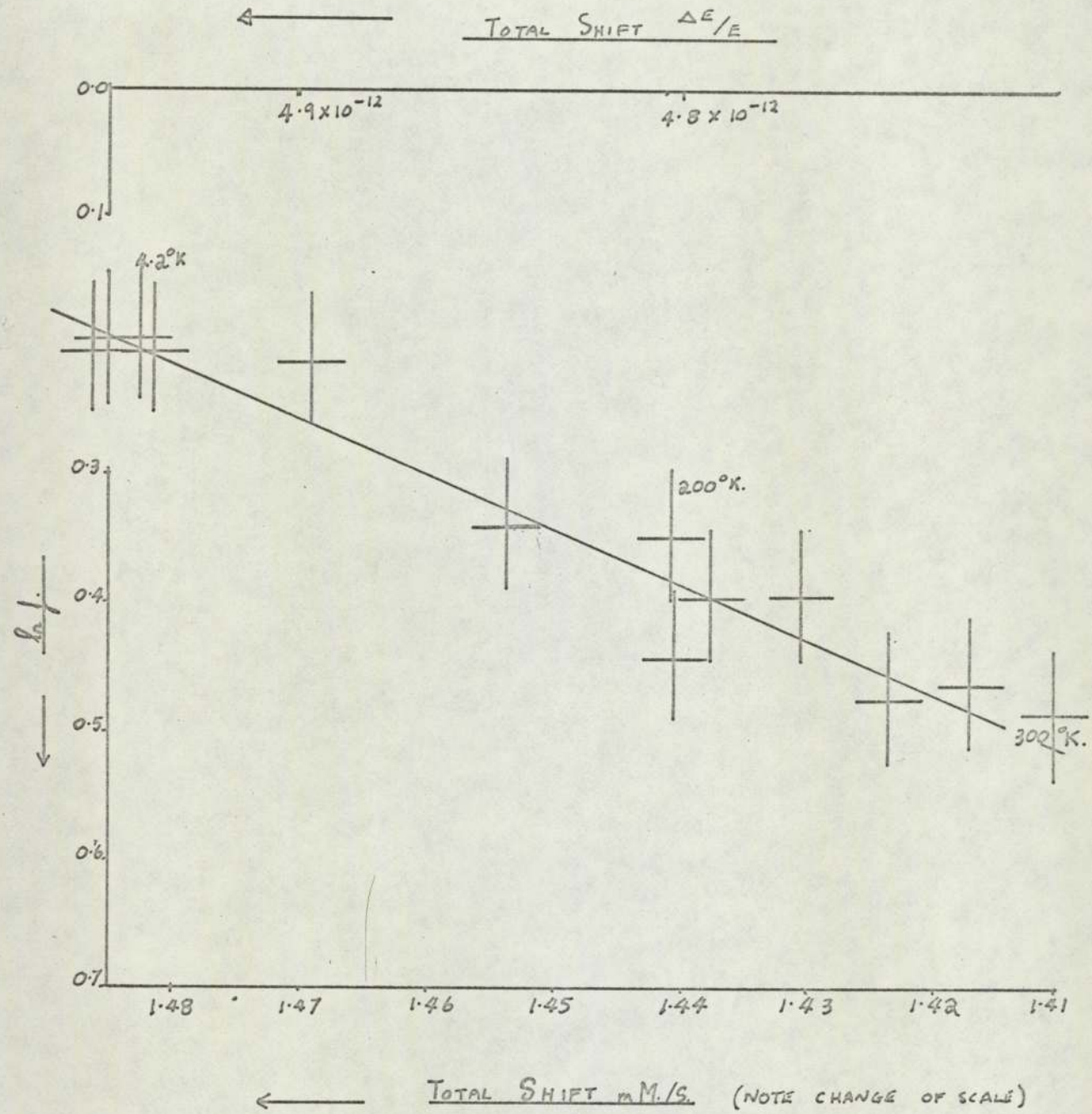

FIG. 5-18

ln f VERSUS ISOMER SHIFT

$CuRh_{2-x}Sn_xS_4$ $x = 0.10$

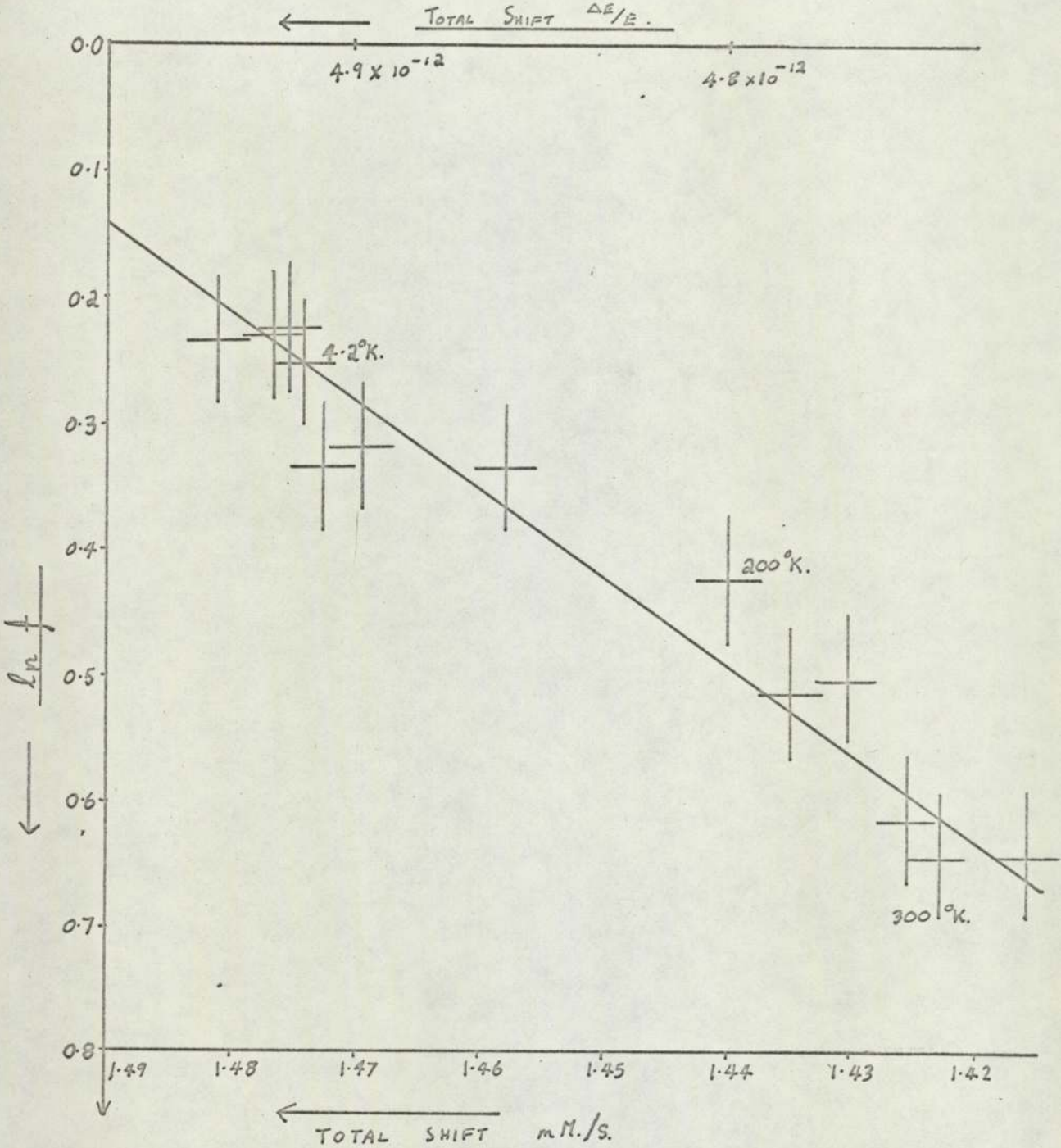

TABLE 5.16

VALUES OF THE ZERO-POINT PARAMETERS

X	S x 10^{11}	ν_{zp} x 10^5 mm/sec. ± 0.1	χ_{zp} x 10^9 mm ± 0.005	z_p ± 0.4	γ ^oK ± 30
$Cu\ Rh_{2-x}\ Sn_x\ Se_4$					
0.05	60 ± 10	1.25	0.0488	1.14	258
0.10	44 ± 5	1.239	0.0413	0.96	272
0.175	37 ± 5	1.270	0.0387	0.92	284
0.6	28 ± 5	1.388	0.0369	0.95	305
$Cu\ Rh_{2-x}\ Sn_x\ S_4$					
0.05	12 ± 2	1.800	0.032	1.08	372
0.10	21 ± 5	1.605	0.037	1.11	327
Sn Te	65.0	1.8	0.076	2.7	154
Nb_3 Sn	23.9	3.0	0.075	4.3	254

They state that for the Debye Model $zp = 0.9186$; on the Einstein Model $zp = 0.866$; and for a square well $zp = 1.391$.

Values of these parameters for the spinels investigated are given in table 5.16. For comparison the results for Nb_3 Sn and Sn Te, from the work of Taylor and Craig are given in table 5.16. Clearly the results for the spinels are of the correct order of magnitude and the variation of zp with x for Cu Rh_{2-x} Sn_x Se_4 is reasonable, bearing in mind that as x increases the temperature dependent anharmonicity reduces. However as has been pointed out by Taylor and Craig the absolute values of the derived zero-point parameters are probably not meaningful in the presence of anharmonicity. It must be recalled that the values of ln f_o used are devoid of any temperature independent f_{AN}.

As stated Taylor and Craig have found γ to be in good agreement with θ_D for Nb_3 Sn. It is noteworthy that the values of γ for Cu Rh_{x-x} Sn_x Se_4 series are in excellent agreement with θ_D determined by Schaeffer and Van Maaren (1968) i.e. $\theta_d = 218^oK$, from their heat capacity data. However for Cu Rh_2 S_4 they found $\theta_D = 230^oK$ which is not in such good agreement.

5.5.2 The Application of the 'S'-parameter to the superconducting spinels

The most important application of the S parameter is in its application to superconductivity, (Taylor and Craig, 1968) which will now be discussed.

By definition, the electron-phonon coupling constant, λ (see equations 1.6 and 1.7) is given by;

$$\lambda = \frac{N(o)\langle J^2\rangle}{M\ (\langle\omega\rangle/\langle\omega^{-1}\rangle)} \qquad 5.13$$

Now McMillan (1968) has shown, by numerically solving the integral equations describing strong coupled superconductivity that λ is given by;

$$\lambda = \frac{1.04 + \mu^* \ln(\theta/1.45\ T_c)}{(1 - 0.62\mu^* \ln(\theta/1.45\ T_c) - 1.04} \qquad 5.14$$

(see equation 1.5). Equation 5.14 contains superconducting parameters that may be determined empirically. Hence providing the appropriate characteristic temperature, θ is used, an empirical value of λ can be derived for any particular material. If the electronic and phonon parameters of equation 5.13 are known this enables a check on either the accuracy of equation 5.14 as a solution of the strong coupling equations, or on whether the material under investigation is a strong coupled superconductor.

For the spinels being investigated details of the electronic band structure are not well known (see section 1.5.3) and so values of λ, computed from equation 5.14 have been used to derive values of $N(o)\langle J^2\rangle$. The S parameter enters via the substitution of equation 5.9 into equation 5.13, allowing an investigation of the McMillan Hypothesis, that $N(o)\langle J^2\rangle$ is constant for a given class of materials (see section 1.3.2.)

$$N(o)\langle J^2\rangle = \frac{2c^2 M K^2}{3} \left(\frac{\lambda}{S}\right) \qquad 5.15$$

Table 5.17 lists values of $N(o)\langle J^2\rangle$ versus x from λ calculated using $\mu^* = 0.13$ (Van Maaren et al, 1970) and $\theta = \gamma$. The latter is reasonable, bearing in mind the agreement noted earlier and the fact that the variation of γ and θ with x would be comparable. Values of λ found using T_c measured in this work are shown in column 2 headed λ(EXPT). Now, as has been pointed out earlier, these values of T_c do not represent the maximum for the particular tin concentration in the spinel and so λ has been calculated using the values found by Van Maaren et al, (1969), headed λ(LIT), column 3. (Note that for $Cu\ Rh_{2-x}\ Sn_x\ S_4$ $x = 0.05$, there is no corresponding T_c and so the experimental value λ(EXPT) has been used throughout). The values of λ calculated here are in good agreement with that for $Cu\ Rh_2\ Se_4$ found using Van Maaren's results, (1968) for θ_D, T_c and μ^*, viz $\lambda = 0.63$.

TABLE 5.17

VALUES OF $N(o)\langle J^2\rangle$ CALCULATED USING THE S PARAMETER

$Cu\ Rh_{2-x}\ Sn_x\ Se_4$

X	λ(EXPT)	λ(LIT)	$(\frac{\lambda_{LIT}}{S}) \times 10^{-13}$	$N(o)\langle J^2\rangle$ e.V./Å^2
0.05	0.575	0.591	0.985	0.64
0.10	0.585	0.565	1.28	0.83
0.175	0.533	0.530	1.43	0.93
0.6	-	-	-	-

$Cu\ Rh_{2-x}\ Sn_x\ S_4$

0.05	0.591	-	0.475	2.1
0.10	-	-	-	-

FIG. 5.19. PLOT OF S VERSUS λ(LIT.) FOR THE SERIES

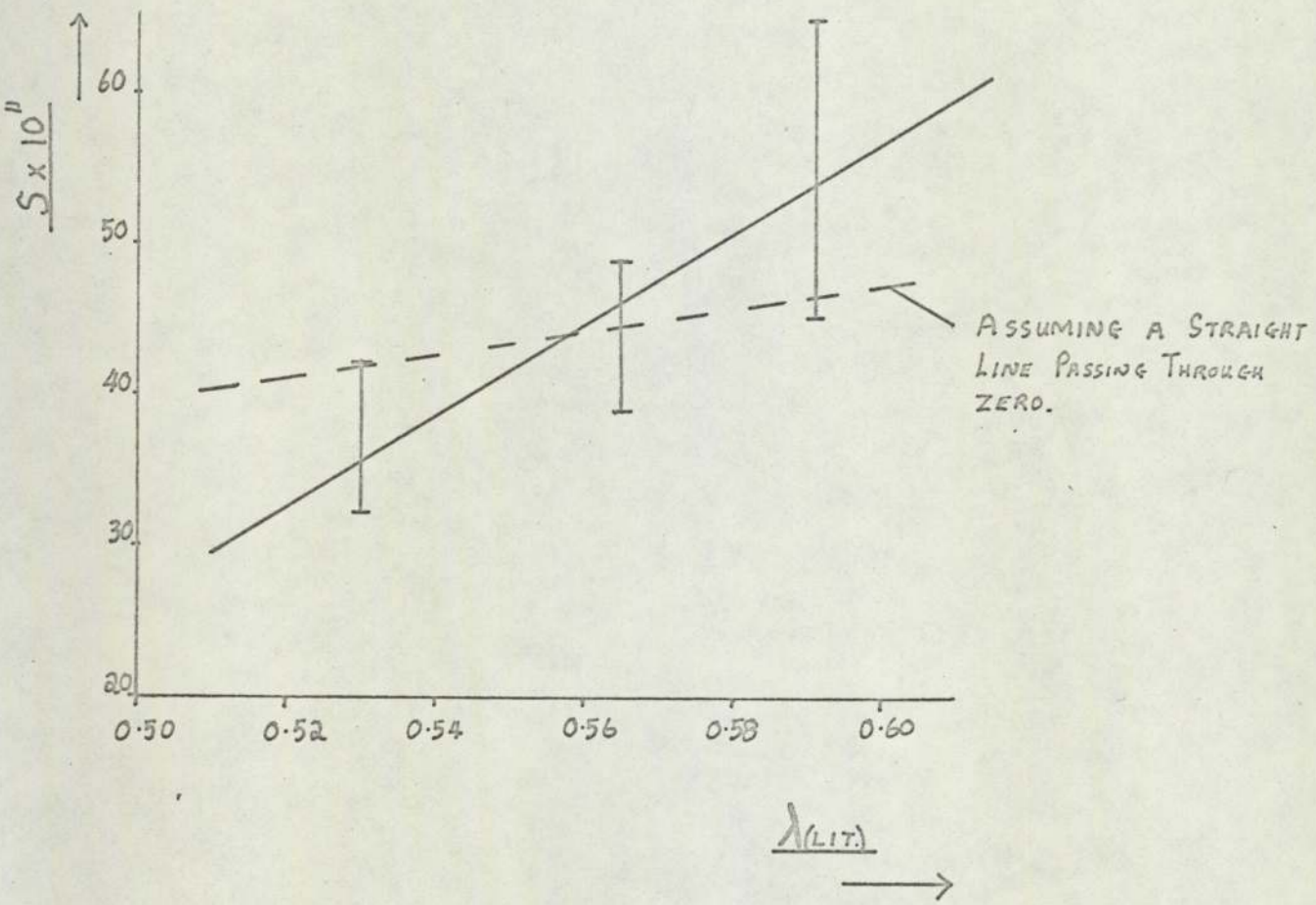

A plot of λ(LIT) versus S is shown in Fig 5.19. The correlation appears good for the available information, but it is clear that S is not solely dependent upon λ since the line drawn does not pass through the origin. (Only a line at the extreme of the errors (shown dotted) would do so). Possibly there is a gradual curvature; the graph flattening out as λ tends to zero. This result indicates that to a limited extent McMillans Hypothesis that $N(0)\langle J^2\rangle$ is a constant is a good approximation for the superconducting spinels and that therefore, in this case, T_c is predominately a function of the lattice phonons.

A similar application of the S parameter has been made by Kimball, Taneja, Weber and Fradin (1975). They performed Mossbauer experiments on the superconducting series V_3 Ga_x Sn_{1-x}, showing appreciable anharmonicity to be present. They state however that they do not find S proportional to λ, although they do not present their results fully. They concluded that the phonon - only part of λ as measured by Mössbauer techniques, has a weaker concentration dependance than T_c in the β-W V_3 Ga_x Sn_{1-x} series. It is possible that evidence of a curvature in S versus λ, as found here, was discovered. This of course would merely indicate that McMillan's Hypothesis is an approximation.

For the superconducting transition metals McMillan found $N(o)\langle J^2\rangle \simeq 7$ e.V./Å^2 within approximately 20% and for the β-W superconductor V_3 Si, $N(o)\langle J^2\rangle = 11.3$ e.V./Å^2. For the series Cu Rh_{2-x} Sn_x Se_4 $N(o)\langle J^2\rangle \simeq$ 0.8 e.V./Å^2, with an error which depends upon the viability of the assumptions made above (e.g. $\theta = \gamma$). For the series Cu Rh_{2-x} Sn_x S_4, $N(o)\langle J^2\rangle$ is larger by a factor of 2.5, implying appreciable differences in the electronic properties between the sulphide and selenide series. It is noteworthy that the sulphide has the higher T_c as well, so that their phonon characteristics could be very similar, the higher T_c being due to differences in electronic band structure.

CHAPTER 6. SUMMARY OF CONCLUSIONS AND SUGGESTIONS FOR FURTHER WORK

6.1 Summary of conclusions

The main conclusion drawn from the experimental work described here is that the $Cu\ Rh_{2-x}\ Sn_x\ Se_4$ and $Cu\ Rh_{2-x}\ Sn_x\ S_4$ series of spinels belong to the class of strong-coupled superconductors which depend upon a mechanism analogous to that operating in the high transition temperature β-tungsten and NbN groups. This is supported not only by the special features of the spinel crystallography, which gave rise to the initial interest in the superconducting behaviour, but more especially by the discovery of low temperature anharmonicity at the octahedral sites, described in this thesis.

The evidence for anharmonicity depends primarily upon the measurements of the Mössbauer recoil-free fraction as a function of temperature, which have revealed that for all of the superconducting compounds, certain characteristic temperatures fail to satisfy the harmonic criterion $\theta\ (-2) \leq \theta\ (-1)$. The results from these experiments, together with the theory developed by Housley and Hess (1966), have also indicated that the mean force constant relating to the chemical bonding at the octahedral site is exceptionally low. This implies the existence of a square well potential, with a central flat zone, similar to that found in $Nb_3\ Sn$ by Shier and Taylor, (1968).

The $T_c MAX$ of the spinel group of compounds has been shown to be at least $13^{\circ}K$ by using McMillan's equation. This result has been borne out by the recent discovery of Johnston et al (1973) that the spinel series $Li_{1+x}\ Ti_{2-x}\ O_4$ has a $T_c MAX$ of the order of $13.7^{\circ}K$.

The Mössbauer experiments have yielded not only characteristic temperatures as a function of spinel composition, but also a measure of the variation of the radius, R of the flat region of the proposed square

potential well at the octahedral site. The implication is that, holding other factors constant an increase in R will yield an increase in T_c.

The observed disappearance of anharmonicity with T_c has reinforced the opinion that anharmonicity is a prerequisite for superconductivity in the spinels, originally put forward by comparison with high T_c superconductors.

Accurate determination of X-ray crystallographic parameters have been made and comparisons between the root mean square displacement of the octahedral ion, from these X-ray and from the Mössbauer measurements, have shown a complicated electron localization/orbital expansion phenomena to be taking place in the series Cu Rh_{2-x} Sn_x Se_4, with changes in the tin concentration. Further, these observations have indicated a correlation between the presence of anharmonicity and superconductivity in these spinels, and the electron orbital situation at their octahedral sites. It is interesting to note that despite the more limited investigation of Cu Rh_{2-x} Sn_x S_4 no unusual electronic behaviour at the octahedral site was detected.

Measurement of the total shifts have given support to the band model of Schaeffer and Van Maaren, (1968) describing the superconducting spinels as having a narrow d-band at the Fermi level occupied by holes. Shift measurements on the non-superconducting spinels have indicated a link between changes in the electronic band structure and superconductivity.

The above observations have enhanced the strong comparisons between the high T_c superconductors, such as Nb_3 Sn and the superconducting spinels. It seems reasonable to suppose that relatively localised electronic activity, at the spinel octahedral sites, is giving rise to anharmonicity and the associated phonons are increasing the amount of electron-phonon coupling.

By using the 'S' parameter of Taylor and Craig, (1968), the applicability of the McMillan Theory to the superconducting spinels has been tested and shown to be true, providing it is borne in mind that the theory

only claims to be a good approximation. Various zero-point parameters have been determined and within the limitations outlined, the results appear reasonable, when compared with other anharmonic compounds.

6.2 Suggestions for further work

The two important areas of study for any superconductor are the phonon density of states and the electronic parameters; and a detailed knowledge of both is necessary for any quantitative analysis. For the former, neutron scattering experiments would be ideal but these are unlikely to be possible in the near future and so, either the thin film tunneling technique or Mössbauer spectrometry must be used. Now, whilst the latter will establish the presence of anharmonicity, the theory is not sufficiently well developed to yield details of specific phonon differences between superconductors. However, this may be determined by using the thin film tunneling technique.

The electronic parameters of interest are also available from thin film measurements, both optical and electrical, as has been pointed out by Hopfield (see section 3.4). It is for this reason that the detailed description of the thin film work performed has been included. Now that it is possible to produce thin films of spinel, improved experimental techniques are required for quantitative measurements.

Mössbauer spectroscopy, of course, also yields information about the electronic band structure, via the isomer shift. Recent improvements in theory (e.g. Housley and Hess, 1967) and high precision measurements would enable detailed quantitative assessment of band structure models.

The usefulness of the 'S' parameter to the study of superconducting materials has been explained in section 5.6.1, but this too requires precision measurements.

For the spinel group of superconductors the discovery of superconductivity in the $Li_{1+x}\ Ti_{2-x}\ O_4$ series is particularly exciting. Not only

because of its high T_c, (the highest T_c known in oxides incidently), but also because this compound has a very low density in comparison to all other superconductors. It seems reasonable to propose from the work of this thesis, that the titanium ions on the octahedral sites are anharmonically bound, with the consequent production of phonons which enhance T_c. This seems particularly reasonable when it is noted that the lattice parameter at 8.4 Å is much larger than that of other lithium cation spinels and also that unlike the latter $Li_{1+x}\ Ti_{2-x}\ O_4$ is not inverse. The presence of instability is implied by the difficulty in preparing stoichiometric samples and the strong dependence of T_c on preparation, (factors which are particularly reminiscent of members of the NbN group of high T_c compounds, e.g. Ta C.)

A detailed study of lithium titanate is therefore desirable in an attempt to clearly identify the details of the mechanism responsible for superconductivity in the spinels. Certainly the success that Matthias et al have enjoyed in obtaining high T_c superconductors, means that their conclusion that our attention must be turned to ternary systems, can not be ignored.

ACKNOWLEDGEMENTS

This work was carried out during the tenure of a University of Aston research studentship.

The advice and assistance of my supervisor, Dr. N. W. Grimes throughout the course of this work is gratefully acknowledged.

Particular thanks are due to Dr. D. A. O'Connor of Birmingham University both for the loan of the Mössbauer equipment and for his advice during these experiments.

I would also like to extend my appreciation to Dr. R. Fane and Mr. G. Cochrane of the physics department of Aston University.

REFERENCES

BACHNER, GOODENOUGH AND CATOS, J. PHYS. CHEM. SOL. 28, 889, 1967

BARDEEN, COOPER AND SCHRIEFFER, PHYS. REV. 108, 1175, 1957

BLOCH, Z. PHYSIK. 52, 555, 1928

BORN AND HUANG IN "DYNAMICAL THEORY OF CRYSTAL LATTICES "OXFORD UNIVERSITY PRESS, 1954

CERVENKA, CZECH. J. PHYS. B15, 747, 1965

CHEARY, PH. D. THESIS, PHYS. DEPT. ASTON UNIVERSITY 1971

CLAESON AND LUNDQVIST, PHYSICA SCRIPTA 10, 5, 1974

CLOGSTON AND JACCARINO, PHYS. REV. 121, 1357, 1961

COHEN AND ANDERSON, IN "SUPERCONDUCTIVITY IN d- AND f- BAND METALS" A.I.P. CONFERENCE PROC. No. 4. 1972

COHEN, CODY AND HALLORAN, PHYS. REV. LETTS 19, 840, 1967

COOPER, PHYS. REV. 104, 1189, 1956

DASH, JOHNSON AND VISCHER, PHYS. REV. 168, 1087, 1968

DAWES AND GRIMES AND O'CONNOR, J. PHYS. C. 7, L387, 1974

DAWES AND GRIMES, SOL. STAT. COMM. 16, 139, 1975

DECKAR, "SOLID STATE PHYSICS" McMILLAN, 1967

DIENNES, COMM. SOL. STATE PHYSICS. 1, 81, 1968

DUNITZ AND ORGEL, J. PHYS. CHEM. SOL. 3, 20, 1957

EVANS, PH. D. THESIS, PHYSICS DEPT. BIRMINGHAM UNIVERSITY, 1972

FRÖHLICH, J. PHYS. REV. 79, 845, 1950

FRÖHLICH, REPTS. ON PROGRESS IN PHYSICS, 1961

GOMMERSALL AND GYORFFY, J. PHYS. F. 3, L138, 1973

GOODENOUGH, J. PHYS. CHEM. SOL. 30, 261, 1969

GORTER, PHILIPS RES. REPTS. 9, 295, 1954

GORTER AND CASIMER, Z. TECH. PHYS. 15, 539, 1934

GORTER AND CASIMER, Z. PHYSIK. 35, 963, 1934

GREENWOOD AND GIBBS, "MÖSSBAUER SPECTROSCOPY" CHAPMAN AND HALL 1971

GRIMES, J. PHYS. C. 4, L342, 1971

GRIMES, PHIL. MAG. 26, 1217, 1972

GRIMES, SPECTROCHIM. ACTA. 28A, 2217, (1972)

GRIMES AND COLLETT, PHYS. STATUS. SOLIDI. (b) 43, 591, 1971

GRIMES AND HILLEARD, J. PHYS. C. 3, 866, 1970

HEISENBERG, Z. NATURFORSCH, 2a, 185, 1947

HILLEARD, PH. D. THESIS, PHYS. DEPT. ASTON UNIVERSITY, 1973

HOPFIELD, PHYS. REV. 186, 443, 1969

HOUSLEY, NUCL. INST. METH. 35, 77, 1965

HOUSLEY, ERIKSON AND DASH NUCL. INST. METH. 27, 29, 1964

HOUSLEY AND HESS, PHYS. REV. 146, 517, 1966

HOUSLEY AND HESS, PHYS. REV. 164, 340, 1967

HWANG, HERBER AND MITCHELL, PHIL. MAG. 28, 241, 1973

INTERNATIONAL TABLES OF X-RAY CRYSTALLOGRAPHY, 1965

JACKSON, THIN SOL. FILMS 5, 209, 1970

JOHNSON, NUCL. INST. METH. 85, 29, 1970

JOHNSON AND DASH, PHYS. REV. 172, 983, 1968

JOHNSTON, SOL. STAT. COMM. 11, 1751, 1972.

KAMERLINGH-ONNES, LEIDEN COMM. 1206, 1226, 1911.

KIMBALL, TANEJA, WEBER AND FRADIN, IN "NINTH SYMPOSIUM ON MOSSBAUER METHODOLOGY", CHICAGO, 1974

KINO, LÜTHI AND MULLEN, J. PHYS. SOC. JAP. 33, 687, 1972

KITCHENS, CRAIG AND TAYLOR, IN "MÖSSBAUER EFFECT METHODOLOGY" VOL. 5, PLENNUM PRESS, 1970

LABBÉ AND FRIEDEL, J. PHYS. RADIUM, 27, 153, AND 303, 1966

LABBÉ AND FRIEDEL, J. PHYS. CHEM. SOL. 28, 2477, 1967

LABBÉ AND FRIEDEL, PHYS. REV. 158, 647 AND 655, 1967

LANGFORD, J. APPL. CRYST. 1, 48, 1968

LIPKIN, ANNAL. PHYS. 9, 332, 1960, (AND 18, 182, 1962)

LITTLE, SCIENTIFIC AMERICAN, 212, 21, 1965

LONDON AND LONDON, PROC. ROY. SOC. A149, 71, 1935

LONDON AND LONDON, PHYSICA, 2, 341, 1935

LOTGERING, J. PHYS. CHEM. SOL. 29, 2193, 1968

LOTGERING AND VAN STEEPLE, SOL. STAT. COMM. 5, 143, 1967

LOTGERING AND VAN STEEPLE, J. APPL. CRYST. 39, 417, 1968

LUTZ AND FEHER, SPECTROCHIM. ACTA. 27A, 357, 1971

LYNTON, "SUPERCONDUCTIVITY", METHUEN, 1969

MAILFERT, BETHERMAN AND HANAK, PHYS. LETS. 24A, 315, 1967

MARADUDIN AND FLINN, PHYS. REV. 129, 2529, 1963

MATTHIAS, IN "SUPERCONDUCTIVITY", VOL. 2, GORDEN AND BREACH, 1969

MATTHIAS, PHYSICS TODAY 24, 23, 1971,a.

MATTHIAS, IN "SUPERCONDUCTIVITY IN d- AND f- BAND METALS"

MATTHIAS, A.I.P. CONFERENCE PROC. No. 3. 1971,b.

MATTHIAS, GEBALLE AND COMPTON, REVS. MOD. PHYS. 35, 1, 1963

MATTHIAS, GEBALLE, GELLER AND GORENZWIT, PHYS. REV. 95, 1435, 1954

MAXWELL, PHYS. REV. 78, 477, 1950

McMILLAN, PHYS. REV. 167, 331, 1968

MEISSNER AND OSCHENFELD, NATURWISS 21, 787, 1933

MOON, FOR A REVIEW SEE METZGER, PROG. IN NUCL. PHYS. 7, 53, 1959

MOREL AND ANDERSON, PHYS. REV. 125, 1263, 1962

MÖSSBAUER, Z. PHYSIK, 151, 124, 1958

MÖSSBAUER EFFECT DATA INDEX, A.I.P. 1968

NAKAGAWA AND WOODS, PHYS. REV. LETS. 11, 271, 1963

NEWMAN, PH. D. THESIS, PHYSICS DEPT. ASTON UNIVERSITY, 1973

NUSSBAUM, HOWARD, NEES AND STEEN, PHYS. REV. 173, 653, 1968

O'CONNOR, NUCL. INST. METH. 218, 318, 1963

O'CONNOR AND SKYRME, NUCL. INST. METH. 106, 77, 1973

PARRISH, IN "X-RAY ANNALYSIS PAPERS" CONTREIX, 1965

PESSALL, GOLD AND JOHANSEN, J. PHYS. CHEM. SOL. 29, 19, 1968

PHILLIPS, PHYS. REV. LETTS. 26, 543, 1971,a.

PHILLIPS, PHYS. REV. B. 3, 3503, 1971,b.

PHILLIPS, J. APPL. PHYS. 43, 3560, 1972

PHILLIPS LTD. X-RAY DIFFRACTOMETER HANDBOOK, P. W. SERIES.

PUTLEY, "THE HALL EFFECT AND RELATED PHENOMENA", BUTTERWORTHS, 1960

PYTTE, PHYS. REV. LETS. 25, 1176, 1970

PYTTE, PHYS. REV. B. 3, 3503, 1971

RAMAKRISHNAN, J. PHYS. C. 6, 3041, 1973

REYNOLDS, SERN, WRIGHT AND NESBITT, PHYS. REV. 78, 487, 1950

ROBBINS, J. PHYS. CHEM. SOL. 28, 897, 1967

ROBBINS, MENTH, MIKSOVSKY, SHERWOOD, J. PHYS. CHEM. SOL. 31, 423, 1970

ROBBINS, WILLENS AND MILLER, SOL. STAT. COMM. 5, 933, 1967

ROSE-INNES AND RHODERICK, "INTRODUCTION TO SUPERCONDUCTIVITY" PERGAMMON, 1969

SALTER, PH. D. THESIS, PHYSICS. DEPT. ASTON UNIVERSITY, 1973

SCHAEFFER AND VAN MAAREN, "PROC. OF THE ELEVENTH INT. CONF. ON LOW TEMP. PHYSICS, ST. ANDREWS, 1968

SHANNON AND PREWITT, ACTA. CRYST. B25, 925, 1969

SHEN, PHYS. REV. LETS. 29, 1082, 1972.

SHENOY "NINTH SYMPOSIUM ON MOSSBAUER EFFECT METHODOLOGY" CHICAGO, 1974

SHIER AND TAYLOR, SOL. STAT. COMM. 5, 147, 1967.

SHIER AND TAYLOR, PHYS. REV. 174, 346, 1968

SHIRANE AND AXE, PHYS. REV. B. 4, 2957, 1971

SHIRANE AND AXE, PHYS. REV. LETS. 27, 1803, 1971

SITEK, NUCL. INST. AND METH. 114, 163, 1974

SMITH, PHYS. REV. LETS. 25, 1483, 1970

SMITH AND GLASSER, PHYS. REV. LETS. 25, 1611, 1970

STAHL-BRADA AND LOW. PHYS. REV. 116, 561, 1959

TANAKA, TOKORO AND AIYAMA, J. PHYS. SOC. JAP. 21, 262, 1966

TAYLOR AND CRAIG, PHYS. REV. 175, 782, 1968

TESTARDI, PHYS. REV. 154, 399, 1967

TESTARDI, PHYS. LETS. 35, A117, 1971,a.

TESTARDI, PHYS. REV. B3, 95 AND 107, 1971,b.

TESTARDI, PHYS. REV. B5, 4342, 1972

TESTARDI, IN "PHYSICAL ACOUSTICS" VOL X ACADEMIC, 1973

TOLANSKY, "MULTIPLE BEAM INTERFEROMETRY" CLARENDON, 1948

VAN DER PAUW, PHILIPS, RES. REPTS. 13, 1, 1958

VAN MAAREN AND HARLAND, PHYS. LETS. 30A, 204, 1969

VAN MAAREN, HARLAND AND HAVINGA 8, 1933, 1970

VAN MAAREN, SCHAEFFER AND LOTGERING, PHYS. LETS. 25A, 238, 1967

VIELAND, COHEN AND ROWALD, PHYS. REV. LETS. 26, 373, 1971

WAKAMURA, ARAI, ONARI, KUDO AND TAKAHASHI, J. PHYS. SOC. JAP. 35, 1430, 1973

WEBER, PHYS. REV. 8, 5093, 1973

WERTHEIM, "MÖSSBAUER EFFECT" ACADEMIC, 1971

WILLIAMSON AND GRIMES, J. PHYS. CHEM. SOL. 3, 44, 1974

WILLIS, ACTA. CRYST. A25, 277, 1969

WILSON, "MATHEMATICAL THEORY OF X-RAY POWDER DIFFRACTOMETRY" CLEAVER-HUME, 1967

WILSON, "ELEMENTS OF X-RAY CRYSTALLOGRAPHY", ADDISON-WESLEY 1970

WOODS, PHYS. REV. 136, A781, 1964

ZELLER, PHYS. REV. B. 5, 1813, 1972

J. Phys. C: Solid State Phys., Vol. 7, 1974. Printed in Great Britain.

LETTER TO THE EDITOR

Direct experimental evidence for low temperature anharmonicity in superconducting spinels

P P Dawes, N W Grimes and D A O'Connor†

Physics Department, University of Aston, Birmingham B4 7ET
† Physics Department, University of Birmingham, Birmingham B15 2TT

Received 23 September 1974

Abstract. Preliminary experimental data are reported for the absolute values and temperature dependence of the Mössbauer recoil-free fraction of ^{119}Sn in the superconducting spinel $CuRh_{1.95}Sn_{0.05}Se_4$. The results are consistent with earlier investigations which indicated the presence of an anharmonic potential well at the octahedral sites.

Following recent x-ray diffraction and related investigations of superconducting spinels, which indicated the presence of anharmonicity at the octahedral sites (Dawes and Grimes 1974), a programme of Mössbauer experiments has been initiated to obtain more direct information. In the first experiments, we have exploited the discovery of van Maaren and Harland (1969) that the system $CuRh_{2-x}Sn_xSe_4$ retains the property of superconductivity over the range $0 \leqslant x < 0{\cdot}5$. The isotope ^{119}Sn is one of the more suitable for investigations by Mössbauer effect. In this brief note, we report preliminary results obtained with a sample of composition $CuRh_{1.95}Sn_{0.05}Se_4$. A more complete account of our experiments is in preparation and will be published elsewhere.

The preparation of the sample whose behaviour is described here was very similar to that of $CuRh_2S_4$ and $CuRh_2Se_4$ (Dawes and Grimes 1974) and measurements of the superconducting transition temperature were carried out as before. X-ray diffraction

Table 1

Compound	a(Å) at 25 °C	u	Octahedral site. Nearest-neighbour distance (Å)	T_c (K)
$CuRh_2Se_4$	10·2603 ± 0·0004	0·384	2·476	3·50 ± 0.05
$CuRh_{1.95}Sn_{0.05}Se_4$	10·2781 ± 0·0004	0·384	2·480	2·70 ± 0.05

examination revealed a single spinel phase with lattice parameter slightly larger than the pure compound $CuRh_2Se_4$ (see table 1) and also confirmed that Sn occupies the octahedral site.

Mössbauer absorbers were prepared from a suspension of the powdered spinel material in Canada balsam by sandwiching an optimum thickness between two aluminium discs. The temperature of an absorber could be controlled to ±0·1 K relative to the

liquid helium or nitrogen. In the experiments a $BaSnO_3$ source, having a recoil-free fraction $f_s = 0{\cdot}64$ at 25 °C, was used with triangular wave velocity modulation. Velocity calibration was carried out by comparison with an iron source line splitting. Measurements of velocity spectra were made with a NaI scintillation counter while the source recoil-free fraction f_s and background corrections to the measured absorption areas, were determined using a lithium-drifted Si detector.

Each of the two absorbers for which results appear here gave single Mössbauer lines slightly broader than twice the natural width of the ^{119}Sn resonance. A Lorentzian profile could be fitted to all the observed lines within a standard deviation of the counting statistics. The effective absorption thickness T_A was determined for each absorber over a range of temperatures by the method of O'Connor and Skyrme (1973).

If the recoil-free fraction of the absorber can be written as the product of a harmonic factor f_H and an anharmonic factor f_{AN} (Dash *et al* 1968) then, in the high-temperature region, T_A depends on temperature as

$$\ln T_A + \frac{\hbar K^2}{12MkT} = -\frac{\hbar^2 K^2 T}{Mk\theta^2(-2)} + \ln Nt\sigma(0) f_{AN} \ldots \tag{1}$$

where K is the wavevector for the γ-ray. Assuming that the anharmonic factor is only weakly dependent on temperature, the left-hand side of (1) may be plotted as a function of temperature to derive values for the -2 moment of the harmonic frequency distribution $\theta(-2)$ and also $Nt\sigma(0) f_{AN}$. f_H is then obtained from $f_H = T_A/Nt\sigma(0) f_{AN}$.

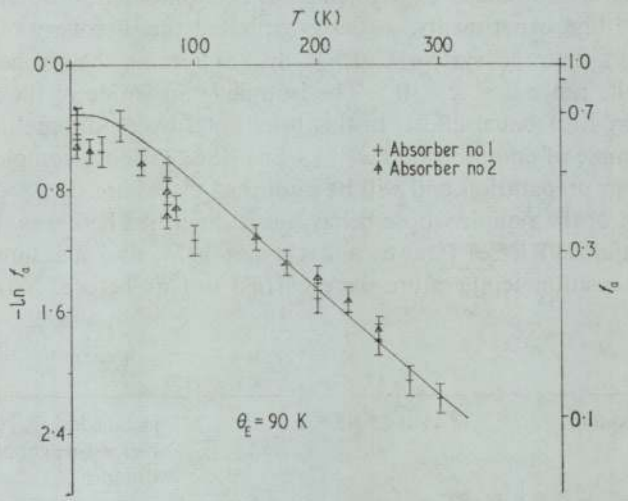

Figure 1. Absolute recoil-free fraction f_a as a function of temperature for two samples of $CuRh_{1\cdot95}Sn_{0\cdot05}Se_4$ spinel. The significance of the limiting curve is discussed in the text.

Our results for $\ln f_a$ for the two absorbers as a function of temperature are shown in figure 1. Ln T_A and therefore $\ln f_H$ were found to vary linearly with temperature as expected above 150 K, with a slope corresponding to a value for $\theta(-2) = 90 \pm 1$ K. Similarly, by fitting the experimental data in the neighbourhood of $T = 0$ K, where $\ln f_H$ tends to the limit (Housley and Hess 1966),

$$\ln f_{\mathrm{H}} = -\frac{\hbar^2 K^2}{2Mk\theta(-1)} \cdots \tag{2}$$

the reciprocal first moment $\theta(-1)$ is found to be 66 ± 6 K.

Now, from their definitions, the moments of the harmonic frequency distribution must obey the relation $\theta(-2) \leqslant \theta(-1)$. The limit $\theta(-2) = \theta(-1)$ corresponds to the Einstein model $\theta(n) = \theta_{\mathrm{E}}$ for which the solid curve in figure 1 has been drawn with $\theta_{\mathrm{E}} = 90$ K. The fact that the low temperature data yields $\theta(-1) < \theta(-2)$ shows that the experimental observations cannot be explained on the basis of a temperature-independent harmonic frequency distribution and that below 100 K there must be an extra anharmonic contribution to the frequency distribution which results in the lowering of $\theta(-1)$ (Dash *et al* 1968, Johnson and Dash 1968).

Such behaviour was first observed in superconductors by Shier and Taylor (1967, 1968) with the compound Nb_3Sn and if we assume with them (see also Maradudin and Flinn 1963) that the displacement of the low-temperature intercept from the harmonic condition can be expressed in the form

$$\ln f_{\mathrm{AN}} \approx \tfrac{1}{3}(K^2R^2), \ldots \tag{3}$$

then R, the radius of the flat zone of the potential well at the octahedral site, is approximately $0{\cdot}06 \pm 0{\cdot}02$ Å, which is roughly comparable with the excess space available (Dawes and Grimes 1974).

We comment finally, and with even greater emphasis than before, that the analogies between the ternary spinel system and the binary NbN and β-tungsten systems are really very striking.

References

Dash J G, Johnson D P and Visscher W M 1968 *Phys. Rev.* **168** 1087–94
Dawes P P and Grimes N W 1974 *Solid St. Commun.* in the press
Housley R M and Hess F 1966 *Phys. Rev.* **146** 517–26
Johnson D P and Dash J G 1968 *Phys. Rev.* **172** 983–90
Maradudin A A and Flinn P A 1963 *Phys. Rev.* **129** 2529–47
O'Connor D A and Skyrme G 1973 *Nucl. Instrum. Meth.* **106** 77–81
Shier J S and Taylor R D 1967 *Solid St. Commun.* **5** 147–9
——1968 *Phys. Rev.* **174** 346–50
van Maaren M H and Harland H B 1969 *Phys. Lett.* **30A** 204–5

Solid State Communications, Vol. 16, pp. 139–141, 1975. Pergamon Press. Printed in Great Britain

SUPERCONDUCTIVITY AMONG COMPOUNDS WITH SPINEL STRUCTURE AND THE STRONG COUPLING MECHANISM

P.P. Dawes and N.W. Grimes

Physics Department, University of Aston, Birmingham, B4 7ET, U.K.

(*Received* 23 *July* 1974 *by C.W. McCombie*)

X-ray diffraction and related investigations of the sulphide and selenide spinels indicate that the mechanism for superconductivity among these materials is very closely allied to that existing in the β-tungsten and NbN systems. The potential well at the octahedral sites is almost certainly anharmonic and the spinels thus appear to be the first ternary compounds for which the high T_c mechanism holds.

IT IS A REMARKABLE though well known fact that all the superconducting compounds presently known to have high transition temperatures ($T_c > 15°K$) belong to one or other of two structural groups. These are the group of compounds with the β-tungsten or A15 structure typified by materials like Nb_3Sn, and the compounds related to NbN whose crystal structure belongs to the NaCl type.

Both of these crystal structures are peculiar in that they possess an intrinsic instability which seems to be connected with an excess volume afforded to one constituent. Thus for example, Phillips[1] has remarked that the B atoms in an A_3B β-tungsten compound are often "situated in cages (formed by the A atoms) which are much too large relative to their atomic volumes". Similarly, Pessall, Gold and Johansen,[2] Phillips[1] and Zeller[3] find a significant correlation between T_c and relative volume available to the transition metal atoms in NbN and related compounds. The shape of the potential well inside the "cage" is thought to be markedly anharmonic in both groups of materials[4] and there is a considerable body of experimental evidence now to suggest that this explanation is along the right lines (see for example, Testardi[5]).

In the spinel group of compounds a very similar model has been used to account for the presence of structural distortions associated with the octahedral or B-sites.[6,7] It has been noted in particular that analogies with the physical behaviour of small off-centre impurity ions in alkali halides include ultrasonic relaxations,[8,9] dielectric phenomena[10] and specific heat anomalies.[11] X-ray diffraction examination of the metallic copper-containing sulphide and selenide spinels on the other hand, shows that these compounds have the higher symmetry $Fd\bar{3}m$, and therefore presumably that the potential conditions at the octahedral site have been modified by good electrical conductivity.[7,12]

Recently, we have extended the X-ray diffraction investigations to the compounds $CuRh_2S_4$ and $CuRh_2Se_4$ which are superconducting spinels.[13,14] Ceramic specimens of these materials were prepared by the usual sintering techniques, compressed pellets of stoichiometric mixtures of the elements being enclosed in silica tubes which were evacuated, flushed with argon and finally sealed under a reduced pressure of argon. $CuRh_2Se_4$ was prepared without detectable impurity by firing at 600°C whilst $CuRh_2S_4$ was found to contain a slight trace (< 1 per cent) of an impurity phase, thought to be CuS. The superconducting transition temperatures were measured for both compounds by a method similar to that of Pessall *et al.*,[2] which exploits the Meissner effect, and the diffraction patterns examined by X-ray diffractometer operated in step-scanning mode.

Table 1.

	$CuCo_2S_4$	$CuRh_2S_4$	$CuRh_2Se_4$
T_c	No Supercond. above 0.05°K	4.07 ± 0.05°K	3.50 ± 0.05°K
a at 25°C	9.478 ± 0.001 A	9.7877 ± 0.0005 A	10.2603 ± 0.0004 A
"u" parameter	0.388 ± 0.001	0.384 ± 0.001	0.384 ± 0.001
Oct. site n.n. distance	2.253 A	2.362 A	2.476 A
D–W factor B	0.4 ± 0.1 A^2	0.2 ± 0.1 A^2	0.1 ± 0.1 A^2

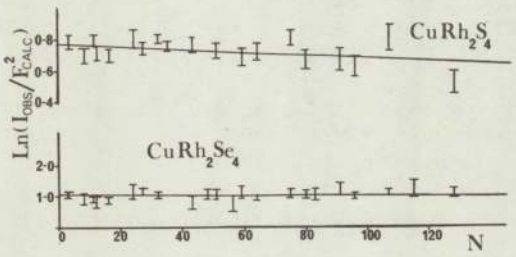

FIG. 1. Ln (I_{obs}/F^2_{calc}) against $N = 4a^2\sin^2\theta/\lambda^2$ for $CuRh_2S_4$ and $CuRh_2Se_4$. (Note the change of scale in the ordinate.) The error bars indicate experimental uncertainty arising from a standard deviation in the total measured counts.

The general appearance of the diffraction patterns from both $CuRh_2S_4$ and $CuRh_2Se_4$ were very similar to that reported by Williamson and Grimes[12] for $CuCo_2S_4$ i.e. once again, no reflections of the type $(hk0)$ with $(h + k) = 4n + 2$. The integrated intensities are easily accounted for on the basis of $Fd3m$ symmetry with no inversion and the structure of both compunds is therefore defined in terms of the three parameters a, u and B, the Debye–Waller or temperature factor B, being derived in the usual way from the slope of the graph of ln (I_{obs}/F^2_{calc}) against $N(= h^2 + k^2 + l^2)$, (see Fig. 1).

Our final results are summarized in Table 1 which also shows that the nearest neighbour distance within the octahedral "hole" is substantially larger for $CuRh_2S_4$ and $CuRh_2Se_4$ than for $CuCo_2S_4$. Indeed, the lattice parameter for the latter substance is among the smallest known for sulphide spinels and the absence of superconductivity in $CuCo_2S_4$ is possibly correlated with this fact.

We note finally that the investigations of van Maaren, Harland and Havinga[15] on the Hall effect and heat capacity in the spinel system $CuRh_{2-x}Sn_xSe_4$ indicate that these new materials should be included among those described by the so called strong coupling theory.[16] Taken together with the present observations, these results now suggest that the mechanism for superconductivity in spinels is very closely allied to that existing in the β-tungsten and NbN systems. It thus emerges that the spinel group of compounds may be the first truly ternary system for which the high T_c mechanism holds.

The significnace of these considerations may be given perspective by using the McMillan formula[16]

$$T_c = \frac{\theta}{1.45}\exp\left[-\frac{1.04\,(1+\lambda)}{\lambda-\mu^*\,(1+0.62\lambda)}\right]$$

to derive the electron–phonon coupling constant λ for say $CuRh_2Se_4$. If we use $\mu^* = 0.13$ according to van Maaren *et al.*[15] and $\theta = 218$°K from the low temperature specific heat,[17] we find $\lambda = 0.63$ and therefore

$$T_c^{max} \simeq 13\text{°K}$$

for the spinel group of compounds. On the other hand, as McMillan points out, the basis of his limit is that the average phonon frequency not only pre-multiplies the exponential factor but also, in simple substances, is the dominant factor in the exponent. The latter may not be true in general however, and the possibility thus exists in principle, that the extra degree of freedom available within a ternary system like the spinels, may be used to relax, at least partially, the restriction inherent in simpler systems.[18]

REFERENCES

1. PHILLIPS J.C., *J. Appl. Phys.* **43**, 3560 (1972).
2. PESSALL N., GOLD R.E. and JOHANSEN H.A., *J. Phys. Chem. Solids* **29**, 19 (1968).
3. ZELLER H.R., *Phys. Rev.* **B5**, 1813 (1972).
4. DASH J.G., JOHNSON D.P. and VISSCHER W.M., *Phys. Rev.* **168**, 1087 (1968).
5. TESTARDI L.R., *Phys. Rev.* **B5**, 4342 (1972).
6. GRIMES N.W., *J. Phys. C.* **4**, L342 (1971).
7. GRIMES N.W., *Phil. Mag.* **26**, 1217 (1972).
8. MORAN T.J. and LÜTHI B., *Phys. Rev.* **187**, 710 (1969).
9. KINO Y., LÜTHI B. and MULLEN M.E., *J. Phys. Soc. Japan* **33**,687 (1972).
10. GRIMES N.W., *J. Phys. C.* **6**, L78 (1973).
11. GRIMES N.W., *Proc. R. Soc.* **A338**, 223 (1974).
12. WILLIAMSON D.P. and GRIMES N.W., *J. Phys. D.* **7**, 1 (1974).
13. VAN MAAREN N.H., SCHAEFFER G.M. and LOTGERING F.K., *Phys. Lett. (Netherlands)* **25A**, 238 (1967).
14. ROBBINS M., WILLENS R.H. and MILLER R.C., *Solid State Commun.* **5**, 933 (1967).
15. VAN MAAREN N.H., HARLAND H.B. and HAVINGA E.E., *Solid State Commun.* 8, 1933 (1970).
16. MCMILLAN W.L., *Phys. Rev.* **167**, 331 (1968).
17. SCHAEFFER G.M. and VAN MAAREN N.H., *Proc. 11th Int. Conf. on Low Temp. Phys.* p. 1033, St. Andrews (1968).
18. MATTHIAS B.T., *Physics Today*, p.23 (Aug. 1971).